Phosphorylation and proteome dynamics in pathogen-resistant tomato plants

4445

1876269

Promotor: Prof. dr. ir. P.J.G.M. de Wit
Hoogleraar in de Fytopathologie
Wageningen Universiteit

Co-promotor: Dr. ir. M.H.A.J. Joosten
Universitair docent bij het Laboratorium voor Fytopathologie
Wageningen Universiteit

Promotiecommissie: Dr. M. Rep, Universiteit van Amsterdam
Dr. F.L.H. Menke, Universiteit Utrecht
Prof. dr. ir. C.M.J. Pieterse, Universiteit Utrecht
Prof. dr. S.C. de Vries, Universiteit Wageningen

Dit onderzoek is uitgevoerd binnen de onderzoekschool Experimental Plant Sciences.

Phosphorylation and proteome dynamics in pathogen-resistant tomato plants

Iris J.E. Stulemeijer

Proefschrift
ter verkrijging van de graad van doctor
op gezag van de rector magnificus
van Wageningen Universiteit,
Prof. dr. M.J. Kropff,
in het openbaar te verdedigen
op maandag 2 juni 2008
des namiddags te vier uur in de aula.

Iris J.E. Stulemeijer

Phosphorylation and proteome dynamics in pathogen-resistant tomato plants

PhD thesis, Wageningen University, Wageningen, The Netherlands, 2008

With summaries in English and Dutch

ISBN 978-90-8504-885-5

Contents

Chapter 1

Introduction and outline of the thesis

INTRODUCTION

An introduction to tomato and *Cladosporium fulvum*

Tomato has been cultivated in most European countries including the Netherlands, since its introduction in the early 16th century and the fruits soon became a popular ingredient in the European kitchen. In the Netherlands, tomato plants grown in approximately six million square meters of greenhouses yield around 675 million kilograms of fruits, which is approximately 16% of the total vegetable production of 2006 in the Netherlands (www.statline.cbs.nl). The wild ancestors of cultivated tomato are thought to originate from Peru and Ecuador, and wild tomato species can still be found in diverse habitats in mainly the Andes region of South America and on the Galapagos (Paran and Van der Knaap, 2007; http://www.sgn.cornell.edu/about/solanum_nomenclature.pl). Cultivated tomato (*Solanum lycopersicum* (syn. *Lycopersicon esculentum*)) and its ancestors belong to the family of the Solanaceae that also includes species such as potato, tobacco, capsicum, eggplant and petunia. One of the closest wild relatives of cultivated tomato is *S. pimpinellifolium*, which produces very small red fruits that are quite different from the tomato fruits as we known them now (Paran and Van der Knaap, 2007). However, the various wild relatives contain several favourable traits that can be used as a basis for breeding to obtain tomato cultivars of high quality that can adapt to different environments and resist various pathogens and pests (Kruijt *et al.*, 2005b).

The fungus *Cladosporium fulvum* (syn. *Passalora fulva*) (Braun *et al.*, 2003) is a pathogen that can infect tomato plants. Most likely, *C. fulvum* also originates from South America, however, not much is known about its history. A sexual stage of *C. fulvum*, which would allow phylogenetic classification, has never been found; however, molecular data suggest that *C. fulvum* is an asexual hyphomycetous member of the Mycosphaerellaceae (Goodwin *et al.*, 2001; Braun *et al.*, 2003). Just recently, analysis of the mating type loci of *C. fulvum* seems to confirm this classification (Stergiopoulos *et al.*, 2007). In Europe, the disease caused by *C. fulvum*, referred to as tomato leaf mould, was first described in England in 1883 (Cooke, 1883). The cultivation of highly susceptible tomato cultivars in greenhouses under high relative humidity provided favourable conditions for *C. fulvum* to become a persistent disease (Thomma *et al.*, 2005). *C. fulvum* caused severe economic losses before the 1970s, however, the introduction of resistance genes in tomato derived from its wild relatives in the

late 1970s, limited its agronomic threat (Thomma *et al.*, 2005). At present, *C. fulvum* is hardly a problem in tomato cultivation anymore.

The interaction between tomato and *C. fulvum*

For molecular phytopathologists, the interaction between tomato and *C. fulvum* serves as a convenient model system to study plant-pathogen interactions (Joosten and De Wit, 1999; Rivas and Thomas, 2005). *C. fulvum* is a biotrophic pathogen that has tomato as its only host. Conidia produced by *C. fulvum* on leaflets of a successfully colonized tomato plant are normally dispersed by wind and water. When they reach the surface of leaflets of susceptible tomato plants, the conidia germinate and form runner hyphae that enter the leaf via stomata that are abundantly present on the lower side of the leaflets. Subsequently, the intercellular spaces (also referred to as the apoplast) between the leaf mesophyll cells are colonized by the rapidly proliferating mycelium, without the formation of feeding structures inside the host cells, such as haustoria. When the fungus has developed sufficient biomass, the mycelium abandons the apoplast through the stomata and produces conidiophores carrying conidia that can again disperse to, and infect other tomato plants. Since the stomata are completely blocked by the in- and outgrowing fungus, plant gas exchange through the stomata is affected, which eventually results in curling of the leaves, the formation of chlorotic spots, wilting, necrosis and abscission of the leaves. Especially in young plants, this can cause severe growth reduction. Normally, the *C. fulvum* infection cycle is completed in approximately two weeks.

To enhance its virulence, *C. fulvum* secretes several small proteins, so-called effectors, into the apoplast of tomato leaves. These effectors play a role in virulence as they are thought to aid in the extraction of nutrients and water from the host tissue and to specifically suppress the defence response, resulting in susceptibility (Jones and Dangl, 2006). These proteins can be divided into two subgroups. The first subgroup consists of race-specific effectors that are recognized by certain resistant tomato genotypes, and are therefore referred to as avirulence factors (Avrs). The second group consists of proteins that are produced by all *C. fulvum* strains and are referred to as extracellular proteins (Ecps). A role in virulence has been shown for some of the Avrs and Ecps (Laugé *et al.*, 1997; Rooney *et al.*, 2005; Van Esse *et al.*, 2007; Bolton *et al.*, 2008).

During the evolution of tomato, several resistance proteins against *C. fulvum* (Cfs) have evolved that mediate specific recognition of Avrs but also of Ecps (Yuan *et al.*, 2002;

Kruijt *et al.*, 2005a; Rivas and Thomas, 2005; Soumpourou *et al.*, 2007). Cf proteins that recognize Ecps were identified in non-commercial tomato genotypes (Laugé *et al.*, 1998; Laugé *et al.*, 2000). Most likely, these resistance traits were not used in breeding programs and therefore no selection pressure was imposed on *C. fulvum* to circumvent recognition by these resistance proteins, as is the case for Avr-triggered recognition (Joosten *et al.*, 1994; Stergiopoulos *et al.*, 2007). So far, four couples of *Cfs* and their matching *Avrs* have been cloned, which include *Cf-9/Avr9*, *Cf-4/Avr4*, *Cf-4E/Avr4E* and *Cf-2/Avr2* (Thomma *et al.*, 2005). Resistance induced by these cognate gene couples follows the typical gene-for-gene model (Flor, 1942), which implies that the plant is fully resistant to the invading pathogen when both members of the Cf/Avr couple are present during the interaction. The resistance proteins seem not to interact directly with their cognate Avr protein, but are in most cases thought to guard the virulence target of the Avr protein. This model has nicely been illustrated by the Cf-2/Avr2 combination, where the Avr2 protein interacts with and inhibits the activity of the apoplastic tomato Rcr3 protease, probably because this protease is hampering *C. fulvum*. Rcr3 is guarded by Cf-2 and the Avr2/Rcr3 complex triggers Cf-2 to initiate defence signalling that inhibits *C. fulvum* proliferation (Rooney *et al.*, 2005).

Rapid downstream responses in tomato upon recognition of *C. fulvum*

Recognition of an effector protein of *C. fulvum* by the cognate Cf protein of resistant tomato eventually leads to the execution of a hypersensitive response (HR) that manifests itself as a form of programmed cell death (PCD) at the site of pathogen penetration (Lam, 2004). In addition, many other defence-related responses are triggered. A very early response is the Cf/Avr-mediated oxidative burst (May *et al.*, 1996) and activation of ion fluxes (Piedras *et al.*, 1998; De Jong *et al.*, 2000). Another early response is the generation of phosphatidic acid (PA), which is mediated by phospholipase C enzymes (PLCs) (De Jong *et al.*, 2004). Downstream of these fast responses, mitogen-activated protein kinases (MAPKs) and calcium-dependent protein kinases (CDPKs) are activated (Romeis *et al.*, 1999; Romeis *et al.*, 2001). Subsequently, a rapid and massive transcriptional reprogramming takes place (Durrant *et al.*, 2000; Gabriëls *et al.*, 2006; Hong *et al.*, 2007), which for example leads to the accelerated *de novo* synthesis of proteins required for defence. For instance, resistant tomato rapidly produces and secretes several defence proteins such as 1,3-ß-glucanases and chitinases into the apoplast to resist the invading pathogen (Joosten and De Wit, 1989). As mentioned

above, the first defence responses of resistant plants occur extremely fast. In transgenic tobacco cell suspensions expressing a Cf resistance protein, defence responses such as the oxidative burst, ion fluxes, PA accumulation and MAPK activation occur within 10 minutes after elicitation with the cognate Avr (Romeis *et al.*, 1999; De Jong *et al.*, 2000; De Jong *et al.*, 2004). Since 10 minutes is too short for transcriptional reprogramming and *de novo* protein synthesis to occur, post-translational modifications (PTMs) of defence-related proteins are likely to play a major role in the early HR initiation. PTMs, such as phosphorylation, glycosylation or nitrosylation, mediate extremely rapid changes in the activity, localization, function and/or conformation of proteins, thereby allowing resistant plants to respond immediately to invading pathogens.

The work described in this thesis focuses on rapid downstream Cf-4-mediated signalling events that occur upon Avr4 perception. Since PTMs are likely to play a major role in plant defence signalling and, as mentioned above, various MAPKs and CDPKs are indeed activated at a very early stage, the role of protein phosphorylation was studied during the activation of the Cf-4/Avr4-triggered HR. In addition, the defence response observed in the apoplast of Cf-4 tomato plants that trigger a HR upon inoculation with a strain of *C. fulvum* secreting Avr4, was compared to the response of susceptible plants inoculated with the same strain of *C. fulvum*.

OUTLINE OF THE THESIS

In nature, many post-translational protein modifications (PTMs) occur during various fundamental and adaptive processes that take place in the cell (Jensen, 2004). PTMs are fast, reversible modifications of proteins that alter their function, localization, conformation and/or activity. Many signalling cascades are regulated by PTMs since they are rapid and versatile and provide an additional level to fine-tune cellular processes. Chapter 2 provides an overview of PTMs that occur in plant defence responses and which are required for efficient host immune responses. Examples of important PTMs in signal perception, but also in signal transduction cascades, are provided. The importance of PTMs in defence is further illustrated by the observation that modified host proteins are specifically targeted by effectors secreted by a pathogen.

An important cascade generally activated during downstream defence signal transduction in many plant-pathogen interactions is the mitogen-activated protein kinase (MAPK) cascade, which is regulated by protein phosphorylation. To study the role of phosphorylation-dependent signalling cascades in Cf-4/Avr4-triggered HR in tomato, a model system was used that exploits the temperature-sensitivity of the HR initiation. Transgenic tomato seedlings co-expressing the *Cf-4* resistance gene and the *Avr4* gene from *C. fulvum*, execute a HR at 20°C. These seedlings can be rescued at 33°C and 100% relative humidity and upon a subsequent shift to 20°C, all Cf-4/Avr4 seedlings execute a synchronized and systemic HR. This phenomenon allows the analysis of specific stages of the HR, from its early induction to its actual execution (De Jong *et al.*, 2002). In the Cf-4/Avr4 seedlings, three MAPKs (LeMPK1, -2 and -3) are rapidly activated after the temperature shift (Chapter 3). These LeMPKs were shown to have different phosphorylation specificities and furthermore, they were shown to have different roles in HR development and resistance to *C. fulvum* (Chapter 3).

The results described in chapter 3 point to an important role for protein phosphorylation in early HR. To further study the role of protein phosphorylation, a quantitative liquid chromatography tandem mass spectrometry (LC-MS/MS) analysis was performed to study the phosphoproteome of Cf-4/Avr4 seedlings at three early time-points after the temperature shift (Chapter 4). Fifty phosphoproteins were identified from total protein extracts, of which 13 had a significantly altered abundance in the Cf-4/Avr4 seedlings as compared to the controls. From this study and additional experiments, it was concluded that the photosynthetic activity in Cf-4/Avr4 seedlings is specifically suppressed at a very early stage upon HR initiation and that this suppression is phosphorylation-dependent. In addition, the Cf-4/Avr4 seedlings seem to shift from aerobic to anaerobic respiration upon HR initiation, which is probably the result of oxygen depletion due to a massive oxidative burst. Furthermore, four phosphorylated isoforms of cytoplasmic heat shock protein 90 (Hsp90) were identified. Three phosphorylated Hsp90s showed a differentially altered abundance in the Cf-4/Avr4 seedlings, suggesting a specific role for the Hsp90 isoforms in defence signalling (Chapter 4).

Tomato plants that express the *Cf-4* resistance gene are fully resistant to strains of *C. fulvum* expressing the *Avr4* avirulence gene. In addition to programmed cell death, these plants mount several associated, active defence responses. One of these responses is the

secretion of defence-related proteins into the apoplast, which is the environment where *C. fulvum* operates. Therefore, the dynamics of the apoplastic proteome of resistant, *Cf-4*-expressing plants and susceptible plants lacking *Cf-4*, were studied after inoculation with a strain of *C. fulvum* that secretes Avr4. For this purpose, quantitative DIGE 2-dimensional gel electrophoresis and quantitative LC-MS/MS^{E} analysis were used (Chapter 5). These studies provided a very detailed overview of the changes in the apoplastic proteome over time in resistant versus susceptible plants. In susceptible plants, *C. fulvum* is able to proliferate although general elicitors, also referred to as microbe-associated molecular patters (MAMPs) (Jones and Dangl, 2006), released by *C. fulvum* probably trigger secretion of host defence proteins into the apoplast. In resistant plants, there will also be MAMP recognition by the host. However, in addition to this, the Cf-4-mediated perception of Avr4 triggers a swift HR, which leads to a much faster and stronger secretion of defence proteins into the apoplast than was observed for the susceptible plants. Most likely, the combination of these responses renders the plants resistant to *C. fulvum*. Microarray analyses revealed that the increase in protein abundance in the apoplast is caused by an increase in transcription of the encoding genes and that in resistant plants this increased transcription is stimulated by the HR. In addition, this study revealed that a subset of genes encoding (structural) cell wall proteins that have been described to play a role in resistance of plants to pathogens is transcriptionally downregulated in heavily colonized leaflets of susceptible tomato plants. This downregulation is most likely the result of active host gene suppression by *C. fulvum* and is possibly mediated by one or more secreted effectors of this extracellular pathogen (Chapter 5).

In the summarizing discussion (Chapter 6), the power of the Cf-4/Avr4 seedlings as a tool to study HR-related defence responses, is discussed. A hypothesis for the temperature sensitivity of the Cf-4/Avr4-triggered HR is proposed and the role of PTMs in Cf-4/Avr4-initiated defence signalling and the link between the HR and other cellular processes that occur in the plant are discussed. Finally, a model is proposed for the signalling cascades leading to the Cf-4-induced HR upon recognition of Avr4, and resistance to *C. fulvum*.

REFERENCES

Bolton MD, Van Esse HP, Vossen JH, De Jonge R, Stulemeijer IJE, Stergiopoulos I, Van den Berg GCM, Borras-Hidalgo O, Dekker HL, De Koster CG, De Wit PJGM, Joosten MHAJ, Thomma BPHJ (2008) The novel *Cladosporium fulvum* lysine motif effector Ecp6 is a virulence factor with orthologs in other fungal species. Mol Microbiol: accepted for publication.

Braun U, Crous PW, Dugan F, Groenewald J, Sybren De Hoog G (2003) Phylogeny and taxonomy of *Cladosporium*-like hyphomycetes, including *Davidiella*, the teleomorph of *Cladosporium*. Mycol Prog 2: 3-18.

Cooke MC (1883) New american fungi. Grevillea 12: 32.

De Jong CF, Honée G, Joosten MHAJ, De Wit PJGM (2000) Early defence responses induced by AVR9 and mutant analogues in tobacco cell suspensions expressing the *Cf9* resistance gene. Physiol Mol Plant Pathol 56: 169-177.

De Jong CF, Laxalt AM, Bargmann BOR, De Wit PJGM, Joosten MHAJ, Munnik T (2004) Phosphatidic acid accumulation is an early response in the Cf-4/Avr4 interaction. Plant J 39: 1-12.

De Jong CF, Takken FLW, Cai X, De Wit PJGM, Joosten MHAJ (2002) Attenuation of Cf-mediated defense responses at elevated temperatures correlates with a decrease in elicitor-binding sites. Mol Plant-Microbe Interact 15: 1040-1049.

Durrant WE, Rowland O, Piedras P, Hammond Kosack KE, Jones JDG (2000) cDNA-AFLP reveals a striking overlap in race-specific resistance and wound response gene expression profiles. Plant Cell 12: 963-977.

Flor HH (1942) Inheritance of pathogenicity in *Melampsora lini*. Phytopathology 32: 653-669.

Gabriëls SHEJ, Takken FLW, Vossen JH, De Jong CF, Liu Q, Turk SCHJ, Wachowski LK, Peters J, Witsenboer HMA, De Wit PJGM, Joosten MHAJ (2006) cDNA-AFLP combined with functional analysis reveals novel genes involved in the hypersensitive response. Mol Plant-Microbe Interact 19: 567-576.

Goodwin SB, Dunkle LD, Zismann VL (2001) Phylogenetic analysis of *Cercospora* and *Mycosphaerella* based on the internal transcribed spacer region of ribosomal DNA. Phytopathology 91: 648-658.

Hong W, Xu YP, Zheng Z, Cao JS, Cai XZ (2007) Comparative transcript profiling by cDNA-AFLP reveals similar patterns of *Avr4/Cf-4*- and *Avr9/Cf-9*-dependent defence gene expression. Mol Plant Pathol 8: 515-527.

Jensen ON (2004) Modification-specific proteomics: characterization of post-translational modifications by mass spectrometry. Curr Opin Chem Biol 8: 33-41.

Jones JDG, Dangl JL (2006) The plant immune system. Nature 444: 323-329.

Joosten MHAJ, Cozijnsen TJ, De Wit PJGM (1994) Host resistance to a fungal tomato pathogen lost by a single base-pair change in an avirulence gene. Nature 367: 384-386.

Joosten MHAJ, De Wit PJGM (1989) Identification of several pathogenesis-related proteins in tomato leaves inoculated with *Cladosporium fulvum* (syn. *Fulvia fulva*) as 1,3-ß-glucanases and chitinases. Plant Physiol 89: 945-951.

Joosten MHAJ, De Wit PJGM (1999) The tomato-*Cladosporium fulvum* interaction: A versatile experimental system to study plant-pathogen interactions. Annu Rev Phytopathol 37: 335-367.

Kruijt M, De Kock MJD, De Wit PJGM (2005a) Receptor-like proteins involved in plant disease resistance. Mol Plant Pathol 6: 85-97.

Kruijt M, Kip DJ, Joosten MHAJ, Brandwagt BF, De Wit PJGM (2005b) The *Cf-4* and *Cf-9* resistance genes against *Cladosporium fulvum* are conserved in wild tomato species. Mol Plant-Microbe Interact 18: 1011-1021.

Lam E (2004) Controlled cell death, plant survival and development. Nat Rev Mol Cell Biol 5: 305-315.

Laugé R, Goodwin PH, De Wit PJGM, Joosten MHAJ (2000) Specific HR-associated recognition of secreted proteins from *Cladosporium fulvum* occurs in both host and non-host plants. Plant J 23: 735-745.

Laugé R, Joosten MHAJ, Haanstra JP, Goodwin PH, Lindhout P, De Wit PJGM (1998) Successful search for a resistance gene in tomato targeted against a virulence factor of a fungal pathogen. Proc Natl Acad Sci USA 95: 9014-9018.

Laugé R, Joosten MHAJ, Van den Ackerveken GFJM, Van den Broek HWJ, De Wit PJGM (1997) The *in planta*-produced extracellular proteins ECP1 and ECP2 of *Cladosporium fulvum* are virulence factors. Mol Plant-Microbe Interact 10: 725-734.

May MJ, Hammond-Kosack KE, Jones JDG (1996) Involvement of reactive oxygen species, glutathione metabolism, and lipid peroxidation in the Cf-gene-dependent defense response of tomato cotyledons induced by race-specific elicitors of *Cladosporium fulvum*. Plant Physiol 110: 1367-1379.

Paran I, Van der Knaap E (2007) Genetic and molecular regulation of fruit and plant domestication traits in tomato and pepper. J Exp Bot 58: 3841-3852.

Piedras P, Hammond Kosack KE, Harrison K, Jones DG (1998) Rapid, Cf-9- and Avr9-dependent production of active oxygen species in tobacco suspension cultures. Mol Plant-Microbe Interact 11: 1155-1166.

Rivas S, Thomas CM (2005) Molecular interactions between tomato and the leaf mold pathogen *Cladosporium fulvum*. Annu Rev Phytopathol 43: 395-436.

Romeis T, Ludwig AA, Martin R, Jones JDG (2001) Calcium-dependent protein kinases play an essential role in a plant defence response. EMBO J 20: 5556-5567.

Romeis T, Piedras P, Zhang SQ, Klessig DF, Hirt H, Jones JDG (1999) Rapid Avr9- and Cf-9-dependent activation of MAP kinases in tobacco cell cultures and leaves: convergence of resistance gene, elicitor, wound, and salicylate responses. Plant Cell 11: 273-287.

Rooney HCE, Van 't Klooster JW, Van der Hoorn RAL, Joosten MHAJ, Jones JDG, De Wit PJGM (2005) Cladosporium Avr2 inhibits tomato Rcr3 protease required for *Cf-2*-dependent disease resistance. Science 308: 1783-1786.

Soumpourou E, Iakovidis M, Chartrain L, Lyall V, Thomas C (2007) The *Solanum pimpinellifolium Cf-ECP1* and *Cf-ECP4* genes for resistance to *Cladosporium fulvum* are located at the Milky Way locus on the short arm of chromosome 1. TAG 115: 1127-1136.

Stergiopoulos I, Groenewald M, Staats M, Lindhout P, Crous PW, De Wit PJGM (2007) Mating-type genes and the genetic structure of a world-wide collection of the tomato pathogen *Cladosporium fulvum*. Fungal Genet Biol 44: 415-429.

Thomma BPHJ, Van Esse HP, Crous PW, De Wit PJGM (2005) *Cladosporium fulvum* (syn. *Passalora fulva*), a highly specialized plant pathogen as a model for functional studies on plant pathogenic Mycosphaerellaceae. Mol Plant Pathol 6: 379-393.

Van Esse HP, Bolton MD, Stergiopoulos I, De Wit PJGM, Thomma BPHJ (2007) The chitin-binding *Cladosporium fulvum* effector protein Avr4 is a virulence factor. Mol Plant-Microbe Interact 20: 1092-1101.

Yuan Y, Haanstra J, Lindhout P, Bonnema G (2002) The *Cladosporium fulvum* resistance gene Cf-ECP3 is part of the Orion cluster on the short arm of tomato Chromosome 1. Mol Breeding 10: 45-50.

Chapter 2

Post-translational modification of host proteins in pathogen-triggered defence signalling in plants

Iris J.E. Stulemeijer and Matthieu H.A.J. Joosten

A slightly modified version of this chapter has been published in Molecular Plant Pathology 9 (2008).

SUMMARY

Microbial plant pathogens impose a continuous threat to global food production. Similar to animals, an innate immune system allows plants to recognise pathogens and swiftly activate defence. To activate a rapid response, receptor-mediated pathogen perception and subsequent downstream signalling depends on post-translational modification (PTM) of components essential for defence signalling. We discuss different types of PTMs that play a role in mounting plant immunity, which include phosphorylation, glycosylation, ubiquitination, sumoylation, nitrosylation, myristoylation, palmitoylation and GPI-anchoring. PTMs are rapid, reversible, controlled and highly specific, and provide a tool to regulate protein stability, activity and localization. Here, we give an overview of PTMs that modify components essential for defence signalling at the site of signal perception, during secondary messenger production and during signalling in the cytoplasm. In addition, we discuss effectors from pathogens that suppress plant defence responses by interfering with host PTMs.

INTRODUCTION

Plants are continuously challenged by microbes such as viruses, bacteria, fungi, oomycetes, nematodes and insects. Microbes that manage to circumvent structural barriers like the cell wall and the cuticle are generally not able to invade a plant because of the activation of a primary defence response resulting in non-host resistance. Most of the microbes that are able to evade or suppress the primary defence response are recognized by the plant via the effector proteins that they secrete, which results in the activation of a secondary defence response that in most cases involves a hypersensitive response (HR). Eventually, only a small subset of microbes has evolved into successful pathogens that are able to suppress and/or circumvent both the primary and the secondary defence responses of the plant (Nürnberger *et al.*, 2004; Chisholm *et al.*, 2006; Jones and Dangl, 2006; Bent and Mackey, 2007; De Wit, 2007). These pathogens cause disease, resulting in severe crop losses.

The primary and secondary defence responses of plants leading to resistance rely on the swift activation of signal transduction cascades, whereby cellular changes caused by the

secondary defence response are generally most pronounced (Jones and Dangl, 2006). Research on the molecular aspects of recognition and subsequent defence signalling was initiated by the proposition of the gene-for-gene hypothesis by Flor (1942). Since then, many sophisticated pathogen recognition mechanisms have been discovered that subsequently initiate highly complex signalling cascades, eventually leading to host genotype-specific resistance. So far, the main focus of molecular phytopathologists has been the identification and functional analysis of resistance (R) proteins and their cognate pathogen effectors, the so-called race-specific elicitors (Bent and Mackey, 2007; Takken and Tameling, 2007). In addition, transcriptional changes that occur upon pathogen recognition have been extensively studied by microarray and cDNA-AFLP experiments (Eulgem, 2005; Wise *et al.*, 2007), and the role of individual genes in resistance has been studied by transient/stable knockdown and knockout studies (Glazebrook *et al.*, 1997; Baulcombe, 1999; Burch-Smith *et al.*, 2004).

Initial plant defence responses occur extremely fast upon recognition of a pathogen (Wojtaszek, 1997; Nürnberger and Scheel, 2001; Laxalt and Munnik, 2002), which implies the involvement of post-translational modifications (PTMs) of pre-existing proteins in signal transduction cascades. A definite role for PTMs in defence signal transduction became apparent with the discovery of protein phosphorylation events in parsley cells upon elicitor treatment (Dietrich *et al.*, 1990), and with the observation that activated mitogen-activated protein kinases (MAPKs), which require phosphorylation for activation, are involved in the primary resistance response of parsley to *Phytophthora sojae* (Ligterink *et al.*, 1997). Furthermore, some receptors contain kinase domains themselves, which enable them to phosphorylate downstream substrates (Martin *et al.*, 2003; Van Ooijen *et al.*, 2007). Over the past years, the general importance of PTMs in signal transduction cascades has become clear (Xing *et al.*, 2002; Thurston *et al.*, 2005) and its relevance for successful plant defence signalling was further confirmed by reports describing direct manipulation of PTMs by pathogens in order to suppress plant immune responses (Kim *et al.*, 2005b; Mudgett, 2005; Shan *et al.*, 2007). In this review we will discuss different types of host protein PTMs that play a role in plant defence signalling. In addition, we will shortly discuss effectors from pathogens that specifically interfere with host PTMs to suppress plant defence responses, thereby underlining the importance of PTMs in defence signalling.

POST-TRANSLATIONAL MODIFICATIONS, HOW DO THEY OCCUR?

Single genes can give rise to a diversity of RNA transcripts because of gene splicing and each of these transcripts is translated into a protein that can subsequently be proteolytically processed and/or post-translationally modified. PTMs are responsible for a major increase in complexity from genome to proteome. For example, the human genome, containing approximately 30,000 open reading frames, is predicted to give rise to approximately 1.8 million different protein species (Jensen, 2004; Kersten *et al.*, 2006). PTMs are involved in protein regulation and are therefore often reversible, rapid, controlled and highly specific but they usually affect only a small percentage of the total pool of a specific protein (Johnson, 2004). Furthermore, PTMs are catalyzed by specific enzymes that in turn are often also regulated by PTMs (Peck, 2006). Currently, more than 300 types of PTMs have been described (Jensen, 2004), but here we focus on the major PTMs that have been implicated in defence signalling.

Phosphorylation

Reversible protein phosphorylation is the most predominant covalent modification of proteins and implies the reversible attachment of a phosphate group to an amino acid residue. Phosphorylation has been described to play a major role in defence signalling cascades (Xing *et al.*, 2002; Peck, 2003; Thurston *et al.*, 2005; De la Fuente van Bentem and Hirt, 2007). Four types of phosphorylation occur of which N-, S- and acyl-phosphorylation are very uncommon. O-phosphorylation is the most common type and here further referred to as phosphorylation. Phosphorylation mainly occurs on the hydroxyl group of hydroxyamino acids such as serine, threonine and tyrosine but can also occur on unusual residues such as hydroxy-proline (Reinders and Sickmann, 2005). Phosphorylation is executed by protein kinases that transfer a phosphoryl (PO_3) group from ATP to the hydroxyl group in the polar rest (R-) group of the amino acid residue, resulting in a phosphoester (R-O-PO_3) bond. Dephosphorylation occurs by protein phosphatases that hydrolyze the phosphoester bond, thereby releasing the phosphoryl group and restoring the hydroxyamino acid into its unphosphorylated state (Sickmann and Meyer, 2001). Generally, only a small percentage of the total pool of a certain protein in the cell is phosphorylated and a transient change of only a few percent can be sufficient to activate signalling. The opposite activity of kinases and

phosphatases balances phosphorylation-based signalling cascades, rendering them very dynamic (Reinders and Sickmann, 2005).

Ubiquitination

Another highly dynamic PTM that is implicated in defence signalling is ubiquitination. Ubiquitination refers to a three-step enzymatic cascade to covalently attach a small conserved polypeptide, ubiquitin, to a protein. First, the C-terminal glycine of ubiquitin, which is maturated by deubiquitination enzymes (DUBs), forms together with the thiol group (SH) of a cysteine in the active site of the ubiquitin-activating enzyme (E1), a thioester (R_{E1}-S-CO-R_{Ub}). Subsequently, the activated ubiquitin is transferred to a cysteine residue of the ubiquitin-conjugating enzyme (E2). Finally, the ubiquitin-ligase protein (E3), which interacts with the ubiquitinated E2 enzyme, initiates attachment of the ubiquitin moiety to the target protein by an isopeptide bond between the C-terminal glycine of ubiquitin and the ε-amino group of a lysine residue of the target protein (Vierstra, 2003). The target protein often requires phosphorylation prior to binding to the E3 complex. To form a polyubiquitinated protein, these three steps are repeated so that each new ubiquitin moiety is attached to a lysine residue of the previous ubiquitin moiety. Polyubiquitination can lead to lysine (K) 48- and K63-linked chains, depending on which lysine in the ubiquitin moiety is targeted for ubiquitination, and on the E2 conjugating enzyme. Proteins modified with a K48-chain are normally targeted to the 26S proteasome for degradation, whereas K63-chains are involved in endocytosis of the protein, its activation or modification of its activity (Angot *et al.*, 2007). Some proteins are only monoubiquitinated and this may also trigger a change in the localization and/or activity of the protein (Haglund *et al.*, 2003). Eventually, DUBs are capable of removing the covalently bound ubiquitin moieties thereby changing the fate of the protein, but they also recycle ubiquitin moieties from ubiquitinated proteins processed by the proteasome (Vierstra, 2003; Kerscher *et al.*, 2006).

Sumoylation

Similar to ubiquitination, proteins can be decorated with a small ubiquitin-related modifier (SUMO) moiety during defence signalling (Novatchkova *et al.*, 2004; Miura *et al.*, 2007). Sumoylation has been reported in cell cycle activity, DNA repair, nuclear localization, enzymatic activity and stability of proteins and in the modulation of transcription factor

activity (Miura *et al.*, 2007). Similar to ubiquitin, SUMO is processed to expose its C-terminal glycine that is subsequently attached to a lysine residue of a target protein, via conjugation machinery similar as for ubiquitination. However, sumoylation differs from ubiquitination since it has only one universal E2-conjugating enzyme that does not always require an E3-ligase to transfer SUMO to the targeted protein. Furthermore, a weak consensus motif for sumoylation has been identified in target proteins and normally only mono-sumoylation occurs although poly-sumoylation has been reported. Finally, the cysteine proteases required for SUMO maturation and desumoylation belong to a distinct family of ubiquitin-like protein proteases (ULPs) (Chosed *et al.*, 2006).

_S_-nitrosylation

S-nitrosylation of proteins is another mechanism to regulate cellular processes and although not very well described, this modification is regarded as influential as protein phosphorylation (Lindermayr *et al.*, 2006). Protein *S*-nitrosylation occurs on cysteine residues, mainly via two mechanisms. Proteins can either become *S*-nitrosylated via an oxygen-dependent reaction where nitrosonium (NO^+) reacts with a thiolate group ($R\text{-}S^-$) of the cysteine in the protein, or nitric oxide (NO) can be transferred from a nitrosothiol (SNO) to the thiol group (SH) of the cysteine (transnitrosylation). SNOs consist of small molecules, like glutathione with a thiol group (GSH), that react with NO resulting in *S*-nitrosoglutathione (GSNO), which are suggested to be the NO reservoirs and NO donors in the cell (Lindermayr *et al.*, 2006). Although reports on *S*-nitrosylation during plant-pathogen interactions are rare, the production of NO and its signalling function during plant-pathogen interactions are well described (Romero-Puertas *et al.*, 2004). The presence of GSNO reductase activity in plants, which releases NO from the GSNO, indicates that the formation of SNOs could play an important role in NO signalling (Lindermayr *et al.*, 2005).

Glycosylation

Covalent linkage of an oligosaccharide side chain to a protein is referred to as protein glycosylation. The two most predominant types are *N*-glycosylation and *O*-glycosylation. Here, we only consider *N*-glycosylation which can affect the asparagine residue in the sequence motif asparagine-X-serine/threonine (X can be any amino acid except proline) and which refers to the oligosaccharide side chain attachment to the asparagine residue. *N*-

glycosylation starts co-translationally at the endoplasmic reticulum (ER) by the transfer of an oligosaccharide precursor, $Glc_3Man_9GlcNAc_2$, onto the amide nitrogen of the asparagine residue. Subsequently, the oligosaccharide matures by the removal of glucose and mannose residues or by the attachment of new sugar residues to generate glycans and complex-type glycans (Saint-Jore-Dupas *et al.*, 2007). Glycosylation occurs quite frequently and can affect the biological activity and the function of proteins, and has been reported to occur also on resistance proteins (Van der Hoorn *et al.*, 2005).

_N_-myristoylation and S-palmitoylation

Next to the attachment of sugars to proteins, proteins can also be modified cotranslationally (*N*-myristoylation) or posttranslationally (S-palmitoylation) with fatty acids. *N*-myristoylation, also referred to as myristoylation, is the modification of a protein with myristate, a hydrophobic 14-carbon fatty acid. Catalyzed by *N*-myristoyltransferase, myristate is in general covalently and irreversibly attached through amide linkage to the N-terminal glycine exposed after removal of the initial methionine residue of the target protein by aminopeptidases. Myristoylation targets proteins to a membrane and thereby promotes interactions between these proteins and membrane-associated protein complexes (Farazi *et al.*, 2001). Protein myristoylation plays an important role in defence signalling in tomato against *Pseudomonas syringae* (Andriotis and Rathjen, 2006). S-palmitoylation, also referred to as S-acylation, is the thioesterification of palmitate (a 16-carbon fatty acid) to a cysteine residue in a protein. S-palmitoylation is catalyzed by palmityl acyltransferases (PAT) or occurs via a spontaneous autoacylation in the presence of long-chain acyl-coenzyme As (CoAs) and lipid vesicles. S-palmitoylation supports initial plasma-membrane binding of proteins (Smotrys and Linder, 2004) including proteins required for the perception of pathogen elicitors and might play a role in protein trafficking (Kim *et al.*, 2005a).

GPI-anchoring

GPI-anchoring implies the attachment of a glycosylphosphatidylinositol (GPI) to anchor cell surface proteins to the plasma membrane, were they can play a role in elicitor perception. GPI is synthesized at the ER via the sequential linkage of sugars and other components to phosphatidylinositol (PI). GPI transamidases recognize and cleave the C-terminal GPI attachment signal peptide of the target and mediate attachment to the GPI

anchor. The GPI-anchored protein is subsequently secreted via the Golgi apparatus and attached to the plasma membrane (Maeda *et al.*, 2006).

PTMS OF HOST PROTEINS INVOLVED IN SIGNAL PERCEPTION

Pathogen recognition is mediated by a group of protein receptors which can be divided in a few major classes. Two classes account for the receptor-like proteins (RLPs) and the receptor-like kinases (RLKs) that are localized in the plasma membrane and contain extracellular leucine-rich repeats (LRRs). The RLPs lack a cytoplasmic signalling domain, while RLKs have a cytoplasmic kinase domain. Two other classes are formed by receptors that are cytoplasmically localized and that contain a nucleotide-binding (NB) site and LRRs. One class is referred to as TIR-NB-LRRs since these NB-LRRs contain an N-terminal domain similar to the *Drosophila* Toll receptor and the interleukin 1 receptor (TIR). The other class is referred to as CC-NB-LRRs, since N-terminal domain structures in which frequently coiled-coil (CC) motifs are predicted are found in addition to the NB-LRR domains (Martin *et al.*, 2003; Van Ooijen *et al.*, 2007). Over the last years, it became clear that the primary (non-host) defence response elicited by microbe-associated molecular patterns (MAMPs) and the secondary (host genotype-specific) defence response induced by race-specific elicitors, are in fact mediated by very similar receptors (Gómez-Gómez and Boller, 2000; Zipfel *et al.*, 2006). Nowadays these receptors are referred to as pattern recognition receptors (PRRs) and R proteins, respectively (Jones and Dangl, 2006; Bent and Mackey, 2007).

Signal perception by RLKs

The best studied model system in Arabidopsis for primary defence signalling is the perception of bacterial flagellin, or its 22-amino-acid conserved epitope, flg22, by the membrane-bound PRR FLS2. FLS2 is an RLK and autophosphorylation of its kinase domain seems to be required for binding of flg22 and might affect the stability of the FLS2-flg22 complex (Gómez-Gómez *et al.*, 2001). Mutation of four, probably not autophosphorylated, phosphorylation sites in the C-terminal region of the protein did not affect flg22 binding but abolished or reduced downstream signalling. Mutation of one of these sites also significantly reduced FLS2 internalization by endocytosis (Robatzek *et al.*, 2006). FLS2 endocytosis might

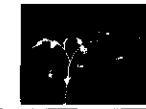

be triggered by ubiquitination since the required conserved (PEST) motif is present in the cytoplasmic region of the FLS2 protein, and FLS2 endocytosis is followed by its degradation (Figure 1; Robatzek *et al.*, 2006). It has been found recently that the FLS2 receptor specifically binds to one of the somatic embryogenesis receptor kinases, SERK3, also referred to as BRI1-associated receptor kinase 1 (BAK1), in a ligand-dependent manner (Chinchilla *et al.*, 2007; Heese *et al.*, 2007). Upon perception of brassinosteroids (BRs), which are plant steroid hormones, BAK1 forms a heterodimer with the plasma membrane receptor kinase BRI1 (BRASSINOSTEROID-INSENSITIVE 1). Both BAK1 and BRI1 display BR-dependent phosphorylation (Wang *et al.*, 2005) which enhances the interaction and complex formation between the two proteins that are subsequently internalized via endocytosis (reviewed by Karlova and De Vries, 2006). Possibly, the ligand-dependent FLS2-BAK1 complex formed *in vivo* is internalized in a similar way as the BRI1-BAK1 complex (Figure 1; Chinchilla *et al.*, 2007). The kinase-associated protein phosphatase (KAPP) might negatively regulate FLS2 signalling since it binds and dephosphorylates FLS2 (Gómez-Gómez *et al.*, 2001). Recently, a very homologous receptor that recognizes an 18 amino acid fragment of the bacterial elongation factor Tu (EF-Tu) was identified (Zipfel *et al.*, 2006). Just like FLS2, this EF-Tu receptor (EFR) requires BAK1 for downstream signalling and upon stimulation both PRRs induce the transcription of a similar set of genes, including a large amount of additional RLKs. Furthermore, they induce a common set of responses including downstream MAPK activation and extracellular alkalization (Zipfel *et al.*, 2006; Chinchilla *et al.*, 2007). Phosphorylation of the EFR receptor itself has not yet been reported, but the homology to the FLS2 signalling cascade suggests a role for EFR-mediated phosphorylation upon EF-Tu perception (reviewed by Nürnberger and Kemmerling, 2006). In addition, a RLK referred to as RPG1 confers resistance of barley to *Puccinia graminis* f. sp. *tritici*. RPG1 contains two tandem kinase domains of which only the C-terminal domain is functional and displays autophosphorylation required for resistance. In accordance with FLS2 signalling, RPG1 appears to be degraded in a proteasome-dependent way upon inoculation with an avirulent strain, which implies that RPG1 becomes ubiquitinated (Nirmala *et al.*, 2006 and 2007). Furthermore, the rice RLK Xa21, that mediates recognition of the effector AvrXa21 from *Xanthomonas oryzae* pv *oryzae* (Song *et al.*, 1995), has a kinase domain that autophosphorylates on several serine and threonine residues which stabilizes the protein and probably protects it from proteolytic cleavage (Liu *et al.*, 2002; Xu *et al.*, 2006). Xa21

phosphorylates the Xa21-binding protein 3 (XB3) that binds *in vivo* to the receptor and which is required for its accumulation. XB3 is a RING finger-containing protein that can function as an E3 ubiquitin ligase and it is hypothesized that XB3 is phosphorylated by Xa21 upon pathogen recognition. XB3 subsequently ubiquitinates a downstream component, which could be a negative regulator of defence signalling that is targeted for degradation (Figure 1; Wang *et al.*, 2006). However, referring back to FLS2, XB3 might also mediate Xa21 ubiquitination and degradation. It is tempting to speculate that RLK-mediated signalling is initiated by phosphorylation and formation of a ligand-dependent protein complex that internalizes and is subsequently degraded in a proteasome-dependent manner.

Signal perception by RLPs

RLPs, that lack a kinase domain and thus lack autophosphorylation, are represented by for example the so-called Cf proteins of tomato plants that mediate resistance to *Cladosporium fulvum* (Rivas and Thomas, 2005). One of the family members is Cf-9, which is highly glycosylated, a feature required for its stability and for a full Cf-9-mediated HR. Probably, Cf-9 *N*-glycosylation is required for a stable structural conformation and/or interactions with the cell wall (Piedras *et al.*, 2000; Van der Hoorn *et al.*, 2005). Cf-9 has no signalling domain but the cytoplasmic C-terminus interacts with a thioredoxin (CITRX; for Cf-9-interacting thioredoxin) that accelerates the Cf-9/Avr9-induced HR upon transcriptional knockdown by virus-induced gene silencing (VIGS) (Rivas *et al.*, 2004). In addition, the Avr9/Cf-9-induced kinase 1 (ACIK1), which encodes a cytoplasmic serine/threonine kinase, compromises the Cf-9/Avr9- and Cf-4/Avr4-induced HR and resistance upon VIGS (Durrant *et al.*, 2000; Rowland *et al.*, 2005). Interestingly, ACIK1 binds and phosphorylates CITRX and binds the C-terminus of Cf-9 with CITRX as an adaptor protein, thereby forming a complex that can mediate downstream signalling (Nekrasov *et al.*, 2006). However, it remains difficult to understand how the downstream signalling from Cf-9 actually takes place since ACIK1 is a positive regulator and CITRX a negative regulator of Cf-9/Avr9-induced defence signalling, and the catalytic domains are not required for the interaction between the different proteins (Nekrasov *et al.*, 2006). We hypothesize that Cf-9, CITRX and ACIK1 form a complex under normal conditions in unchallenged plants. Upon elicitation by Avr9, ACIK1 phosphorylates CITRX which destabilizes the complex and releases CITRX and ACIK1 into the cytoplasm where they can activate downstream signalling components resulting in a

balanced defence response (Figure 1). In addition to race-specific elicitor recognition, RLPs also mediate MAMP-induced defence responses. The MAMP xylanase from *Trichoderma viride* triggers signalling through the ethylene-inducing xylanase (EIX) PRR, which is an RLP (Ron and Avni, 2004). Chitin, a major component from fungal cell walls, is a MAMP that triggers signalling by the chitin oligosaccharide elicitor-binding protein CEBiP, which is an RLP that is highly glycosylated, just like Cf-9 (Kaku *et al.*, 2006). However, for these PRRs it remains to be elucidated how the perceived signal is transferred further downstream to the cytoplasm.

Signal perception by NB-LRRs

Resistance to *Pseudomonas* species is in most cases conferred by NB-LRRs. The interaction between tomato and *Pseudomonas syringae* pv *tomato* (Pst) is a well studied model system. Resistance to Pst expressing the elicitor genes *AvrPto* and/or *AvrPtoB* requires the *Pto* and the *Prf* gene (Salmeron *et al.*, 1994; Kim *et al.*, 2002). *Pto* encodes a serine/threonine protein kinase (Loh and Martin, 1995) and originally, Pto was reported as the AvrPto-matching R protein (Martin *et al.*, 1993). However, further analysis revealed Prf as a CC-NB-LRR protein, which is capable of signalling in the absence of Pto, while Pto is incapable of signalling in the absence of Prf (Salmeron *et al.*, 1996). It was also shown that Prf and Pto interact *in vivo* and that Prf accumulates to higher amounts in the presence of Pto (Mucyn *et al.*, 2006). Therefore, Prf is now classified as the R protein that activates downstream signalling (Van Ooijen *et al.*, 2007). Still, Pto plays an important role in AvrPto and AvrPtoB perception since Pto specifically binds both elicitors and several other Pto-interacting (Pti) proteins (Tang *et al.*, 1996; Sessa *et al.*, 2000b; Kim *et al.*, 2002). Pti1 represents a serine/threonine kinase which is phosphorylated by the Pto kinase, and this phosphorylation is required for Pto/Pti1 interaction (Sessa *et al.*, 2000a). *In vitro*, Pto autophosphorylates at eight sites of which three are required for HR development and AvrPto binding, and one is only required for HR development, indicating that Pto kinase activity is required for the AvrPto/Prf-dependent HR elicitation (reviewed by Pedley and Martin, 2003). Further research revealed two additional phosphorylation sites in the activation loop of Pto required for AvrPto binding. Substitution of these residues by aspartic acid (D), which mimics the negative charge introduced by phosphorylation, resulted in a Prf-dependent and AvrPto-independent HR in tomato (Rathjen *et al.*, 1999). To further complicate Pto-mediated AvrPto

perception, Pto was also found to be myristoylated at the N-terminus, which negatively regulates its kinase activity (Andriotis and Rathjen, 2006). A model summarizing these results has been proposed: Pto is myristoylated to suppress its kinase activity and to be target to a cellular membrane, most likely the plasma membrane, where it binds to Prf. AvrPto targets the complex and causes displacement of the myristoylated N terminus of Pto which results in derepression of the kinase domain, Pto phosphorylation and activation, and subsequent signalling via Prf (Andriotis and Rathjen, 2006; Balmuth and Rathjen, 2007). Furthermore, AvrPto and phosphorylated Pto form a complex with AvrPto-dependent Pto-interacting protein 3 (Adi3). Adi3 is a member of the AGC family of protein kinases (protein kinase A, G and C family) and negatively regulates the Pto-AvrPto-induced host cell death when phosphorylated by 3-phosphoinositide-dependent protein kinase-1 (PDK1) or Pto. In contrast to the AvrPto-dependent Pto/Adi3 interaction, Adi3 phosphorylation by Pto is independent of AvrPto and not required for Pto/AvrPto/Adi3 complex formation. Therefore, it is hypothesized that Adi3-mediated negative regulation is released when bound to the Pto-AvrPto complex (Devarenne *et al.*, 2006). Possibly, phosphorylated Adi3 negatively regulates elicitor-independent Pto signalling under normal conditions to avoid activation of defence responses. Upon elicitation, Adi3 is dephosphorylated and binds to Pto, which leads to Pto-mediated signalling. As described in other defence signalling cascades, secondary messengers such as phosphatidic acid might be produced (see below) that bind and possibly activate PDK1 (Testerink *et al.*, 2004). PDK1 might subsequently phosphorylate Adi3 to negatively regulate Pto signalling again, thereby forming a negative feed-back loop (Figure 1).

Interactions between *Pseudomonas syringae* and Arabidopsis are also intensively studied and several intracellular NB-LRRs have been described to mediate recognition of elicitors from different *P. syringae* strains (Nimchuk *et al.*, 2003). The R proteins RPS2 and RPS5 provide resistance to *P. syringae* pathovars expressing AvrRpt2 or AvrPphB, respectively, whereas RPM1 provides resistance to *P. syringae* pathovars expressing AvrRpm1 or AvrB (reviewed by Belkhadir *et al.*, 2004b). In a yeast two-hybrid screen, two RPM1-interacting proteins (RINs), RIN2 and RIN3, were identified which represent RING-finger ubiquitin E3 ligases and which also weakly interact with RPS2. These RINs seem to enhance the RPM1- and RPS2-mediated HR; however, they do not restrict bacterial growth in the plant. Although RIN2 and RIN3 encode proteins that show E3 ligase activity *in vitro*, a target protein that might serve as a negative regulator of the HR and is degraded still has to be

identified (Kawasaki *et al.*, 2005). Another protein that physically interacts with RPM1 and RPS2 is RIN4, a protein that negatively regulates RPM1- and RPS2-mediated resistance (Belkhadir *et al.*, 2004a). RIN4 is C-terminally palmitoylated which is required for RIN4 localization to the plasma membrane and its functioning (Belkhadir *et al.*, 2004a; Day *et al.*, 2005; Kim *et al.*, 2005a). It is hypothesized that RIN4 is bound to RPM1 and RPS2 under normal conditions to negatively regulate defence signalling and that RIN4 is released from the complex upon R protein triggering (Figure 1). In addition, defence signalling by RPM1 or RPS2 requires the non-race-specific disease resistance 1 (NDR1) protein, which is glycosylated and C-terminally processed. NDR1 is thought to undergo GPI modification at its processed C-terminus and this GPI-anchor places the protein on the outer surface of the plasma membrane with a short part of the N-terminus in the cytoplasm, where it binds the C-terminal half of RIN4 (Coppinger *et al.*, 2004; Day *et al.*, 2006). Upon inoculation with an AvrRpt2-producing Pst strain, RIN4 is cleaved by the cysteine protease activity of the AvrRpt2 effector after which the negative regulation of RPS2 by RIN4 is released (Figure 1; Takemoto and Jones, 2005). A C-terminal membrane-embedded RIN4 fragment is not degraded after cleavage and positively regulates RPS2-mediated signalling by its interaction with NDR1 (Day *et al.*, 2006). Probably, RIN4-mediated RPM1 activation by AvrRpm1/AvrB elicitation occurs via a different mechanism, since RIN4 degradation abolishes RPM1 signalling, and RPM1 activation depends on RIN4 phosphorylation (Kim *et al.*, 2005a; Kim *et al.*, 2005b). In addition to RPM1 and RPS2, also RPS5-mediated resistance depends on NDR1 but RPS5 does not require RIN4 (Coppinger *et al.*, 2004). Instead, RPS5-mediated resistance to *P. syringae* depends on a serine/threonine protein kinase PBS1 that binds to RPS5 in unchallenged plants (Swiderski and Innes, 2001; Ade *et al.*, 2007). Similar to AvrRpt2-mediated cleavage of RIN4 and the subsequent activation of RPS2, the cysteine protease AvrPphB cleaves PBS1 which activates RPS5. PBS1 requires a functional kinase domain that is probably involved in autophosphorylation; however, neither the phosphorylation nor the elimination of PBS1 is sufficient to activate RPS5. Therefore, it is hypothesized that a phosphorylated cleavage product of PBS1 is required for RPS5-activation (Shao *et al.*, 2003).

PTMS OF PLASMA MEMBRANE-LOCALIZED HOST PROTEINS INVOLVED IN DOWNSTREAM SIGNALLING

In addition to the above described complexes that are at least partially localized and/or bound to the plasma membrane, several other post-translationally modified membrane-localized proteins exist that are not directly involved in signal perception but play a role in downstream responses.

Transport of secondary messengers over the plasma membrane by ATPases

Secondary messengers are transported over membranes by pumps that are driven by the hydrolysis of ATP and are referred to as ATPases. An important subclass of ATPases is formed by the H^+-ATPases that mediate the generation of electrochemical gradients across the plasma membrane, which is the energy source for most transport proteins (Palmgren, 2001). H^+-ATPases require phosphorylation on a threonine residue in the N-terminus for their activity and are inactivated by dephosphorylation of this site. However, a plasma membrane H^+-ATPase from Arabidopsis was also inactivated by phosphorylation on a serine residue by the PKS5 serine/threonine protein kinase. This phosphorylation event prevents interaction with a 14-3-3 protein and therefore inhibits the activity of the H^+-ATPase (Figure 1; Fuglsang *et al.*, 2007). Furthermore, plasma membrane-bound H^+-ATPases are dephosphorylated upon recognition of the Avr5 elicitor of *C. fulvum* by Cf-5 tomato suspension cells (Vera-Estrella *et al.*, 1994). In addition to H^+-ATPases, also Ca^{2+}-ATPases seem to be regulated via phosphorylation. For example, in closing *Vicia* guard cells, Ca^{2+}-ATPases become phosphorylated which enhances Ca^{2+} import in the cell (Köhler and Blatt, 2002). Furthermore, elicitation of the plasma membrane of Cf-5 tomato protoplasts with the Avr5 elicitor activates a Ca^{2+}-ATPase by G-protein-dependent phosphorylation (Figure 1; Gelli *et al.*, 1997). Also K^+ channel activity seems to depend on phosphorylation. The stimulation of the K^+ outward channels and the suppression of the K^+ inward channels upon elicitation of transgenic Cf-9-expressing *N. tabacum* cells with Avr9, is completely blocked by broad-range protein kinase inhibitors (Blatt *et al.*, 1999). K^+ channels might also be nitrosylated since NO blocks outward K^+ channels in guard cells (Figure 1; Sokolovski and Blatt, 2004).

Syntaxins and other membrane-bound proteins in defence signalling

To identify plasma membrane-bound proteins in Arabidopsis that are (de)phosphorylated upon defence signalling, ^{32}P pulse-labelled suspension-cultured cells were elicited with flg22 and plasma membrane proteins were analysed by two-dimensional gel electrophoresis (Nühse *et al.*, 2003). This revealed several differentially phosphorylated proteins such as the syntaxin AtSyp122. Syntaxins are part of the SNARE complex and play a central role in exocytosis as they mediate vesicle fusion to the plasma membrane (Fasshauer, 2003). Phosphorylation of AtSyp122 is Ca^{2+}-dependent which leads to the hypothesis that a Ca^{2+} influx stimulates exocytosis of defence proteins and other compounds via syntaxins (Figure 1). In agreement with this hypothesis, the same phosphoproteomics screen revealed a second syntaxin, AtSyp132, of which the *N. benthamiana* orthologue, NbSyp132, contributes to the exocytosis of pathogenesis-related (PR) proteins into the apoplast upon Pto/AvrPto-induced defence signalling (Kalde *et al.*, 2007). Furthermore, NbSyp132 contributes to basal- and salicylate-associated defence against bacterial pathogens in plants (Kalde *et al.*, 2007). Another plasma membrane-localized syntaxin, Syp121 or PEN1, is required for resistance to powdery mildew in barley but does not play a role in Pto-mediated resistance to Pst (Figure 1; Collins *et al.*, 2003; Kalde *et al.*, 2007). The orthologue NtSyp121 is phosphorylated upon Cf-9/Avr9-activated signalling, which appeared to be specific as this syntaxin is not phosphorylated upon elicitation with flg22 (Heese *et al.*, 2005).

Recent technical advances in phosphoproteomics now enable phosphopeptide or –protein purification and their immediate analysis by mass spectrometry. A non-quantitative analysis of phosphorylated plasma membrane-bound proteins from flg22-elicited Arabidopsis cells revealed over 300 phosphorylation sites although it remains unclear to what extent these phosphorylation sites play a role during signalling cascades (Nühse *et al.*, 2004). Recently, quantitative phosphoproteome studies of flg22- or xylanase-treated Arabidopsis cells revealed several differentially phosphorylated proteins. Some of these proteins, like calcium-dependent protein kinases (CDPKs) and ATPases, have already been described to be regulated by phosphorylation, but for other proteins like auxin efflux carriers and respiratory burst oxidase protein D, phosphorylation-mediated regulation is novel (Benschop *et al.*, 2007; Nühse *et al.*, 2007). Further functional analysis of the identified phosphoproteins will reveal new insights in defence-related signalling cascades.

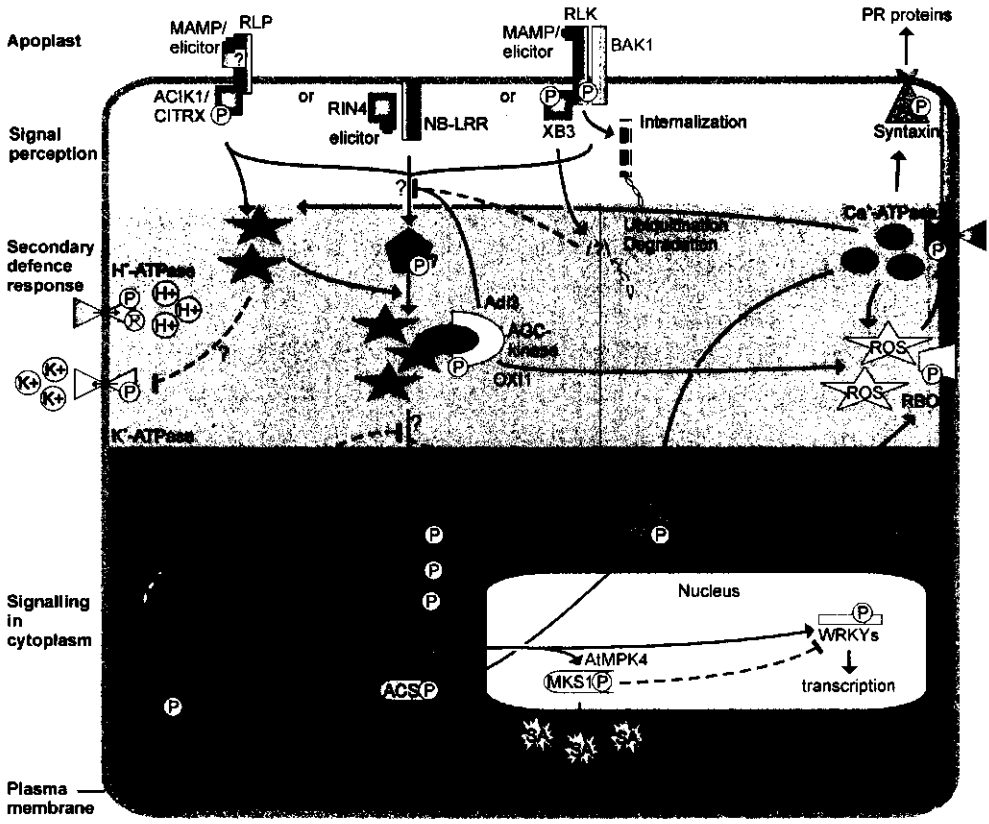

Figure 1. Defence-related signal transduction cascades that depend on post-translational modifications. Receptors mediate recognition of microbe-associated molecular patterns (MAMPs) and race-specific elicitors (elicitor), but they require additional proteins for their function. Proteins with nucleotide-binding and leucine rich repeat domains (NB-LRR) recognize their cognate elicitors intracellularly, while receptor-like proteins (RLP) and receptor-like kinases (RLK) are probably activated outside the cell. RLPs require additional proteins that bind the cytoplasmically localized part of the protein to mediate downstream signalling, while RLKs require their kinase domain to autophosphorylate and form complexes with additional proteins. Furthermore, RLKs might become ubiquitinated after which they are internalized and targeted for proteasome-mediated degradation. Signalling downstream from the receptor eventually leads to the formation of secondary messengers such as phosphatidic acid (PA), possibly via phospholipase C (PLC) phosphorylation, and nitric oxide (NO). Furthermore, the concentrations of ions such as H^+, K^+, Ca^{2+} are controlled by (de)phosphorylation of the respective ATPase while the production of ROS is stimulated upon phosphorylation of the NADPH oxidases (RBOH). The secondary messengers also mediate phosphorylation of proteins such as calcium-dependent protein kinases (CDPK), or syntaxins which might promote the release of pathogenesis-related (PR) proteins into the apoplast. The mitogen-activated protein kinase (MAPK) cascades are activated by phosphorylation of the individual components which eventually leads to the phosphorylation of WRKY transcription factors and the phosphorylation of 1-aminocyclopropane-1-carboxylic acid synthase (ACS) and MAP kinase substrate 1 (MKS1) which influences the production of ethylene (Et) and salicylic acid (SA), respectively. Also E3-ligases are activated which might result in the ubiquitination and subsequent degradation of negative regulators of the signalling cascades, thereby providing a positive feedback loop. In addition, negative feedback loops are required to prevent an uncontrolled hypersensitive response (HR). For example, MAPK (MPK)-mediated ethylene production negatively regulates the MAPK activation. The secondary messengers influence each other and fine-tune the downstream signal while proteins modified by secondary messengers might inhibit receptor-mediated signals. Eventually, a balanced signal will lead to increased (basal) resistance and possibly a HR.

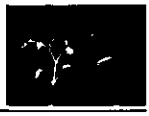

Phosphorylation states as presented in this figure represent the active state of the protein. Protein names indicated in grey might be specific for specific plant-pathogen interaction. ACIK1; Avr9/Cf-9-induced kinase 1, CITRX; Cf-9-interacting thioredoxin, RIN4; RPM1-interacting protein 4, BAK1; BRASSINOSTEROID-INSENSITIVE 1, XB3; Xa21-binding protein 3, Adi3; AvrPto-dependent Pto-interacting protein 3, PDK1; 3-phosphoinositide-dependent protein kinase-1, AGC-kinase; protein kinase A, G and C family, OXI1; oxidative signal-inducible 1.

PTMS LEADING TO THE FORMATION OF HOST SECONDARY MESSENGERS

When a microbe is recognized by the plant, defence signalling cascades are activated. So far, it is unclear how signals are transferred from the receptor to one or more downstream pathways such as the MAPK pathway. Studies using suspension-cultured cells indicate that in intact plants, secondary messengers are produced upon elicitation and they are thought to play a role in amplifying and transferring the signal downstream into the signalling cascade (Laxalt and Munnik, 2002).

NO signalling

Elicitation of tomato cells with xylanase results in the production of the secondary messenger NO (Figure 1; Laxalt *et al.*, 2007). In Arabidopsis, NO is synthesized by the NO synthase enzyme, AtNOS1 (Guo *et al.*, 2003), or results from the reduction of nitrate by nitrate reductase (NR) (Romero-Puertas *et al.*, 2004). However, other mechanisms to generate NO are also likely to exist (Neill *et al.*, 2007). To transfer a signal, the highly reactive NO molecules can modify a variety of target proteins by *S*-nitrosylation. An extensive study in Arabidopsis led to the identification of many proteins that can be modified by *S*-nitrosylation, of which some proteins like superoxide dismutases and Hsp90 have been reported in defence signalling as well (Lindermayr *et al.*, 2005).

PA signalling

Another secondary messenger is the phospholipid-derived molecule phosphatidic acid (PA) that is produced upon signal perception via the phospholipase C or D (PLC/PLD) pathway (Laxalt and Munnik, 2002; Testerink and Munnik, 2005; Bargmann and Munnik, 2006). Most elicitors reported to induce PA production stimulate PLC-mediated formation of PA via the phosphorylation of the intermediate diacylglycerol (DAG) by DAG kinase (DGK), although some elicitors also activate the PLD pathway (Van der Luit *et al.*, 2000; De Jong *et*

al., 2004; Andersson *et al.*, 2006). The PLCs might be activated by upstream kinases that have been activated as a result of receptor triggering, since an Arabidopsis PLC was reported to be phosphorylated upon flagellin elicitation (Figure 1; Nühse *et al.*, 2007). In soybean, PA generated upon wounding has been shown to activate the MAPK cascade since the addition of exogenous PA to suspension-cultured cells specifically activates a MAPK (Figure 1). The PA formation in wound-induced leaves can be blocked with PLD inhibitors (Lee *et al.*, 2001). Furthermore, PA stimulates the oxidative burst upon elicitation (De Jong *et al.*, 2004; Andersson *et al.*, 2006). In xylanase-treated tomato suspension cells, PA is produced via the PLC/DGK pathway which is activated by a xylanase-triggered NO accumulation. How NO exactly activates the PLC/DGK pathway remains unclear, although NO might act directly on PLC and/or DGK by protein *S*-nitrosylation (Figure 1). NO might also affect the PLC/DGK pathway indirectly via the MAPK signalling cascade, via altered Ca^{2+} levels or via a change in redox potential in the cell (Lee *et al.*, 2001; Laxalt *et al.*, 2007). In Arabidopsis, PA targets have been identified and include heat shock protein 90, serine/threonine kinases and phosphatases (Testerink *et al.*, 2004). Another target is the previously described phosphoinositide-dependent kinase PDK1 (Figure 1, see above) (Anthony *et al.*, 2006). PDK1 interacts with the OXI1 kinase (oxidative signal-inducible 1; also referred to as AGC2-1) and subsequently phosphorylates and activates OXI1, which is involved in oxidative burst-mediated signalling in Arabidopsis (Figure 1; Anthony *et al.*, 2004 and 2006; Rentel *et al.*, 2004). OXI1 in its turn phosphorylates the serine/threonine kinase PTI1-2, which has high sequence homology to the tomato Pti1 kinase. The signalling pathway PDK1/OXI1/PTI1-2 was shown to be specific for lipid signalling, whereas ROS and flagellin signals converge further downstream in the OXI1/PTI1-2 pathway, independently of PDK1 (Anthony *et al.*, 2006). Since the AGC kinase Adi3 is also phosphorylated by PDK1 (see above), we suggest that PDK1 functions as a spider in the web for transferring receptor-mediated PA signals to downstream signalling cascades via AGC kinases (Figure 1). To balance the signalling cascade, PA signals are attenuated by PA kinase (PAK), which converts PA into the lipid DAG pyrophosphate (DGPP) (Munnik *et al.*, 1996). However, since DGPP accumulation is associated with PA-induced signalling, DGPP itself might also function as a secondary messenger. The observation that DGPP is broken down by the DGPP phosphatase (DPP) might confirm this hypothesis (reviewed by Van Schooten *et al.*, 2006).

ROS signalling

Reactive oxygen species (ROS) are important secondary messengers responsible for the oxidative burst. Upon pathogen recognition, the plant responds with a bi-phasic production of ROS (Lamb and Dixon, 1997). ROS can be produced inside the plant cell in several organelles, however, a membrane-bound respiratory oxidative burst protein (RBOHD; an NADPH oxidase) is considered as the source of ROS upon elicitation by pathogens (Torres and Dangl, 2005). The Arabidopsis RBOHD protein is heavily phosphorylated at seven different amino acid residues and differentially phosphorylated at three residues upon elicitation with flg22 or xylanase (Benschop *et al.*, 2007; Nühse *et al.*, 2007). In accordance, another member from the RBOH family, RBOHB, is phosphorylated by calcium-dependent protein kinases (CDPKs) in potato, which causes a subsequent oxidative burst (Figure 1; Kobayashi *et al.*, 2007). Upon signal-induced phosphorylation, the activated oxidase converts O_2 into O_2^- which subsequently forms the stable component hydrogen peroxide (H_2O_2) that is removed by catalases or peroxidases when the signal is transferred further down. Besides a signalling role, H_2O_2 also has direct antimicrobial effects, cross-links cell walls and activates transcription of defence-related genes (Lamb and Dixon, 1997).

Calcium signalling

A secondary messenger that links several defence-related processes is the ubiquitous messenger calcium (Ca^{2+}) (Lecourieux *et al.*, 2006). Ca^{2+} is in- and exported to/from the cell and the vacuole by Ca^{2+}-ATPases that are regulated via phosphorylation, and stimulates the production of NO and ROS upon recognition of an avirulent pathogen (Figure 1; Delledonne, 2005). Strikingly, H_2O_2 also stimulates rapid Ca^{2+} influxes upon elicitation which reveals a role for Ca^{2+}-signalling up- and downstream of ROS (Figure 1; Lamb and Dixon, 1997). These data imply that secondary messengers produced via pathways that rely on PTMs connect several components of the defence signalling cascades, but also influence each other to balance the downstream responses.

PTMS OF HOST PROTEINS IN THE CYTOPLASM

The MAPK cascade

A major conserved signalling cascade which is activated by a large range of biotic and abiotic stress stimuli in plants, is the MAPK cascade (Figure 1; Pedley and Martin, 2005; Zhang *et al.*, 2006). MAPK cascades consist of three functionally linked protein kinases that transfer the stress signals. A stress signal causes phosphorylation and activation of the most upstream MAPK kinase kinase (MAPKKK). Subsequently, the MAPKKK phosphorylates and activates a MAPK kinase (MAPKK) which in turn does the same with a MAPK (MPK). The MAPK then phosphorylates downstream target(s) thereby transferring the signal further downstream (Figure 1). The Arabidopsis genome encodes 20 MAPKs, 10 MAPKKs and 60 putative MAPKKKs and in addition, it contains several protein phosphatases that control the cascade by dephosphorylating the MAPK cascade components (Ichimura *et al.*, 2002; Martín *et al.*, 2005). For example the AtMPK6 protein, activated upon most stress stimuli, is controlled by the phosphatases ABI1, AP2C1, MKP1 and MKP2 in Arabidopsis (Ulm *et al.*, 2002; Leung *et al.*, 2006; Lee and Ellis, 2007; Schweighofer *et al.*, 2007). The AtMPK4 protein negatively regulates defence responses upon phosphorylation, which implies that also the activation of protein phosphatases can mediate the transfer of stress-related signals (Ichimura *et al.*, 2006; Suarez-Rodriguez *et al.*, 2007). It is interesting to note that most stress stimuli mainly activate AtMPK6, -3 and -4 and their orthologues in other plant species during stress-related signalling. Therefore, stress-related signalling cascades are considered to converge in the MAPK cascades after which the signal is transferred into different downstream pathways (Pedley and Martin, 2005; Zhang *et al.*, 2006). In Cf-4 tomato, three highly homologous MAPKs, LeMPK1, -2 and -3, are activated upon Avr4-elicitation. LeMPK1 and -2 are the orthologues of AtMPK6 and LeMPK3 is the orthologue of AtMPK3. These LeMPKs appeared to have different phosphorylation specificities and a different role in defence signalling, suggesting that the signal can eventually be transferred to different substrates and possibly different downstream signalling cascades (Chapter 3). So far, only a few MAPK targets have been described. The AtMPK6 protein phosphorylates 1-aminocyclopropane-1-carboxylic acid synthase 6 and 2 (ACS6/2), which are key enzymes in ethylene biosynthesis, and WRKY transcription factors upon flg22 elicitation (Figure 1) (Asai *et al.*, 2002; Liu and Zhang, 2004; Menke *et al.*, 2005). The AtMPK4 protein phosphorylates

MAP kinase substrate 1 (MKS1), which negatively regulates salicylic acid-dependent resistance upon phosphorylation (Figure 1) (Andreasson *et al.*, 2005). Furthermore, AtMPK3 was recently found to phosphorylate the transcription factor VIP1, which is involved in regulating the expression of the PR1 pathogen-related gene (Djamei *et al.*, 2007).

CDPK-mediated signalling

CDPKs contain a calmodulin-like domain with Ca^{2+} binding sites and represent another class of kinases. In the absence of Ca^{2+}, the kinase domain of CDPKs is not phosphorylated, which points to a direct regulation by Ca^{2+} (Figure 1; Ludwig *et al.*, 2004). Tobacco NtCDPK2 was the first CDPK reported to be involved in plant defence signalling in transgenic Cf-9 tobacco upon elicitation with the Avr9 effector. NtCDPK2 is required for HR development and is activated by phosphorylation (Figure 1). Furthermore, NtCDPK2 enhances ethylene production that subsequently negatively regulates the MAPK signalling cascade (Figure 1). In addition, a tomato CDPK phosphorylates the tomato ACS2 (Tatsuki and Mori, 2001) of which the orthologue in Arabidopsis was shown to be phosphorylated by AtMPK6 (Liu and Zhang, 2004). This observation suggests that two kinase signalling cascades both leading to an ethylene-dependent cell death, can cross-talk to fine-tune the final outcome (Ludwig *et al.*, 2005). Finally, the potato CDPK, StCDPK5, phosphorylates StRBOHB thereby regulating the oxidative burst (Figure 1; Kobayashi *et al.*, 2007).

Ubiquitination in defence signalling

Over the last years, several proteins with E3 ubiquitin ligase activity that play a role in defence signalling have been reported, indicating that ubiquitination is important for resistance of plants to pathogens (Figure 1). An extensive transcriptional analysis of Cf-9 transgenic tobacco cells elicited with Avr9 revealed two genes, *ACRE189* and *ACRE276*, of which the encoded proteins possess *in vitro* E3 ligase activity and which are required for Cf-9- and Cf-4-mediated defence signalling (Durrant *et al.*, 2000; Yang *et al.*, 2006). The closest orthologue of ACRE276 in Arabidopsis, PUB17, is also required for RPM1- and RPS4-mediated resistance to *Pseudomonas syringae* pv *tomato* expressing the elicitors *AvrB* or *AvrRPS4*, respectively (Yang *et al.*, 2006). ACRE74, which encodes another tobacco E3 ligase (NtCMPG1), is also required for Cf-9/Avr9-induced signalling in addition to defence responses induced by Pto/AvrPto and the *Phytophthora infestans* elicitor Inf1 (González-

Lamothe *et al.*, 2006). Furthermore, a functional tomato E3 ligase, ATL6, is transcriptionally upregulated upon elicitation with a cell wall protein fraction from *Pythium oligandrum* (Hondo *et al.*, 2007). In addition to E3 ubiquitin ligase activity, transient-induced gene silencing (TIGS) of the ubiquitin encoding gene itself and subsequent complementation studies in powdery mildew-inoculated resistant barley, suggest a role for K48-linked polyubiquitination in defence signalling. Although K48-linked polyubiquitination normally results in proteasome-mediated protein degradation, here the polyubiquitination event but not the subsequent degradation is required for the defence response (Dong *et al.*, 2006). Finally, the Arabidopsis E1 ubiquitin-activating enzyme UBA1 is required for defence responses induced upon recognition of the AvrRpt2 effector (Goritschnig *et al.*, 2007).

Sumoylation in defence signalling

In addition to ubiquitination, also sumoylation plays a role in defence signalling, although the evidence remains scarce. So far, there are only two reports that show an increase in protein sumoylation upon exposure to abiotic stress conditions such as heat shock, H_2O_2, ethanol and the defensive compound against herbivores, canavanine (Kurepa *et al.*, 2003; Saracco *et al.*, 2007). However, overexpression of SUMO in tobacco appears to block HR development upon xylanase infiltration (Hanania *et al.*, 1999) and a SUMO E3 ligase, SIZ1, was reported to regulate salicylic acid-mediated innate immunity in Arabidopsis (Lee *et al.*, 2007). SIZ1 also appears to negatively regulate systemic-acquired resistance and the expression of PR genes. The best evidence for the importance of sumoylation in defence signalling originates from the observation that pathogen effectors interfere with the host sumoylation cascade. The *Xanthomonas campestris* effector XopD is injected into the host cell upon infection and encodes an active cysteine protease with plant-specific SUMO substrate specificity. XopD specifically desumoylates host proteins, thereby most likely interfering with the host defence signalling cascade upon infection (Hotson *et al.*, 2003). Another effector from *X. campestris*, AvrXv4, requires its protease activity to reduce the amount of SUMO-conjugated proteins in the host cell, which leads to suppression of localized cell death in inoculated plants (Roden *et al.*, 2004). The effector AvrBsT, that also possesses protease activity, requires its catalytic domain to induce cell death in *N. benthamiana* (Orth *et al.*, 2000; reviewed by Hotson and Mudgett, 2004). Additionally, some effectors seem to interact with proteins from the host sumoylation machinery. Xylanase interacts with SUMO

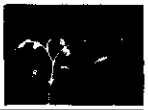

in a yeast-two-hybrid system (Hanania *et al.*, 1999) and the replication protein RepAC1 from geminiviruses interacts with the SUMO E3 ligase SCE1 from *N. benthamiana* (Castillo *et al.*, 2004). However, the biological relevance of these observations still remains to be elucidated. Still, if sumoylation would not play any role in defence signalling, the various effectors mentioned above would not enhance virulence for the pathogen and they would probably have been eliminated for the population during evolution to avoid recognition by resistant plants.

EFFECTORS OF PATHOGENS MODIFY PTMS IN DEFENCE SIGNALLING

It has become apparent from the information given above that plants depend on rapid PTMs in signalling cascades to defend themselves against intruding pathogens. An active defence response is triggered by the recognition of elicitors that are secreted by the invading pathogen. Therefore, the intriguing question remains why pathogens still secrete elicitors that induce avirulence. More and more evidence is accumulating that these elicitors act as effectors that specifically interfere with the host defence mechanisms to increase the virulence of pathogens in the absence of the cognate R protein (Alfano and Collmer, 2004; Mudgett, 2005; Abramovitch *et al.*, 2006a; He *et al.*, 2007). To reach this goal, effectors regularly modify the PTM status of host proteins, thereby targeting primary and/or secondary defence responses. Here, we describe the virulence function of some effectors of *P. syringae*.

The RIN4 protein is targeted by two effectors from Pst, AvrRpm1 and AvrB, which indirectly induce RIN4 phosphorylation, thereby enhancing the negative regulation of the primary defence response by RIN4 which leads to increased host susceptibility and pathogen virulence (Mackey *et al.*, 2002; Kim *et al.*, 2005b). The effector HopAI1 dephosphorylates AtMPK6 and AtMPK3 in the MAPK cascade through phosphothreonine lyase activity, which is an alternative cleavage of the phosphate from the threonine residue (Zhang *et al.*, 2007). Similarly, the HopPtoD2 effector functions as a protein tyrosine phosphatase downstream of the host MAPKKs (Espinosa *et al.*, 2003). Since MAPK cascades are activated in most stress-related responses, the position of interference is strategic since the effectors might interfere in many signalling cascades. Even more intriguing is the abuse of the MAPK cascade by *Agrobacterium* of which the T-DNA hitch-hikes with a phosphorylated AtMPK3 substrate,

the transcription factor VIP1, into the nucleus thereby circumventing the defence response (Djamei *et al.*, 2007). Finally, it was shown that AvrPto of *P. syringae* inhibits plant immunity triggered by diverse MAMPs. The bacterial effector suppresses early defence gene transcription and intercepts MAPK signalling upstream of MAPKKK at the plasma membrane (He *et al.*, 2006). Recently, it has been shown that AvrPto binds the MAMP-triggered receptor-kinases FLS2 and EFR, which inhibits kinase activity of these receptors (Xiang *et al.*, 2008). As a result of this, MAPK cascade activation is inhibited and MAMP-induced immune responses are suppressed. Effectors do not only modify protein phosphorylation but can also modify protein ubiquitination. The effector AvrPtoB, of which the N-terminal part is recognized by the Fen kinase, has a C-terminal E3 ubiquitin ligase domain. AvrPtoB ubiquitinates the Fen kinase and subsequently targets it for degradation, thereby abolishing the recognition of its own N-terminal region (Abramovitch *et al.*, 2006b; Janjusevic *et al.*, 2006; Rosebrock *et al.*, 2007). Probably, AvrPtoB will not remain the only effector that mediates ubiquitination of host proteins, since a screen of the available bacterial genomes revealed several new putative effectors that are predicted to mimic subunits of the ubiquitination pathway (Angot *et al.*, 2007).

CONCLUDING REMARKS

Rapid PTMs of proteins in defence signalling are essential tools for plants to respond swiftly to pathogen invasion. In this review, we gave an overview of PTMs that modify components essential for defence signalling at the site of signal perception, during secondary messenger production and during signalling in the cytoplasm. PTMs regulate protein localization and activity and provide complex mechanisms to balance responses in the cell without the prerequisite of protein synthesis. Since recent technological developments allow high-throughput analysis of modified proteins, we expect that many previously unidentified components of defence signalling cascades, that are not transcriptionally regulated, will be revealed in the coming years.

REFERENCES

Abramovitch RB, Anderson JC, Martin GB (2006a) Bacterial elicitation and evasion of plant innate immunity. Nat Rev Mol Cell Biol 7: 601-611.

Abramovitch RB, Janjusevic R, Stebbins CE, Martin GB (2006b) Type III effector AvrPtoB requires intrinsic E3 ubiquitin ligase activity to suppress plant cell death and immunity. Proc Natl Acad Sci USA 103: 2851-2856.

Ade J, DeYoung BJ, Golstein C, Innes RW (2007) Indirect activation of a plant nucleotide binding site-leucine-rich repeat protein by a bacterial protease. Proc Natl Acad Sci USA 104: 2531-2536.

Alfano JR, Collmer A (2004) Type III secretion system effector proteins: Double agents in bacterial disease and plant defense. Annu Rev Phytopathol 42: 385-414.

Andersson MX, Kourtchenko O, Dangl JL, Mackey D, Ellerström M (2006) Phospholipase-dependent signalling during the AvrRpm1- and AvrRpt2-induced disease resistance responses in *Arabidopsis thaliana*. Plant J 47: 947-959.

Andreasson E, Jenkins T, Brodersen P, Thorgrimsen S, Petersen NHT, Zhu S, Qiu J-L, Micheelsen P, Rocher A, Petersen M, Newman M-A, Bjorn Nielsen H, Hirt H, Somssich I, Mattsson O, Mundy J (2005) The MAP kinase substrate MKS1 is a regulator of plant defense responses. EMBO J 24: 2579-2589.

Andriotis VME, Rathjen JP (2006) The Pto kinase of tomato, which regulates plant immunity, is repressed by its myristoylated N terminus. J Biol Chem 281: 26578-26586.

Angot A, Vergunst A, Genin S, Peeters N (2007) Exploitation of eukaryotic ubiquitin signaling pathways by effectors translocated by bacterial type III and type IV secretion systems. PLoS Pathog 3: 1-13.

Anthony RG, Henriques R, Helfer A, Meszaros T, Rios G, Testerink C, Munnik T, Deak M, Koncz C, Bögre L (2004) A protein kinase target of a PDK1 signalling pathway is involved in root hair growth in Arabidopsis. EMBO J 23: 572-581.

Anthony RG, Khan S, Costa J, Pais MS, Bögre L (2006) The Arabidopsis protein kinase PTI1-2 is activated by convergent phosphatidic acid and oxidative stress signaling pathways downstream of PDK1 and OXI1. J Biol Chem 281: 37536-37546.

Asai T, Tena G, Plotnikova J, Willmann MR, Chiu WL, Gomez Gomez L, Boller T, Ausubel FM, Sheen J (2002) MAP kinase signalling cascade in Arabidopsis innate immunity. Nature 415: 977-983.

Balmuth A, Rathjen JP (2007) Genetic and molecular requirements for function of the Pto/Prf effector recognition complex in tomato and *Nicotiana benthamiana*. Plant J 51: 978-990.

Bargmann BOR, Munnik T (2006) The role of phospholipase D in plant stress responses. Curr Opin Plant Biol 9: 515-522.

Baulcombe DC (1999) Fast forward genetics based on virus-induced gene silencing. Curr Opin Plant Biol 2: 109-113.

Belkhadir Y, Nimchuk Z, Hubert DA, Mackey D, Dangl JL (2004a) Arabidopsis RIN4 negatively regulates disease resistance mediated by RPS2 and RPM1 downstream or independent of the NDR1 signal modulator and is not required for the virulence functions of bacterial type III effectors AvrRpt2 or AvrRpm1. Plant Cell 16: 2822-2835.

Belkhadir Y, Subramaniam R, Dangl JL (2004b) Plant disease resistance protein signaling: NBS-LRR proteins and their partners. Curr Opin Plant Biol 7: 391-399.

Benschop JJ, Mohammed S, O'Flaherty M, Heck AJR, Slijper M, Menke FLH (2007) Quantitative phosphoproteomics of early elicitor signalling in Arabidopsis. Mol Cell Proteomics 6: 1198-1214.

Bent A, Mackey D (2007) Elicitors, effectors, and *R* genes: The new paradigm and lifetime supply of questions. Annu Rev Phytopathol 45: 399-436.

Blatt MR, Grabov A, Brearley J, Hammond-Kosack K, Jones JDG (1999) K+ channels of Cf-9 transgenic tobacco guard cells as targets for *Cladosporium fulvum* Avr9 elicitor-dependent signal transduction. Plant J 19: 453-462.

Burch-Smith TM, Anderson JC, Martin GB, Dinesh-Kumar SP (2004) Applications and advantages of virus-induced gene silencing for gene function studies in plants. Plant J 39: 734-746.

Castillo AG, Kong LJ, Hanley-Bowdoin L, Bejarano ER (2004) Interaction between a geminivirus replication protein and the plant sumoylation system. J Virol 78: 2758-2769.

Chinchilla D, Zipfel C, Robatzek S, Kemmerling B, Nürnberger T, Jones JDG, Felix G, Boller T (2007) A flagellin-induced complex of the receptor FLS2 and BAK1 initiates plant defence. Nature 448: 497-500.

Chisholm ST, Coaker G, Day B, Staskawicz BJ (2006) Host-microbe interactions: Shaping the evolution of the plant immune response. Cell 124: 803-814.

Chosed R, Mukherjee S, Lois LM, Orth K (2006) Evolution of a signalling system that incorporates both redundancy and diversity: Arabidopsis SUMOylation. Biochem J 398: 521-529.

Collins NC, Thordal-Christensen H, Lipka V, Bau S, Kombrink E, Qiu JL, Hückelhoven R, Steins M, Freialdenhoven A, Somerville SC, Schulze-Lefert P (2003) SNARE-protein-mediated disease resistance at the plant cell wall. Nature 425: 973-977.

Coppinger P, Repetti PP, Day B, Dahlbeck D, Mehlert A, Staskawicz BJ (2004) Overexpression of the plasma membrane-localized NDR1 protein results in enhanced bacterial disease resistance in *Arabidopsis thaliana*. Plant J 40: 225-237.

Day B, Dahlbeck D, Huang J, Chisholm ST, Li D, Staskawicz BJ (2005) Molecular basis for the RIN4 negative regulation of RPS2 disease resistance. Plant Cell 17: 1292-1305.

Day B, Dahlbeck D, Staskawicz BJ (2006) NDR1 interaction with RIN4 mediates the differential activation of multiple disease resistance pathways in Arabidopsis. Plant Cell 18: 2782-2791.

De Jong CF, Laxalt AM, Bargmann BOR, De Wit PJGM, Joosten MHAJ, Munnik T (2004) Phosphatidic acid accumulation is an early response in the Cf-4/Avr4 interaction. Plant J 39: 1-12.

De la Fuente van Bentem S, Hirt H (2007) Using phosphoproteomics to reveal signalling dynamics in plants. Trends Plant Sci 12: 404-411.

De Wit PJGM (2007) How plants recognize pathogens and defend themselves. Cell Mol Life Sci 64: 2726-2732.

Delledonne M (2005) NO news is good news for plants. Curr Opin Plant Biol 8: 390-396.

Devarenne TP, Ekengren SK, Pedley KF, Martin GB (2006) Adi3 is a Pdk1-interacting AGC kinase that negatively regulates plant cell death. EMBO J 25: 255-265.

Dietrich A, Mayer JE, Hahlbrock K (1990) Fungal elicitor triggers rapid, transient, and specific protein phosphorylation in parsley cell suspension cultures. J Biol Chem 265: 6360-6368.

Djamei A, Pitzschke A, Nakagami H, Rajh I, Hirt H (2007) Trojan horse strategy in Agrobacterium transformation: abusing MAPK defense signaling. Science 318: 453-456.

Dong W, Nowara D, Schweizer P (2006) Protein polyubiquitination plays a role in basal host resistance of barley. Plant Cell 18: 3321-3331.

Durrant WE, Rowland O, Piedras P, Hammond Kosack KE, Jones JDG (2000) cDNA-AFLP reveals a striking overlap in race-specific resistance and wound response gene expression profiles. Plant Cell 12: 963-977.

Espinosa A, Guo M, Tam VC, Fu ZQ, Alfano JR (2003) The *Pseudomonas syringae* type III-secreted protein HopPtoD2 possesses protein tyrosine phosphatase activity and suppresses programmed cell death in plants. Mol Microbiol 49: 377-387.

Eulgem T (2005) Regulation of the Arabidopsis defense transcriptome. Trends Plant Sci 10: 71-78.

Farazi TA, Waksman G, Gordon JI (2001) The biology and enzymology of protein *N*-myristoylation. J Biol Chem 276: 39501-39504.

Fasshauer D (2003) Structural insights into the SNARE mechanism. Biochim Biophys Acta 1641: 87-97.

Flor HH (1942) Inheritance of pathogenicity in *Melampsora lini*. Phytopathology 32: 653-669.

Fuglsang AT, Guo Y, Cuin TA, Qiu Q, Song C, Kristiansen KA, Bych K, Schulz A, Shabala S, Schumaker KS, Palmgren MG, Zhu J-K (2007) *Arabidopsis* protein kinase PKS5 inhibits the plasma membrane H^+-ATPase by preventing interaction with 14-3-3 protein. Plant Cell 19: 1617-1634.

Gelli A, Higgins VJ, Blumwald E (1997) Activation of plant plasma membrane Ca^{2+}-permeable channels by race-specific fungal elicitors. Plant Physiol 113: 269-279.

Glazebrook J, Rogers EE, Ausubel FM (1997) Use of Arabidopsis for genetic dissection of plant defense responses. Annu Rev Genet 31: 547-569.

Gómez-Gómez L, Bauer Z, Boller T (2001) Both the extracellular leucine-rich repeat domain and the kinase activity of FSL2 are required for flagellin binding and signaling in Arabidopsis. Plant Cell 13: 1155-1163.

Gómez-Gómez L, Boller T (2000) FLS2: an LRR receptor-like kinase involved in the perception of the bacterial elicitor flagellin in Arabidopsis. Mol Cell 5: 1003-1011.

González-Lamothe R, Tsitsigiannis DI, Ludwig AA, Panicot M, Shirasu K, Jones JDG (2006) The U-box protein CMPG1 is required for efficient activation of defense mechanisms triggered by multiple resistance genes in tobacco and tomato. Plant Cell 18: 1067-1083.

Goritschnig S, Zhang Y, Li X (2007) The ubiquitin pathway is required for innate immunity in Arabidopsis. Plant J 49: 540-551.

Guo FQ, Okamoto M, Crawford NM (2003) Identification of a plant nitric oxide synthase gene involved in hormonal signaling. Science 302: 100-103.

Haglund K, Di Fiore PP, Dikic I (2003) Distinct monoubiquitin signals in receptor endocytosis. Trends Biochem Sci 28: 598-604.

Hanania U, Furman-Matarasso N, Ron M, Avni A (1999) Isolation of a novel SUMO protein from tomato that suppresses EIX-induced cell death. Plant J 19: 533-541.

He P, Shan L, Lin NC, Martin GB, Kemmerling B, Nürnberger T, Sheen J (2006) Specific bacterial suppressors of MAMP signaling upstream of MAPKKK in Arabidopsis innate immunity. Cell 125: 563-575.

He P, Shan L, Sheen J (2007) Elicitation and suppression of microbe-associated molecular pattern-triggered immunity in plant-microbe interactions. Cell Microbiol 9: 1385-1396.

Heese A, Hann DR, Gimenez-Ibanez S, Jones AME, He K, Li J, Schroeder JI, Peck SC, Rathjen JP (2007) The receptor-like kinase SERK3/BAK1 is a central regulator of innate immunity in plants. PNAS 104: 12217-12222.

Heese A, Ludwig AA, Jones JDG (2005) Rapid phosphorylation of a syntaxin during the Avr9/Cf-9-race-specific signaling pathway. Plant Physiol 138: 2406-2416.

Hondo D, Hase S, Kanayama Y, Yoshikawa N, Takenaka S, Takahashi H (2007) The LeATL6-associated ubiquitin/proteasome system may contribute to fungal elicitor-activated defense response via the jasmonic acid-dependent signaling pathway in tomato. Mol Plant-Microbe Interact 20: 72-81.

Hotson A, Chosed R, Shu H, Orth K, Mudgett MB (2003) Xanthomonas type III effector XopD targets SUMO-conjugated proteins in planta. Mol Microbiol 50: 377-389.

Hotson A, Mudgett MB (2004) Cysteine proteases in phytopathogenic bacteria: identification of plant targets and activation of innate immunity. Curr Opin Plant Biol 7: 384-390.

Ichimura K, Casais C, Peck SC, Shinozaki K, Shirasu K (2006) MEKK1 is required for MPK4 activation and regulates tissue-specific and temperature-dependent cell death in Arabidopsis. J Biol Chem 281: 36969-36976.

Ichimura K, Shinozaki K, Tena G, Sheen J, Henry Y, Champion A, Kreis M, Zhang S, Hirt H (2002) Mitogen-activated protein kinase cascades in plants: a new nomenclature. Trends Plant Sci 7: 301-308.

Janjusevic R, Abramovitch RB, Martin GB, Stebbins CE (2006) A bacterial inhibitor of host programmed cell death defenses is an E3 ubiquitin ligase. Science 311: 222-226.

Jensen ON (2004) Modification-specific proteomics: characterization of post-translational modifications by mass spectrometry. Curr Opin Chem Biol 8: 33-41.

Johnson ES (2004) Protein modification by SUMO. Annu Rev Biochem 73: 355-382.

Jones JDG, Dangl JL (2006) The plant immune system. Nature 444: 323-329.

Kaku H, Nishizawa Y, Ishii-Minami N, Akimoto-Tomiyama C, Dohmae N, Takio K, Minami E, Shibuya N (2006) Plant cells recognize chitin fragments for defense signaling through a plasma membrane receptor. Proc Natl Acad Sci U S A 103: 11086-11091.

Kalde M, Nühse TS, Findlay K, Peck SC (2007) The syntaxin SYP132 contributes to plant resistance against bacteria and secretion of pathogenesis-related protein 1. Proc Natl Acad Sci USA 104: 11850-11855.

Karlova R, De Vries SC (2006) Advances in understanding brassinosteroid signaling. Sci. STKE 2006: pe36.

Kawasaki T, Nam J, Boyes DC, Holt III BF, Hubert DA, Wiig A, Dangl JL (2005) A duplicated pair of Arabidopsis RING-finger E3 ligases contribute to the RPM1- and RPS2-mediated hypersensitive response. Plant J 44: 258-270.

Kerscher O, Felberbaum R, Hochstrasser M (2006) Modification of proteins by ubiquitin and ubiquitin-like proteins. Annu Rev Cell Dev Biol 22: 159-180.

Kersten B, Agrawal GK, Iwahashi H, Rakwal R (2006) Plant phosphoproteomics: A long road ahead. Proteomics 6: 5517-5528.

Kim HS, Desveaux D, Singer AU, Patel P, Sondek J, Dangl JL (2005a) The *Pseudomonas syringae* effector AvrRpt2 cleaves its C-terminally acylated target, RIN4, from Arabidopsis membranes to block RPM1 activation. Proc Natl Acad Sci USA 102: 6496-6501.

Kim MG, da Cunha L, McFall AJ, Belkhadir Y, DebRoy S, Dangl JL, Mackey D (2005b) Two *Pseudomonas syringae* type III effectors inhibit RIN4-regulated basal defense in Arabidopsis. Cell 121: 749-759.

Kim YJ, Lin N-C, Martin GB (2002) Two distinct Pseudomonas effector proteins interact with the Pto kinase and activate plant immunity. Cell 109: 589-598.

Kobayashi M, Ohura I, Kawakita K, Yokota N, Fujiwara M, Shimamoto K, Doke N, Yoshioka H (2007) Calcium-dependent protein kinases regulate the production of reactive oxygen species by potato NADPH oxidase. Plant Cell 19: 1065-1080.

Köhler B, Blatt MR (2002) Protein phosphorylation activates the guard cell Ca^{2+} channel and is a prerequisite for gating by abscisic acid. Plant J 32: 185-194.

Kurepa J, Walker JM, Smalle J, Gosink MM, Davis SJ, Durham TL, Sung DY, Vierstra RD (2003) The small ubiquitin-like modifier (SUMO) protein modification system in Arabidopsis. Accumulation of SUMO1 and -2 conjugates is increased by stress. J Biol Chem 278: 6862-6872.

Lamb C, Dixon RA (1997) The oxidative burst in plant disease resistance. Annu Rev Plant Biol 48: 251-275.

Laxalt AM, Munnik T (2002) Phospholipid signalling in plant defence. Curr Opin Plant Biol 5: 332-338.

Laxalt AM, Raho N, Ten Have A, Lamattina L (2007) Nitric oxide is critical for inducing phosphatidic acid accumulation in xylanase-elicited tomato cells. J Biol Chem 282: 21160-21168.

Lecourieux D, Ranjeva R, Pugin A (2006) Calcium in plant defence-signalling pathways. New Phytol 171: 249-269.

Lee J, Nam J, Park HC, Na G, Miura K, Jin JB, Yoo CY, Baek D, Kim DH, Jeong JC, Kim D, Lee SY, Salt DE, Mengiste T, Gong Q, Ma S, Bohnert HJ, Kwak S-S, Bressan RA, Hasegawa PM, Yun D-J (2007) Salicylic acid-mediated innate immunity in Arabidopsis is regulated by SIZ1 SUMO E3 ligase. Plant J 49: 79-90.

Lee JS, Ellis BE (2007) Arabidopsis MAPK phosphatase MKP2 positively regulates oxidative stress tolerance and inactivates the MPK3 and MPK6 mitogen-activated protein kinases. J Biol Chem 282: 25020-25029.

Lee S, Hirt H, Lee Y (2001) Phosphatidic acid activates a wound-activated MAPK in *Glycine max*. Plant J 26: 479-486.

Leung J, Orfanidi S, Chefdor F, Mészáros T, Bolte S, Mizoguchi T, Shinozaki K, Giraudat J, Bögre L (2006) Antagonistic interaction between MAP kinase and protein phosphatase 2C in stress recovery. Plant Sci 171: 596-606.

Ligterink W, Kroj T, Zur Nieden U, Hirt H, Scheel D (1997) Receptor-mediated activation of a MAP Kinase in pathogen defense of plants. Science 276: 2054-2057.

Lindermayr C, Saalbach G, Bahnweg G, Durner J (2006) Differential inhibition of *Arabidopsis* methionine adenosyltransferases by protein S-nitrosylation. J Biol Chem 281: 4285-4291.

Lindermayr C, Saalbach G, Durner J (2005) Proteomic identification of *S*-nitrosylated proteins in Arabidopsis. Plant Physiol 137: 921-930.

Liu GZ, Pi LY, Walker JC, Ronald PC, Song WY (2002) Biochemical characterization of the kinase domain of the rice disease resistance receptor-like kinase XA21. J Biol Chem 277: 20264-20269.

Liu Y, Zhang S (2004) Phosphorylation of 1-aminocyclopropane-1-carboxylic acid synthase by MPK6, a stress-responsive mitogen-activated protein kinase, induces ethylene biosynthesis in Arabidopsis. Plant Cell 16: 3386-3399.

Loh Y-T, Martin GB (1995) The *Pto* bacterial resistance gene and the *Fen* insecticide sensitivity gene encode functional protein kinases with serine/threonine specificity. Plant Physiol 108: 1735-1739.

Ludwig AA, Romeis T, Jones JDG (2004) CDPK-mediated signalling pathways: specificity and cross-talk. J Exp Bot 55: 181-188.

Ludwig AA, Saitoh H, Felix G, Freymark G, Miersch O, Wasternack C, Boller T, Jones JDG, Romeis T (2005) Ethylene-mediated cross-talk between calcium-dependent protein kinase and MAPK signaling controls stress responses in plants. Proc Natl Acad Sci USA 102: 10736-10741.

Mackey D, Holt III BF, Wiig A, Dangl JL (2002) RIN4 interacts with *Pseudomonas syringae* type III effector molecules and is required for RPM1-mediated resistance in *Arabidopsis*. Cell 108: 743-754.

Maeda Y, Ashida H, Kinoshita T, Minoru F (2006) CHO glycosylation mutants: GPI anchor, Methods in Enzymology, Vol 416. Academic Press, pp 182-205

Martin GB, Bogdanove AJ, Sessa G (2003) Understanding the functions of plant disease resistance proteins. Annu Rev Plant Biol 54: 23-61.

Martin GB, Brommonschenkel SH, Chunwongse J, Frary A, Ganal MW, Spivey R, Wu T, Earle ED, Tanksley SD (1993) Map-based cloning of a protein kinase gene conferring disease resistance in tomato. Science 262: 1432-1436.

Martín H, Flández M, Nombela C, Molina M (2005) Protein phosphatases in MAPK signalling: We keep learning from yeast. Mol Microbiol 58: 6-16.

Menke FLH, Kang HG, Chen Z, Jeong MP, Kumar D, Klessig DF (2005) Tobacco transcription factor WRKY1 is phosphorylated by the MAP kinase SIPK and mediates HR-like cell death in tobacco. Mol Plant-Microbe Interact 18: 1027-1034.

Miura K, Jin JB, Hasegawa PM (2007) Sumoylation, a post-translational regulatory process in plants. Curr Opin Plant Biol 10: 1-8.

Mucyn TS, Clemente A, Andriotis VME, Balmuth AL, Oldroyd GED, Staskawicz BJ, Rathjen JP (2006) The tomato NB-ARC-LRR protein Prf interacts with Pto kinase *in vivo* to regulate specific plant immunity. Plant Cell 18: 2792-2806.

Mudgett MB (2005) New insights to the function of phytopathogenic bacterial type III effectors in plants. Annu Rev Plant Biol 56: 509-531.

Munnik T, De Vrije T, Irvine RF, Musgrave A (1996) Identification of diacylglycerol pyrophosphate as a novel metabolic product of phosphatidic acid during G-protein activation in plants. J Biol Chem 271: 15708-15715.

Neill S, Bright J, Desikan R, Hancock J, Harrison J, Wilson I (2007) Nitric oxide evolution and perception. J Exp Bot doi:10.1093

Nekrasov V, Ludwig AA, Jones JDG (2006) CITRX thioredoxin is a putative adaptor protein connecting Cf-9 and the ACIK1 protein kinase during the Cf-9/Avr9- induced defence response. FEBS Lett 580: 4236-4241.

Nimchuk Z, Eulgem T, Holt III BF, Dangl JL (2003) Recognition and response in the plant immune system. Annu Rev Genet 37: 579-609.

Nirmala J, Brueggeman R, Maier C, Clay C, Rostoks N, Kannangara CG, von Wettstein D, Steffenson BJ, Kleinhofs A (2006) Subcellular localization and functions of the barley stem rust resistance receptor-like serine/threonine-specific protein kinase Rpg1. Proc Natl Acad Sci USA 103: 7518-7523.

Nirmala J, Dahl S, Steffenson BJ, Kannangara CG, von Wettstein D, Chen X, Kleinhofs A (2007) Proteolysis of the barley receptor-like protein kinase RPG1 by a proteasome pathway is correlated with Rpg1-mediated stem rust resistance. Proc Natl Acad Sci USA 104: 10276-10281.

Novatchkova M, Budhiraja R, Coupland G, Eisenhaber F, Bachmair A (2004) SUMO conjugation in plants. Planta 220: 1-8.

Nühse TS, Boller T, Peck SC (2003) A plasma membrane syntaxin is phosphorylated in response to the bacterial elicitor flagellin. J Biol Chem 278: 45248-45254.

Nühse TS, Bottrill AR, Jones AME, Peck SC (2007) Quantitative phosphoproteomic analysis of plasma membrane proteins reveals regulatory mechanisms of plant innate immune responses. Plant J 51: 931-940.

Nühse TS, Stensballe A, Jensen ON, Peck SC (2004) Phosphoproteomics of the Arabidopsis plasma membrane and a new phosphorylation site database. Plant Cell 16: 2394-2405.

Nürnberger T, Brunner F, Kemmerling B, Piater L (2004) Innate immunity in plants and animals: striking similarities and obvious differences. Immunol Rev 198: 249-266.

Nürnberger T, Kemmerling B (2006) Receptor protein kinases - pattern recognition receptors in plant immunity. Trends Plant Sci 11: 519-522.

Nürnberger T, Scheel D (2001) Signal transmission in the plant immune response. Trends Plant Sci 6: 372-379.

Orth K, Xu Z, Mudgett MB, Bao ZQ, Palmer LE, Bliska JB, Mangel WF, Staskawicz BJ, Dixon JE (2000) Disruption of signaling by *Yersinia* effector YopJ, a ubiquitin-like protein protease. Science 290: 1594-1597.

Palmgren MG (2001) Plant plasme membrane H+-ATPases: powerhouses for nutrient uptake. Annu rev plant physiol plant mol biol 52: 817-845.

Peck SC (2003) Early phosphorylation events in biotic stress. Curr Opin Plant Biol 6: 334-338.

Peck SC (2006) Phosphoproteomics in Arabidopsis: Moving from empirical to predictive science. J Exp Bot 57: 1523-1527.

Pedley KF, Martin GB (2003) Molecular basis of Pto-mediated resistance to bacterial speck disease in tomato. Annu Rev Phytopathol 41: 215-243.

Pedley KF, Martin GB (2005) Role of mitogen-activated protein kinases in plant immunity. Curr Opin Plant Biol 8: 541-547.

Piedras P, Rivas S, Droge S, Hillmer S, Jones JD (2000) Functional, c-myc-tagged Cf-9 resistance gene products are plasma-membrane localized and glycosylated. Plant J 21: 529-536.

Rathjen JP, Chang JH, Staskawicz BJ, Michelmore RW (1999) Constitutively active Pto induces a Prf-dependent hypersensitive response in the absence of avrPto. EMBO J 18: 3232-3240.

Reinders J, Sickmann A (2005) State-of-the-art in phosphoproteomics. Proteomics 5: 4052-4061.

Rentel MC, Lecourieux D, Ouaked F, Usher SL, Petersen L, Okamoto H, Knight H, Peck SC, Grierson CS, Hirt H, Knight MR (2004) OXI1 kinase is necessary for oxidative burst-mediated signalling in Arabidopsis. Nature 427: 858-861.

Rivas S, Rougon-Cardoso A, Smoker M, Schauser L, Yoshioka H, Jones JD (2004) CITRX thioredoxin interacts with the tomato Cf-9 resistance protein and negatively regulates defence. EMBO J 23: 2156-2165.

Rivas S, Thomas CM (2005) Molecular interactions between tomato and the leaf mold pathogen *Cladosporium fulvum*. Annu Rev Phytopathol 43: 395-436.

Robatzek S, Chinchilla D, Boller T (2006) Ligand-induced endocytosis of the pattern recognition receptor FLS2 in *Arabidopsis*. Genes Dev. 20: 537-542.

Roden J, Eardley L, Hotson A, Cao Y, Mudgett MB (2004) Characterization of the Xanthomonas AvrXv4 effector, a SUMO protease translocated into plant cells. Mol Plant-Microbe Interact 17: 633-643.

Romero-Puertas MC, Perazzolli M, Zago ED, Delledonne M (2004) Nitric oxide signalling functions in plant-pathogen interactions. Cell Microbiol 6: 795-803.

Ron M, Avni A (2004) The receptor for the fungal elicitor ethylene-inducing xylanase is a member of a resistance-like gene family in tomato. Plant Cell 16: 1604-1615.

Rosebrock TR, Zeng L, Brady JJ, Abramovitch RB, Xiao F, Martin GB (2007) A bacterial E3 ubiquitin ligase targets a host protein kinase to disrupt plant immunity. Nature 448: 370-374.

Rowland O, Ludwig AA, Merrick CJ, Baillieul F, Tracy FE, Durrant WE, Fritz-Laylin L, Nekrasov V, Sjolander K, Yoshioka H, Jones JDG (2005) Functional analysis of Avr9/Cf-9 rapidly elicited genes identifies a protein kinase, ACIK1, that is essential for full Cf-9-dependent disease resistance in tomato. Plant Cell 17: 295-310.

Saint-Jore-Dupas C, Faye L, Gomord V (2007) From planta to pharma with glycosylation in the toolbox. Trends Biotechnol 25: 317-323.

Salmeron JM, Barker SJ, Carland FM, Mehta AY, Staskawicz BJ (1994) Tomato mutants altered in bacterial disease resistance provide evidence for a new locus controlling pathogen recognition. Plant Cell 6: 511-520.

Salmeron JM, Oldroyd GED, Rommens CMT, Scofield SR, Kim H-S, Lavelle DT, Dahlbeck D, Staskawicz BJ (1996) Tomato Prf is a member of the leucine-rich repeat class of plant disease resistance genes and lies embedded within the Pto kinase gene cluster. Cell 86: 123-133.

Saracco SA, Miller MJ, Kurepa J, Vierstra RD (2007) Genetic analysis of SUMOylation in Arabidopsis: conjugation of SUMO1 and SUMO2 to nuclear proteins is essential. Plant Physiol 145: 119-134.

Schweighofer A, Kazanaviciute V, Scheikl E, Teige M, Doczi R, Hirt H, Schwanninger M, Kant M, Schuurink R, Mauch F, Buchala A, Cardinale F, Meskiene I (2007) The PP2C-type phosphatase AP2C1, which negatively regulates MPK4 and MPK6, modulates innate immunity, jasmonic acid, and ethylene levels in Arabidopsis. Plant Cell 19: 2213-2224.

Sessa G, D'Ascenzo M, Martin GB (2000a) The major site of the pti1 kinase phosphorylated by the pto kinase is located in the activation domain and is required for pto-pti1 physical interaction. Eur J Biochem 267: 171-178.

Sessa G, D'Ascenzo M, Martin GB (2000b) Thr38 and Ser198 are Pto autophosphorylation sites required for the AvrPto-Pto-mediated hypersensitive response. EMBO J 19: 2257-2269.

Shan L, He P, Sheen J (2007) Intercepting host MAPK signaling cascades by bacterial type III effectors. Cell Host Microbe 1: 167-174.

Shao F, Golstein C, Ade J, Stoutemyer M, Dixon JE, Innes RW (2003) Cleavage of Arabidopsis PBS1 by a bacterial type III effector. Science 301: 1230-1233.

Sickmann A, Meyer HE (2001) Phosphoamino acid analysis. Proteomics 1: 200-206.

Smotrys JE, Linder ME (2004) Palmitoylation of intracellular signaling proteins: regulation and function. Annu Rev Biochem 73: 559-587.

Sokolovski S, Blatt MR (2004) Nitric oxide block of outward-rectifying K+ channels indicates direct control by protein nitrosylation in guard cells. Plant Physiol 136: 4275-4284.

Song WY, Wang GL, Chen LL, Kim HS, Pi LY, Holsten T, Gardner J, Wang B, Zhai WX, Zhu LH, Fauquet C, Ronald P (1995) A receptor kinase-like protein encoded by the rice disease resistance gene, *Xa21*. Science 270: 1804-1806.

Suarez-Rodriguez MC, Adams-Phillips L, Liu Y, Wang H, Su SH, Jester PJ, Zhang S, Bent AF, Krysan PJ (2007) MEKK1 is required for flg22-induced MPK4 activation in Arabidopsis plants. Plant Physiol 143: 661-669.

Swiderski MR, Innes RW (2001) The Arabidopsis PBS1 resistance gene encodes a member of a novel protein kinase subfamily. Plant J 26: 101-112.

Takemoto D, Jones DA (2005) Membrane release and destabilization of Arabidopsis RIN4 following cleavage by *Pseudomonas syringae* AvrRpt2. Mol Plant-Microbe Interact 18: 1258-1268.

Takken FLW, Tameling WI (2007) Resistance proteins: scouts of the plant innate immune system. Eur J Plant Pathol: DOI 10.1007/s10658-10007-19187-10658

Tang X, Frederick RD, Zhou J, Halterman DA, Jia Y, Martin GB (1996) Initiation of plant disease resistance by physical interaction of AvrPto and Pto kinase. Science 274: 2060-2063.

Tatsuki M, Mori H (2001) Phosphorylation of tomato 1-aminocyclopropane-1-carboxylic acid synthase, LE-ACS2, at the C-terminal region. J Biol Chem 276: 28051-28057.

Testerink C, Dekker HL, Lim ZY, Johns MK, Holmes AB, Koster CG, Ktistakis NT, Munnik T (2004) Isolation and identification of phosphatidic acid targets from plants. Plant J 39: 527-536.

Testerink C, Munnik T (2005) Phosphatidic acid: A multifunctional stress signaling lipid in plants. Trends Plant Sci 10: 368-375.

Thurston G, Regan S, Rampitsch C, Xing T (2005) Proteomic and phosphoproteomic approaches to understand plant-pathogen interactions. Physiol Mol Plant Pathol 66: 3-11.

Torres MA, Dangl JL (2005) Functions of the respiratory burst oxidase in biotic interactions, abiotic stress and development. Curr Opin Plant Biol 8: 397-403.

Ulm R, Ichimura K, Mizoguchi T, Peck SC, Zhu T, Wang X, Shinozaki K, Paszkowski J (2002) Distinct regulation of salinity and genotoxic stress responses by Arabidopsis MAP kinase phosphatase 1. EMBO J 21: 6483-6493.

Van der Hoorn RAL, Wulff BBH, Rivas S, Durrant MC, Van der Ploeg A, De Wit PJGM, Jones JDG (2005) Structure-function analysis of Cf-9, a receptor-like protein with extracytoplasmic leucine-rich repeats. Plant Cell 17: 1000-1015.

Van der Luit AH, Piatti T, van Doorn A, Musgrave A, Felix G, Boller T, Munnik T (2000) Elicitation of suspension-cultured tomato cells triggers the formation of phosphatidic acid and diacylglycerol pyrophosphate. Plant Physiol 123: 1507-1516.

Van Ooijen G, Van den Burg HA, Cornelissen BJC, Takken FLW (2007) Structure and function of resistance proteins in Solanaceous plants. Annu Rev Phytopathol 45: 43-72.

Van Schooten B, Testerink C, Munnik T (2006) Signalling diacylglycerol pyrophosphate, a new phosphatidic acid metabolite. Biochim Biophys Acta 1761: 151-159.

Vera-Estrella R, Barkla BJ, Higgins VJ, Blumwald E (1994) Plant defense response to fungal pathogens. Activation of host-plasma membrane H+-ATPase by elicitor-induced enzyme dephosphorylation. Plant Physiol 104: 209-215.

Vierstra RD (2003) The ubiquitin/26S proteasome pathway, the complex last chapter in the life of many plant proteins. Trends Plant Sci 8: 135-142.

Wang X, Goshe MB, Soderblom EJ, Phinney BS, Kuchar JA, Li J, Asami T, Yoshida S, Huber SC, Clouse SD (2005) Identification and functional analysis of *in vivo* phosphorylation sites of the Arabidopsis BRASSINOSTEROID-INSENSITIVE1 receptor kinase. Plant Cell 17: 1685-1703.

Wang YS, Pi LY, Chen X, Chakrabarty PK, Jiang J, De Leon AL, Liu GZ, Li A, Benny U, Oard J, Ronald PC, Song WY (2006) Rice XA21 binding protein 3 is a ubiquitin ligase required for full *Xa21*-mediated disease resistance. Plant Cell 18: 3635-3646.

Wise RP, Moscou MJ, Bogdanove AJ, Whitham SA (2007) Transcript profiling in host-pathogen interactions. Annu Rev Phytopathol 45: 329-369.

Wojtaszek P (1997) Oxidative burst: An early plant response to pathogen infection. Biochem J 322: 681-692.

Xiang T, Zong N, Zou Y, Wu Y, Zhang J, Xing W, Li Y, Tang X, Zhu L, Chai J, Zhou J-M (2008) *Pseudomonas syringae* effector AvrPto blocks innate immunity by targeting receptor kinases. Curr Biol 18: 74-80.

Xing T, Ouellet T, Miki BL (2002) Towards genomic and proteomic studies of protein phosphorylation in plant-pathogen interactions. Trends Plant Sci 7: 224-230.

Xu WH, Wang YS, Liu GZ, Chen X, Tinjuangjun P, Pi LY, Song WY (2006) The autophosphorylated Ser686, Thr688, and Ser689 residues in the intracellular juxtamembrane domain of XA21 are implicated in stability control of rice receptor-like kinase. Plant J 45: 740-751.

Yang C-W, Gonzalez-Lamothe R, Ewan RA, Rowland O, Yoshioka H, Shenton M, Ye H, O'Donnell E, Jones JDG, Sadanandom A (2006) The E3 ubiquitin ligase activity of Arabidopsis PLANT U-BOX17 and its functional tobacco homolog ACRE276 are required for cell death and defense. Plant Cell 18: 1084-1098.

Zhang J, Shao F, Li Y, Cui H, Chen L, Li H, Zou Y, Long C, Lan L, Chai J, Chen S, Tang X, Zhou JM (2007) A *Pseudomonas syringae* effector inactivates MAPKs to suppress PAMP-induced immunity in plants. Cell Host and Microbe 1: 175-185.

Zhang T, Liu Y, Yang T, Zhang L, Xu S, Xue L, An L (2006) Diverse signals converge at MAPK cascades in plant. Plant Physiol Biochem 44: 274-283.

Zipfel C, Kunze G, Chinchilla D, Caniard A, Jones JDG, Boller T, Felix G (2006) Perception of the bacterial PAMP EF-Tu by the receptor EFR restricts *Agrobacterium*-mediated transformation. Cell 125: 749-760.

Chapter 3

Tomato mitogen-activated protein kinases LeMPK1, -2 and -3 are activated during the Cf-4/Avr4-induced hypersensitive response and have distinct phosphorylation specificities

Iris J.E. Stulemeijer, Johannes W. Stratmann and Matthieu H.A.J. Joosten

A slightly modified version of this chapter has been published in Plant Physiology 144: 1481-1494 (2007).

SUMMARY

Tomato (*Solanum lycopersicum*, in this chapter further referred to as *Lycopersicon esculentum*) plants with the *Cf-4* resistance gene recognize strains of the pathogenic fungus *Cladosporium fulvum* that secrete the avirulence protein Avr4. Transgenic tomato seedlings co-expressing *Cf-4* and *Avr4* mount a hypersensitive response (HR) at 20°C, which is suppressed at 33°C. Within 120 minutes after a shift from 33°C to 20°C, *L. esculentum* MAP kinase (LeMPK) activity increases in the Cf-4/Avr4 seedlings. Searching tomato genome databases revealed at least 16 *LeMPK* sequences, including the sequence of *LeMPK1*, *-2* and *-3* that cluster with biotic stress-related MAPK orthologues from Arabidopsis (*Arabidopsis thaliana*) and *Nicotiana tabacum*. LeMPK1, -2 and -3 are simultaneously activated in the Cf-4/Avr4 seedlings and to reveal whether they are functionally redundant or not, recombinant LeMPKs were incubated on PepChip Kinomics® slides carrying peptides with potential phosphorylation sites. Phosphorylated peptides and motifs present in them discriminated between the phosphorylation specificities of LeMPK1, -2 and -3. LeMPK1, -2 or -3 activity was specifically suppressed in Cf-4-tomato by virus-induced gene silencing and leaflets were either injected with Avr4 or challenged with *C. fulvum* secreting Avr4. The results of these experiments suggested that the LeMPKs have different but also overlapping roles with regard to HR and full resistance in tomato.

INTRODUCTION

Plants are able to prevent or stop colonization by pathogens via highly effective defence systems. The constant battle between plants and pathogens can be described by a so-called zigzag model and consists of several layers of resistance responses of the plant which are suppressed by the pathogen (Jones and Dangl, 2006). The primary resistance response is based on the recognition of common features of pathogens, also referred to as pathogen-associated molecular pattern (PAMP)-triggered innate immunity. Successful pathogens suppress this primary immune response with specific effectors. In turn, plants have developed resistance (R) proteins that mediate recognition of the pathogen via the secreted effector proteins, rendering them avirulence (Avr) factors. As a result of this co-evolution R/Avr-

based host-pathogen interactions have evolved that follow the gene-for-gene model (Flor *et al.*, 1942). When an R protein and its cognate Avr protein are present, a swift resistance response is initiated which consists of localized cell death, the so-called hypersensitive response (HR), and associated defence responses (Jones and Dangl, 2006; Chisholm *et al.*, 2006). The immediate response of the plant relies on rapid post-translational modifications that alter the function of signalling proteins by changing their activity and/or localization.

Along this line, mitogen-activated protein kinase (MAPK) cascades, one of the major signalling modules in eukaryotes, are rapidly activated by post-translational modification upon recognition of pathogens by resistant plants (Pedley and Martin, 2005). MAPK cascades transfer signals from upstream receptors to downstream cellular effectors and rapid MAPK activation allows instantaneous modification of downstream signalling proteins (Krens *et al.*, 2006; Zhang *et al.*, 2006). In plants, these cascades have been implicated in typical defence responses, such as the production of pathogenesis-related (PR) proteins, reactive oxygen species (ROS), ethylene and cell death (Pedley and Martin, 2005). The phospho-relay system is based on specific activation of three types of kinases; MAPKK kinases (MAPKKKs), MAPK kinases (MAPKKs or MKKs) and MAPKs, which are also referred to as MPKs. Perception of external stimuli leads to MAPKKK activation, which subsequently phosphorylate the [Ser/Thr]-x(3,5)-[Ser/Thr] motif present in the target MAPKKs, thereby activating them. In their turn, MAPKKs phosphorylate the Thr (T) and Tyr (Y) residues in the TxY motif of the target MAPKs, which then become active and can phosphorylate downstream proteins that initiate the cellular response (Pedley and Martin, 2005). Plants trigger MAPK cascades upon biotic stress, but also when challenged by abiotic stresses such as wounding, drought, ozone and UV light (Mishra *et al.*, 2006; Nakagami *et al.*, 2005)). Thus, signals from diverse stresses eventually converge into various overlapping, but also distinct MAPK cascades (Zhang *et al.*, 2006) which is reflected by the presence of, for example, 20 MAPK-, 10 MAPKK- and 60 putative MAPKKK-encoding genes in Arabidopsis (*Arabidopsis thaliana*) (Ichimura *et al.*, 2002).

Upstream signalling components that activate MAPK cascades remain largely unknown, although ROS, auxin and abscisic acid (ABA), and phosphatidic acid (PA) have been reported to be involved (Lee *et al.*, 2001; Mishra *et al.*, 2006). Signalling events downstream of activated MAPK cascades also remain a black box, as hardly any MAPK substrates have been identified. So far, 1-aminocyclopropane-1-carboxylic acid synthase

(ACS), the rate-limiting enzyme in ethylene biosynthesis (Liu and Zhang, 2004) and MKS1 which is required for full salicylic acid-dependent resistance (Andreasson *et al.*, 2005), have been reported to be phosphorylated by MAPKs in Arabidopsis. Furthermore, plant-specific WRKY transcription factors that contain the WRKYGQK core sequence followed by a zinc-finger motif are phosphorylated by MAPKs (Menke *et al.*, 2005). Many putative MAPK-substrates were identified by employing a high-throughput proteomic screen in Arabidopsis (Feilner *et al.*, 2005).

In tomato (*Solanum lycopersicum*, here further referred to as *Lycopersicon esculentum* (*Le*)), several components of MAPK signalling cascades have been identified. The tomato MAPKs LeMPK1, -2 and -3 are activated upon stress responses caused by the wound signalling peptide systemin, oligosaccharide elicitors, ultraviolet-B radiation and the fungal toxin fusicoccin (Higgins *et al.*, 2006; Holley *et al.*, 2003). Furthermore, LeMPK2 and -3 are activated in a Pto-specific manner upon expression of AvrPto and AvrPtoB, and upon expression of LeMAPKKKα (Pedley and Martin, 2004). The authors also identified four MAPKKs, of which LeMKK2 and -4 activate LeMPK2 and -3 *in vivo*. *In vitro* experiments revealed that both LeMKKs are able to phosphorylate LeMPK1, -2 and -3. In addition to its activation by phosphorylation, *LeMPK3* mRNAs are specifically induced in resistant tomato upon inoculation with the bacterial strains *Xanthomonas campestris* pv *vesicatoria* and *Pseudomonas syringae* pv *tomato*, and upon treatment with a fungal ethylene-inducing xylanase (Mayrose *et al.*, 2004). Finally, virus-induced gene silencing (VIGS) of both LeMPK1 and -2, LeMPK3 or LeMKK2 revealed a role for these kinases in Mi-1-mediated aphid resistance (Li *et al.*, 2006).

We study the resistance response of tomato to the fungal pathogen *Cladosporium fulvum*. Several *Cf* resistance genes of tomato and their cognate avirulence genes (*Avrs*) from *C. fulvum* have been identified (Thomma *et al.*, 2005), including the gene pairs *Cf-4/Avr4* and *Cf-9/Avr9* (Rivas and Thomas, 2005). To study specific activation of kinases in typical defence responses leading to cell death, tobacco (*Nicotiana tabacum*) cell suspensions expressing *Cf* genes were elicited with its cognate Avr protein. In accordance with these studies, *Cf-9*-expressing cells were reported to activate calcium-dependent protein kinases (CDPKs) and the MAP kinases salicylic acid- and wound-induced protein kinase (SIPK and WIPK, respectively) (Romeis *et al.*, 1999 and 2000). The activation of the latter two kinases was confirmed in *Cf-9*-transgenic tobacco leaves. Furthermore, LeMAPKKKα has been

shown to be a positive regulator of the Cf-9-mediated HR and overexpression of the encoding gene causes MAPK activation and cell death (Del Pozo *et al.*, 2004). Interestingly, *Cf-9*-expressing cells also showed an increase in MAPK activity after treatment with Avr9 (De Jong *et al.*, 2000).

To study HR-related signalling processes in intact tomato plants, transgenic tomato lines lacking a functional *Cf* gene (Money Maker (MM)-Cf0) and expressing Avr4 were crossed to MM-Cf-4 tomato, resulting in Cf-4/Avr4 offspring that displays lethality at the seedling stage (Cai *et al.*, 2001; Thomas *et al.*, 1997). Since specific Avr perception appeared to be temperature-sensitive, Cf-4/Avr4 seedlings can be rescued upon incubation at 33°C (De Jong *et al.*, 2002). When the seedlings are subsequently transferred to 20°C, a synchronous systemic HR-related cell death program is initiated and this biological system has successfully been employed to study early transcriptional changes by cDNA-AFLP analysis (Gabriëls *et al.*, 2006). This study revealed that in these plants the typical defence-related genes are up regulated and novel genes were identified that play a role in plant defence.

Here we report on the specific Cf-4/Avr4-mediated activation of the tomato MAPKs LeMPK1, -2 and -3 upon initiation of the HR. Interestingly, analysis of the phosphorylation specificity of these LeMPKs using PepChip Kinomics® slides revealed overlapping, but also different phosphorylation preferences for each kinase, indicating different downstream roles for the LeMPKs. VIGS of the genes encoding the individual kinases suggested that LeMPK1, -2 and -3 play different but also overlapping roles in the establishment of the HR and resistance of tomato to *C. fulvum*.

RESULTS

Kinase activation upon Cf-4/Avr4-induced defence signalling

Tomato seedlings expressing both *Cf-4* and *Avr4* develop systemic necrosis at 20°C but can be rescued from lethality at 33°C. When incubated at 33°C and subsequently transferred to 20°C, defence signalling leading to systemic HR is induced in the Cf-4/Avr4 seedlings but not in seedlings from the parental lines (De Jong *et al.*, 2002). A video covering a five-day period shows the seedlings from the moment of the temperature shift until the Cf-4/Avr4 seedlings had become completely necrotic (Supplementary Figure S1). To study the

activation of kinases during Cf-4/Avr4-induced defence signalling, the HR was induced in one-week-old Cf-4/Avr4 seedlings and seedlings from the parents by a temperature shift to 20°C. Cotyledons were sampled at intervals of 30 minutes starting from the actual temperature shift and were analyzed for kinase activity using myelin basic protein (MBP) as a substrate in in-gel kinase assays. MBP-kinase activity in the parents, representing a mixture of the Cf-4 and transgenic Avr4-expressing lines, remained at basal levels throughout the experiment (Figure 1A). However, in the Cf-4/Avr4 seedlings the MBP-kinase activity had significantly increased at 120 minutes after the temperature shift, reached its maximum at 180 minutes and subsequently stabilized over the next 60 minutes (Figure 1A). The activity was quantified and expressed as a percentage of the maximum activity per experiment (Figure 1B). Statistical analysis revealed that the MBP-kinase activity in Cf-4/Avr4 seedlings is significantly increased compared to the parental lines at t=0 and from 120 minutes onwards ($P \leq 0.05$). MBP-kinase activity was present in a band with a molecular weight of about 50 kDa, suggesting that this is a reflection of MAP kinase activity. Samples taken from primary leaves of older Cf-4/Avr4 seedlings that were subjected to the same treatment showed a similar MBP-kinase activation pattern (results not shown), indicating that the response in cotyledons is representative for the response in true leaves.

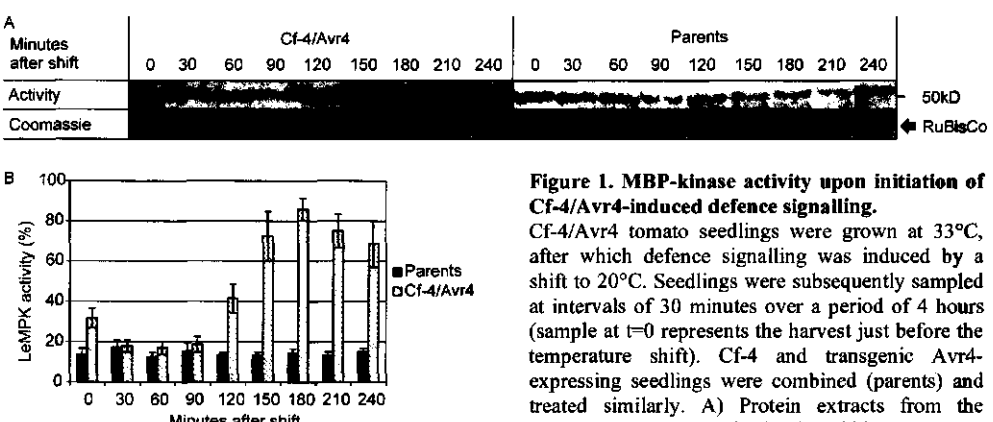

Figure 1. MBP-kinase activity upon initiation of Cf-4/Avr4-induced defence signalling.
Cf-4/Avr4 tomato seedlings were grown at 33°C, after which defence signalling was induced by a shift to 20°C. Seedlings were subsequently sampled at intervals of 30 minutes over a period of 4 hours (sample at t=0 represents the harvest just before the temperature shift). Cf-4 and transgenic Avr4-expressing seedlings were combined (parents) and treated similarly. A) Protein extracts from the seedlings were analyzed using in-gel kinase assays with MBP as a substrate. In each lane, similar amounts of protein were loaded as shown by Coomassie-staining of the RuBisCo large subunit. B) MBP-kinase activity represented by the 50 kDa band was quantified by phospho-imaging and expressed as the percentage of the maximum activity determined per experiment, which was set to 100%. For each time-point, the average activity (bars) of five independent experiments is presented and standard errors of mean (SEM) are shown by error bars.

LeMPK family analysis

In most cases, MBP-kinase activity reflects MAP kinase activity. For Arabidopsis(*At*), 20 *AtMPKs* were described to cluster in group A to D (Ichimura *et al.*, 2002) and *MAPKs* that cluster in group A have been described to be positive regulators of defence signalling (Mishra *et al.*, 2006). Some members of group B are negative regulators of defence signalling, whereas only in rice two MAPKs of group D were activated by pathogens (Song *et al.*, 2006; Zhang *et al.*, 2006). Since information of the tomato *MAPK* gene family is limited, the size of the *LeMPK* family and the variation between the family members was studied to identify potential additional homologues of the already described *LeMPK1*, *-2* and *-3* (Holley *et al.*, 2003) that cluster in group A. The open reading frames (ORFs) of these *LeMPKs* were used in BLAST queries on the TIGR, NCBI and the SOL Genomics Network (SGN) databases and additional *LeMPKs* were identified which, to identify all homologues, were in turn also used in BLAST queries on the same databases. Thirteen additional sequences that putatively encode a LeMPK were identified (Table I). The *LeMPK* sequences were translated into protein sequences and the ORFs were aligned with those of LeMPK1, -2 and -3, the ORFs from AtMPK1 to -20, the *Nicotiana tabacum* (Nt) ORFs from NtWIPK, NtSIPK, NtNTF4 and NtNTF6 and the ORF of *Homo sapiens* (Hs) HsERK1 that was assigned as out-group. As presented in Figure 2, the 13 additional LeMPKs cluster over groups B to D. LeMPKs present in groups A, B and C all have a Thr-Glu-Tyr (TEY) activation domain, whereas those of group D have a Thr-Asp-Tyr (TDY) activation domain, except for two incomplete sequences lacking this part of the sequence. LeMPK6 might represent a non-functional homologue because the Met-Glu-Tyr (MEY) sequence that

Table I. The tomato MAP kinases.
The Unigene identifier, type of activation domain (TxY), the number of residues of the protein and the clustering in the groups presented in Figure 2 are indicated for the 16 LeMPKs.

Name	Unigene identifier	TxY[a]	Residues	Group
LeMPK1	SGN-U316697	TEY	397	A
LeMPK2	SGN-U316695	TEY	395	A
LeMPK3	SGN-U313928	TEY	374	A
LeMPK4	SGN-U323634	TEY	373	B
LeMPK5	SGN-U313996	TEY	281	B
LeMPK6	SGN-U313995	MEY	377	B
LeMPK7	SGN-U323219	TEY	380	B
LeMPK8	SGN-U318773	TEY	371	C
LeMPK9	SGN-U316113	TEY	373	C
LeMPK10	SGN-U317229	TDY	576	D
LeMPK11[b]	SGN-U322516 & TC168576	-	395	D
LeMPK12	SGN-U318438	TDY	622	D
LeMPK13	SGN-U316366 & SGN-U316367	TDY	596	D
LeMPK14	SGN-U318361	TDY	496	D
LeMPK15[b]	SGN-U332259	-	207	D
LeMPK16	SGN-U318101	TDY	576	D

[a] TEY: Thr-Glu-Tyr; TDY: Thr-Asp-Tyr; MEY: Met-Glu-Tyr.
[b] These sequences lack the N-terminal region and do therefore not contain the TDY domain.

replaces the TEY domain in this MAP kinase probably renders the protein inactive. Since the tomato genome has not been fully sequenced yet, additional *LeMPKs* might be found in the near future. However, it is unlikely that large numbers of novel *LeMPKs* will be identified since all groups presented in the cladogram contain *LeMPK* sequences. Furthermore, other higher plant species of which the genome has been fully sequenced, such as *Populus trichocarpa* and *Oryza sativa*, contain comparable numbers of MAP kinases (21 and 15, respectively) (Hamel *et al.*, 2006). The results mentioned above suggest that group A is complete and therefore, to identify the MAPKs responsible for the MBP phosphorylation shown in Figure 1, we focused on LeMPK1, -2 and -3.

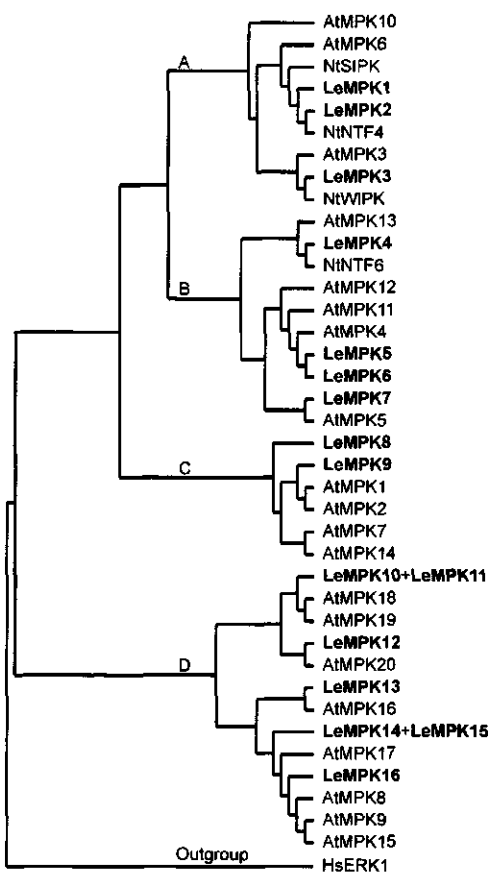

Figure 2. Relationships among the MAPKs of *Lycopersicon esculentum* (Le), *Arabidopsis thaliana* (At) and *Nicotiana tabacum* (Nt).
Thirteen sequences homologous to the ORF of *LeMPK1, -2* or *-3* were obtained from the tomato TIGR, NCBI and SGN databases and translated. All 16 LeMPK protein sequences were aligned with the known AtMPK and NtMPK sequences and a cladogram showing four distinct groups was generated in which LeMPK4 to -16 are numbered from top to bottom according to their position in the cladogram. LeMPK11 and -13 each represent a fusion of two database entries with an identical overlapping part. LeMPK11 and -15 are positioned manually next to their closest homologue since their sequence is not complete and in this way miss-clustering in the ClustalX alignment is avoided.

Cf-4/Avr4-induced defence signalling causes activation of LeMPK1, -2 and -3

To identify which LeMPK is activated upon Cf-4/Avr4-induced defence signalling, LeMPK1, -2 and -3 were immunoprecipitated from protein extracts of Cf-4/Avr4 and the parents, of which the MBP-kinase activity is shown in Figure 1, using antiserum raised against either LeMPK1, -2 or -3 (Holley *et al.*, 2003). Subsequently, the precipitated kinases were incubated with MBP to reveal whether they had been activated in the responding plants. Interestingly, the activity of all three LeMPKs had increased upon the initiation of Cf-4/Avr4-induced defence signalling when compared to the LeMPK activity in the parents (Figure 3). Although the MAPK protein levels were unaltered (results not shown), in contrast to *LeMPK1* and *-2*, *LeMPK3* transcription was significantly up regulated at 180 minutes after the temperature shift in the Cf-4/Avr4 seedlings (Stulemeijer and Joosten, unpublished results). This observation matches with the earlier described transcriptional regulation of *LeMPK3* upon recognition of a bacterial avirulence factor (Mayrose *et al.*, 2004). Furthermore, the transcript levels of *LeMPK1* and *-2* were not altered.

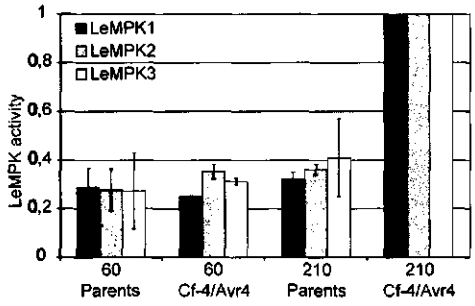

Figure 3. Initiation of Cf-4/Avr4-induced defence signalling causes activation of LeMPK1, -2 and -3. Cf-4/Avr4 tomato seedlings were grown at 33°C, after which defence signalling was induced by a temperature shift to 20°C. Seedlings were subsequently sampled at 60 and 210 minutes after the temperature shift. MM-Cf-4 and transgenic Avr4-expressing seedlings were combined (parents) and treated similarly. LeMPK1, LeMPK2 or LeMPK3 was immunoprecipitated from total protein extracts using specific antisera and incubated with MBP and radio-labelled ATP and protein bands were quantified. Bars represent the average activity of two independent experiments and standard errors of mean (SEM) are shown by error bars. LeMPK1, -2 and -3 activities in the Cf-4/Avr4 seedlings after 210 minutes were set to 1 and the remaining bars were related to these. Note that the bars do not represent absolute levels of LeMPK activity.

LeMPK1, -2 and -3 have overlapping and distinct specificities based on PepChip Kinomics® slide analysis

The experiments described above show that LeMPK1, -2 and -3 are specifically activated after triggering Cf-4/Avr4-induced defence signalling. To investigate whether the different LeMPKs have overlapping and/or distinct phosphorylation specificities, recombinant (r) LeMPKs were produced in *E. coli* and their peptide phosphorylation specificity was tested.

We included rAtMPK6 as a control in this assay, as for this MAPK a substrate has been identified (Liu and Zhang, 2004), and AtMPK6 clusters with LeMPK1, -2 and -3 in group A (Figure 2). The four rMAPKs were expressed as HIS-tagged proteins, purified and visualized by Coomassie staining and kinase assays were performed to confirm basal MAPK activity (Figure 4, upper and middle panel). MAPKs produced in *E. coli* autophosphorylate the Tyr residue in the TEY motif (Crews at al., 1991; Mayrose *et al.*, 2004), thereby gaining activity that is probably controlled by specific MAPK phosphatases *in vivo*. Monoclonal anti-phospho-Tyr (α-pY) antiserum recognizes the rMAPKs, indicating that the rMAPKs are indeed phosphorylated on a tyrosine residue (Figure 4, lower panel). To show that loss of activity is coupled to a loss of phosphorylation, rLeMPK3 was stored in a solution without kinase storage buffer which results in an inactive enzyme (rLeMPK3*; Figure 4). Probing with the α-pY antiserum revealed that this inactive rMAPK is indeed no longer phosphorylated (Figure 4). Thus, MAPKs that are produced in *E. coli* have basal activity. This conclusion is supported by the observations of Feilner *et al.* (2005), who produced AtMPK3 and AtMPK6 in *E. coli* and used the active MAP kinases to perform protein microarray-based kinase assays.

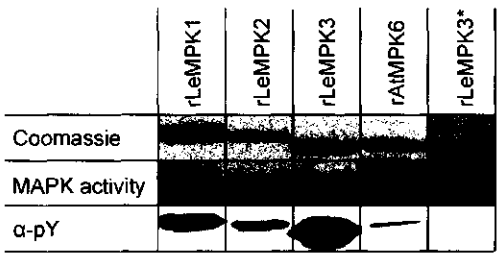

Figure 4. Recombinant MAPKs of group A have basal kinase activity and are phosphorylated on a Tyr residue.
Recombinant MAP kinases stored in kinase storage buffer (rLeMPKs and rAtMPK6; see Materials and Methods for details) were run on SDS-PAGE gels and stained with Coomassie brilliant blue. Basal kinase activity was determined by incubation of the rMAPKs with MBP and radio-labelled ATP (middle panel) and a blot carrying the rMAPK proteins was incubated with antiserum specific for phospho-Tyr (α-pY). rLeMPK3* represents an inactive form of the LeMPK3 enzyme obtained by storage in a solution without kinase storage buffer.

To investigate peptide phosphorylation specificities of the individual MAPKs, PepChip Kinomics® slides, further referred to as PepChips, were incubated with the rMAPKs showing basal activity. PepChips carry a triplicate set of 976 peptides containing experimentally verified phosphorylation sites for different types of human kinases (see Materials and Methods for details). Each of the rMAPKs phosphorylated an overlapping but also partially different subset of the peptides (Figure 5A). In the magnified region of the slide

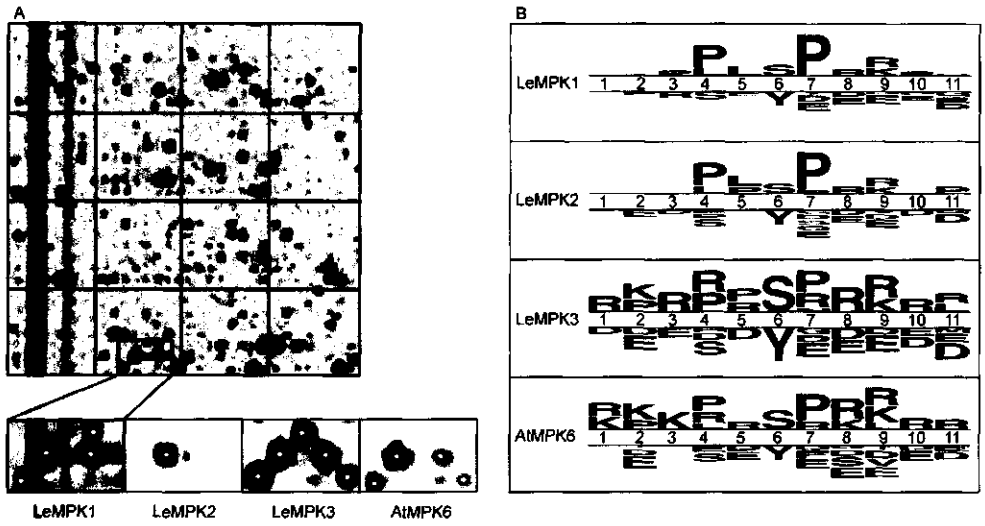

Figure 5. PepChips reveal different phosphorylation patterns for LeMPK1, -2 and -3. PepChips were incubated with rMAPKs in the presence of radio-labelled ATP.
A) Peptides phosphorylated on the PepChips were visualized with phospho-imaging. The upper panel shows one of the triplicate sets of peptides phosphorylated by rLeMPK1, whereas the lower panels show a subset of peptides differentially phosphorylated by rLeMPK1, -2, -3 and rAtMPK6, respectively. Spots marked by a white dot are represented in the selected subset of phosphorylated peptides presented in (B). B) The selected phosphorylated and non-phosphorylated peptides were compared with Two Sample Logo (TSL) software. Putative phosphorylation sites (Ser (S), Thr (T) or Tyr (Y)) are aligned on position 6, and above the double line the TSL plots show for positions 1 to 11 whether a particular amino acid residue has an increased frequency in the phosphorylated peptides compared to the same position in the non-phosphorylated peptides. For the latter, the most frequently occurring residues are depicted below the double line (t-test, $P<0.05$). The size of the symbols is proportional to the relative frequencies of the residues in the phosphorylated and non-phosphorylated peptides. The largest (stack of) symbols in the TSL-plots for rLeMPK1, -2, -3 and rAtMPK6 have a frequency of 62%, 58%, 34% and 34%, respectively. L: Leu; R: Arg; K: Lys; D: Asp; E: Glu; F: Phe; V: Val.

(Figure 5A, small panels), only one of the spotted peptides is phosphorylated by all three rLeMPKs and rAtMPK6, whereas two peptides are phosphorylated by both rLeMPK1 and -3 as well as by rAtMPK6. Additionally, three peptides spotted in this area were only phosphorylated by rLeMPK1 or -3. The peptide phosphorylation specificity of rAtMPK6 is most similar to that of rLeMPK1, although it has similarities with rLeMPK3 as well.

The phosphorylation intensity of most of the peptides did not exceed background levels and these peptides probably do not contain motifs that could be present in putative *in vivo* substrates. For further analysis, only peptides showing a phosphorylation intensity above the average peptide phosphorylation intensity of a complete PepChip and peptides with a phosphorylation intensity of zero were selected and will be referred to as phosphorylated and non-phosphorylated peptides, respectively (Supplementary Figure S2; see Material and

Table II. Phosphorylation motifs present in the peptides phosphorylated on the PepChips by rLeMPK1, -2 or -3 or rAtMPK6.

Phosphorylated peptides were divided into subgroups based on common characteristics and phosphorylation motifs were predicted with TEIRESIAS software (Rigoutsos and Floratos, 1998). Motifs present in at least 40% of the sequences of a subgroup are presented.

Phosphorylation motif	LeMPK1	LeMPK2	LeMPK3	AtMPK6
P x **S** P[a]	21[b]	21	14	16
S P x [KR][c]	19	19	19	19
[KR] R x **S**	10	-[d]	-	-
[KR] x x x x **S**	-	-	21	18
S x x [KR]	-	-	20	-

[a] P: Pro; S: Ser; x: any residue. The phosphorylation site (S) is indicated in bold.
[b] The number of phosphorylated peptides containing this motif in the subgroup of sequences.
[c] [KR] refers to the presence of either a Lys (K) or an Arg (R) at this position of the phosphorylation motif.
[d] This motif is not present in the peptides phosphorylated by this kinase.

Methods for details). Comparison of the phosphorylated peptides for LeMPK1, -2 or -3 revealed that 30% of the peptides were phosphorylated by LeMPK1, -2 and -3, 19% by LeMPK1 and -2, 5% by LeMPK1 and -3 and 4% by LeMPK2 and -3. The remaining phosphorylated peptides were specifically phosphorylated by either LeMPK1, -2 or -3 (see also Table II). To determine the specificity of the rMAPKs, the phosphorylated peptides were compared to the non-phosphorylated peptides with Two Sample Logo software (TSL; Crooks *et al.*, 2004). The peptides consist of 11 residues of which the central residue represents the putative phosphorylation site, which is either a Ser, Thr or Tyr residue. The TSL plots show for the 11 positions whether a residue is more represented in the phosphorylated peptides as compared to the non-phosphorylated peptides (Figure 5B; t-test, $P<0.05$). As expected for MAPKs, which are Ser/Thr-specific kinases (Nakagami *et al.*, 2005), the rMAPKs prefer Ser- instead of Tyr-phosphorylation (position 6). In addition, rLeMPK1 and -2 prefer to phosphorylate sequences containing Pro residues, whereas rLeMPK3 and rAtMPK6 have a preference for sequences containing the positively charged amino acid residues Arg and Lys, in addition to Pro residues. Sequences containing negatively charged residues, such as Asp and Glu, are hardly phosphorylated by any rMAPK (Figure 5B) which might be caused by static hindrance of the negatively charged phosphate group at the phosphorylation site. These results demonstrate that phosphorylation of the peptides on the PepChips by the various rMAPKs is significantly influenced by the sequence of the peptides and that each of the rLeMPKs phosphorylates a different subset of peptides, since clear differences are observed between the TSL plots.

The sequences of the phosphorylated peptides were loaded into TEIRESIAS software (Rigoutsos and Floratos, 1998) and preferred phosphorylation motifs consisting of 3 or 2 residues were predicted for each rMAPK (Table II). These motifs are too short to identify

relevant putative *in vivo* substrates from databases; however they allow discrimination between the phosphorylation specificities of the individual rMAPKs. To verify whether the results from the PepChip analysis match reported biological substrates, phosphorylation motifs predicted for rAtMPK6 were compared to the phosphorylation sites of its known *in vivo* substrates, ACS6 and -2. The predicted Pro-x-Ser-Pro (PxSP) phosphorylation motif matches for the position of two of the three phosphorylated serine residues (Ser483 and Ser488) described for ACS6 (Liu and Zhang, 2004). However, the third phosphorylated serine residue (Ser480) is only followed by a proline. Such serine residues were frequently phosphorylated on the PepChip but motifs matching these Ser-Pro sites did not exceed the threshold set to predict motifs. These data reveal phosphorylation motifs for rLeMPK1, -2 and -3 that only partially overlap, indicating that the LeMPKs share common substrates but also have different substrate specificities (Table II).

VIGS of *LeMPK1*, *-2* or *-3* results in decreased activity of the encoded MAP kinase

LeMPK1, -2 and -3 are activated upon specific Cf-4-mediated recognition of *C. fulvum* avirulence factor Avr4. To elucidate the role of the individual LeMPKs in HR and resistance of tomato to *C. fulvum*, VIGS of *LeMPK1*, *-2* or *-3* was performed. Therefore, MM-Cf-4-tomato seedlings were inoculated with recombinant tobacco rattle virus (TRV)-silencing constructs (Liu *et al.*, 2002a and 2002b) each containing part of the unique 3' UTR region of the *LeMPK1, -2* or *-3* genes. LeMPK1, -2 and -3 have very low activity in untreated leaf disks (results not shown). However, they can be rapidly activated by wounding (Higgins *et al.*, 2006). To test MAPK activity in silenced plants, we induced MAPK activity by punching leaf disks, which results in a wound stimulus, and floated the disks on water to prevent desiccation (Menke *et al.*, 2004; see Materials and Methods). Subsequently, in gel kinase assays were performed. Overall LeMPK activity was decreased in TRV:LeMPK1-, -2- and -3-inoculated plants when compared to control plants that had been inoculated with TRV containing the ORF of green fluorescent protein (TRV:GFP; Figure 6A). To confirm decreased activity of only the targeted LeMPK, immunocomplex assays for LeMPK1, -2 and -3 were performed on the TRV:LeMPK- and TRV:GFP-inoculated plants. In the TRV:LeMPK1-inoculated plants, LeMPK1 activity was decreased when compared to the LeMPK1 activity in the TRV:GFP-inoculated plants, whereas the LeMPK2 and -3 activities did not change when compared to those in TRV:GFP-inoculated plants (Figure 6B). Also, a clear specific decrease in LeMPK2

and -3 activity was observed in TRV:LeMPK2- and -3-inoculated plants, respectively. From these observations, we conclude that inoculation of tomato with the different TRV:LeMPK constructs results in specific suppression of the respective MAP kinase activities.

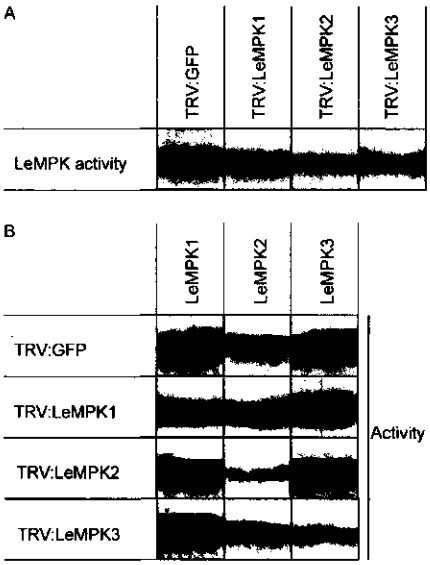

Figure 6. VIGS of *LeMPK1*, *-2* or *-3* decreases the activity of the encoded MAP kinase.
Disks were taken from leaflets of TRV-GFP and TRV-LeMPK-inoculated plants three weeks after inoculation and they were floated on water for 15 minutes, after which protein extracts were made. A) An in-gel kinase assay was performed for each individual leaf disc and representative overall LeMPK activities are shown. Bands represent a combination of LeMPK1-, -2- and -3 activities, since the slightly smaller LeMPK3 protein was not separated from LeMPK1 and -2 on these gels. Equal amounts of protein were loaded in each lane (not shown). B) LeMPK1, -2 and -3 proteins were individually immunoprecipitated from the protein extracts shown in (A) and subjected to a kinase assay. Representative results from three independent experiments are shown. Note that only the activity of the targeted LeMPK is decreased when compared to the activity levels from TRV:GFP-inoculated plants.

LeMPKs have different and overlapping roles in Cf-4-mediated HR and resistance to *C. fulvum*

Three weeks after inoculation of MM-Cf-4 tomato with the various TRV VIGS constructs described above, eight leaflets of compound leaves at similar positions on the plant were injected with Avr4 protein at ten sites per leaflet. Sites that developed necrosis, reflecting Cf-4/Avr4-induced HR, were counted (see Materials and Methods for details). The maximum response to Avr4 of 7.6 necrotic spots per leaflet (± 0.2 SEM) was obtained in TRV:GFP-inoculated MM-Cf-4 plants, whereas inoculation with TRV:Cf-4 resulted in a significant decrease of the response to Avr4 (Figure 7A). Interestingly, inoculation with TRV:LeMPK2 or -3 also caused a significant decrease in the responsiveness of the plant, whereas inoculation with TRV:LeMPK1 did not affect the Cf-4/Avr4-induced HR in this experimental setup ($P \leq 0.05$; Figure 7A).

To determine whether, in addition to their requirement for a full HR, the LeMPKs are also required for Cf-4-mediated resistance, MM-Cf-4 tomato plants that had been inoculated

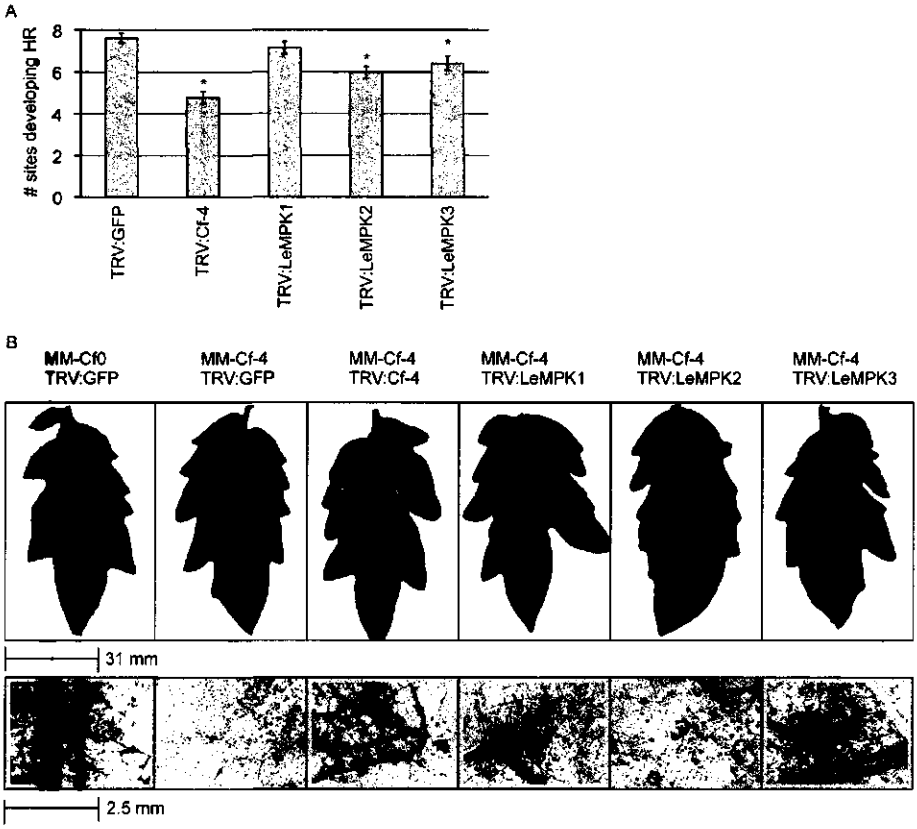

Figure 7. The role of LeMPK1, -2 and -3 in Cf-4-mediated HR and resistance to *C. fulvum*.
Tomato plants were inoculated with TRV:GFP, TRV:Cf-4, TRV:LeMPK1, TRV:LeMPK2 or TRV:LeMPK3 and injected with Avr4 or challenged with *C. fulvum* expressing *Avr4*. A) After three weeks, a total of 160 leaflets of the TRV-inoculated MM-Cf-4 plants were injected with Avr4 protein at ten sites. The average number of sites per leaf that developed a specific HR, visible as necrosis, is shown (see Materials and Methods for details). The asterisks indicate a significantly decreased response as compared to TRV:GFP-inoculated plants ($P \leq 0.05$). B) MM-Cf0 plants that are fully susceptible to *C. fulvum* and MM-Cf-4 plants that are fully resistant were inoculated with the indicated recombinant TRV VIGS constructs. After three weeks, the plants were inoculated with a strain of *C. fulvum* expressing *Avr4* and *GUS* and leaflets were stained for GUS activity after 14 days. Leaflets representative for five independent experiments are shown in the upper panel and a magnification of GUS-stained areas is shown in the lower panel. In this panel the margins indicate compromised resistance.

with the various TRV constructs were challenged with a strain of *C. fulvum* expressing *Avr4*. As a control, fully susceptible MM-Cf0 plants lacking functional resistance genes to *C. fulvum* were inoculated with TRV:GFP and challenged with the fungus. The *C. fulvum* strain also expresses the *pGPD:GUS* transgene, thereby allowing detection of the mycelium of the fungus in the leaves. Two weeks after inoculation with *C. fulvum*, leaflets from fully developed compound leaves were treated with X-gluc, resulting in staining of leaf sections

that are successfully colonized. As shown in Figure 7B (upper panels), leaflets of susceptible TRV:GFP-inoculated MM-Cf0 tomato plants were colonized by *C. fulvum*, as reflected by the staining in the leaflet. Magnification of the stained areas clearly revealed the presence of fungal mycelium growth in the leaf (lower panels). MM-Cf-4 tomato plants inoculated with TRV:GFP did not show any colonization by *C. fulvum*, indicating that these TRV-inoculated plants are still fully resistant to the fungus. Inoculation of the MM-Cf-4 plants with TRV:Cf-4 compromised resistance to *C. fulvum* as mycelium of the fungus is observed in the leaflets. Interestingly, loss of full resistance to *C. fulvum* was also observed in the TRV:LeMPK1- and -3-inoculated MM-Cf-4 plants, since the intercellular spaces in certain patches of the leaflets were successfully colonized (Figure 7B). Surprisingly, although VIGS of LeMPK2 significantly affected the Cf-4/Avr4-induced HR (Figure 7A), we did not find compromised resistance to *C. fulvum* in TRV:LeMPK2-inoculated MM-Cf-4 plants (Figure 7B).

DISCUSSION

To reveal differences in LeMPK1, -2 and -3 peptide substrate specificity, PepChip analysis was performed. We have incubated two different PepChips, each carrying a triplicate peptide set, with rLeMPK1 in two independent experiments and found that the peptides selected as phosphorylated peptides were identical when both experiments were compared (results not shown). Therefore, the other rMAPKs were incubated on only one PepChip. The PepChip Kinomics® slides that we employed carry peptides containing phosphorylation motifs for human kinases and therefore we focused on the overall phosphorylation patterns rather than on the phosphorylation of individual peptides. Analysis with TEIRESIAS motif prediction software revealed motifs in the sequences of the phosphorylated peptides (Table II). To enable comparison of rMAPK-specific phosphorylation motifs obtained from the PepChip analysis, different amounts of the rMAPK proteins with similar MBP kinase activities were applied to the slides. This implies that the relevance of a certain phosphorylation motif identified for a LeMPK could be different *in vivo*, as LeMPK protein concentrations and specific activities differ in the plant tissue. Each rMAPK phosphorylated approximately 80 to 100 peptides consisting of 11 amino acid residues, which allowed identification of motifs of two or three residues. Table II shows motifs for the individual

rLeMPKs present in 40% or more of the sequences in a subgroup, which could match with motifs present in *in vivo* substrates. In contrast to Figure 5B where residues with a higher frequency in phosphorylated, as compared to non-phosphorylated peptides are presented, these motifs consist of residues that have a high frequency in the phosphorylated peptides. Unfortunately, motifs consisting of two or three residues are not discriminative in database searches. However, manual annotation revealed that the PxSP motif, which has been previously described by Schwartz and Gygi (2005), matches for Ser483 and Ser488 of ACS6, which are phosphorylated by AtMPK6 (Liu and Zhang, 2004). The third phosphorylated Ser of ACS6 (Ser480) was only followed by a Pro. Peptides with a central Ser residue followed by a Pro are frequently phosphorylated on the slides and only a subset of the sequences matches the PxSP motif. The remaining Ser-Pro sequences were not part of a pattern exceeding the threshold set for motif prediction. Furthermore, many potential AtMPK6 substrates have been described by Feilner *et al.* (2005). However, the exact phosphorylation sites are not known for these substrates, rendering verification of the motifs not possible. In addition to rAtMPK6, rLeMPK1, -2 and -3 also phosphorylate the PxSP motif (Table II) and in tomato this motif matches the orthologues LeACS6 and LeACS2, suggesting that these enzymes are substrates of LeMPK1, -2 and -3. The identification of motifs phosphorylated by only one of the tested rLeMPKs (Table II) implies that, in addition to overlapping specificities, these LeMPKs have also different substrate-specificities *in vivo*. Alternatively, the LeMPKs could target different phosphorylation sites of the same protein which implies a different regulatory function for each of the LeMPKs.

Since our PepChip analysis points to different, and also overlapping, regulatory functions for the LeMPKs *in vivo*, the role of these MAP kinases in the initiation of Cf-4/Avr4-induced HR and disease resistance was studied. The *LeMPK*s were individually targeted in MM-Cf-4 tomato plants by VIGS, which resulted in a decreased LeMPK activity compared to the control TRV:GFP-inoculated plants. To avoid off-target silencing, the sequences to target the individual *LeMPK*s were designed on the highly unique 3' UTR-regions and these sequences have less than 21 base pairs homology to any other tomato gene present in the NCBI or SGN databases (results not shown). Furthermore standardized immunoprecipitations, with equal amounts of LeMPK antibodies, protein A agarose beads and input protein for each sample, did not reveal decreased activity of the homologous, non-

targeted LeMPKs (Figure 6B). Therefore it is unlikely that the expression of other genes is affected in the different TRV:LeMPK-inoculated plants.

VIGS in tomato is patchy and usually only results in a partial knock-down of gene expression. Therefore, we only observed a slight decrease in the Avr4-induced HR even upon silencing of the *Cf-4* resistance gene itself (Figure 7A). However, the decrease is significant and also correlates with a clear loss of full resistance to *Avr4*-expressing strains of *C. fulvum* (Figure 7B). In many cases, silencing of a gene encoding a protein that functions downstream of Cf-4 in the HR signalling cascade even has a smaller effect on the responsiveness of the plant to Avr4, which is probably due to redundancy (Gabriëls *et al.*, 2006). Still, significant suppression of the Avr4-induced HR was found in MM-Cf-4 plants in which either LeMPK2 or -3 activity was decreased, whereas decreased LeMPK1 activity did not affect the Avr4-induced HR (Figure 7A). The latter could be caused by the relatively slight decrease in LeMPK1 activity (Figure 6B). The TRV:LeMPK-inoculated MM-Cf-4 plants were also challenged with the *Avr4*-expressing strain of *C. fulvum*. Surprisingly, in this assay the LeMPK1-silenced plants showed a phenotype, as localized patches of blue-stained intercellular mycelium were visible upon treatment of the inoculated leaves with X-gluc (Figure 7B). Although the LeMPK1 activity is only slightly decreased and the HR is not affected (Figure 7A), it does cause suppressed resistance, indicating that the degree of *LeMPK1* silencing is sufficient to observe a phenotype. The lower LeMPK2 activity did not affect resistance, whereas for silencing of LeMPK3, in addition to its effect on the HR, suppressed resistance was found (Figure 7B).

The role in disease resistance of various orthologues of the LeMPKs studied here appears to match with our results. VIGS of *NtSIPK* and *NtWIPK*, the tobacco orthologues of *LeMPK1* and *-3* respectively, in *N. benthamiana* compromised resistance to the bacterial pathogen *Pseudomonas cichorii* and tobacco mosaic virus (TMV) (Jin *et al.*, 2003; Sharma *et al.*, 2003). Furthermore, enhanced susceptibility to *Peronospora parasitica* was found upon silencing of the *LeMPK1* orthologue *AtMPK6* in Arabidopsis (Menke *et al.*, 2004). Silencing of *LeMPK1* and *-2* or silencing of *LeMPK3* only was reported to result in a loss of full *Mi-1*-mediated aphid resistance (Li *et al.*, 2006) and inoculation of tomato with TRV:NtWIPK compromised resistance to *Pseudomonas syringae* pv *tomato* (Ekengren *et al.*, 2003). Finally, constitutive overexpression of *StMEK1* thereby activating the LeMPK1 orthologue StMPK1, enhanced resistance to *Phytophthora infestans* and *Alternaria solani* (Yamamizo *et al.*, 2006).

Interestingly, TRV:NtSIPK inoculation, which should cause simultaneous silencing of *LeMPK1* and *-2* in tomato, did not affect the resistance response to *P. syringae* pv *tomato* (Ekengren *et al.*, 2003).

Solanaceous species like tomato and tobacco possess two homologous MAPKs in group A, LeMPK1/2 and NtSIPK/NTF4, and it is not clear whether these homologues are fully redundant or have different specificities. Here, we show that LeMPK1 and the 95.4% identical LeMPK2 protein have overlapping but also different peptide phosphorylation specificities *in vitro* and that both MAPKs are clearly involved in the resistance response. The VIGS data indicate that LeMPK1 and LeMPK2 may have different functions with regard to HR and full resistance in tomato. However, a definite result would require complete knockouts of *LeMPK1* and/or *LeMPK2*, which are not available. VIGS of *LeMPK3* affects the execution of the HR and in this case also full resistance is lost (Figure 7), suggesting that LeMPK3 has a role in both the initiation of the HR and other defence responses. This hypothesis is supported by the broader phosphorylation specificity of LeMPK3 (Table II).

In transgenic tobacco cell suspensions expressing *Cf-9*, MAPKs are activated within 5 minutes after elicitation with the Avr9 avirulence factor of *C. fulvum* (Romeis *et al.*, 1999; De Jong *et al.*, 2002). Such cell suspensions are also temperature-sensitive and it was found that this sensitivity resides at the level of elicitor perception, as the amount of Avr9 binding sites was significantly decreased at 33°C (De Jong *et al.*, 2002). The cell suspensions required at least 45 minutes to regain their ability to perceive Avr9 when transferred from 33°C to 15°C, indicating that *de novo* protein synthesis is required for this recovery. The Cf-4/Avr4 seedlings also need to recover when shifted from 33°C to 20°C, in this case resulting in a lag phase of 90 to 120 minutes before MAPK activation is observed (Figure 1). Furthermore, a significantly higher basal MAPK activity was observed in Cf-4/Avr4 seedlings at 33°C as compared to the parents (t=0 min, Figure 1B), although immunocomplex assays did not reveal an increased activity for LeMPK1, -2 or -3 at this time point. Possibly, at this stage during which HR is suppressed, other MAPKs which act as negative regulators of the HR are active. Putative candidates are LeMPK4 and/or -7 from group B (Figure 2), which are orthologues of the negative regulator of resistance AtMPK4 (Ichimura *et al.*, 2006). Due to their similar size (Table I) these MAPKs are indistinguishable from LeMPK1, -2 and -3 on the gel shown in Figure 1. We did not further separate LeMPK3 from the other LeMPKs as this allowed to quantify the total MAPK activity present in one band. Correspondingly, LeMPK4 and/or -7 or

other LeMPKs might be activated simultaneously with LeMPK1, -2 and -3 from 120 minutes onwards since the immunoprecipitation data do not provide absolute qualitative data as this depends on the titer and affinity of the antibodies. Recently, for example, the activation of the negative regulator AtMPK4 simultaneously with AtMPK3 and -6 has been reported upon elicitation of Arabidopsis with the bacterial elicitor flagellin (Mészáros *et al.*, 2006).

Cotyledons of Cf-4/Avr4 seedlings develop localized necrotic lesions that become macroscopically visible at about 12 hours after the temperature shift and eventually spread over the complete surface of the cotyledons. Interestingly, Cf-4/Avr4 seedlings that are incubated at 20°C for 240 minutes and subsequently shifted back to 33°C, survive and do not develop necrosis (results not shown). In addition, Cf-4/Avr4 seedlings incubated at 20°C for 24 hours develop localized necrotic lesions but when shifted back to 33°C, these lesions do not further expand and the remaining tissue survives (results not shown). Alvarez *et al.* (1998) observed the initiation of systemic 'micro-HRs' at certain confined locations in the tissue leaving no visible trace, upon inoculation of Arabidopsis with avirulent *P. syringae*. Furthermore, it was found that reactive oxygen intermediates that are generated at defined sites by the plant upon perception of an avirulent pathogen are able to suppress the spread of cell death (Torres *et al.*, 2005). Our observations indicate that similar phenomena take place in the Cf-4/Avr4 seedlings upon the temperature shift. The reversibility of the system and the more or less constant total LeMPK activity level after 180 minutes suggest that at least during the early stages after the temperature shift, a controlled HR takes place in the Cf-4/Avr4 seedlings. This control mechanism prevents superfluous cell death in Cf-4/Avr4 seedlings and illustrates that the response of the seedlings is a proper reflection of the response of a resistant host plant to invasion by an avirulent pathogen.

MATERIALS AND METHODS

Plants

To generate tomato (*Lycopersicon esculentum*) offspring expressing both the *Hcr9-4D* (= *Cf-4*) gene and its cognate avirulence (*Avr*) gene *Avr4* from *Cladosporium fulvum*, transgenic Money Maker (MM)-Cf0 plants expressing *Avr4* (MM-Cf0:*Avr4*) were crossed to transgenic MM-Cf0:*Hcr9-4D* (MM-Cf-4) plants, as described earlier (Cai *et al.*, 2001;

Thomas *et al.*, 1997). In addition, the MM-Cf-4 and MM-Cf0:*Avr4* parental lines were selfed. The resulting Cf-4/Avr4 and parental seeds were isolated from the fruits and germination was stimulated by a treatment with 25% (v/v) Lodik (containing 4% (v/v) sodium hypochlorite), for 20 min. After germination under normal daylight conditions at room temperature (RT) for approximately seven days, seedlings were incubated at 33°C under 16hr/8hr light/dark regime (Elbanton, Kerkdriel, The Netherlands) for at least another seven days. For the activation of Cf-4/Avr4-induced defence signalling, the seedlings were shifted to 20°C and at several time points after this temperature shift cotyledons were harvested, immediately frozen in liquid nitrogen and stored at -80°C. The parental lines were subjected to the same treatment. MM-Cf-4 and MM-Cf0 plants used for VIGS assays were grown under standard greenhouse conditions.

Monitoring HR development in Cf-4/Avr4 seedlings

Cf-4/Avr4 seedlings and seedlings of the parents were rescued at 33°C as described above. Seedlings were transferred to 20°C and a webcam, which was placed in the incubator, took photographs from the seedlings every 5 min over a period of 5 days. Images were cropped by Irfanview software Version 3.98 (http://www.irfanview.com/), batch conversed to centralize the seedlings in the photograph and merged to avi-format by VideoMach 2.7.2 software (http://www.gromada.com/).

Kinase assays

Cotyledons of the seedlings were homogenized in immunoprecipitation (IP) buffer [10 mM Tris, pH 7.5, 150 mM NaCl, 1 mM EDTA, 1 mM EGTA, 1 mM Na_3VO_4, 1 mM NaF, 10 mM β-glycerophosphate, 1% (w/v) Triton X-100, 0.5% (w/v) Nonidet P-40, 2 mM dithiothreitol and one complete protease inhibitor tablet (Roche)] and the homogenate was centrifuged at 16,000*g* for 20 min at 4°C, after which the supernatant was recovered. For in-gel kinase assays with myelin basic protein (MBP) as an artificial substrate (Shibuya *et al.*, 1992), a volume containing 25 μg of total protein (Bradford protein assay (Bio-Rad)) was loaded per lane. MPK activity was measured by phospho-imaging (Storm, Molecular Dynamics) and quantified with ImageQuant software (Amersham). The data obtained from 5 individual in-gel kinase assays were subjected to a two-way design ANOVA (Genstat release

8.1). Furthermore, 25 µg of protein was loaded on SDS-PAGE gels and stained with Coomassie Brilliant Blue to verify even loading.

Immunocomplex kinase assays were performed as described earlier (Holley *et al.*, 2003) with minor modifications. For IPs, 200 µg of protein was incubated with LeMPK1, -2 or -3 antiserum in a 100:1 dilution and the antibodies were pulled down with 15 µl of protein A beads (3 mg/mL). To determine the activity of recombinant MPKs (see below), dilution series of these proteins were incubated with 20 µl kinase reaction buffer [20 mM Hepes, pH 7.5, 15 mM $MgCl_2$, 2 mM EGTA, 1 mM DTT, 0.25 mg/mL MBP, 25 µM ATP and 1 µl 10 µCi [gamma-^{32}P]ATP] for 30 min at 30°C. Proteins were subsequently separated on 15% SDS-PAGE gels and a phospho-imaging screen was exposed to the dried gel. MPK activity was measured by phospho-imaging and quantified with ImageQuant software.

Analysis of relationships between MAPK protein sequences

To identify the sequences of all putative *LeMPK* homologues, BLAST searches with the DNA sequence of *LeMPK1*, *-2* and *-3* open reading frames (ORFs) were performed on the TIGR Tomato Gene Index (LeGI), the NCBI database and the SOL Genomics Network (SGN). Each newly found homologue was subsequently BLASTed until no new sequences were identified and in this way, the ORFs from 13 putative additional *LeMPK* homologues were obtained. The sequences were translated to protein sequences with the Expasy Proteomics server translate tool (http://us.expasy.org/tools/dna.html) and protein sequences encoded by the ORFs were aligned in ClustalX (Supplementary Figure S3; Thompson *et al.*, 1997) with the sequences encoded by the ORFs of AtMPK1 to -20 from Arabidopsis, NtSIPK, NtWIPK, NtNTF4 and NtNTF6 from *Nicotiana tabacum*, and the *Homo sapiens* HsERK1, which also encodes a MAPK (Ichimura *et al.* 2002; Zhang and Klessig, 2001). Pairwise distances between sequences were calculated with neighbour joining (NJ) in ClustalX and a cladogram rooted with HsERK1 was made with Treeview software (Page, 1996).

Cloning and expression of recombinant MAPKs

To express LeMPK1, -2 and -3 as soluble HIS-tagged proteins, primers were designed to PCR amplify the ORFs of the encoding genes. Respective primers were for *LeMPK1*: forward: 5'-GATCGGATCCATGGATGGTTCCGTTCCGC-3'; reverse: 5'-

GATCCTCGAGTCACATGCGCTGGTATTCAGG-3', for *LeMPK2*: forward: 5'-GATCGGATCCATGGATGGTTCAGCTCCGC-3'; reverse: 5'-GATCCTCGAGTCACATGTGCTGGTATTCGGG-3' and for *LeMPK3*: forward: 5'-GATCGGATCCATGGTTGATGCTAATATGGG-3' and reverse: 5'-GATCCTCGAGTTAAGCATATTCAGGATTCAACG-3' (*Bam*HI and *Xho*I sites are underlined in the forward and reverse primers respectively). The amplification products were ligated into *Bam*HI/*Xho*I-digested pET28a+ vector (Novagen, Madison, WI). The plasmids were transformed to *Escherichia coli* BL21 (DE3) cells and the integrity of the constructs was confirmed by sequencing. The pET28a+-*AtMPK6* construct has been described previously (Liu and Zhang, 2004; Menke *et al.*, 2004). Bacteria were cultured in Luria Broth (LB) medium at 37°C and protein expression was induced at OD 0.6 by adding IPTG to a final concentration of 1 mM. The cells were cultured for another 4 h, washed in cold 20 mM Tris, pH 7.5, (in 25% of the original volume) and stored at -80°C as a cell pellet.

Proteins were recovered from the cell pellet by adding 10 mL/g pellet of CellLytic™ B bacterial cell lysis extraction reagent (Sigma) plus complete protease inhibitor cocktail (EDTA-free, Roche) and subsequent incubation at RT for 20 min. After centrifuging at 25,000*g* (4°C), the soluble HIS-tagged proteins present in the supernatant were bound to 1 mL Ni-NTA superflow resin that had been pre-treated with 4 volumes of MilliQ water and 10 volumes of buffer [20 mM Tris-HCl, pH 7.9, 0.5 M NaCl] containing 5 mM imidazole. The resin was washed with 10 volumes of the buffer containing 20 mM imidazole and the protein was eluted with 4 volumes of the buffer containing 200 mM imidazole. The eluate was dialyzed against kinase storage buffer [25 mM Hepes, pH 7.5, 2 mM DTT, 50 mM KCl, 5% (v/v) glycerol] using Vivaspin 4 columns and stored in aliquots at -80°C. Protein concentrations were determined using the BCA reducing agent kit (Pierce) and kinase activity was determined from dilution series of the MAPK proteins as described above. The intensity of MBP phosphorylation quantified by phospho-imaging per µg of the different MAPK proteins (the specific activities), show a ratio of 8 : 5 : 40 : 4 for rLeMPK1 : rLeMPK2 : rLeMPK3 : rAtMPK6, respectively. Non-active control rLeMPK3* was obtained by storage of the eluted protein in elution buffer instead of kinase storage buffer.

Immunoblot analysis

Proteins present in extracts obtained as described for the in-gel kinase assays or recombinant MAPK proteins were separated on 10% SDS-PAGE gels and transferred to polyvinylidene difluoride (PVDF) membranes (Bio-Rad). For detection of phosphorylated tyrosine (pY) in recombinant MAPKs, membranes were blocked in 50 mM Tris, pH 7.5, 150 mM NaCl, 0.1% (w/v) Tween-20 and 3% BSA and incubated with 1:2,000 diluted monoclonal Phospho-Tyrosine IgG (CST #9411) in the same solution o/n. After three washes with 50 mM Tris, pH 7.5, 150 mM NaCl and 0.1% (w/v) Tween-20, the membranes were incubated with HRP-linked anti-mouse IgG, (1:3,000 diluted) (CST #7076) and developed using the ECL detection kit (Pierce).

PepChip Kinomics® slide analysis

PepChip Kinomics® slides (Pepscan, NL) are spotted with a triplicate set of 976 peptides (excluding controls) that resemble experimentally verified phosphorylation sites for human kinases (PhosphoBase) and their original surrounding residues (sequences available at: http://www.pepscan.nl/index5.htm). The peptides mostly consist of 11 amino acids of which the central position is the putative phosphorylation site. Six peptides are spotted that consist of only 9 or 10 amino acids in which the phosphorylation site is not centralized.

For the incubation of the PepChips, respectively 11, 3.6, 0.8 and 1.1 µg (representing equal kinase activities) of purified rLeMPK1, rLeMPK2, rLeMPK3 or rAtMPK6 protein in kinase storage buffer was mixed with 5 µl of ^{33}P-γ-ATP (3000 Ci/mmol; 50 µCi/PepChip) in a final volume of 30 µl and added to 30 µl of 2x PepChip Mastermix [40 mM Hepes, pH 7.5, 30 mM $MgCl_2$, 4 mM EGTA, 2 mM DTT, 40% (v/v) glycerol, 0.02 mg/mL BSA, 0.02% (v/v) Brij-35 and 0.56 mM ATP]. The mix was brought onto a cover slide after which the PepChip was posed over the sample and turned around. The PepChip was incubated for 4 h at 30°C in a closed box with wet paper to prevent drying of the chip. The cover slides were rinsed off the PepChip with TBST [50 mM Tris, pH 7.5, 150 mM NaCL, 0.02 % Tween-20] and the PepChips were washed twice with 2 M NaCl, once with 2 M Urea, twice with 10% SDS and three times with MilliQ water in a washing tube (provided with the PepChips) by manual shaking. Phosphorylation intensity of the various spotted peptides was determined by phospho-imaging (50 micron scan resolution) and quantitative values were obtained with ImageQuant software by adding the numerical values of each pixel within a prescribed area

(=spot), subtracted by the background value. Data were exported and collected in a Microsoft Excel worksheet and the average phosphorylation intensity per set was calculated after which the sets were normalized. In addition, the data obtained from the different PepChips were normalized based on the average PepChip phosphorylation intensity.

The average phosphorylation intensity from the triplicates was calculated for each peptide and peptides with an average phosphorylation intensity equal to, or higher than, 1.5 times the average PepChip phosphorylation intensity were selected for further phosphorylation pattern analysis (referred to as phosphorylated peptides; approximately 10% of all peptides). Phosphorylated peptides with a standard deviation exceeding 1.5 times the average PepChip phosphorylation intensity were removed from the dataset. The subset of non-phosphorylated peptides represents the peptides that had a phosphorylation intensity of zero (approximately 10% of all peptides). Significant differences between the sequences of the phosphorylated and non-phosphorylated peptides were calculated by Two Sample Logo software with a t-test ($P \leq 0.05$), and TSL-plots were drawn (Crooks *et al.*, 2004).

Sequences of the phosphorylated peptides were combined in subsets based on common phosphorylation by one or more LeMPKs and TEIRESIAS software (Rigoutsos and Floratos, 1998) calculated phosphorylation motifs in these sequences. Peptides phosphorylated by AtMPK6 were combined in subsets based on the overlapping phosphorylation with LeMPK1. Calculated phosphorylation motifs present in at least 40% of the sequences in the respective subset were included in Table II. Motifs indicated in Table II as not being phosphorylated were absent in the motif prediction for the respective kinase.

Virus-induced gene silencing (VIGS) of LeMPKs in tomato

The tobacco rattle virus-based binary VIGS vectors TRV:RNA1 and TRV:RNA2 (pYL156) have been described before (Liu *et al.*, 2002a; Liu *et al.*, 2002b). For TRV:LeMPK construction, the following primers were used to PCR amplify *LeMPK* sequences of genomic DNA isolated from MM-Cf0 tomato (*Bam*HI (forward) and *Acc*65I (reverse) sites are underlined): for *LeMPK1* (forward: 5'-CAGGATCCATAATTGCTGACAGATTGTTGCAG-3'; reverse: 5'-CAGGTACCGTACTCGCTCGTTTGCTGTTGGAT-3'), for *LeMPK2* (forward: 5'-CAGGATCCCAGTTCTTCTCTTGCTTACCTAGT-3'; reverse: 5'-CAGGTACCCTCTCCATACATAAGTCAGCTTC-3') and for *LeMPK3* (forward: 5'-CAGGTACCTGAACCACTTTCTTGGAGTACAG-3'; reverse: 5'-

CAGGTACCACACAAGCTAGCCCGAACACCAC-3'). This resulted in fragments of 166, 199 and 205 base pairs corresponding to the 3' UTR region of LeMPK1, -2 and -3 respectively. The fragments were ligated into *Bam*HI/*Acc*65I-digested TRV:RNA2 and the resulting TRV:LeMPK constructs were transformed to *Agrobacterium tumefaciens* strain GV3101. Construction of TRV:GFP, TRV:Cf-4 and TRV:PDS was described previously (Gabriëls *et al.*, 2007; Liu *et al.*, 2002b). For VIGS, cultures of *A. tumefaciens* containing TRV:RNA1 were mixed 1:1 with the various TRV:LeMPK cultures to an OD of 1.0 and infiltrated in cotyledons of ten-day-old tomato seedlings. In each experiment, four plants were infiltrated per TRV:LeMPK construct. Phytoene desaturase (PDS)-silenced plants, that develop white patches on the leaflets upon successful silencing, were used to visually monitor the development of the silencing process.

Assessment of Avr4-induced HR development and statistical analysis

Three weeks after agroinfiltration of the VIGS constructs, leaflets of comparable compound leaves were injected parallel to the midvein with 150 µg/mL *Pichia pastoris*-produced His-FLAG-Avr4 protein (Rooney *et al.*, 2005), using a micro-syringe (Ito Corporation, Fuji). Per day, two leaflets of four plants were injected at ten sites and each plant was injected on four different days (80 sites per plant, resulting in 320 sites per pTRV:LeMPK construct per experiment). The experiment was repeated five times. After 4 to 7 days the number of sites per leaflet showing HR, visible as necrosis, was scored. An arcsin$\sqrt{x}$ transformation was performed to obtain a normally distributed dataset. The data were analyzed with a split-plot design analysis of variance, after which multiple comparisons of all constructs were performed with a Student-Newman-Keuls test in Genstat (Version 8.1.0.155, VSN International Ltd).

***C. fulvum* inoculations and GUS staining**

A strain of *C. fulvum* race 5, expressing *Avr4* and containing a *pGPD::GUS* transgene, which contains the β-glucuronidase gene under control of the constitutive *GPD* promoter, was sub-cultured on 2% (w/v) potato dextrose agar to which 1.5% (w/v) technical agar was added. Conidia were obtained from ten-day-old plates, washed three times in water by centrifuging (4,000*g*) and decanting the supernatant and diluted to 6 x 10^5 spores/mL water. Plants were dip-inoculated three weeks after agroinfiltration with the VIGS constructs described above

and were kept in closed cages covered with transparent plastic for 2 days. Two weeks after inoculation, two to four leaflets were harvested and vacuum-infiltrated with X-gluc buffer [0.1 M NaPi, pH 7.0, 1% (v/v) Triton X100, 1% (v/v) DMSO, 10 mM EDTA and 1 mg/mL 5-bromo-4-chloro-3-indoxyl-beta-D-glucuronic acid sodium salt (X-gluc)]. Leaves were incubated overnight in the dark at 37°C and destained with 70% ethanol at RT after which photographs were taken using an Axioskop Zeiss microscope equipped with a Coolsnap camera. This experiment was repeated five times.

Confirmation of *MAPK* silencing

Disks with a diameter of 1.5 cm were taken close to the midvein from different leaflets at 4 (HR assays) or 6 (*C. fulvum*-inoculation studies) weeks after TRV-inoculation of plants of which the other leaflets were used for HR-scoring or GUS-analysis, respectively. Punching leaf disks allows for a targeted sampling in regions that probably have the most pronounced silencing, based on the PDS results. The leaf disks were floated on water for 15 minutes to allow MAPK activation by the wound response from punching the disks and to prevent the leaf disks from desiccating (Menke *et al.*, 2004). Leaf disks were individually analyzed for total inducible LeMPK activity by in gel kinase assays. For extracts that showed decreased LeMPK activity in the in-gel kinase assays, the activity of LeMPK1, -2 and -3 was determined by immunocomplex kinase assays. This experiment was repeated three times.

ACKNOWLEDGMENTS

We thank D. Klessig and S. Zhang for the pET28a+-AtMPK6 construct, G. van den Berg for cloning the TRV:LeMPK constructs, H. Smid for horticultural assistance and M. Hartog of the department of Molecular Biology (WUR) for the use of the phospho-imager.

REFERENCES

Alvarez ME, Pennell RI, Meijer PJ, Ishikawa A, Dixon RA, Lamb C (1998) Reactive oxygen intermediates mediate a systemic signal network in the establishment of plant immunity. Cell 92: 773-784.

Andreasson E, Jenkins T, Brodersen P, Thorgrimsen S, Petersen NHT, Zhu S, Qiu J, Micheelsen P, Rocher A, Petersen M, Newman M, Nielsen HB, Hirt H, Somssich I, Mattsson O, Mundy J (2005) The MAP kinase substrate MKS1 is a regulator of plant defence responses. EMBO J 24: 2579-2589.

Cai X, Takken FLW, Joosten MHAJ, De Wit PJGM (2001) Specific recognition of AVR4 and AVR9 results in distinct patterns of hypersensitive cell death in tomato, but similar patterns of defence-related gene expression. Mol Plant Pathol 2: 77-86.

Chisholm ST, Coaker G, Day B, Staskawicz BJ (2006) Host-microbe interactions: shaping the evolution of the plant immune response. Cell 124: 803-814.

Crews CM, Alessandrini AA, Erikson RL (1991) Mouse *Erk-1* gene product is a serine/threonine protein kinase that has the potential to phosphorylate tyrosine. Proc Natl Acad Sci USA 88: 8845-8849.

Crooks GE, Hon G, Chandonia JM, Brenner SE (2004) WebLogo: A sequence logo generator. Genome Res 14: 1188-1190.

De Jong CF, Honée G, Joosten MHAJ, De Wit PJGM (2000) Early defence responses induced by AVR9 and mutant analogues in tobacco cell suspensions expressing the *Cf-9* resistance gene. Physiol Mol Plant Pathol 56: 169-177.

De Jong CF, Takken FLW, Cai X, De Wit PJGM, Joosten MHAJ (2002) Attenuation of Cf-mediated defence responses at elevated temperatures correlates with a decrease in elicitor-binding sites. Mol Plant Microbe Interact 15: 1040-1049.

Del Pozo O, Lam E (1998) Caspases and programmed cell death in the hypersensitive response of plants to pathogens. Curr Biol 8: 1129-1132.

Del Pozo O, Pedley KF, Martin GB (2004) MAPKKKα is a positive regulator of cell death associated with both plant immunity and disease. EMBO J 23: 3072-3082.

Ekengren SK, Liu Y, Schiff M, Dinesh-Kumar SP, Martin GB (2003) Two MAPK cascades, NPR1, and TGA transcription factors play a role in Pto-mediated disease resistance in tomato. Plant J 36: 905-917.

Feilner T, Hultschig C, Justin L, Meyer S, Immink RGH, Koenig A, Possling A, Seitz H, Beveridge A, Scheel D, Cahill DJ, Lehracht H, Kreutzberger J, Kersten B (2005) High throughput identification of potential *Arabidopsis* mitogen-activated protein kinases substrates. Mol Cell Proteomics 4: 1558-1568.

Flor HH (1942) Inheritance of pathogenicity in *Melampsora lini*. Phytopathology 32: 653-669.

Gabriëls SHEJ, Takken FLW, Vossen JH, De Jong CF, Turk SC, Wachowski LK, Peters J, Witsenboer HMA, De Wit PJGM, Joosten MHAJ (2006) cDNA-AFLP combined with functional analysis reveals novel genes involved in the hypersensitive response. Mol Plant-Microbe Interact 19: 567-576.

Gabriëls SHEJ, Vossen JH, Ekengren SK, Van Ooijen G, Abd-El-Haliem AM, Van den Berg GCM, Rainey DY, Martin GB, Takken FLW, De Wit PJGM, Joosten MHAJ (2007) An NB-LRR protein required for HR signalling mediated by both extra- and intracellular resistance proteins. Plant J 50: 14-28.

Hamel LP, Nicole M, Sritubtim S, Morency M, Ellis M, Ehlting J, Beaudoin N, Barbazuk B, Klessig D, Lee J, Martin GB, Mundy J, Ohashi Y, Scheel D, Sheen J, Xing T, Zhang S, Seguin A, Ellis BE (2006) Ancient signals: comparative genomics of plant MAPK and MAPKK gene families. Trends Plant Sci 11: 192-198.

Higgins R, Lockwood T, Holley S, Yalamanchili R, Stratmann JW (2006) Changes in the extracellular pH are neither required nor sufficient for activation of mitogen-activated protein kinases (MAPKs) in response to systemin and fusicoccin in tomato. Planta 225: 1535-1546.

Holley SR, Yalamanchili RD, Moura DS, Ryan CA, Stratmann JW (2003) Convergence of signalling pathways induced by systemin, oligosaccharide elicitors, and ultraviolet-B radiation at the level of mitogen-activated protein kinases in *Lycopersicon peruvianum* suspension-cultured cells. Plant Physiol 132: 1728-1738.

Ichimura K, Shinozki K, Tena G, Sheen J, Henry Y, Champion A, Kreis M, Zhang S, Hirt H, Wilson C, Heberle-Bors E, Ellis BE, Morris PC, Innes RW, Ecker JR, Scheel D, Klessig DF, Machida Y, Mundy J, Ohashi Y, Walker JC (2002) Mitogen-activated protein kinase cascades in plants: a new nomenclature. Trends Plant Sci 7: 301-308.

Ichimura K, Casais C, Peck SC, Shinozaki K, Shirasu K (2006) MEKK1 is required for MPK4 activation and regulates tissue-specific and temperature-dependent cell death in Arabidopsis. J Biol Chem 281: 36969-36976.

Jin H, Liu Y, Yang K, Kim CY, Baker B, Zhang S (2003) Function of a mitogen-activated protein kinase pathway in *N* gene-mediated resistance in tobacco. Plant J 33: 719-731.

Jones JDG, Dangl JL (2006) The plant immune system. Nature 444: 323-329.

Krens SFG, Spaink HP, Snaar-Jagalska E (2006) Functions of the MAPK family in vertebrate-development. FEBS Lett 580: 4984-4990.

Lee S, Hirt H, Lee Y (2001) Phosphatidic acid activates a wound-activated MAPK in *Glycine max*. Plant J 26: 479-486.

Li Q, Xie Q, Smith-Becker J, Navarre DA, Kaloshian I (2006) *Mi-1*-mediated aphid resistance involves salicylic acid and mitogen-activated protein kinase signalling cascades. Mol Plant Microbe Interact 6: 655-664.

Liu Y, Schiff M, Marathe R, Dinesh-Kumar SP (2002a) Tobacco Rar1, EDS1 and NPR1/NIM1 like genes are required for N-mediated resistance to tobacco mosaic virus. Plant J 30: 415-429.

Liu Y, Schiff M, Dinesh-Kumar SP (2002b) Virus-induced gene silencing in tomato. Plant J 31: 777-786.

Liu Y, Zhang S (2004) Phosphorylation of 1-aminocyclopropane-1-carboxylic acid synthase by MPK6, a stress-responsive mitogen-activated protein kinase, induces ethylene biosynthesis in *Arabidopsis*. Plant Cell 16: 3386-3399.

Mayrose M, Bonshtien A, Sessa G (2004) LeMPK3 is a mitogen-activated protein kinase with dual specificity induced during tomato defence and wounding responses. J Biol Chem 279: 14819-14827.

Menke FLH, Van Pelt JA, Pieterse CMJ, Klessig DF (2004) Silencing of the mitogen-activated protein kinase MPK6 compromises disease resistance in *Arabidopsis*. Plant Cell 16: 897-907.

Menke FLH, Kang H, Chen Z, Park JM, Kumar D, Klessig DF (2005) Tobacco transcription factor WRKY1 is phosphorylated by the MAP kinase SIPK and mediates HR-like cell death in tobacco. Mol Plant Microbe Interact 18: 1027-1034.

Mészáros T, Helfer A, Hatzimasoura E, Magyar Z, Serazetdinova L, Rios G, Bardóczy V, Teige M, Koncz C, Peck S, Bögre L (2006) The Arabidopsis MAP kinase kinase MKK1 participates in defence responses to the bacterial elicitor flagellin. Plant J 48: 485-498.

Mishra NS, Tuteja R, Tuteja N (2006) Signalling through MAP kinase networks in plants. Arch Biochem Biophys 452: 55-68.

Nakagami H, Pitzschke A, Hirt H (2005) Emerging MAP kinase pathways in plant stress signalling. Trends Plant Sci. 10: 339-349.

Page RDM (1996) TREEVIEW: An application to display phylogenetic trees on personal computers. Comput Appl Biosci 12: 357-358.

Pedley KF, Martin GB (2004) Identification of MAPKs and their possible MAPK kinase activators involved in the Pto-mediated defence response of tomato. J Biol Chem 279: 49229-49235.

Pedley KF, Martin GB (2005) Role of mitogen-activated protein kinases in plant immunity. Curr Opin Plant Biol 8: 541-547.

Rigoutsos I, Floratos A (1998) Combinatorial pattern discovery in biological sequences: the TEIRESIAS Algorithm. Bioinformatics 14: 55-67.

Rivas S, Thomas CM (2005) Molecular interactions between tomato and the leaf mold pathogen *Cladosporium fulvum*. Annu Rev Phytopathol 43: 395-436.

Romeis T, Piedras P, Zhang S, Klessig DF, Hirt H, Jones JDG (1999) Rapid Avr9- and Cf-9-dependent activation of MAP kinases in tobacco cell cultures and leaves: convergence of resistance gene, elicitor, wound, and salicylate responses. Plant Cell 11: 273-287.

Romeis T, Piedras P, Jones JDG (2000) Resistance gene-dependent activation of a calcium-dependent protein kinase in the plant defence response. Plant Cell 12: 803-816.

Rooney HCE, Van't Klooster JW, Van der Hoorn RAL, Joosten MHAJ, Jones JDG, De Wit PJGM (2005) Cladosporium Avr2 inhibits tomato Rcr3 protease required for *Cf-2*-dependent disease resistance. Science 308: 1783-1786.

Schwartz D, Gygi SP (2005) An iterative statistical approach to the identification of protein phosphorylation motifs from large-scale data sets. Nature Biotech 23: 1391-1398.

Sharma PC, Ito A, Shimizu T, Terauchi R, Kamoun S, Saitoh H (2003) Virus-induced silencing of WIPK and SIPK genes reduces resistance to a bacterial pathogen, but has no effect on the INF1-induced hypersensitive response (HR) in *Nicotiana benthamiana*. Mol Genet Genomics 269: 583-591.

Shibuya EK, Boulton TG, Cobb MH, Ruderman JV (1992) Activation of p42 MAP kinase and the release of oocytes from cell cycle arrest. EMBO J. 11: 3963-3975.

Song D, Chen J, Song F, Zheng Z (2006) A novel rice MAPK gene, *OsBIMK2*, is involved in disease-resistance responses. Plant Biol 8: 587-596.

Thomas CM, Jones DA, Parniske M, Harrison K, Balint-Kurti PJ, Hatzixanthis K, Jones JDG (1997) Characterization of the tomato *Cf-4* gene for resistance to *Cladosporium fulvum* identifies sequences that determine recognitional specificity in *Cf-4* and *Cf-9*. Plant Cell 9: 2209-2224.

Thomma BPHJ, Van Esse HP, Crous PW, De Wit PJGM (2005) *Cladosporium fulvum* (syn. *Passalora fulva*), a highly specialized plant pathogen as a model for functional studies on plant pathogenic *Mycosphaerellaceae*. Mol Plant Pathol 6: 379-393.

Thompson JD, Gibson TJ, Plewniak F, Jeanmougin F, Higgins DG (1997) The ClustalX windows interface: flexible strategies for multiple sequence alignement aided by quality analysis tools. Nucleic Acids Res 24: 4876-4882.

Torres MA, Jones JDG, Dangl JL (2005) Pathogen-induced, NADPH oxidase-derived reactive oxygen intermediates suppress spread of cell death in *Arabidopsis thaliana*. Nature 37: 1130-1134.

Yamamizo C, Kuchimura K, Kobayashi A, Katou S, Kawakita K, Jones JDG, Doke N, Yoshioka H (2006) Rewiring mitogen-activated protein kinase cascade by positive feedback confers potato blight resistance. Plant Physiol 140: 681-692.

Zhang S, Klessig DF (2001) MAPK cascades in plant defence signalling. Trends Plant Sci 15: 2285-2295.

Zhang T, Yang T, Zhang L, Xu S, Xue L, An L (2006) Diverse signals converge at MAPK cascades in plant. Plant Physiol Biochem 44: 274-283.

SUPPLEMENTARY DATA

Supplementary Figure S1. Monitoring systemic HR development in a Cf-4/Avr4 seedling after a temperature shift.

The video, which can be seen at http://www.planphysiol.org/cgi/content/full/pp.107.101063/DC1, shows the development of systemic HR over a five-day period in a Cf-4/Avr4 seedling (left). A control MM-Cf-4 seedling is shown on the right. Plants were incubated at 33°C and subsequently transferred to 20°C at t=0 days to initiate the Cf-4/Avr4-induced HR. The unaffected MM-Cf-4 seedling is representative for both *Cf-4*- and *Avr4*-containing seedlings.

Representative images from the video are printed above the odd numbered pages of this thesis. An impression of the video can be obtained by flapping this book from start to end.

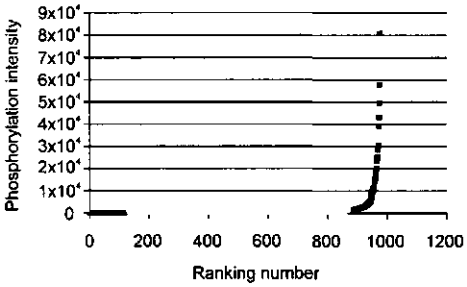

Supplementary Figure S2. Phosphorylation intensities of the rLeMPK1-phosphorylated and non-phosphorylated peptides.

Average phosphorylation intensities (from the triplicates on one slide) of each of the 976 peptides were sorted from low to high and a corresponding ranking number was assigned. Peptides with an average phosphorylation intensity equal to, or higher than, 1.5 times the average overall phosphorylation intensity are represented by the black dots (referred to as phosphorylated peptides). Peptides with an average phosphorylation intensity of zero are represented by the dark grey dots (referred to as non-phosphorylated peptides). These two subsets of peptides were selected for further analysis. Similar graphs were obtained for rLeMPK2, -3 and rAtMPK6 and subsets of peptides were selected for further analysis in a similar way.

Supplementary Figure S3. Alignment of the MAPK protein sequences (See following pages).

Protein sequences encoded by the ORF of 16 *LeMPK* homologues identified in databases were aligned using ClustalX with the sequences encoded by the ORFs of AtMPK1 to -20 from Arabidopsis, NtSIPK, NtWIPK, NtNTF4 and NtNTF6 from *N. tabacum*, and the *H. sapiens* HsERK1. See Materials and Methods for details.

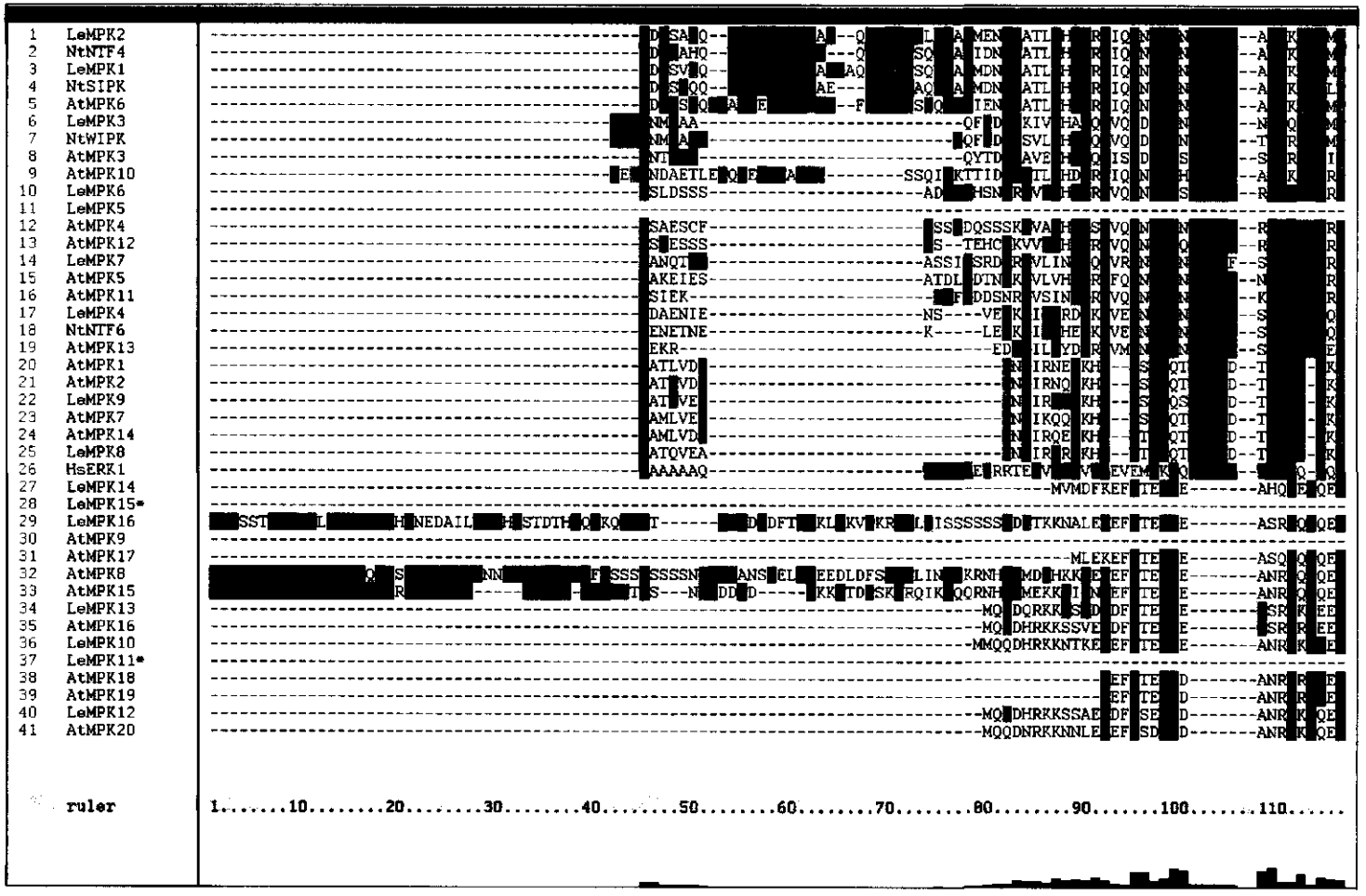
1 LeMPK2
2 NtNTF4
3 LeMPK1
4 NtSIPK
5 AtMPK6
6 LeMPK3
7 NtWIPK
8 AtMPK3
9 AtMPK10
10 LeMPK6
11 LeMPK5
12 AtMPK4
13 AtMPK12
14 LeMPK7
15 AtMPK5
16 AtMPK11
17 LeMPK4
18 NtNTF6
19 AtMPK13
20 AtMPK1
21 AtMPK2
22 LeMPK9
23 AtMPK7
24 AtMPK14
25 LeMPK8
26 HsERK1
27 LeMPK14
28 LeMPK15*
29 LeMPK16
30 AtMPK9
31 AtMPK17
32 AtMPK8
33 AtMPK15
34 LeMPK13
35 AtMPK16
36 LeMPK10
37 LeMPK11*
38 AtMPK18
39 AtMPK19
40 LeMPK12
41 AtMPK20
ruler
1.....10.....20.....30.....40.....50.....60.....70.....80.....90.....100.....110.....

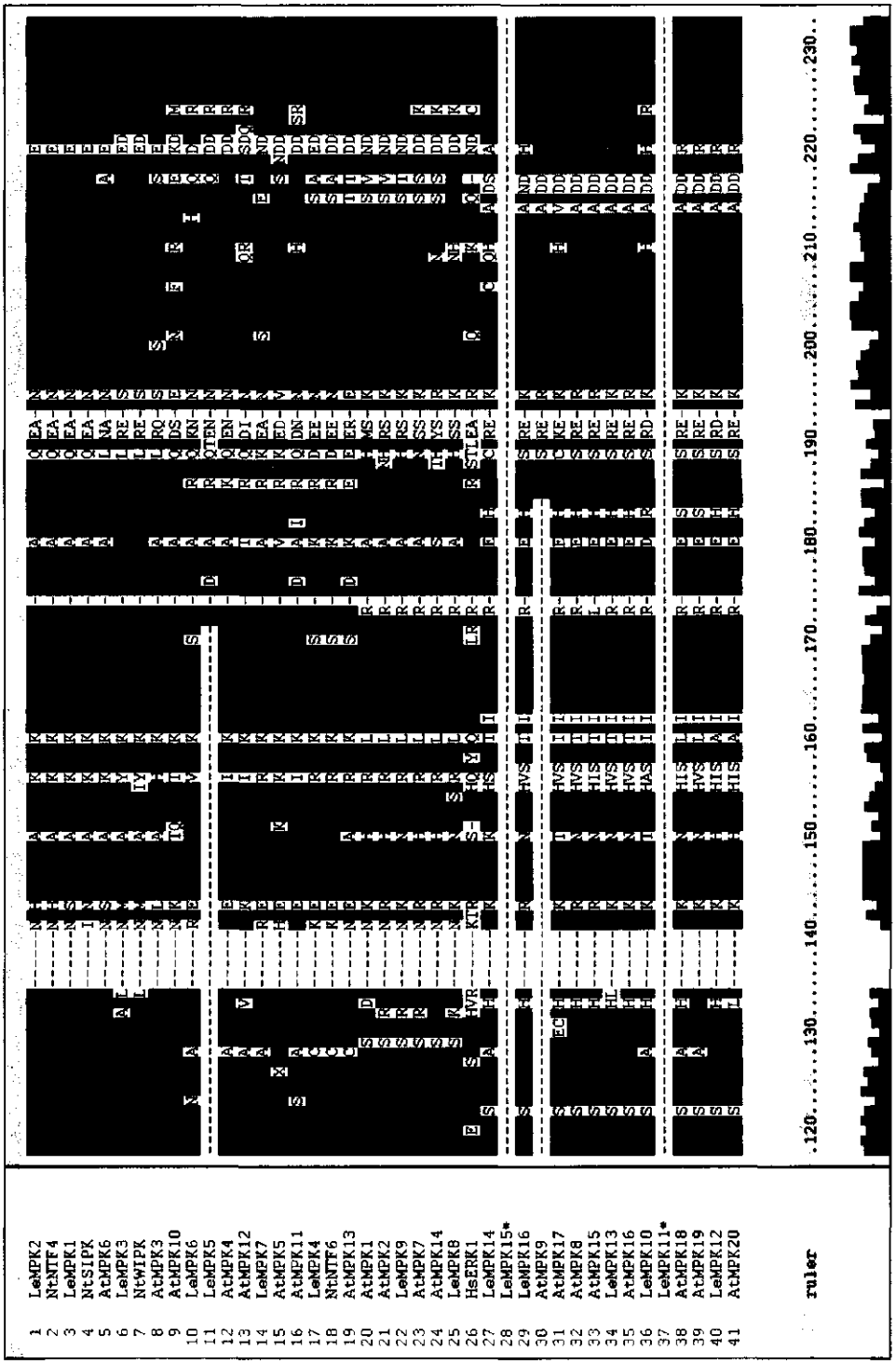
1 LeMPK2
2 NtNTF4
3 LeMPK1
4 NtSIPK
5 AtMPK6
6 LeMPK3
7 NtWIPK
8 AtMPK3
9 AtMPK10
10 LeMPK5
11 LeMPK4
12 AtMPK4
13 AtMPK12
14 LeMPK7
15 AtMPK5
16 AtMPK11
17 LeMPK4
18 NtNTF6
19 AtMPK13
20 AtMPK1
21 AtMPK2
22 LeMPK9
23 AtMPK7
24 AtMPK14
25 LeMPK8
26 HsERK1
27 LeMPK14
28 LeMPK15*
29 LeMPK16
30 AtMPK9
31 AtMPK17
32 AtMPK8
33 AtMPK15
34 LeMPK13
35 AtMPK16
36 LeMPK10
37 LeMPK11*
38 AtMPK18
39 AtMPK19
40 LeMPK12
41 AtMPK20
ruler
120
130
140
150
160
170
180
190
200
210
220
230

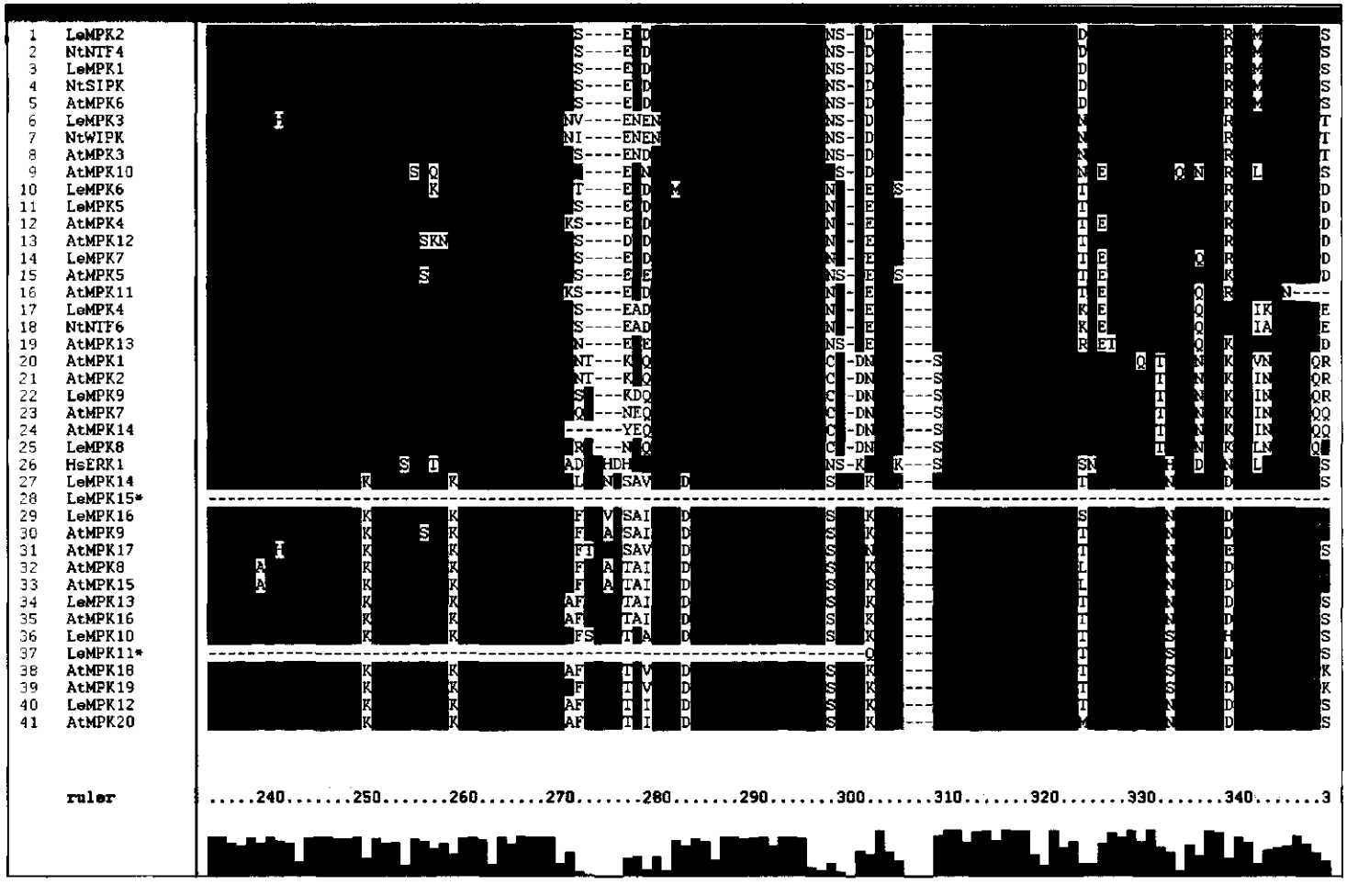
1 LeMPK2
2 NtNTF4
3 LeMPK1
4 NtSIPK
5 AtMPK6
6 LeMPK3
7 NtWIPK
8 AtMPK3
9 AtMPK10
10 LeMPK6
11 LeMPK5
12 AtMPK4
13 AtMPK12
14 LeMPK7
15 AtMPK5
16 AtMPK11
17 LeMPK4
18 NtNTF6
19 AtMPK13
20 AtMPK1
21 AtMPK2
22 LeMPK9
23 AtMPK7
24 AtMPK14
25 LeMPK8
26 HsERK1
27 LeMPK14
28 LeMPK15*
29 LeMPK16
30 AtMPK9
31 AtMPK17
32 AtMPK8
33 AtMPK15
34 LeMPK13
35 AtMPK16
36 LeMPK10
37 LeMPK11*
38 AtMPK18
39 AtMPK19
40 LeMPK12
41 AtMPK20
ruler
.....240.....250.....260.....270.....280.....290.....300.....310.....320.....330.....340.....3

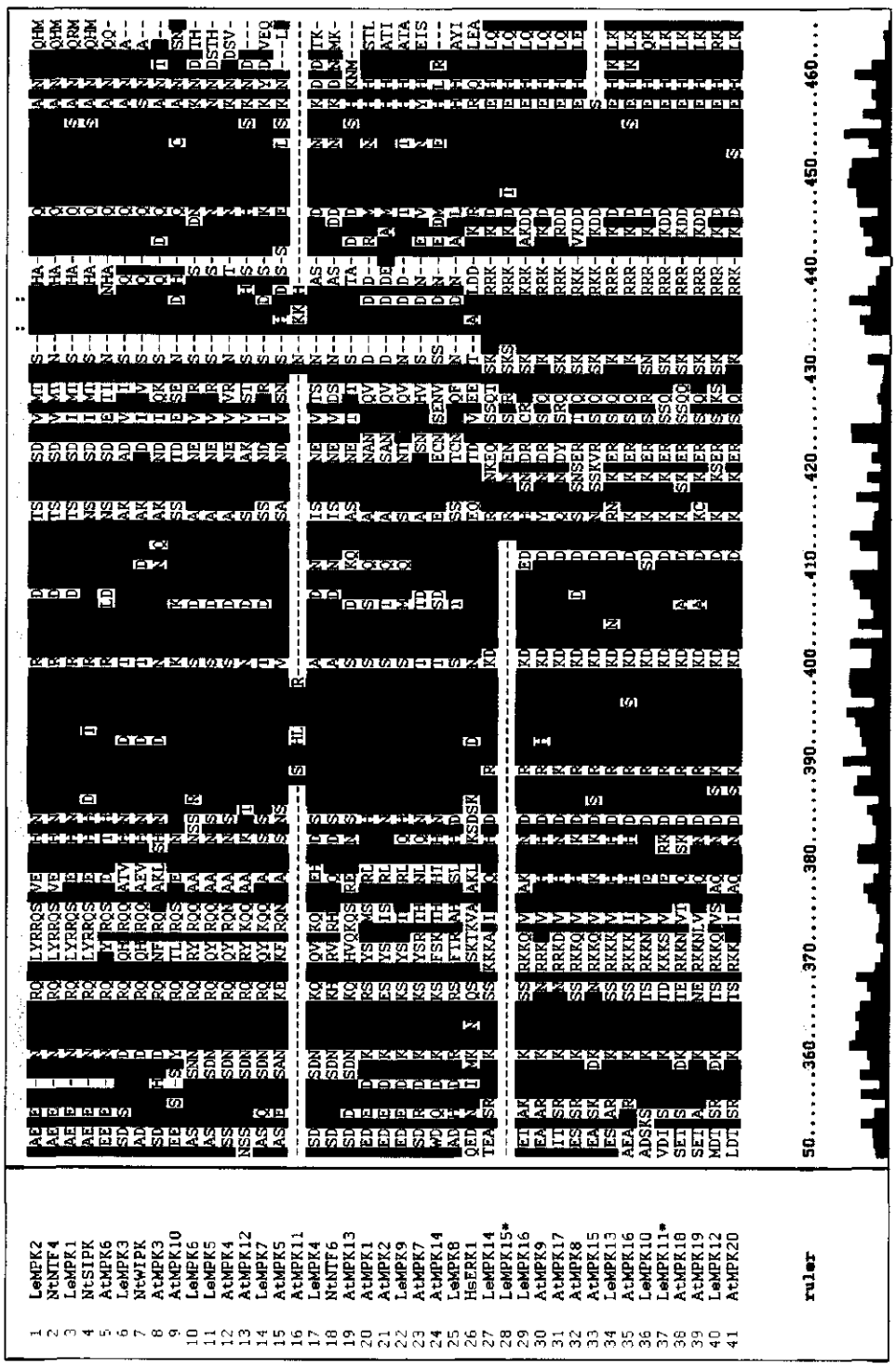
1 LeMPK2
2 NtNTF4
3 LeMPK1
4 NtSIPK
5 AtMPK6
6 LeMPK3
7 NtWIPK
8 AtMPK3
9 AtMPK10
10 LeMPK6
11 LeMPK5
12 AtMPK4
13 AtMPK12
14 LeMPK7
15 AtMPK5
16 AtMPK11
17 LeMPK4
18 NtNTF6
19 AtMPK13
20 AtMPK1
21 AtMPK2
22 LeMPK9
23 AtMPK7
24 AtMPK14
25 LeMPK8
26 HsERK1
27 LeMPK14
28 LeMPK15*
29 LeMPK16
30 AtMPK9
31 AtMPK17
32 AtMPK8
33 AtMPK15
34 LeMPK13
35 AtMPK16
36 LeMPK10
37 LeMPK11*
38 AtMPK18
39 AtMPK19
40 LeMPK12
41 AtMPK20
ruler
50.....360.....370.....380.....390.....400.....410.....420.....430.....440.....450.....460.....

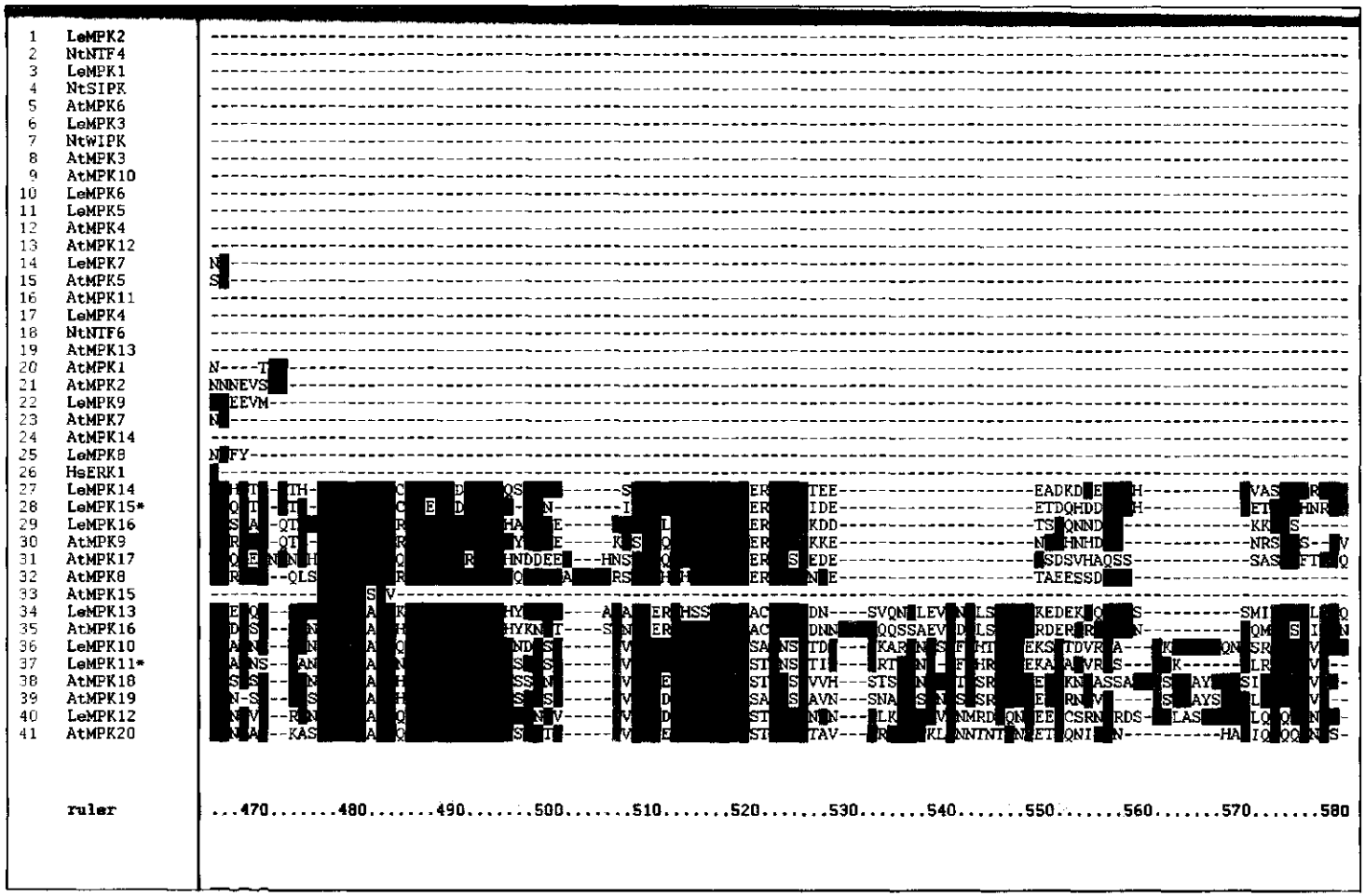
1 LeMPK2
2 NtNTF4
3 LeMPK1
4 NtSIPK
5 AtMPK6
6 LeMPK3
7 NtWIPK
8 AtMPK3
9 AtMPK10
10 LeMPK6
11 LeMPK5
12 AtMPK4
13 AtMPK12
14 LeMPK7
15 AtMPK5
16 AtMPK11
17 LeMPK4
18 NtNTF6
19 AtMPK13
20 AtMPK1
21 AtMPK2
22 LeMPK9
23 AtMPK7
24 AtMPK14
25 LeMPK8
26 HsERK1
27 LeMPK14
28 LeMPK15*
29 LeMPK16
30 AtMPK9
31 AtMPK17
32 AtMPK8
33 AtMPK15
34 LeMPK13
35 AtMPK16
36 LeMPK10
37 LeMPK11*
38 AtMPK18
39 AtMPK19
40 LeMPK12
41 AtMPK20
ruler
...470.....480.....490.....500.....510.....520.....530.....540.....550.....560.....570.....580

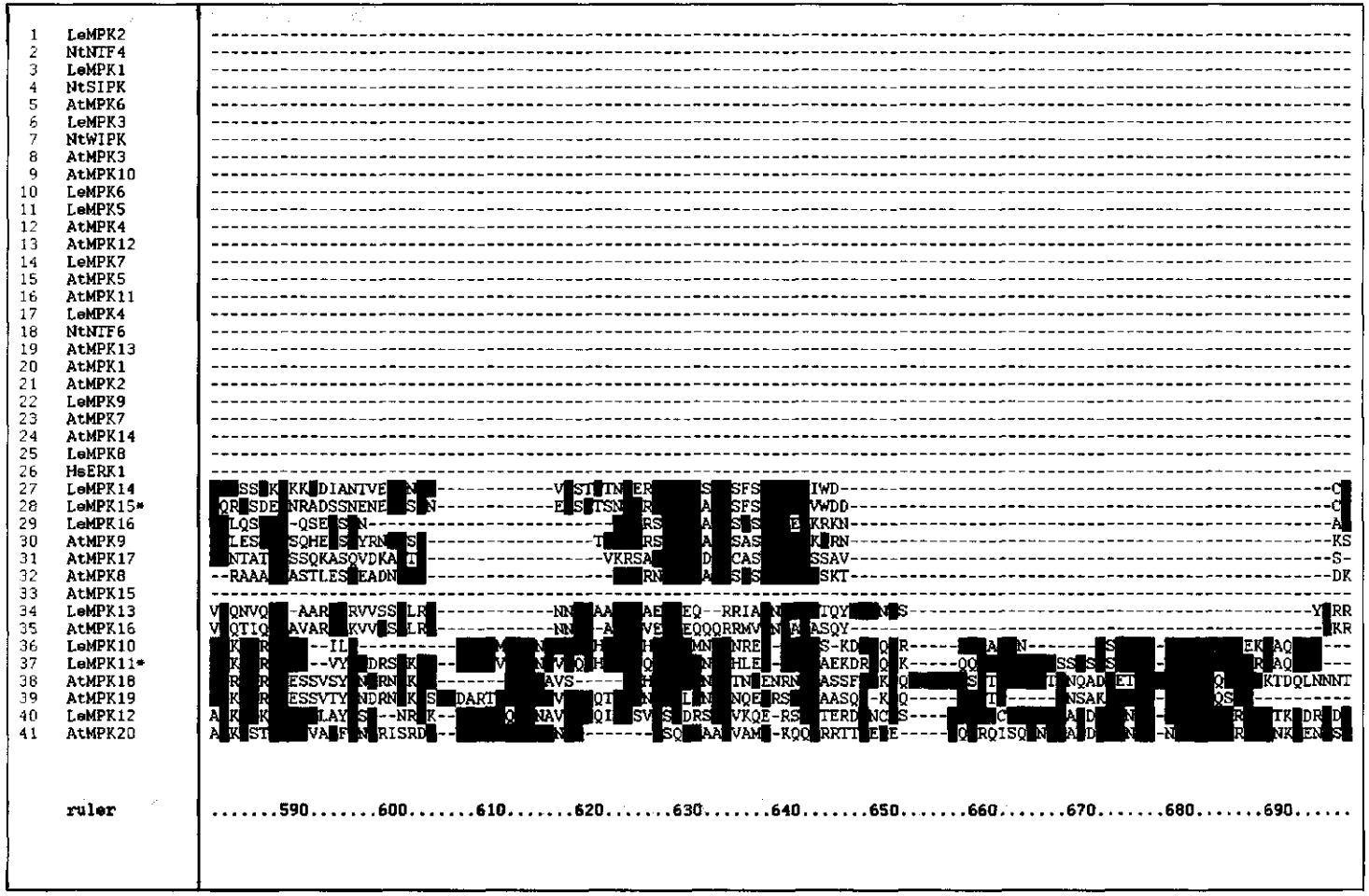
1 LeMPK2
2 NtNTF4
3 LeMPK1
4 NtSIPK
5 AtMPK6
6 LeMPK3
7 NtWIPK
8 AtMPK3
9 AtMPK10
10 LeMPK6
11 LeMPK5
12 AtMPK4
13 AtMPK12
14 LeMPK7
15 AtMPK5
16 AtMPK11
17 LeMPK4
18 NtNTF6
19 AtMPK13
20 AtMPK1
21 AtMPK2
22 LeMPK9
23 AtMPK7
24 AtMPK14
25 LeMPK8
26 HsERK1
27 LeMPK14
28 LeMPK15*
29 LeMPK16
30 AtMPK9
31 AtMPK17
32 AtMPK8
33 AtMPK15
34 LeMPK13
35 AtMPK16
36 LeMPK10
37 LeMPK11*
38 AtMPK18
39 AtMPK19
40 LeMPK12
41 AtMPK20
ruler
.....590.....600.....610.....620.....630.....640.....650.....660.....670.....680.....690.....

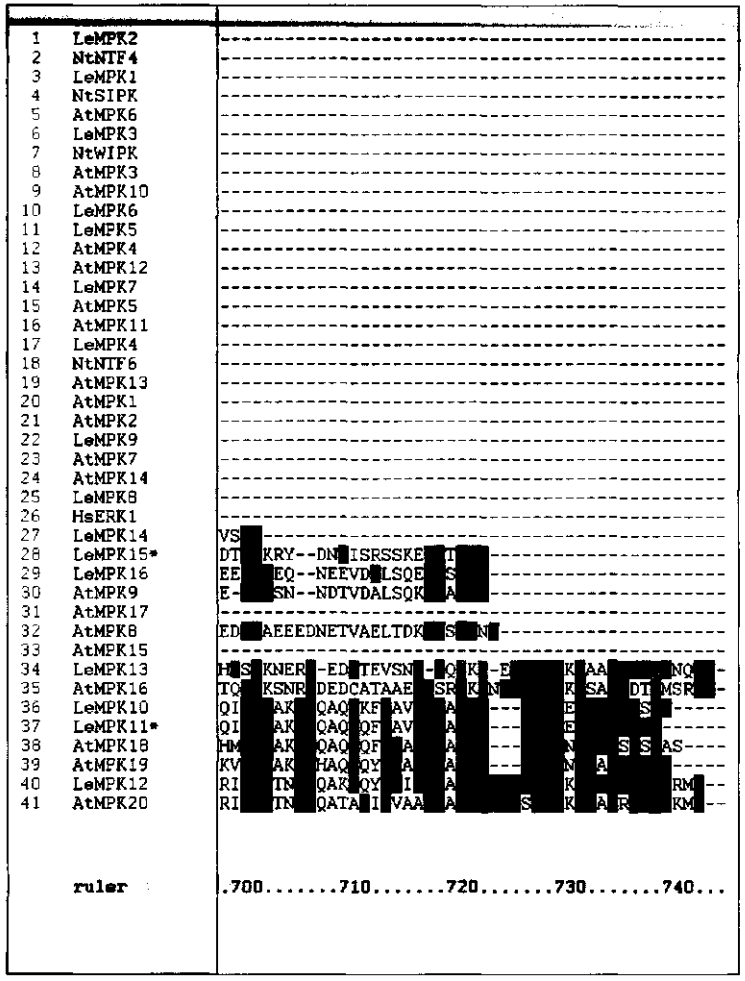
1 LeMPK2
2 NtNTF4
3 LeMPK1
4 NtSIPK
5 AtMPK6
6 LeMPK3
7 NtWIPK
8 AtMPK3
9 AtMPK10
10 LeMPK6
11 LeMPK5
12 AtMPK4
13 AtMPK12
14 LeMPK7
15 AtMPK5
16 AtMPK11
17 LeMPK4
18 NtNTF6
19 AtMPK13
20 AtMPK1
21 AtMPK2
22 LeMPK9
23 AtMPK7
24 AtMPK14
25 LeMPK8
26 HsERK1
27 LeMPK14
28 LeMPK15*
29 LeMPK16
30 AtMPK9
31 AtMPK17
32 AtMPK8
33 AtMPK15
34 LeMPK13
35 AtMPK16
36 LeMPK10
37 LeMPK11*
38 AtMPK18
39 AtMPK19
40 LeMPK12
41 AtMPK20
ruler
.700.....710.....720.....730.....740...

Chapter 4

Quantitative phosphoproteomics reveals a swift suppression of photosynthetic activity and a differential role for Hsp90 isoforms in tomato defence signalling

Iris J.E. Stulemeijer, Matthieu H.A.J. Joosten and Ole N. Jensen

A slightly modified version of this chapter has been submitted for publication.

SUMMARY

Plants are continuously exposed to pathogens. An important mechanism by which plants defend themselves is the rapid execution of a hypersensitive response (HR) to prevent colonization of its tissue by the pathogen. Tomato plants containing the Cf-4 resistance protein mount a HR that relies on the activation of phosphorylation cascades, when challenged with the Avr4 elicitor that is secreted by the pathogenic fungus *Cladosporium fulvum*. To study the phosphoproteome of leaf tissue undergoing a Cf-4/Avr4-induced HR, phosphopeptides were isolated from tomato seedlings expressing both Cf-4 and Avr4 and from control seedlings, at one, three and five hours after HR initiation using titanium dioxide columns. LC-MS/MS analysis of the phosphopeptides led to the identification of 50 phosphoproteins, most of which have not been described in tomato before. In addition, phosphopeptides were quantified using a relative label-free approach based on the MS peak areas, which was validated using a novel approach. Eventually, 13 phosphopeptides were identified with an altered abundance upon HR initiation as compared to control seedlings. These changes and additional experiments showed that photosynthetic activity is specifically suppressed in a phosphorylation-dependent way during the very early stages of HR development. In addition, a shift from aerobic to anaerobic respiration appears to occur in the Cf-4/Avr4 seedlings, which might be the result of oxygen depletion caused by the HR-associated oxidative burst. Furthermore, four Hsp90 isoforms are (de)phosphorylated to a different extent at one conserved phosphorylation site, suggesting that Hsp90 isoforms have a different function in defence signalling. Our data demonstrate that relative label-free quantification of the phosphoproteome of complex samples is feasible and extends our knowledge on the biochemistry and physiology of tomato plants undergoing HR.

INTRODUCTION

Plants are continuously exposed to all types of stress. To resist attacking pathogens, plants possess a primary and secondary line of active defence to prevent colonization. The primary defence response is triggered upon recognition of microbe-associated molecular patterns (MAMPs) by pattern recognition receptors. The secondary response is induced by

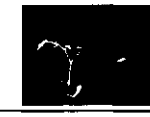

resistance (R) proteins that mediate recognition of specific pathogen-secreted effectors, which are required during pathogenesis (Jones and Dangl, 2006; De Wit, 2007). The latter response is commonly associated with a fast and highly effective hypersensitive-response (HR), which is a localized programmed cell death at the site of pathogen penetration. It is clear that when a resistant plant detects a pathogen, rapid defence signalling cascades need to be activated to prevent the pathogen from further proliferation and to avoid extensive damage. A rapid and reversible process that greatly increases protein dynamics in the cell is post-translational modification of proteins (Sun *et al.*, 2006; Chapter 2). Especially protein phosphorylation has been shown to play an important role in swift activation of defence signalling in plants (Xing *et al.*, 2002; Peck, 2003; Pedley and Martin, 2005). Phosphorylation mainly takes place on serine, threonine and tyrosine residues and can modulate the activity, subcellular localization, stability and/or three-dimensional structure of proteins. In addition, phosphorylation can affect interactions with other proteins and non-proteinaceous molecules (Sun *et al.*, 2006). Thus, phosphorylation-dependent signalling is required for an efficient and fast defence response that eventually determines the difference between host susceptibility and resistance.

So far, a few plant-pathogen interactions have been described in which phosphorylation events play an essential role during defence signalling. In some cases, phosphorylation already takes place at the site of signal perception. For example, the serine/threonine kinase domains of the resistance proteins Pto, FLS2 and Xa21, which mediate recognition of the bacterial effector AvrPto, the MAMP flagellin and an elicitor of the bacterium *Xanthomonas campestris* respectively, require (auto)phosphorylation to be functionally active (Sessa *et al.*, 2000b; Gómez-Gómez *et al.*, 2001; Mucyn *et al.*, 2006; Xu *et al.*, 2006). Signalling of most of these receptors leads to the phosphorylation of downstream components (Sessa *et al.*, 2000a; Devarenne *et al.*, 2006; Wang *et al.*, 2006) and triggers for example the mitogen-activated protein kinase (MAPK) cascade (Romeis *et al.*, 1999; Asai *et al.*, 2002; Pedley and Martin, 2005; Suarez-Rodriguez *et al.*, 2007). In addition, several other signalling components become (de)phosphorylated, such as calcium-dependent protein kinases (CDPKs) (Romeis *et al.*, 2001; Cheng *et al.*, 2002) and the basal defence inhibitor RIN4 that interacts with the R proteins RPM1 and RPS2 in Arabidopsis (Kim *et al.*, 2005). These reports and the recent observation that effectors of successful pathogens intercept MAPK signalling cascades or target receptor kinases to block innate immunity (Shan *et al.*,

2007; Xiang *et al.*, 2008), indicate that phosphorylation plays a major role during early defence signalling.

Fortunately, many tools to study the phosphoproteome of a particular organism or a specific tissue have been developed over the last years. For example, protein or peptide arrays are available that can be used to identify downstream targets of activated kinases. These arrays are spotted with full length proteins or peptides that are potential kinase substrates and to reveal potential *in vivo* substrates they are incubated with the pure active kinase of interest, in the presence of radio-labelled phosphate (Feilner *et al.*, 2005; Ritsema *et al.*, 2007; Chapter 3). Although these studies provide new insight in potential downstream targets of kinases, they are restricted to only one or a few kinases that can be tested. Alternatively, a large-scale analysis of the radio-labelled phosphoproteome by two-dimensional electrophoresis allows to reveal changes in the phosphorylation pattern of many proteins upon pathogen recognition (Peck *et al.*, 2001; Nühse *et al.*, 2003a). Although this method is very sensitive and has a high resolution, protein identification remains difficult in most cases and is often time and resource consuming (Peck, 2006). To avoid these problems, analysis of the phosphoproteome by liquid chromatography coupled to tandem mass spectrometry (LC-MS/MS) is a rapidly developing technique. Several protocols have been developed to specifically separate the phosphoproteome from the complete protein pool (Nühse *et al.*, 2003b; Nühse *et al.*, 2004; Gruhler *et al.*, 2005; Larsen *et al.*, 2005; Reinders and Sickmann, 2005), allowing detection of low abundant phosphopeptides. The technical specifications of the latest mass spectrometers allow very accurate identification of sets of phosphopeptides and even of the exact phosphorylation site of the protein. Eventually, the dynamics of phospho-regulation upon perception of a stimulus are biologically most relevant. To this aim, several tools have been developed to quantify the (phospho)proteome upon detection in LC-MS/MS experiments (Ong *et al.*, 2003; Thelen and Peck, 2007). So far, only a few large-scale quantitative LC-MS/MS studies have been performed to study changes in the phosphoproteome of defence-induced plants (Benschop *et al.*, 2007; Nühse *et al.*, 2007). To enable *in vivo* protein labelling, these studies have been performed in cell suspensions, a system which only partly represents intact green plants. Other labelling approaches, such as iTRAQ^{TM} labelling, are performed *in vitro* after protein extraction prior to MS analysis and might introduce technical errors in quantification (Jones *et al.*, 2006a; Zieske, 2006). The latest development in quantitative proteomics is relative label-free quantification of peptides identified by LC-MS/MS, which is

based on the peptide peak area of the mass spectrum (Ong *et al.*, 2003; Steen *et al.*, 2005; Beck *et al.*, 2006; Ono *et al.*, 2006). This approach allows quantitative (phospho) proteome analysis without the requirement to label samples prior to LC-MS/MS analysis, a method particularly suited for the analysis of systems such as intact plants in which incorporation of a label is difficult or not feasible.

We use the interaction between tomato (*Solanum lycopersicum*) and the fungal leaf pathogen *Cladosporium fulvum* as a model system to study the gene-for-gene interaction between plants and pathogens (Flor, 1942; Rivas and Thomas, 2005). *C. fulvum* secretes several effectors that enhance virulence of the fungus in susceptible tomato genotypes (Joosten and De Wit, 1999; Thomma *et al.*, 2005; Van Esse *et al.*, 2007). In tomato plants carrying the appropriate *Cf* resistance gene, the effectors are recognized and in such a case referred to as avirulence factors (Avrs). Recognition eventually results in a HR and resistance to the fungus (Rivas and Thomas, 2005). The involvement of phosphorylation cascades in Cf-mediated signalling has been reported by several research groups. Studies using tomato cell suspensions expressing Cf resistance proteins revealed the specific dephosphorylation of a membrane-bound H^+-ATPase after treatment with *C. fulvum* elicitor preparations (Xing *et al.*, 1996). Furthermore, recognition of an Avr of *C. fulvum* in Cf-transgenic tobacco cell suspensions was found to activate MAPKs and CDPKs (Romeis *et al.*, 1999; De Jong *et al.*, 2000; Romeis *et al.*, 2000; Romeis *et al.*, 2001). *In planta* studies using *Nicotiana* spp. revealed that protein phosphatase 2A is involved in Cf/Avr-dependent HR suppression (He *et al.*, 2004) and that a tobacco syntaxin is rapidly phosphorylated upon Cf/Avr-triggered defence signalling (Heese *et al.*, 2005). In addition, the protein kinase ACIK1 is required for full Cf/Avr-induced HR and resistance (Rowland *et al.*, 2005). Finally, we observed fast phosphorylation events in intact tomato plants undergoing a synchronized HR. To this aim, tomato plants carrying *Cf-4* were crossed to transgenic tomato plants expressing *Avr4* of *C. fulvum*. The resulting seeds germinate, but the seedlings develop a constitutive HR at 20°C that can be suppressed by incubating the plants at 33°C and 100% relative humidity (RH) (De Jong *et al.*, 2002; Wang *et al.*, 2005). A subsequent transfer to 20°C induces the HR and allows the collection of leaf material at a specific, synchronized stage of HR development, while control seedlings (consisting of a mixture of *Cf-4*- and *Avr4*-expressing parental seedlings that are exposed to the same treatment) remain healthy (De Jong *et al.*, 2002). We found specific activation of the MAPKs LeMPK1, -2 and -3 in these Cf-4/Avr4 seedlings,

within two hours after the temperature shift. By using peptide arrays, we demonstrated that these MAPKs have overlapping but also different phosphorylation specificities. This observation suggests that a diverse set of downstream target proteins is phosphorylated by the activated MAPKs. Furthermore, virus-induced gene silencing (VIGS) of the three individual LeMPK-encoding genes revealed a role for these kinases in Avr4-triggered resistance to *C. fulvum* (Chapter 3).

Here, we present a relative quantitative phosphoproteome analysis of total leaf extracts of Cf-4/Avr4 tomato seedlings, without sample prefractionation and without having the complete genomic sequence available. We describe LC-MS/MS analysis of the phosphoproteome of Cf-4/Avr4 seedlings compared to control tomato seedlings, at 1, 3 and 5h after the shift from 33°C to 20°C that initiates the HR. Using TiO_2 affinity enrichment followed by LC-ESI-QTOF tandem mass spectrometry, we identified a total of 50 phosphoproteins, with novel phosphorylation sites. Relative label-free quantification of the phosphopeptides revealed previously unidentified changes in the phosphoproteome upon HR induction. Based on these changes we conclude that photosynthetic activity is swiftly suppressed upon the initiation of the HR and that anaerobic respiration is promoted in the seedlings, probably as a result of low oxygen stress. Furthermore, four Hsp90 isoforms with a different phosphorylation status were identified in Cf-4/Avr4 seedlings compared to control seedlings.

RESULTS

Experimental setup

Resistant tomato plants protect themselves from *Cladosporium fulvum* invasion by the execution of a hypersensitive response (HR). The HR is induced by the Cf-4 resistance protein that mediates recognition of the cognate Avr4 elicitor from *C. fulvum*. Transgenic tomato seedlings expressing both *Cf-4* and *Avr4* (Cf-4/Avr4 seedlings) do not execute a HR at elevated temperature, but a specific synchronized HR is initiated after a shift to a lower temperature (De Jong *et al.*, 2002). We have shown that HR signalling in these seedlings involves protein phosphorylation and that MAPK activation precedes the appearance of HR

symptoms (Chapter 3). Therefore, HR-related changes in the phosphoproteome of Cf-4/Avr4 and control seedlings were studied.

Phosphopeptides were isolated from total protein extracts of cotyledons of Cf-4/Avr4 and control seedlings using TiO_2 columns and analyzed by LC-MS/MS. Three independent experiments were performed (t=1h, t=3h and t=5h after the temperature shift; time points which are based on the time course of MAPK activation in the Cf-4/Avr4 seedlings (Chapter 3; See below) and each experiment comprised the analysis of six samples representing three independent biological replicates from Cf-4/Avr4 and control seedlings. In each experiment, the first biological replicate (biological replicate 1) was analyzed in triplicate to determine the technical variation in an experiment, while biological replicates 2 and 3 were analyzed once by LC-MS/MS, resulting in 10 LC-MS/MS runs per experiment (Figure 1).

To study peptide carry-over between the individual LC-MS/MS runs, identical phosphopeptide samples were analyzed by LC-MS/MS in triplicate but separated by runs of trypsin-digested bovine serum albumin (BSA). No (phospho)peptides from tomato were identified in the BSA runs, indicating that there was no carry-over from one run to another (results not shown). Therefore, no BSA runs were included between the triplicate runs in the LC-MS/MS experiments described here, to reduce the size of the experiment. A BSA run was only included after each biological replicate consisting of a Cf-4/Avr4 and control seedling sample.

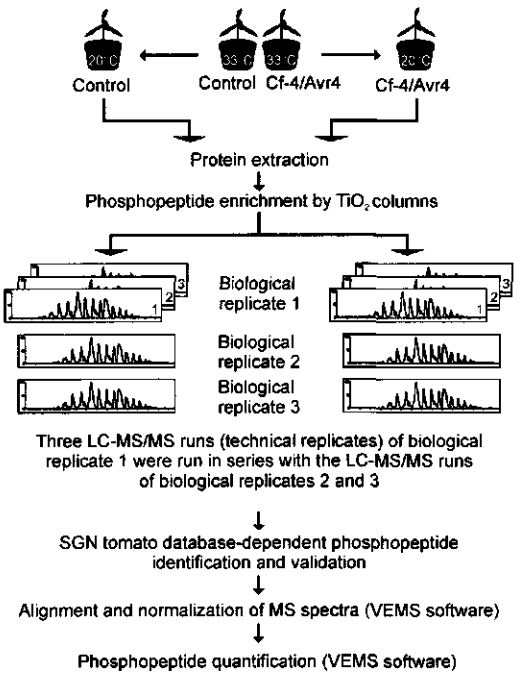

Figure 1. Overview of the experimental approach.
Setup of the experiments performed at t=1h, t=3h or t=5h of Cf-4/Avr4 and control seedlings, from HR initiation by the temperature shift, to quantification of the phosphopeptides.

Phosphopeptide identification

Three experiments (t=1h, t=3h and t=5h) were performed to analyze phosphopeptides purified from the tomato seedlings mounting a HR and the controls, using two different mass spectrometers (Table I). One-third of the phosphopeptides purified from 200μg of trypsin-digested protein was injected into the mass spectrometer using a 2h elution gradient on the reverse phase column. This procedure resulted in good ion currents without column saturation. Using VEMS software, LC-MS/MS data from each experiment were searched against the translated SGN tomato database containing approximately 34,000 unigenes that cover about 40% of the tomato genome. Global analysis of the non-redundant search results revealed that 40-60% of the identifications were not phosphopeptides, thereby indicating that phosphopeptides were enriched to 50% by TiO_2 columns under the described conditions. Since the focus of this study was the identification of phosphoproteins, all identified proteins that match only non-phosphorylated peptides were removed from the search result. All remaining (phospho)peptides were manually validated in each of the three experiments. This resulted in the identification of 50 phosphoproteins that match 75 unique phosphopeptides and 6 non-phosphorylated peptides with an average accuracy smaller than 4.7 ppm (Tables I and II). In the technical replicates of the samples representing biological replicate 1, 91-98% of the phosphopeptides were repeatedly identified (Table I). In addition, 56-61% of the phosphopeptides were repeatedly identified in the three biological replicates of Cf-4/Avr4 as well as control samples, while 81-100% of the peptides were identified in at least two biological replicates (Table I). This indicates that identified peptides largely overlap between biological replicates. Furthermore, 20% of the identified peptides were found in all three experiments (t=1h, t=3h and t=5h) while an additional 30% was found in two experiments (Table II).

Table I. Experimental details.

Experiment	t=1h	t=3h	t=5h
LC-MS/MS analysis [a]	QTOF-Micro	QTOF-Ultima	QTOF-Micro
Average ppm [b]	4.7 ± 5.3	2.4 ± 2.5	3.7 ± 6.1
Label free quantification (mDa - minutes)	79 - 11.0	21 - 3.4	75 - 4.3
Technical reproducibility [c] (Control - Cf-4/Avr4)	92 - 95%	91 - 96%	95 - 98% [d]
Biological reproducibility (3 or >2 replicates)	61 - 100%	56 - 99%	56 - 81% [e]

[a] The type of mass spectrometer used for LC-MS/MS analysis. See Methods for further details.
[b] Average ppm represents all reported peptides.
[c] Percentage of reported peptides identified in each of the three technical replicates.
[d] The percentage for the control sample is based on two technical LC-MS/MS replicates.
[e] Percentage of reported peptides identified in each of the three biological replicates.

Of the 50 phosphoproteins, 30 have previously been described as phosphoprotein in other organisms (Table III), but not in tomato whereas the remaining 20 phosphoproteins have not been described before. In addition, several high quality MS/MS spectra of potential phospho- and non-phosphopeptides were obtained, which could not be assigned to a peptide sequence since the tomato genomic sequence is not complete. The 75 unique phosphopeptides matching the 50 phosphoproteins represent 58 phosphorylation sites, which are reported in Table III. Phosphopeptides covering the same phosphorylation site because of missed tryptic cleavages are reported only by the shortest peptide sequence, resulting in a set of 55 phosphopeptides representing the 58 phosphorylation sites (and 6 non-phosphorylated peptides; Table III). These phosphorylation sites include 45 serine and 13 threonine residue phosphorylation sites (Tables II and III). No tyrosine phosphorylation sites were observed, which confirms the already described low occurrence of tyrosine phosphorylation in plants (Kersten *et al.*, 2006). The MS/MS spectra, m/z, z values, mass errors and scores for each peptide are reported in Supplementary Table SI. Comparison of the phosphorylation sites to sites described in literature and to the Arabidopsis phosphorylation database (PhosAtbase; http://phosphat.mpimp-golm.mpg.de/) revealed that 22 of the 55 phosphorylation sites are conserved in orthologous proteins in other organisms (Table III, indicated with L). These conserved phosphoproteins include Hsp90, ATPases, aquaporins and several proteins involved in photosynthesis and glycolysis. In many cases, (de)phosphorylation of these proteins has been reported to regulate their activity. Another 8 proteins were previously identified as phosphoprotein, however, the reported site of phosphorylation has not been determined before (Table III, indicated with P).

Table II. Summary of data obtained from three independent LC-MS/MS experiments (t=1h, t=3h and t=5h).

Data summary	
# phosphoproteins	50
# phosphopeptides	55
# serine phosphorylation sites	45
# threonine phosphorylation sites	13
# tyrosine phosphorylation sites	0
% of (phospho)peptides at t=1, 3 and 5h	20
% of (phospho)peptides at 2 time points	30
% of (phospho)peptides at 1 time point	50
# differentially phosphorylated peptides*	13

*These phosphorylated peptides are observed in at least two biological replicates.

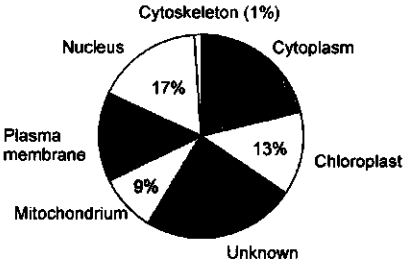

Figure 2. Phosphoproteins originate from different subcellular localizations.
Phosphoprotein localization was predicted by WoLF PSORT software, based on the protein sequences.

Table III. Phosphopeptides identified and quantified in experiments t=1h, t=3h and t=5h.

SGN-ID [a]	Peptide sequence [b]	Phosphorylation of Cf-4/Avr4 vs Control [c]			Annotation	Literature [d]
		Ratio t=1h	Ratio t=3h	Ratio t=5h		
SGN-U312354 SGN-U312357 SGN-U313363	EDQLEYLEER	1.47 ± 0.36	1.06 ± 0.27	1.09	Hsp90	
SGN-U313365	ELISNSSDALDK	1.40 ± 0.36		1.18 ± 0.32		
SGN-U312354	EI**S**DDEDEEEK	0.60 ± 0.36	0.82 ± 0.21	**1.83 ± 0.41***	Hsp90-1	L
SGN-U312357	EI**S**DDEEEEEK	0.93 ± 0.32	1.16 ± 1.46	**6.30 ± 2.30**	Hsp90-2	L
SGN-U313363 SGN-U313365	EI**S**DDEDDEPK	1.22 ± 0.62	0.46 ± 0.74*	0.91 ± 0.36	Hsp90-3/4	
SGN-U313363	EI**S**DDEDDEPKKDEEGAVEEVDEDK		2.14 ± 0.52		Hsp90-3	L
SGN-U313365	EI**S**DDEDDEPKKEQEGDIEEVDEDK		1.14 ± 0.19		Hsp90-4	L
SGN-U312661	NLAGDIIG**t**R**t**EVADVK		2.01 ± 0.58	0.97 ± 0.26	Chlorophyll a-b binding protein CP29 (LHCB4)	P
SGN-U312844	SI**S**TPF**m**NTASK[#]	1.08 ± 0.25*		1.33 ± 0.28	Nitrate reductase	L
SGN-U312863	AALAAGADKDEEDSEGR	1.21 ± 0.26*			Ankyrin-repeat protein (HBP1)	
	K**S**PESSTVEAPSGEGR	1.00 ± 0.30*				
SGN-U313210 SGN-U313218	FGEAVWFK			0.70 ± 0.20*	Chlorophyll a-b binding protein	
SGN-U313210	SAPSSSPWYGPDR			1.79 ± 0.40	Chlorophyll a-b binding protein (LHCII type I CAB-1B)	L
	SAPSSSPWYGPDR					
SGN-U313218	PASSGSPWYGPDR	10.93 ± 4.08		1.04 ± 0.19	Chlorophyll a-b binding protein (LHCII type I CAB-3C)	L
	TAAKPKPASSGSPWYGPDR	**0.73 ± 0.12***		1.50		
SGN-U313242	GG**mts**HAAVVAR			0.79 ± 0.28	Pyruvate phosphate dikinase (PPDK)	L
SGN-U313311	VETPIDANEIR	**0.69 ± 0.12***		1.98	putative DNA/RNA binding protein	
	VSTDFDYDGEG**S**PSGGR	0.47 ± 0.51	1.26 ± 0.25	0.81 ± 0.15		
SGN-U313649 SGN-U313650	GLDIETIQQSY**T**V[#]		1.23 ± 0.45	0.86	Plasma membrane H $^{+}$-ATPase LHA1/2	L
SGN-U313547 SGN-U315949	GLDIETIQQHY**T**V[#]		1.52 ± 0.39	1.49 ± 0.35	Plasma membrane H $^{+}$-ATPase LHA4	L
SGN-U313599	RFGTTGTVK				putative extracellular calcium sensing receptor	

Table III (continued).

SGN-ID [a]	Peptide sequence [b]	Phosphorylation of Cf-4/Avr4 vs Control [c]			Annotation	Literature [d]
		Ratio t=1h	Ratio t=3h	Ratio t=5h		
SGN-U313650	TLHGLQVPDTK#	0.98 ± 0.33*		1.28 ± 0.28	Plasma membrane H +-ATPase LHA2	L
SGN-U313858	KEEPKEESDDDmGFSLFD#	0.67 ± 0.49*	2.19 ± 0.46	1.08 ± 0.51	Acidic ribosomal protein P1a-like	L
SGN-U314961	IASESDVSVHSTFASR		2.14 ± 0.36*	1.25 ± 0.41*	Glutamate decarboxylase isozyme 1 (GAD1)	
SGN-U315162	VADSGASPPASSANPQHPASR			1.03 ± 0.36*	Beta-adaptin-like protein B	
SGN-U315274	TPVTEsAsFK			1.34 ± 0.35	putative SEC14 protein	
SGN-U315305	YHGHsmsDPGSTYR	3.24 ± 0.91		0.87 ± 0.35	Pyruvate dehydrogenase	L
SGN-U315592	VSSFEALQPVNR#	0.98 ± 0.33*	1.07 ± 0.19	1.45 ± 0.29	Putative GDP-mannose pyrophosphorylase	L
SGN-U315632	LRDGEASDEEEEYEAK		0.90 ± 0.23	0.85	Eukaryotic translation initiation factor 3 subunit 9, PRT1	
SGN-U315720	SHAVDASDDEmDDDENDANIK		0.82 ± 0.29*		TPR containing protein, putative heat shock chaperonin-binding	
SGN-U315821	ALGSFRSNATN		0.82 ± 0.12*		Plasma membrane intrinsic protein, aquaporin	L
SGN-U315990	AAATIAKEPEEK	1.35 ± 0.37	3.05 ± 1.97*	1.32	putative IMP dehydrogenase/ GMP reductase	
	ANEESDAQVA TVR	0.89 ± 0.50	1.25 ± 0.26	0.46		
SGN-U316572	ALGsFRsNQTN#		0.58 ± 0.12	0.72 ± 0.22	Plasma membrane intrinsic protein PIP2, aquaporin	L
	ALGSFRSNQTN		1.36 ± 0.28*	1.30 ± 0.28		
SGN-U317145	QLmLEYAGSER		1.50 ± 0.39		CHUP1, chloroplast unusual positioning 1	
SGN-U317356	NSAEGYVPIHALsEsPK		2.35 ± 0.60		RNA recognition motif (RRM)-containing protein	
SGN-U317388	VSTLPSENPQ SPSDQPK		0.80 ± 0.19	0.83 ± 0.18*	UDP-glucose glycosyltransferase	P
SGN-U317660	EAVAD mSEDLSEGEK		0.91 ± 0.18*		Sucrose phosphate synthase	L
SGN-U317742 SGN-U317743	SVVELTSGT SDDGHDK		5.15 ± 0.99*		Oligouridylate binding protein	
SGN-U317758	KVSPIPESR	0.76 ± 0.18			emp24/gp25L/p24 family protein	

Table III (continued).

SGN-ID[a]	Peptide sequence[b]	Phosphorylation of Cf-4/Avr4 vs Control[c]			Annotation	Literature[d]
		Ratio t=1h	Ratio t=3h	Ratio t=5h		
SGN-U317838	QL**S**IDQFENEGR[#]		2.46 ± 0.69		Kelch repeat-containing serine/threonine phosphoesterase family protein	L
SGN-U318020	VDGLL**tssssss**PR		0.83 ± 0.11*		Uridine kinase-like protein	P
SGN-U318050	GLEHSF**S**TGFR[#]		0.91 ± 0.20	0.84 ± 0.18	Calcium-dependent protein kinase 2	L
SGN-U318935	LHFSNHSSSPAPASSSSD **S**DDEK		1.06 ± 0.26*		putative IMP dehydrogenase/ GMP reductase	
SGN-U319866	ISSEDE**m**AG**m**DLTR[#]	1.35 ± 1.49	1.09 ± 0.22*		Ammonium transporter 1 (LeAMT1;1)	L
SGN-U319978	**m**A**S**IDAQLR[#]		0.50	1.39 ± 0.31	Phosphoenolpyruvate (PEP) carboxylase 1	L
SGN-U320093	VEEPHNVAEQPI **S**PKDER			1.25 ± 0.18	YT521-B-like protein	
SGN-U320785	TDVGEG **S**FHAISR	0.95 ± 0.51		0.92 ± 0.28*	Phototropin-2	P
	SIDVFDPASTHDGANLASSSR			0.88		
	TSEESNLGAEFPRV **S**QDLK			0.99 ± 0.22		
SGN-U322822	GR**S**FDDSPVSITDR		1.80 ± 0.29*		putative IMP dehydrogenase/ GMP reductase	
SGN-U323143	EIEAG **S**DLEVK			0.96 ± 0.20*	putative IMP dehydrogenase/ GMP reductase	
SGN-U323433	DDHWDEE **S**LQR				Putative hexose transporter	P
	IYLHQEAGP **ss**R		0.73 ± 0.32			
SGN-U325962	AT**S**PQTGSQQVGGNLK[#]		**0.59 ± 0.17**	1.39 ± 0.29*	Dynamin-like protein	L
SGN-U327750	EANGGFI **ms**A**s**HNPGGPEYDWGIK			0.92 ± 0.21	Plastidic phosphoglucomutase	P
SGN-U328413	LPEMP**S**SKGLKR			0.81 ± 0.16	Protein kinase family	P
SGN-U333128	GEN**S**SSEINIVRS				Sucrose transport protein	P
SGN-U337595	QEEP**T**KGKLEK	0.76 ± 0.12			Putative glycolate oxidase	

[a] Gene identifier from the *Solanaceae* Genomics Network (SGN).
[b] The phosphorylated residue in the peptide sequence is indicated in bold, or in lower case bold when it is unclear from the spectrum which residue is phosphorylated. Methionine (M) oxidation is indicated in lower case bold. [#] indicates phosphopeptides that have also been identified and quantified in xylanase-treated Arabidopsis cells (Benschop *et al.*, 2007).
[c] The ratio represents the average of the ion intensities of a peptide in the Cf-4/Avr4 seedlings versus the control seedlings, determined from three biological replicates. Ratios indicated with an asterisk are determined from two biological replicates while ratios without SE originate from one biological replicate. The ratios indicated in light or dark grey are significantly different from 1.00 with 95% and 99% confidence, respectively.
[d] Phosphopeptides indicated with 'L' contain a phosphorylation site that has been described before. Phosphopeptides indicated with 'P' correspond to proteins that were described as phosphoproteins before, but of which the phosphorylation site was not known.

Since a total leaf protein extract was made for phosphoproteome analysis, the identified proteins are expected to originate from different organelles. Prediction of their localization using WoLF PSORT (Protein Subcellular Localization Prediction) software (http://wolfpsort.seq.cbrc.jp) indeed revealed that the phosphoproteins originate from the cytoplasm, chloroplast, mitochondria, plasma membrane, nucleus and the cytoskeleton, thus confirming that they represent a cross section of the phosphoproteome of the complete leaf (Figure 2).

Relative quantification of phosphopeptides

Relative quantification based on peptide ion peak area, also known as label-free quantification, was used to identify differentially phosphorylated peptides. Using the VEMS software package (Matthiesen *et al.*, 2005), (phospho)peptides were quantified based on the peak area of the MS spectrum. Chromatograms of the ten samples of each experiment were aligned and calibrated with respect to RT and mass to enable peak area comparison of MS spectra between individual samples. To set an accurate window for alignment and calibration, mass and RT deviation was determined. The largest mass deviation per experiment was determined from the peptide selected for MS/MS analysis that deviated most from the theoretical mass. The RT deviation was determined by the drift in RT of a peptide selected for MS/MS analysis in all of the ten samples of each experiment. For the experiments t=1h, t=3h and t=5h, the mass deviation was 79, 21 and 75 mDa respectively, and the RT deviation was 11.0, 3.4 and 4.3 minutes, respectively. VEMS-mediated alignment of the MS spectra based on these parameters led to proper peak alignment and quantification (Figure 3*a* and 3*b*). Different intensities of a phosphopeptide are reflected by a difference in peak area (Figure 3*b*).

To validate the quality of the label-free quantification, the technical replicates of biological replicate 1 (Figure 1) were analyzed by a new approach. For each peptide, the average abundance was plotted against the corresponding SE and a polynomial function y=a*x, in which 'a' represents the technical error of the experiment was fitted to the data (Figure 3*c*, *upper panels*). To verify whether the polynomial function correctly represents the data, residual plots were made (Figure 3c, *lower panels*) and as expected for data that are correctly fitted, the residuals scatter around zero. The technical error of the quantified data remains below 10% ($a < 0.1$) for all three experiments and this label-free quantification approach was therefore accepted for further analysis. Since ten samples were analyzed in series within one experiment, they should all have the same technical error. Therefore, the technical errors (0.096, 0.072 and 0.080 for t=1h, t=3h and t=5h, respectively) were used to estimate the SE of the peptide intensities in biological replicates 2 and 3. Subsequently, the phosphopeptide ratio ± SE of the Cf-4/Avr4 seedlings compared to the control seedlings was calculated for each biological replicate in each experiment (Supplementary Table SII). Finally, the average abundance ratio ± SE was calculated for each peptide in which the SE represents the technical and biological variation (Table III). Average abundance ratios that significantly differ from 1.00 are indicated in grey ($P \leq 0.01$) or light grey ($P \leq 0.05$). In total, we identified 13 phosphopeptides, each representing a different phosphoprotein, with a ratio that significantly differs from 1.00 in at least one of the three experiments (Table III). These results show that label-free quantification is feasible on phosphopeptides isolated from total protein extracts of tomato leaves.

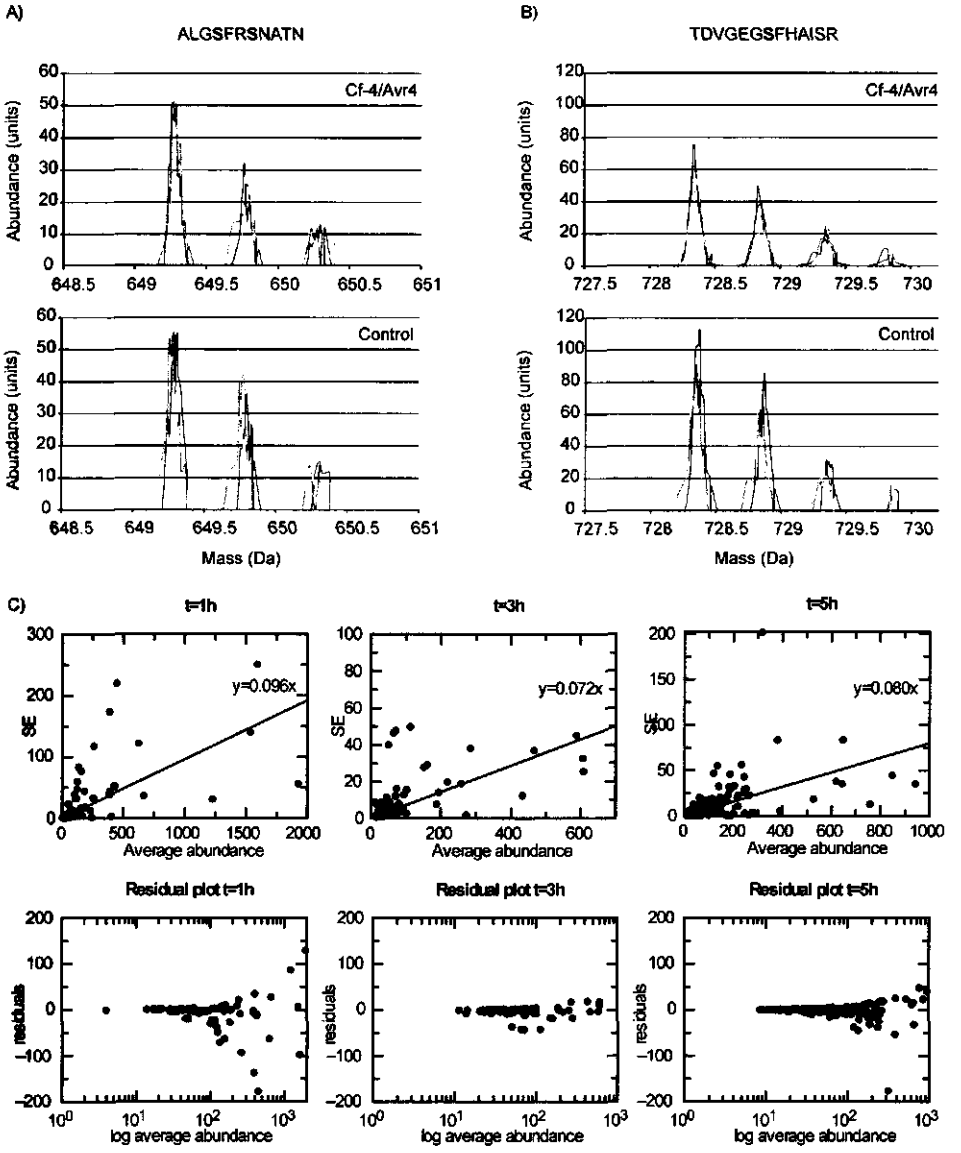

Figure 3. Validation of the relative label-free quantification procedure.
The procedure for quantification of the (phospho) peptides was validated to determine the reliability of the relative label-free quantification approach. MS spectra of all peptides were aligned and calibrated by VEMS, based on the mass and retention time deviation per experiment (see Methods for more details). A and B) Quantification based on peptide ion peak area gives similar results for phosphopeptides ALGSFRSNATN and TDVGEGSFHAISR in the three technical replicates of biological replicate 1 at t=3h. In all cases, a similar peak area was observed for the carbon isotope peaks. Phosphopeptide ALGSFRSNATN shows a similar abundance (A), whereas phosphopeptide TDVGEGSFHAISR has a decreased abundance in the Cf-4/Avr4 seedlings as compared to the control (B). C) To determine the technical error of each experiment, the SE of the average abundance of each peptide was plotted against the average abundance (upper panels). A polynomial function y=a*x was fitted to the data, in which 'a' represents the technical error. The residual plots of the fitted data, shown in the lower panels, indicate that this function fits the data.

Transcriptional regulation of genes encoding phosphoproteins

The commercially available Affymetrix tomato microarray contains the coding sequences of 29 of the 50 phosphoproteins that were identified in the phosphoproteome analysis. From these 29 genes, only four were significantly transcriptionally regulated at t=5h ($P \leq 0.01$; Table IV, SGN-U318050, SGN-U317660, SGN-U313242 and SGN-U319866), whereas the average abundance ratio of the encoded phosphoproteins was unaltered. For the phosphoproteins with an altered abundance in the Cf-4/Avr4 seedlings as compared to the controls, four encoding genes were present on the microarray (Table IV, SGN-U312354, SGN-U312357, SGN-U313599 and SGN-U315305). None of these genes were differentially transcribed with 99% confidence; however, one was transcriptionally regulated with 95% confidence (Table IV; SGN-U312354). These results indicate that the genes encoding most of the identified phosphoproteins are not transcriptionally regulated within the first five hours of the Cf-4/Avr4-induced HR.

Table IV. Transcriptional regulation of genes encoding phosphoproteins.

SGN-ID[a]	Microarray ID[b]	Annotation	Cf-4/Avr4 vs Control[c]		
			t=1h	t=3h	t=5h
SGN-U318050	Les.1558.1.S1_at	Calcium-dependent protein kinase 2	1.10	1.49	**2.24**[d]
	Les.1558.2.A1_at		1.41	1.48	**3.39**
SGN-U317660	Les.3522.1.S1_at	Sucrose phosphate synthase	0.75	0.69	**0.40**
SGN-U313242	Les.4356.2.S1_at	Pyruvate phosphate dikinase (PPDK)	**0.60**	0.72	**0.21**
	Les.4356.3.S1_at		**0.41**	0.63	**0.20**
SGN-U319866	Les.797.1.S1_at	Ammonium transporter 1 (LeAMT1;1)	0.96	1.25	**1.76**
SGN-U312354	Les.321.1.S1_at	Hsp90-1	0.95	0.91	1.82[e]
SGN-U312357	Les.1146.1.S1_at	Hsp90-2	1.01	0.99	1.07
SGN-U313599	Les.3180.1.S1_at	putative extracellular calcium receptor	0.72	0.84	0.50
	Les.3180.2.S1_at		0.75	0.89	0.54
	Les.3180.3.A1_at		0.97	0.89	0.77
SGN-U315305	Les.3167.1.S1_at	Pyruvate dehydrogenase	0.99	0.90	1.05

[a] Gene identifier from the Solanaceae Genomics Network (SGN).
[b] Gene identifier from the Affymetrix tomato microarray. Some SGN-IDs are represented by more than one microarray ID.
[c] Numbers represent the ratio of transcript levels in the Cf-4/Avr4 seedlings compared to the control seedlings, based on three independent biological replicates.
[d] Ratios indicated in bold are significantly different from 1.00 with $P \leq 0.01$.
[e] This ratio is significantly different from 1.00 with $P \leq 0.05$.
Supplementary Table SII. Replicate phosphopeptide quantification at t=1h, t=3h and t=5h.

Biological validation of the phosphorylation events occurring in Cf-4/Avr4 seedlings

We have described earlier that the MAPKs LeMPK1, -2 and -3 are activated in the Cf-4/Avr4 seedlings within 2h after the temperature shift (Chapter 3). MAPK activity observed at

t=0h in the Cf-4/Avr4 seedlings disappeared after the temperature shift, preceding their subsequent HR-specific activation at t=2h after the temperature shift (Chapter 3). These results provided evidence for HR-related phosphorylation events in the Cf-4/Avr4 seedlings, since MAPKs are activated through phosphorylation by upstream MAP(K)KKs and phosphorylate downstream targets themselves. Therefore, the time points for phosphoproteome analysis were based on the timing of MAPK activation in the seedlings. To avoid possible background protein phosphorylation induced by heat stress (33°C, at t=0h), the phosphoproteome from the Cf-4/Avr4 and control seedlings was analyzed at t=1h, t=3h and t=5h after the temperature shift. At the latter two time points massive MAPK activation has occurred in the Cf-4/Avr4 seedlings (Chapter 3). Our analysis did not reveal a higher percentage of phosphopeptides with an altered average abundance ratio at t=3h or t=5h as compared to t=1h. However, the average abundance ratios seem to deviate more from 1.00 at the later time points.

HR-related regulation of photosynthesis, sugar transport and glycolysis

Protein phosphorylation plays a major role in basic physiological processes such as photosynthesis, glycolysis and sugar transport. Many enzymes that participate in these processes are (in)activated by phosphorylation, to eventually stimulate or suppress the pathway. This regulation is required to respond rapidly to changing environmental conditions, such as light intensity. Several phosphopeptides identified in this study play a role in these processes, and some of these phosphoproteins showed significant changes in their abundance ratio, suggesting phosphorylation-mediated regulation of these processes during the Cf-4/Avr4-induced HR (Table III). Three phosphoproteins were identified that function in the chloroplast during photosynthesis. The phosphorylation of plastidic phosphoglucomutase (SGN-U327750), which controls the flow of photosynthetic carbon to either starch synthesis or glycolysis, appeared unaltered at t=5h. However, the pool of two different phosphorylated chlorophyll a/b binding proteins (CABs) present in light-harvesting complex II (LHCII type I), was found to be smaller in the Cf-4/Avr4 seedlings, at respectively t=1h (SGN-U313218) and t=5h (SGN-U313210). LHCII CABs are phosphorylated under light conditions after which they migrate to photo system I (PSI) to increase photosynthetic activity, and are dephosphorylated in the dark when photosynthesis is suppressed (Vener, 2007). Our data indicate that photosynthetic activity is swiftly suppressed in Cf-4/Avr4 seedlings. This

hypothesis is supported by the observation that phosphorylated phototropin-2 (SGN-U320785; Table III) is less abundant in Cf-4/Avr4 seedlings at t=3h. Phototropins are serine/threonine kinases that are activated by autophosphorylation and are involved in optimizing the efficiency of photosynthesis (Christie, 2007). Phosphorylated phototropin stimulates stomatal opening, and a smaller pool of phosphorylated phototropin is expected to lead to stomatal closure and a decreased CO_2 uptake, leading to inhibition of photosynthesis. Interestingly, we also found a phosphopeptide derived from the tomato orthologue of the Arabidopsis calcium sensing receptor (CAS; SGN-U313599), which has a significantly lower abundance in the Cf-4/Avr4 seedlings at t=3h. CAS is located in chloroplast membranes and is an important regulator of stomatal opening (Nomura *et al.*, 2008). Our results indicate that CAS activity is regulated by phosphorylation and that CAS dephosphorylation is correlated with stomatal closure.

Two sugar transporters, a hexose transporter and a sucrose transport protein, have a significant lower average abundance ratio at t=3h (SGN-U323433) and t=5h (SGN-U333128), respectively (Table III). Phosphorylation of hexose and sucrose transporters inhibits their activity (Roblin *et al.*, 1998; Norholm *et al.*, 2006), which suggests that sugar transporters are activated in the Cf-4/Avr4 seedlings. Although the link between sugar transporters and plant defence is unclear, there are several examples of increased transcript levels of sugar transporters in plants that have mounted a defence response (Norholm *et al.*, 2006). From our results, it appears that in addition to gene induction also dephosphorylation takes place to increase sugar transport activity.

During glycolysis, sugars synthesized by photosynthesis are metabolized to phosphoenolpyruvate (PEP) and subsequently to pyruvate, which in its turn is converted by the pyruvate dehydrogenase complex (PDC) into acetyl-CoA that enters the citric acid cycle eventually leading to ATP generation. At t=3h, a strong increase in the abundance of phosphorylated pyruvate dehydrogenase (SGN-U315305) was observed in the Cf-4/Avr4 seedlings. Pyruvate dehydrogenase is one of the three enzymes in the PDC and is inactivated by phosphorylation, resulting in a decreased rate of the conversion of pyruvate to acetyl-CoA in the mitochondria (Rubin and Randall, 1977). The subsequent depletion of acetyl-CoA interrupts mitochondrial functioning, which by itself might already lead to cell death (Newmeyer and Ferguson-Miller, Cell, 2003).

Our data on the dynamics of the phosphoproteome indicate that photosynthetic activity is swiftly inhibited in the Cf-4/Avr4 seedlings upon HR initiation. Therefore we performed chlorophyll fluorescence measurement and imaging on Cf-4/Avr4 and control seedlings to determine the actual efficiency of photosynthesis over a time course after triggering the HR (De Ruiter *et al.*, 2007). The seedlings were transferred from 33°C to room temperature and every 10 minutes, the leaf surface was scanned with a laser over a total period of 18 h. When the efficiency of photosynthesis decreases, the laser light is still absorbed but less energy is used for photosynthesis and more is emitted as fluorescence by the chlorophyll pigments in the leaves. In this way the photosynthetic activity can be determined. A significant decrease in photosynthetic activity was observed for the Cf-4/Avr4 seedlings compared to the control seedlings within 1.5 h after the temperature shift ($P \leq 0.05$; Figure 4), an observation which fully supports our conclusion from the phosphoproteome analysis.

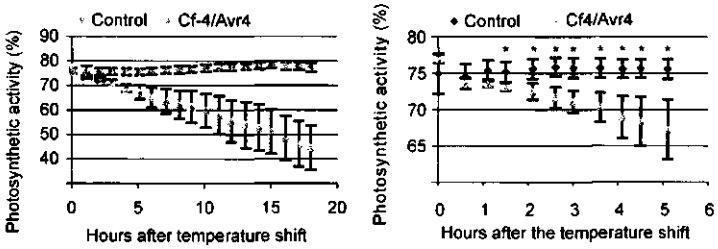

Figure 4. Photosynthetic activity decreases upon initiation of the Cf-4/Avr4-induced HR.
Seedlings were transferred from 33°C to room temperature and every 10 minutes, the leaf surface was scanned with a laser over a period of 18 h. When photosynthetic activity decreases, the laser light is still absorbed but less energy is used for photosynthesis and more is emitted by the chlorophyll pigments in the leaves as fluorescence, which is captured by a camera. Therefore, increased fluorescence reflects a decrease in photosynthetic activity (De Ruiter *et al.*, 2007). Healthy plants have a photosynthetic activity of approximately 75-80%. In Cf-4/Avr4 seedlings photosynthetic activity decreases to a level below 50% over the 18 h period after the temperature shift (left panel) and a significant decrease was already observed within 1.5 h after HR initiation (right panel; $P \leq 0.05$, indicated with an asterisk).

In addition, the transcriptional regulation of genes encoding proteins involved in photosynthesis, glycolysis and defence was studied. Genes involved in photosynthesis and glycolysis were hardly transcriptionally regulated in the first 5h after the temperature shift in Cf-4/Avr4 seedlings, except for the 3.5 to 4.5 times upregulation of the two L-lactate dehydrogenases that convert pyruvate to lactate (Figure 5) (Germain and Ricard, 1997). In contrast, most of the genes encoding characteristic defence-associated proteins such as the pathogenesis-related (PR) genes are upregulated in the Cf-4/Avr4 seedlings at t=5h after the temperature shift (Figure 5). PR genes become typically upregulated after recognition of a

pathogen by resistant plants and encode proteins that limit pathogen proliferation. Together, these data show that transcriptional regulation of defence genes occurs at t=5h, whereas the rapid physiological reprogramming of the plant required for mounting the defence response mainly occurs via differential phosphorylation.

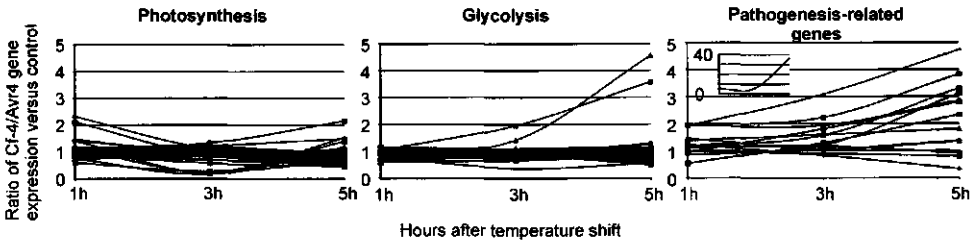

Figure 5. HR-associated regulation of the expression of genes involved in photosynthesis, glycolysis and pathogenesis-related genes.
Microarray gene expression analysis was performed using RNA isolated from Cf-4/Avr4 and control seedlings at 1h, 3h and 5h after the temperature shift. Gene expression is presented as the ratio between the expression in Cf-4/Avr4 seedlings and control seedlings. Details about the genes used for this figure are reported in Supplementary Table SIII.

HR-related phosphorylation of Hsp90 isoforms

Heat-shock protein 90 (Hsp90) is a multifunctional molecular chaperone that facilitates the folding of newly synthesized polypeptides into stable, functional, mature proteins (Richter *et al.*, 2007). Hsp90 has a role in highly diverse cellular functions and plays a critical role in innate immune responses of both animals and plants (Sangster and Queitsch, 2005; Mayor *et al.*, 2007). In this study, four different Hsp90-derived phosphopeptides were identified, each containing the same highly conserved serine-phosphorylation site EISDDE (Table III) (Krishna and Gloor, 2001; Ogiso *et al.*, 2004). One of these phosphopeptides originates from SGN-U312354 and one from SGN-U312357, which are known as tomato Hsp90-1 and Hsp90-2, respectively. Differences in the peptide sequence containing the phosphorylation site allowed discrimination between these two Hsp90s and two additional phosphorylated Hsp90 isoforms, which are annotated as Hsp90-3 for SGN-U313363 and Hsp90-4 for SGN-U313365 (Table III). In Arabidopsis also four cytoplasmic Hsp90 isoforms (AtHsp90-1 to -4) have been described, in which the orthologous conserved phosphorylation site is indicated as a casein kinase II phosphorylation site, a site which is phosphorylated in animals (Dougherty *et al.*, 1987; Krishna and Gloor, 2001). Detailed sequence analysis did not provide clues on the functional relevance of the different Hsp90s in Arabidopsis (Krishna

and Gloor, 2001). However, a mutational analysis of the different Hsp90 isoforms indicated that the cytosolic Hsp90s have diverged in function (Sangster and Queitsch, 2005). Interestingly, the abundance of phosphorylated Hsp90-1 and Hsp90-2 has increased in the Cf-4/Avr4 seedlings at t=5h, while the abundance of phosphorylated Hsp90-4 has decreased at this stage. In agreement with the observation that only AtHsp90-1 is transcriptionally upregulated by heat and pathogen infection (Takahashi *et al.*, 2003; Sangster and Queitsch, 2005), transcriptional profiling of the Cf-4/Avr4 seedlings revealed an increase in the amount of Hsp90-1 transcripts compared to the controls at t=5h, whereas the transcript abundance of Hsp90-2 remains unaltered at all time points ($P \leq 0.05$; Table IV). Therefore, the increase in phosphopeptide abundance of Hsp90-1 could be caused by an increase in protein abundance, whereas Hsp90-2 appears to be differentially phosphorylated. The abundance of the non-phosphorylated Hsp90-derived peptides, EDQLEYLEER and ELISNSSDALDK, was unaltered between Cf-4/Avr4 and control seedlings. However, these peptides match all four Hsp90 isoforms and might therefore hide changes in average abundance ratio for a specific Hsp90 protein (Table III).

Additional phosphopeptides with an altered abundance in the Cf-4/Avr4 seedlings

Two additional phosphopeptides matching SGN-U313311 and SGN-U315274, which are annotated as a putative DNA/RNA binding protein and a putative SEC14 protein, respectively, were identified with a significantly decreased average abundance ratio at t=1h. The phosphopeptide matching SEC14 also has a decreased abundance at t=3h. Interestingly, both proteins seem to have a role in the early Cf-4/Avr4-triggered HR and these proteins are interesting candidates for further research.

DISCUSSION

Phosphoprotein identification from samples that are complex and that originate from an organism without a complete genomic sequence

The purification of phosphopeptides on TiO_2 columns is based on the binding of phosphate to TiO_2 by a bridging bidentate surface complex (Larsen *et al.*, 2005). However, non-phosphorylated peptides can bind aspecifically to TiO_2, thereby contaminating the

phosphopeptide fraction. In this study, peptides were loaded on the TiO_2 column in 5% TFA although it has been described that aspecific binding of non-phosphorylated peptides can be reduced by loading the peptides in 2,5-dihydroxy-benzoic acid (DHB) in TFA (Larsen *et al.*, 2005). However, DHB caused contamination of the ESI ion source during LC-MS/MS analysis and it was therefore excluded from the phosphopeptide purification protocol, allowing some aspecific peptide binding to the TiO_2 columns (Thingholm *et al.*, 2006). Analysis of the LC-MS/MS data revealed that approximately 50% of the peptides are phosphorylated. This column performance is similar to the efficiency obtained with TiO_2 purification of phosphopeptides from membrane fractions (Benschop *et al.*, 2007). In addition, approximately 60% of the peptides were repeatedly identified in the 3 biological replicates present in each experiment (Table I), while Benschop *et al* (2007) reported approximately 30% overlap between two biological replicates. This indicates that prefractionation does not increase the overlap in identified peptides between biological replicates. Therefore, we conclude that sufficient peptide coverage is obtained with the more direct approach that we have followed, especially when a shallow HPLC gradient is used. Furthermore, we show that TiO_2 columns are suitable to enrich phosphopeptides from complex protein samples that have not been pre-fractionated.

In this study, 50 phosphoproteins were identified, which is a relatively low number when compared to the study of Benschop *et al* (2007). One reason for this is that only 40% of the genomic sequence of tomato is available. Therefore, several MS/MS spectra with good ion intensities could not be assigned to a protein since their sequence is not present in the database. In addition, several of the sequences that are present in the database are not full length, which will also lead to unassigned spectra. Taking these database restrictions into account, a re-examination of our results is expected to reveal at least 125 phosphoproteins when the complete genomic sequence of tomato has become available. In addition to database restrictions, a stringent manual validation was applied to the reported (phospho) peptides. Furthermore, the MS/MS exclusion time during LC-MS/MS analysis has been too small in some cases, leading to multiple MS/MS spectra from the same (phospho) peptide, thereby decreasing MS/MS sequence coverage. Finally, total leaf protein extracts were analyzed to study the feasibility of phosphoproteome analysis of complex samples, without prefractionation and/or enrichment for proteins present in specific subcellular compartments. We identified phosphopeptides from at least 6 different cellular localizations (Figure 2)

providing information on general physiological processes taking place in leaf tissue of plants that mount a defence response. Although specific enrichment and/or prefractionation of phosphopeptide samples might lead to a higher amount of phosphoprotein identifications (Benschop *et al.*, 2007), a faster and more direct approach as described here is still very useful. Since more sensitive mass spectrometers with a high resolution become available, this approach can be a good alternative for a time and resources intensive large-scale phosphoproteome analysis that includes several prefractionation steps. In subsequent studies, for instance, the role of suppression of photosynthetic activity immediately upon HR-initiation in Cf-4/Avr4 seedlings could be further studied by the analysis of phosphopeptide samples purified from chloroplasts only.

Relative label-free quantification of phosphopeptides

Relative label-free quantification of a phosphopeptide is performed based on the peak area of its MS spectrum. To be able to compare the abundance of a given peptide in different samples, MS spectra of the peptide have to be aligned based on their RT and mass to allow comparison of the correct MS peak areas (Beck *et al.*, 2006; Jensen, 2006; Wang *et al.*, 2007). The ΔRT and Δmass was determined for each experiment and set in VEMS, allowing the program to search for matching MS spectra in the set window (Table I). In experiment t=5h, the first LC-MS/MS run deviated in RT from the other nine. By discarding this run from the experiment, the ΔRT remained small which is theoretically best for quantification. In experiment t=1h, the RTs deviated between all ten runs. Although the label-free quantification was approved by the validation method described in Figure 3 and the results are biologically relevant (Table III), the quantification in experiment t=1h was further analyzed. MS alignment with the presented ΔRT (11 minutes) led to an increased amount of quantified peptides compared to MS alignment with a smaller ΔRT (5.25 minutes), although most calculated peptide abundances did not differ between the two MS alignments. This shows that MS alignment with ΔRT=11 minutes does not decrease data quality. Finally, the experiments t=1h, t=3h and t=5h have been performed independently employing different mass spectrometers and using different reverse phase columns. Therefore, it is not possible to determine the dynamics of the abundance of the phosphopeptides over the 4h period as the RT deviates too much between the individual experiments.

The reported changes in average abundance ratio of a given phosphopeptide are proposed to represent a change in the phosphorylation status of the pool of the corresponding protein. However, constitutive phosphorylation in combination with altered amounts of protein as a result of transcriptional regulation of the encoding gene cannot be excluded for several of the identified peptides, as quantitative data from unphosphorylated peptides was not available.

Biological interpretation of the results

One of the most abundant proteins in plants is ribulose-1,5-bisphosphate carboxylase/oxygenase (RuBisCo) and although the large subunit of RuBisCo has been described to be phosphorylated, it was not identified in this analysis (Guitton and Mache, 1987; Spreitzer and Salvucci, 2002; Jones *et al.*, 2006a). Since RuBisCo is so abundant and often interferes in the various analyses, we followed a protein isolation method (Tsunezuka *et al.*, 2005) that minimizes RuBisCo extraction, as validated by 2-dimensional protein electrophoresis (Stulemeijer *et al*, unpublished results). Therefore, the samples were depleted for RuBisCo and this might explain why this phosphoprotein was not detected in our analysis.

Tomato cell suspensions expressing the Cf-5 resistance protein revealed the dephosphorylation of an H^+-ATPase after treatment with *C. fulvum* elicitor preparations containing Avr5 (Xing *et al.*, 1996). We also identified several phosphorylated H^+-ATPases but these did not show a change in abundance in the Cf-4/Avr4 seedlings (Table III). Possibly, the Cf-4/Avr4-induced response is different from the Cf-5 response, as is also apparent from the observed Cf-5-mediated medium acidification, in contrast to the reported Cf-4-mediated medium alkalization (Xing *et al.*, 1996; De Jong *et al.*, 2002). However, Cf-5-mediated dephosphorylation might also occur on an H^+-ATPase not identified in this study, or on another yet unidentified phosphorylation site. In addition, Cf-9- and Cf-4-triggered defence signalling in tobacco cell suspensions has been found to result in specific phosphorylation of the tobacco calcium-dependent protein kinase NtCDPK2 (Romeis *et al.*, 2001). Although we identified a phosphopeptide from tomato CDPK2, we did not observe a difference in its abundance between the Cf-4/Avr4 and the control seedlings. Also in this case, the exact site that becomes phosphorylated in the kinase is not known but mutational analysis have shown that the phosphorylated site is located outside the kinase domain (Ludwig *et al.*, 2005), which matches with the location of the phosphorylation site identified

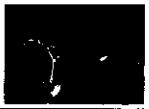

in our study. Possibly, Cf-4/Avr4-dependent phosphorylation of CDPK2 requires more than five hours in intact plants. Finally, three different LeMPKs were shown to become specifically activated in the Cf-4/Avr4 seedlings within 2h after initiation of the HR (Stulemijer *et al.*, 2007). Activation of these MAPKs is the result of their phosphorylation by upstream MAPKKs. However, we did not identify phosphopeptides originating from LeMPKs, which is possibly a reflection of their low abundance.

Changes in the phosphoproteome of the Cf-4/Avr4 seedlings point to a specific suppression of the activity of pyruvate dehydrogenase, the enzyme that converts pyruvate (the end product of glycolysis) into acetyl-CoA in the mitochondria. Interestingly, microarray analysis revealed a specific transcriptional upregulation of both of the genes encoding L-lactate dehydrogenase in tomato (Table IV) that catalyzes the conversion of pyruvate into lactate under anaerobic conditions. Interestingly, these genes are also upregulated under low-oxygen stress (Germain *et al.*, 1997; Germain and Ricard, 1997) and it has been described that the massive oxidative burst induced upon Avr9 recognition in Cf-9 tobacco suspension cells leads to an increase in oxygen consumption, creating low-oxygen stress (Piedras *et al.*, 1998). Also in cotyledons of tomato plants carrying Cf-2 or Cf-9, a fast production of reactive oxygen intermediates takes place upon recognition of Avr2 or Avr9 respectively (May *et al.*, 1996). We propose that in a similar way, the Cf-4-triggered oxidative burst (De Jong *et al.*, 2004) in combination with stomatal closure, leads to low-oxygen stress and a switch from aerobic to anaerobic respiration in order to maintain energy production.

Other interesting observations are the changes in average abundance ratio during HR development of the phosphorylated form of the different Hsp90 isoforms. The Hsp90 phosphorylation site is conserved in animal systems and here we show for the first time specific *in vivo* phosphorylation of plant Hsp90 isoforms at this conserved serine-phosphorylation site (Krishna and Gloor, 2001). Jones *et al* (2006a) reported Hsp90 phosphorylation in Arabidopsis during the defence response to *Pseudomonas syringae* but no unequivocal proof of phosphorylation was shown. Hsp90 was already shown to play a role in the Cf-4/Avr4-induced HR, as simultaneous VIGS of Hsp90-1 and Hsp90-2 compromises the Avr4-induced HR in *Nicotiana benthamiana* (Gabriëls *et al.*, 2006), as well as in tomato (Gabriëls *et al*, unpublished results). In addition, Hsp90s are thought to stabilize resistance proteins since they have been shown to interact with resistance proteins such as I-2 and N, which confer resistance to the fungus *Fusarium oxysporum* and the tobacco mosaic virus (Liu

et al., 2004; De la Fuente van Bentem *et al.*, 2005). Furthermore, Hsp90 is required for accumulation of the resistance protein Rx that confers resistance to potato virus X (Botër *et al.*, 2007). Our data suggest that Hsp90 isoforms have a different function in Cf-4/Avr4-triggered HR development and that Hsp90-2 and Hsp90-4 might be regulated by differential protein phosphorylation. Interestingly, NbHsp90c-1 from *N. benthamiana* interacts in a yeast two-hybrid screen with the MAP kinase NbSIPK (Kanzaki *et al.*, 2003), which is the orthologue of LeMPK1, one of the MAPKs that is activated during Cf-4/Avr4 signalling (Chapter 3). Possibly, LeMPK1 also interacts with Hsp90, thereby phosphorylating one or more of the Hsp90 isoforms. However, further analysis should reveal the function of (de)phosphorylation of the various Hsp90 isoforms during HR development and resistance.

Conclusions

This analysis shows that TiO_2 columns are suitable to enrich for phosphopeptides from complex protein extracts. In addition, LC-MS/MS analysis leads to sufficient peptide coverage between biological replicates when a shallow HPLC gradient is used, although the protein samples have not been pre-fractionated. Therefore, this approach can be a good alternative for a time and resources intensive large-scale phosphoproteome analysis that includes several prefractionation steps. Furthermore, our data show that relative label-free quantification is feasible for phosphopeptides isolated from total protein extracts of tomato leaves.

Our analysis has resulted in the identification and quantification of new phosphoproteins of tomato that change in abundance during HR development. As we have used intact plants in stead of cell suspensions, we have obtained insight in some general physiological changes that occur in plants that mount a defence response. Biological interpretation of our data revealed that photosynthetic activity is specifically suppressed immediately upon initiation of Cf-4/Avr4-triggered HR. In addition, the Cf-4/Avr4 seedlings seem to switch from aerobic to anaerobic respiration by favouring the lactic acid fermentation pathway. Furthermore, different levels of phosphorylated Hsp90 isoforms in Cf-4/Avr4 seedlings compared to controls point to a different role for the specific Hsp90 isoforms in HR development. Together, our results show that quantitative phosphoproteome analysis on intact plants leads to the identification of highly interesting key proteins, of which further analysis

will reveal their role in defence and metabolic reprogramming of plants responding to pathogens.

METHODS

Chemicals and materials

Formic acid (FA) was obtained from Merck (Darmstadt, Germany), trifluoroacetic acid (TFA) from Applied Biosystems (Warrington, UK), analytical-grade acetonitrile (ACN) from Fisher Scientific (Loughborough, UK) and acetic acid (HAc) from AppliChem (Darmstadt, Germany). Modified trypsin was obtained from Promega (Madison, WI) and modified lysyl endopeptidase from Wako Pure Chemical Industries, Ltd. (Neuss, Germany). Tips were from Eppendorff (Eppendorff, Hamburg, Germany). Plugs of 3M Empore^{tm} C8 disks (3M Bioanalytical Technologies, St. Paul, MN) were made with a 0.5 mm diameter HPLC syringe from SGE (Victoria, Australia), whereas plugs of 3M Empore^{tm} C18 disks were made with a 1 mm diameter HPLC syringe from the same manufacturer. Ultrapure water was obtained from an Elga system (Glostrup, Denmark). Titanium dioxide (TiO_2) beads were obtained from a disassembled TiO_2 cartridge (4.0 mm ID – 5020-08520-5u-TiO_2) purchased from GL sciences Inc, Japan. All other chemicals and reagents were of the highest grade commercially available.

Induction of a hypersensitive response in tomato seedlings

Cf-4/Avr4 seeds were obtained from crossings between *Cf-4*- and *Avr4*-expressing tomato plants. Seeds from *Cf-4*- or *Avr4*-expressing tomato plants were mixed and taken as control as described previously (De Jong *et al.*, 2002; Chapter 3). Germination of the seeds was stimulated and synchronized by a 20 min treatment with 25% (v/v) Lodik containing 4% (v/v) sodium hypochlorite, followed by extensive washing with tap water. After germination in soil under normal daylight conditions at room temperature, seedlings were incubated at 33°C and 100% RH under 16h/8h light/dark regime in an incubator (Elbanton, Kerkdriel, The Netherlands) for at least 7 days. The seedlings were subsequently shifted to 20°C and cotyledons were harvested at 1h, 3h and 5h after the temperature shift, immediately frozen in liquid nitrogen and stored at -80°C. This was done for three independent biological replicates.

Protein extraction and digestion

Cotyledon tissue was thawed in a solution containing 7M urea, 2M thiourea, 60mM DTT, 4% CHAPS and 2% IPG buffer pH 3-10 (GE Healthcare) and immediately ground with mortar and pestle (Tsunezuka *et al.*, 2005). Samples were vortexed and rotated for maximal 30 min and subsequently centrifuged at 16,000g for 15 min. The supernatant was transferred to a new vial and centrifuged for another 15 min (16,000g) until all solid particles were pelleted. Proteins present in the supernatant were precipitated by adding TCA to a final concentration of 10% (w/v), incubated at -20°C and centrifuged into a pellet at 4°C (16,000g; 15 min). Protein pellets were washed and stored at -80°C in 100% acetone until further use. Then protein pellets were washed with 70% acetone, dried, and dissolved in 6M urea and 2M thiourea by short sonication and shaking. After centrifugation at 16,000 g (15 min), the protein concentration of the supernatant was determined with a Bradford protein assay from Bio-Rad (Herlev, Denmark).

200 µg of each protein sample was treated with 4 µl DTT (1µg/µl) for 40 min to denature the proteins, after which the proteins were treated with 2 µl iodoacetamide (10µg/µl) for 40 min to reduce the cysteine residues. Subsequently, the proteins were digested with 4 µl lysyl endopeptidase (1µg/µl) for 4h after which the samples were 5 times diluted with 50 mM NH_4HCO_3, pH 8. Then, 4 µl of trypsin (1 µg/µl) was added and proteins were further digested overnight. All treatments were performed at room temperature unless stated otherwise.

Purification of phosphorylated peptides using TiO_2 columns

A small plug of C8 material was taken from a 3M Empore^{tm} C8 extraction disk and placed in the end of a P10-tip to retain the approximately 5 mm long column of TiO_2 beads (Thingholm *et al.*, 2006). The volume of the P10-tip was increased by placing a P200-tip, of which about 5 mm of the top was removed, into the P10-tip. The protein digest was diluted five times in 15% H_2O/ 80% ACN/ 5% TFA (v/v/v) and 50 µg of the digested proteins was loaded onto the TiO_2 column with gentle air pressure created by a plastic syringe (Gobom *et al.*, 1999; Larsen *et al.*, 2005). The column was subsequently washed twice with 15% H_2O/ 80% ACN/ 5% TFA (v/v/v), after which bound peptides were eluted with 50 µl NH_4OH (pH 10.5). Samples were acidified with 10% formic acid (FA) in H_2O (v/v).

To clean the samples before LC-MS/MS analysis, eight plugs of 3M Empore^{tm} C18 material were placed in the end of a P200-tip, washed with 100% ACN and equilibrated with

5% FA in H_2O (v/v). The peptides eluted from four TiO_2 column were loaded onto the equilibrated C18 column with gentle air pressure created with a plastic syringe and the column was washed with 5% FA in H_2O (v/v). Peptides were subsequently eluted with 240 µl of 25% H_2O/ 70% ACN/ 5% FA. The volume was decreased by vacuum drying and the peptides were dissolved in 0.5% HAc in H_2O (v/v). Peptides purified from 200 µg of digested protein provided material for three LC-MS/MS runs.

Nano-flow liquid chromatography electrospray ionization tandem mass spectrometry analysis (LC-ESI-MS/MS)

Three LC-ESI-MS/MS experiments were performed each of which experiment represents a different time point after the temperature shift (t=1h, t=3h and t=5h). For each experiment, three biologically independent samples were obtained from the Cf-4/Avr4 and the control seedlings. The samples from the first biological replicate were analyzed in triplicate to determine the technical variation per experiment, whereas the other samples were analyzed only once. Therefore, one experiment consisted of ten LC-MS/MS runs which were run in series. The technical replicates of the first biological replicate were run successively. Standard BSA runs were included to separate the biological replicates per experiment, although carry-over between the runs was not observed.

Automated nanoflow liquid chromatography/tandem mass spectrometric (nano-LC-MS and MS/MS) analysis was performed using a QTOF mass spectrometer (Micromass UK Ltd., Manchester, UK) employing automated data-dependent acquisition (DDA). For the t=3h experiment, a QTOF Ultima mass spectrometer coupled to an Ultimate/Switchos2/Famos nanoflow-HPLC system (LC Packings, The Netherlands) was used, whereas we employed a QTOF Micro mass spectrometer coupled to an Ultima 3000 nanoflow-HPLC system (Dionex, The Netherlands) for the t=1h and t=5h experiments. The HPLC systems delivered a flow rate of 100 nl/min over a silica transfer line (75 µm inner diameter, 360 µm outer diameter) connected to a homemade 1 cm fused silica pre-column (75 µm inner diameter, 360 µm outer diameter; ReproSil-pur AQ-C18 3µm (Dr. Maisch, GmbH, Germany). Chromatographic separation was accomplished by loading peptide samples onto the pre-column using an auto sampler. Peptides were sequentially eluted using a linear gradient from 100% of solution A (0% ACN, 0.5% HAc in H_2O) to 50% of solution A and 50% of solution B (80% ACN in 0.5% HAc in H_2O) in 120 minutes over the pre-column in series with a homemade 8 cm

resolving column (50 µm inner diameter; 360 µm outer diameter; ReproSil-pur AQ-C18 3 µm, Dr. Maisch GmbH, Germany). The resolving column was connected to a distally coated fused silica PicoTip™ emitter (360 µm outer diameter, 50 µm inner diameter, 8 µm tip inner diameter, New Objective, Cambridge, MA, USA). The mass spectrometer was operated in the positive ion mode with a resolution of 4500-8000 at full-width half-maximum (FWHM) for QTOF Micro and 6500-8000 for QTOF Ultima, using a source temperature of 150°C and 80°C respectively, and a counter current nitrogen flow rate of 60 liter/h. Data-dependent analysis was employed (four most abundant ions in each cycle); 1 second MS (m/z 350-1500) and a maximum of 2 (QTOF Ultima) or 3 (QTOF Micro) seconds MS/MS (m/z 50-2000), with 45 seconds dynamic exclusion.

Data processing and quantitative analysis using virtual expert mass spectrometrist (VEMS) software

Raw data were processed using ProteinLynx Global Server 2.0.5 (smooth 2/3 Savitzky Golay and center 4 channels/80% centroid) and the resulting MS/MS dataset was exported in Micromass pkl format for automated peptide identification using the Virtual Expert Mass Spectrometrist (VEMS v3_209 update 25-06-2007) software (Matthiesen *et al.*, 2005). To identify peptides, the SGN tomato database (Tomato_200607_build_1) containing ~34,000 expressed sequence tags (ESTs) was translated into protein sequences by ESTScan (http://www.sgn.cornell.edu/). The data from one experiment (t=1h, t=3h or t=5h) were loaded into VEMS software (Matthiesen *et al.*, 2004; Matthiesen *et al.*, 2005) and searched against the SGN database. The following constraints were used: only tryptic peptides and up to 2 missed cleavages sites, initial tolerance of 0.6 Da for MS ions and for MS/MS fragment ions and carbamidomethyl cysteine, methionine oxidation and serine, threonine and tyrosine phosphorylation were anticipated to occur. Based on the initial search, high confidence peptides were recalibrated in VEMS and the search was repeated with 50 ppm for MS ions and 0.6 Da for MS/MS fragment ions. For the experiment at t=3h, asparagine and glutamine deamidation was allowed. Since the focus of this study was the identification and quantification of phosphopeptides, all non-phosphoproteins were removed from the result file, resulting in a set of phosphopeptides and non-phosphopeptides that match a phosphoprotein. All phosphopeptide assignments reported by VEMS were manually validated to check the sequence and phosphorylation site assignment. No threshold score was applied to the

identified peptides before manual validation since phosphopeptides usually have a lower score than regular peptides and searches against small databases might lead to inaccurate scores. Spectra, VEMS scores, E-values, m/z, z values and mass errors of each peptide are reported in Supplementary Table SI. Relative label-free quantification of all peptides (threshold intensity = 0) was performed on the peak area using VEMS (version v3_209 update 25062007) (Matthiesen *et al.*, 2004; Matthiesen *et al.*, 2005) that includes the features to align and calibrate the LC-MS/MS data with respect to peptide retention time (RT) and mass, as also described by Beck *et al* (2006). Some peptides were selected for MS/MS in all ten samples per experiment and these peptides were used to determine the variation in RT (ΔRT; in minutes) per experiment. The mass deviation (Δmass; in mDa) was determined for the peptide with the largest mass deviation in an experiment. This information was subsequently used to set ΔRT and Δmass during peptide quantification. For the three experiments (t=1h, t=3h and t=5h), the ΔRT was 11.0, 3.4 and 4.3 minutes and the Δmass was 79, 21 and 75 mDa, respectively. The peak area from all identified peptides was extracted from the LC-MS part of the datasets and quantitative data were obtained for all identified peptides (Table III).

Tomato protein database

To have the most recent annotation of the SGN tomato database, the protein sequences as provided by SGN (ftp://ftp.sgn.cornell.edu/proteins/; Tomato_200607_build_1_pep) were matched against the UniProt Release 11.0 database by NCBI blastp 2.2.13 using default settings (Altschul *et al.*, 1997; Consortium, 2007). GO terms were assigned by IPRscan versie 4.2 and IPRscan data updates (30-5-2007) for InterPro release 15.1 (Zdobnov and Apweiler, 2001). The SGN tomato database is redundant, leading to multiple protein identifications for one phosphopeptide. When a phosphopeptide matches multiple proteins, all entries are reported in Table III. When a phosphopeptide matches multiple proteins originating from the same gene product, the entry with the longest sequence is reported. Since the tomato genome is not fully sequenced, we cannot exclude that phosphopeptides match proteins encoded by genes that have not been sequenced yet.

Data analysis and validation

Quantitative data from different phosphopeptides that cover the same phosphorylation site (resulting from missed cleavages) were combined to allow correct quantification of the phosphorylated form of a particular peptide. All data were normalized to the total abundance of all peptides per sample that were identified in all ten LC-MS/MS runs for one experiment. The data analysis described below was performed for each experiment (t=1h, t=3h and t=5h). Based on the triplicate analysis of biological replicate 1, the technical error of the quantification was determined by calculating the average abundance and the standard error (SE) of each peptide. The absolute SEs were plotted against the average peptide abundance and the data could be fitted with one parameter (ProFit, Zürich; y=ax). This revealed a linear correlation between the peptide abundance and the SEs and thus a constant technical error in each experiment (Figure 2; Vetterling *et al.*, 1992). The technical error was used to estimate the SE of the peptide abundance detected in the other samples that were analyzed only once (biological replicates 2 and 3). The peptide abundance in samples originating from the Cf-4/Avr4 seedlings (x) was divided by the peptide abundance of the control samples (y) to calculate the relative abundance ratio (f; $f = x / y$) per peptide for each biological replicate. The SE of the relative abundance ratio was calculated according to the equation $(\sigma_f/f)^2 = (\sigma_x/x)^2 + (\sigma_y/y)^2$, in which σ represents the SE. Subsequently, a relative average abundance ratio ($f = (a + b + c)/3$, in which a, b and c represent the relative abundance ratios of biological replicates 1, 2 and 3, respectively) was calculated per peptide for each experiment (t=1h, t=3h and t=5h). The SE for this ratio was subsequently calculated according to the equation $\sigma_f^2 = \sigma_a^2 + \sigma_b^2 + \sigma_c^2$ (Vetterling *et al.*, 1992).

Microarray experiment and analysis

Total RNA was extracted and purified (NucleoSpin RNA/Protein kit, Machery-Nagel, GmbH & Co., Dueren, Germany) from cotyledons of Cf-4/Avr4 and control seedlings at t=1h, t=3h and t=5h after the temperature shift. Three independent biological replicates were performed. RNA-labeling, hybridization of the microarray (GeneChip® Tomato Genome Array, Affymetrix, Santa Clara, CA, USA) and data extraction was performed at ServiceXS (Leiden, The Netherlands) according to standard protocols provided by the manufacturer. In short, RNA concentrations were determined with the Nanodrop (type ND-1000) and RNA quality was assessed with the RNA 6000 Nano Labchip kit (Agilent Technologies, Palo Alto,

CA, USA). Biotin-labeled cRNA was synthesized from 2 μg of total RNA using the Affymetrix one-cycle target labeling and control agents (Affymetrix, Part nr. 900493). The tomato GeneChips were hybridized with 20 μg of fragmented biotin-labeled cRNA. After automated washing and staining, the GeneChips were scanned with an Affymetrix scanner, type G7. Raw data were converted to CEL files with Affymetrix GCOS software and data analysis was performed by packages from the Bioconductor project (Gentleman *et al.*, 2004) implemented in the Management and Analysis Database for Microarray Experiments (MADMAX, Gavai, de Groot and Leunissen, unpublished results). MADMAX microarray quality control analysis (Jones *et al.*, 2006b) revealed that one array deviated from the others (Cf-4/Avr4, t=3h) and this array was excluded from further analysis. Subsequently, the arrays were normalized using quartile normalization, and expression estimates were compiled using GC-RMA, applying the empirical Bayes approach (Wu *et al.*, 2004). Differentially expressed probe sets were identified using linear models, applying moderate t-statistics that implement empirical Bayes regularization of standard errors (Smyth, 2004). Sequences present on the microarray entries were matched to a SGN-ID based on their sequence, by NCBI stand-alone blast (blast-2.2.12-ia32-win32; http://www.ncbi.nlm.nih.gov/BLAST/download.shtml).

Determination of photosynthetic activity by chlorophyll fluorescence measurement and imaging

Cf-4/Avr4 and control seedlings were subjected to a temperature shift from 33°C to room temperature and were analyzed to determine their photosynthetic activity over a period of 18 h. Plants were scanned each 10 minutes with a fast (F_0) and a slow (F_m) scanning red laser light line and a 16 bit CCD camera was used to record the reflected light from the leaf surface, observed as fluorescence. The relative increase in fluorescence is expressed as $((F_m - F_0)/F_m)*100\%$, which reflects the quantum efficiency of photosystem II reaction centers and thus reflects the photosynthetic activity. In healthy plants, quantum efficiency is generally 75-80% (De Ruiter *et al.*, 2007).

ACKNOWLEDGEMENTS

We are very thankful to Rune Matthiesen for VEMS assistance, Kate Rafn and David Selby for technical assistance during LC-MS/MS analysis, Christian Ravnsborg, Andreas Schlattl and Jan Poulsen for assistance in bioinformatics, Pieter Neerincx for SGN database annotation, Philip de Groot for assistance during microarray analysis, and Tine Thingholm and Martin Larsen for useful discussions. Furthermore, we thank Henk Jalink and Rob van der Schoor for chlorophyll fluorescence measurement and imaging of the seedlings. This work was supported by a personal grant to Iris Stulemeijer from the Netherlands Genomics Initiative (Fellowship: 050-72-416).

REFERENCES

Altschul SF, Madden TL, Schaffer AA, Zhang J, Zhang Z, Miller W, Lipman DJ (1997) Gapped BLAST and PSI-BLAST: a new generation of protein database search programs. Nucl Acids Res 25: 3389-3402.

Asai T, Tena G, Plotnikova J, Willmann MR, Chiu WL, Gomez Gomez L, Boller T, Ausubel FM, Sheen J (2002) MAP kinase signalling cascade in Arabidopsis innate immunity. Nature 415: 977-983.

Beck HC, Nielsen EC, Matthiesen R, Jensen LH, Sehested M, Finn P, Grauslund M, Hansen AM, Jensen ON (2006) Quantitative proteomic analysis of post-translational modifications of human histones. Mol Cell Proteomics 5: 1314-1325.

Benschop JJ, Mohammed S, O'Flaherty M, Heck AJR, Slijper M, Menke FLH (2007) Quantitative phosphoproteomics of early elicitor signalling in Arabidopsis. Mol Cell Proteomics 6: 1198-1214.

Botër M, Amigues B, Peart J, Breuer C, Kadota Y, Casais C, Moore G, Kleanthous C, Ochsenbein F, Shirasu K, Guerois R (2007) Structural and functional analysis of SGT1 reveals that its interaction with HSP90 is required for the accumulation of Rx, an R protein involved in plant immunity. Plant Cell 19: 3791-3804.

Cheng SH, Willmann MR, Chen HC, Sheen J (2002) Calcium signaling through protein kinases. The Arabidopsis calcium-dependent protein kinase gene family. Plant Physiol 129: 469-485.

Christie JM (2007) Phototropin blue-light receptors. Annu Rev Plant Biol 58: 21-45.

Consortium TU (2007) The universal protein resource (UniProt). Nucl Acids Res 36 (Database issue): 190-195.

De Jong CF, Honée G, Joosten MHAJ, De Wit PJGM (2000) Early defence responses induced by AVR9 and mutant analogues in tobacco cell suspensions expressing the *Cf9* resistance gene. Physiol Mol Plant Pathol 56: 169-177.

De Jong CF, Laxalt AM, Bargmann BOR, De Wit PJGM, Joosten MHAJ, Munnik T (2004) Phosphatidic acid accumulation is an early response in the Cf-4/Avr4 interaction. Plant J 39: 1-12.

De Jong CF, Takken FLW, Cai X, De Wit PJGM, Joosten MHAJ (2002) Attenuation of Cf-mediated defense responses at elevated temperatures correlates with a decrease in elicitor-binding sites. Mol Plant-Microbe Interact 15: 1040-1049.

De la Fuente van Bentem S, Vossen JH, De Vries KJ, Van Wees S, Tameling WIL, Dekker HL, Koster CG, Haring MA, Takken FLW, Cornelissen BJC (2005) Heat shock protein 90 and its co-chaperone protein phosphatase 5 interact with distinct regions of the tomato I-2 disease resistance protein. Plant J 43: 284-298.

De Ruiter H, Mack B, Van der Schoor R, Jalink H (2007) Fluoresence imaging as a non-invasive technology to monitor the performance of glyphosate adjuvants and formulations. J ASTM Internat 4: 1-8.

De Wit PJGM (2007) How plants recognize pathogens and defend themselves. Cell Mol Life Sci 64: 2726-2732.

Devarenne TP, Ekengren SK, Pedley KF, Martin GB (2006) Adi3 is a Pdk1-interacting AGC kinase that negatively regulates plant cell death. EMBO J 25: 255-265.

Dougherty JJ, Rabideau DA, Iannotti AM, Sullivan WP, Toft DO (1987) Identification of the 90 kDa substrate of rat liver type II casein kinase with the heat shock protein which binds steroid receptors. Biochim Biophys Acta 927: 74-80.

Feilner T, Hultschig C, Lee J, Meyer S, Immink RGH, Koenig A, Possling A, Seitz H, Beveridge A, Scheel D, Cahill DJ, Lehrach H, Kreutzberger J, Kersten B (2005) High throughput identification of potential Arabidopsis mitogen-activated protein kinases substrates. Mol Cell Proteomics 4: 1558-1568.

Flor HH (1942) Inheritance of pathogenicity in *Melampsora lini*. Phytopathology 32: 653-669.

Gabriëls SHEJ, Takken FLW, Vossen JH, De Jong CF, Liu Q, Turk SCHJ, Wachowski LK, Peters J, Witsenboer HMA, De Wit PJGM, Joosten MHAJ (2006) cDNA-AFLP combined with functional analysis reveals novel genes involved in the hypersensitive response. Mol Plant-Microbe Interact 19: 567-576.

Gentleman RC, Carey VJ, Bates DM, Bolstad B, Dettling M, Dudoit S, Ellis B, Gautier L, Ge Y, Gentry J, Hornik K, Hothorn T, Huber W, Iacus S, Irizarry RA, Leisch F, Li C, Maechler M, Rossini AJ, Sawitzki G, Smith C, Smyth G, Tierney L, Yang JYH, Zhang J (2004) Bioconductor: open software development for computational biology and bioinformatics. Genome Biol 5

Germain V, Raymond P, Ricard B (1997) Differential expression of two toamto lactate dehydrogenase genes in reponse to oxygen deficit. Plant Mol Biol 35: 711-721.

Germain V, Ricard B (1997) Two ldh genes from tomato and their expression in different organs, during fruit ripening and in response to stress. Plant Mol Biol 35: 949-954.

Gobom J, Nordhoff E, Mirgorodskaya E, Ekman R, Roepstorff P (1999) Sample purification and preparation technique based on nano-scale reversed-phase columns for the sensitive analysis of complex peptide mixtures by matrix-assisted laser desorption/ionization mass spectrometry. J Mass Spectrom 34: 105-116.

Gómez-Gómez L, Bauer Z, Boller T (2001) Both the extracellular leucine-rich repeat domain and the kinase activity of FSL2 are required for flagellin binding and signaling in Arabidopsis. Plant Cell 13: 1155-1163.

Gruhler A, Olsen JV, Mohammed S, Mortensen P, Faergeman NJ, Mann M, Jensen ON (2005) Quantitative phosphoproteomics applied to the yeast pheromone signaling pathway. Mol Cell Proteomics 4: 310-327.

Guitton C, Mache R (1987) Phosphorylation *in vitro* of the large subunit of the ribulose-1,5-bisphosphate carboxylase and of the glyceraldehyde-3-phosphate dehydrogenase. Eur J Biochem 166: 249-254.

He X, Anderson JC, Del Pozo O, Gu YQ, Tang X, Martin GB (2004) Silencing of subfamily I of protein phosphatase 2A catalytic subunits results in activation of plant defense responses and localized cell death. Plant J 38: 563-577.

Heese A, Ludwig AA, Jones JDG (2005) Rapid phosphorylation of a syntaxin during the Avr9/Cf-9-race-specific signaling pathway. Plant Physiol 138: 2406-2416.

Jensen ON (2006) Interpreting the protein language using proteomics. Nature Rev Mol Cell Biol 7: 391-403.

Jones AM, Bennett MH, Mansfield JW, Grant M (2006a) Analysis of the defence phosphoproteome of *Arabidopsis thaliana* using differential mass tagging. Proteomics. 6: 4155-4165.

Jones JDG, Dangl JL (2006) The plant immune system. Nature 444: 323-329.

Jones L, Goldstein DR, Hughes G, Strand AD, Collin F, Dunnett SB, Kooperberg C, Aragaki A, Olson JM, Augood SJ, Faull RLM, Luthi-Carter R, Moskvina V, Hodges AK (2006b) Assessment of the relationship between pre-chip and post-chip quality measures for Affymetrix GeneChip expression data. BMC Bioinformatics 7

Joosten MHAJ, De Wit PJGM (1999) The tomato-*Cladosporium fulvum* interaction: A versatile experimental system to study plant-pathogen interactions. Annu Rev Phytopathol 37: 335-367.

Kanzaki H, Saitoh H, Ito A, Fujisawa S, Kamoun S, Katou S, Yoshioka H, Terauchi R (2003) Cytosolic HSP90 and HSP70 are essential components of INF1-mediated hypersensitive response and non-host resistance to *Pseudomonas cichorii* in *Nicotiana benthamiana*. Mol Plant Pathol 4: 383-391.

Kersten B, Agrawal GK, Iwahashi H, Rakwal R (2006) Plant phosphoproteomics: A long road ahead. Proteomics 6: 5517-5528.

Kim MG, da Cunha L, McFall AJ, Belkhadir Y, DebRoy S, Dangl JL, Mackey D (2005) Two *Pseudomonas syringae* type III effectors inhibit RIN4-regulated basal defense in Arabidopsis. Cell 121: 749-759.

Krishna P, Gloor G (2001) The Hsp90 family of proteins in *Arabidopsis thaliana*. Cell Stress Chaperon 6: 238-246.

Larsen MR, Thingholm TE, Jensen ON, Roepstorff P, Jørgensen TJD (2005) Highly selective enrichment of phosphorylated peptides from peptide mixtures using titanium dioxide microcolumns. Mol Cell Proteomics 4: 873-886.

Liu Y, Burch-Smith T, Schiff M, Feng S, Dinesh-Kumar SP (2004) Molecular chaperone Hsp90 associates with resistance protein N and its signaling proteins SGT1 and RAR1 to modulate an innate immune response in plants. J Biol Chem 279: 2101-2108.

Ludwig AA, Saitoh H, Felix G, Freymark G, Miersch O, Wasternack C, Boller T, Jones JDG, Romeis T (2005) Ethylene-mediated cross-talk between calcium-dependent protein kinase and MAPK signaling controls stress responses in plants. Proc Natl Acad Sci USA 102: 10736-10741.

Matthiesen R, Bunkenborg J, Stensballe A, Jensen ON, Welinder KG, Bauw G (2004) Database-independent, database-dependent, and extended interpretation of peptide spectra in VEMS V2.0. Proteomics 4: 2583-2593.

Matthiesen R, Trelle MB, Højrup P, Bunkenborg J, Jensen ON (2005) VEMS 3.0: Algorithms and computational tools for tandem mass spectrometry based identification of post-translational modifications in proteins. J Proteome Res 4: 2338-2347.

May MJ, Hammond-Kosack KE, Jones JDG (1996) Involvement of reactive oxygen species, glutathione metabolism, and lipid peroxidation in the Cf-gene-dependent defense response of tomato cotyledons induced by race-specific elicitors of *Cladosporium fulvum*. Plant Physiol 110: 1367-1379.

Mayor A, Martinon F, De Smedt T, Petrilli V, Tschopp J (2007) A crucial function of SGT1 and HSP90 in inflammasome activity links mammalian and plant innate immune responses. Nat Immunol 8: 497-503.

Mucyn TS, Clemente A, Andriotis VME, Balmuth AL, Oldroyd GED, Staskawicz BJ, Rathjen JP (2006) The tomato NB-ARC-LRR protein Prf interacts with Pto kinase *in vivo* to regulate specific plant immunity. Plant Cell 18: 2792-2806.

Norholm MHH, Nour-Eldin HH, Brodersen P, Mundy J, Halkier BA (2006) Expression of the Arabidopsis high-affinity hexose transporter STP13 correlates with programmed cell death. FEBS Lett 580: 2381-2387.

Nühse TS, Boller T, Peck SC (2003a) A plasma membrane syntaxin is phosphorylated in response to the bacterial elicitor flagellin. J Biol Chem 278: 45248-45254.

Nühse TS, Bottrill AR, Jones AME, Peck SC (2007) Quantitative phosphoproteomic analysis of plasma membrane proteins reveals regulatory mechanisms of plant innate immune responses. Plant J 51: 931-940.

Nühse TS, Stensballe A, Jensen ON, Peck SC (2003b) Large-scale analysis of *in vivo* phosphorylated membrane proteins by immobilized metal ion affinity chromatography and mass spectrometry. Mol Cell Proteomics 2: 1234-1243.

Nühse TS, Stensballe A, Jensen ON, Peck SC (2004) Phosphoproteomics of the Arabidopsis plasma membrane and a new phosphorylation site database. Plant Cell 16: 2394-2405.

Ogiso H, Kagi N, Matsumoto E, Nishimoto M, Arai R, Shirouzu M, Mimura J, Fujii-Kuriyama Y, Yokoyama S (2004) Phosphorylation analysis of 90 kDa heat shock protein within the cytosolic arylhydrocarbon receptor complex. Biochemistry 43: 15510-15519.

Ong S-E, Foster LJ, Mann M (2003) Mass spectrometric-based approaches in quantitative proteomics. Methods 29: 124-130.

Ono M, Shitashige M, Honda K, Isobe T, Kuwabara H, Matsuzuki H, Hirohashi S, Yamada T (2006) Label-free quantitative proteomics using large peptide data sets generated by nanoflow liquid chromatography and mass spectromery. Mol Cell Proteomics 5: 1338-1347.

Peck SC (2003) Early phosphorylation events in biotic stress. Curr Opin Plant Biol 6: 334-338.

Peck SC (2006) Phosphoproteomics in Arabidopsis: Moving from empirical to predictive science. J Exp Bot 57: 1523-1527.

Peck SC, Nühse TS, Hess D, Iglesias A, Meins F, Boller T (2001) Directed proteomics identifies a plant-specific protein rapidly phosphorylated in response to bacterial and fungal elicitors. Plant Cell 13: 1467-1475.

Pedley KF, Martin GB (2005) Role of mitogen-activated protein kinases in plant immunity. Curr Opin Plant Biol 8: 541-547.

Piedras P, Hammond Kosack KE, Harrison K, Jones DG (1998) Rapid, Cf-9- and Avr9-dependent production of active oxygen species in tobacco suspension cultures. Mol Plant-Microbe Interact 11: 1155-1166.

Reinders J, Sickmann A (2005) State-of-the-art in phosphoproteomics. Proteomics 5: 4052-4061.

Richter K, Hendershot LM, Freeman BC (2007) The cellular world according to Hsp90. Nat Struct Mol Biol 14: 90-94.

Ritsema T, Joore J, van Workum W, Pieterse C (2007) Kinome profiling of Arabidopsis using arrays of kinase consensus substrates. Plant Methods 3: 3.

Rivas S, Thomas CM (2005) Molecular interactions between tomato and the leaf mold pathogen *Cladosporium fulvum*. Annu Rev Phytopathol 43: 395-436.

Roblin G, Sakr S, Bonmort J, Delrot S (1998) Regulation of a plant plasma membrane sucrose transporter by phosphorylation. FEBS Lett 424: 165-168.

Romeis T, Ludwig AA, Martin R, Jones JDG (2001) Calcium-dependent protein kinases play an essential role in a plant defence response. EMBO J 20: 5556-5567.

Romeis T, Piedras P, Jones JDG (2000) Resistance gene-dependent activation of a calcium-dependent protein kinase in the plant defense response. Plant Cell 12: 803-815.

Romeis T, Piedras P, Zhang SQ, Klessig DF, Hirt H, Jones JDG (1999) Rapid Avr9- and Cf-9-dependent activation of MAP kinases in tobacco cell cultures and leaves: convergence of resistance gene, elicitor, wound, and salicylate responses. Plant Cell 11: 273-287.

Rowland O, Ludwig AA, Merrick CJ, Baillieul F, Tracy FE, Durrant WE, Fritz-Laylin L, Nekrasov V, Sjolander K, Yoshioka H, Jones JDG (2005) Functional analysis of Avr9/Cf-9 rapidly elicited genes identifies a protein kinase, ACIK1, that is essential for full Cf-9-dependent disease resistance in tomato. Plant Cell 17: 295-310.

Rubin PM, Randall DD (1977) Regulation of plant pyruvate dehydrogenase complex by phosphorylation. Plant Physiol 60: 34-39.

Sangster TA, Queitsch C (2005) The HSP90 chaperone complex, an emerging force in plant development and phenotypic plasticity. Curr Opin Plant Biol 8: 86-92.

Sessa G, D'Ascenzo M, Martin GB (2000a) The major site of the pti1 kinase phosphorylated by the pto kinase is located in the activation domain and is required for pto-pti1 physical interaction. Eur J Biochem 267: 171-178.

Sessa G, D'Ascenzo M, Martin GB (2000b) Thr38 and Ser198 are Pto autophosphorylation sites required for the AvrPto-Pto-mediated hypersensitive response. EMBO J 19: 2257-2269.

Shan L, He P, Sheen J (2007) Intercepting host MAPK signaling cascades by bacterial type III effectors. Cell Host Microbe 1: 167-174.

Smyth GK (2004) Linear models and empirical bayes methods for assessing differential expression in microarray experiments. Stat Appl Genet Mol Biol 3

Spreitzer RJ, Salvucci ME (2002) RUBISCO: structure, regulatory interactions, and possibilities for a better enzyme. Annu Rev Plant Biol 53: 449-475.

Steen H, Jebanathirajah JA, Springer M, Kirschner MW (2005) Stable isotope-free relative and absolute quantitation of protein phosphorylation stoichiometry by MS. Proc Natl Acad Sci USA 102: 3948-3953.

Suarez-Rodriguez MC, Adams-Phillips L, Liu Y, Wang H, Su SH, Jester PJ, Zhang S, Bent AF, Krysan PJ (2007) MEKK1 is required for flg22-induced MPK4 activation in Arabidopsis plants. Plant physiology 143: 661-669.

Sun JK, Eun YC, Yoon JC, Ji HA, Park OK (2006) Proteomics studies of post-translational modifications in plants. J Exp Bot 57: 1547-1551.

Takahashi A, Casais C, Ichimura K, Shirasu K (2003) HSP90 interacts with RAR1 and SGT1 and is essential for RPS2-mediated disease resistance in Arabidopsis. Proc Natl Acad Sci USA 100: 11777-11782.

Thelen JJ, Peck SC (2007) Quantitative proteomics in plants: choices in abundance. Plant Cell 19: 3339-3346.

Thingholm TE, Jørgensen TJD, Jensen OL, Larsen MR (2006) Highly selective enrichment of phosphorylated peptides using titanium dioxide. Nature Protoc 1: 1929-1935.

Thomma BPHJ, Van Esse HP, Crous PW, De Wit PJGM (2005) *Cladosporium fulvum* (syn. *Passalora fulva*), a highly specialized plant pathogen as a model for functional studies on plant pathogenic Mycosphaerellaceae. Mol Plant Pathol 6: 379-393.

Tsunezuka H, Fujiwara M, Kawasaki T, Shimamoto K (2005) Proteome analysis of programmed cell death and defense signaling using the rice lesion mimic mutant cdr2. Mol Plant-Microbe Interact 18: 52-59.

Van Esse HP, Bolton MD, Stergiopoulos I, De Wit PJGM, Thomma BPHJ (2007) The chitin-binding *Cladosporium fulvum* effector protein Avr4 is a virulence factor. Mol Plant-Microbe Interact 20: 1092-1101.

Vener AV (2007) Environmentally modulated phosphorylation and dynamics of proteins in photosynthetic membranes. BBA - Bioenergetics 1767: 449-457.

Vetterling WT, Press WH, Teukolski SA, Flannery BP (1992) Numerical recipes in C, Ed 2nd. http://www.computer-books.us/c_4.php

Wang C, Cai X, Zheng Z (2005) High humidity represses *Cf-4/Avr4*- and *Cf-9/Avr9*-dependent hypersensitive cell death and defense gene expression. Planta 222: 947-956.

Wang P, Tang H, Fitzgibbon MP, McIntosh M, Coram M, Zhang H, Yi E, Aebersold R (2007) A statistical method for chromatographic alignment of LC-MS data. Biostat 8: 357-367.

Wang YS, Pi LY, Chen X, Chakrabarty PK, Jiang J, De Leon AL, Liu GZ, Li A, Benny U, Oard J, Ronald PC, Song WY (2006) Rice XA21 binding protein 3 is a ubiquitin ligase required for full *Xa21*-mediated disease resistance. Plant Cell 18: 3635-3646.

Wu Z, Irizarry RA, Gentleman R, Martinez-Murillo F, Spencer F (2004) A model-based background adjustment for oligonucleotide expression arrays. J Am Stat Assoc 99: 909-917.

Xiang T, Zong N, Zou Y, Wu Y, Zhang J, Xing W, Li Y, Tang X, Zhu L, Chai J, Zhou J-M (2008) *Pseudomonas syringae* effector AvrPto blocks innate immunity by targeting receptor kinases. Curr Biol 18: 74-80.

Xing T, Higgins VJ, Blumwald E (1996) Regulation of plant defense response to fungal pathogens: two types of protein kinases in the reversible phosphorylation of the host plasma membrane H+-ATPase. Plant Cell 8: 555-564.

Xing T, Ouellet T, Miki BL (2002) Towards genomic and proteomic studies of protein phosphorylation in plant-pathogen interactions. Trends Plant Sci 7: 224-230.

Xu WH, Wang YS, Liu GZ, Chen X, Tinjuangjun P, Pi LY, Song WY (2006) The autophosphorylated Ser686, Thr688, and Ser689 residues in the intracellular juxtamembrane domain of XA21 are implicated in stability control of rice receptor-like kinase. Plant J 45: 740-751.

Zdobnov EM, Apweiler R (2001) InterProScan - an integration platform for the signature-recognition methods in InterPro. Bioinformatics 17: 847-848.

Zieske LR (2006) A perspective on the use of iTRAQ reagent technology for protein complex and profiling studies. J Exp Bot 57: 1501-1508.

SUPPLEMENTARY DATA

Supplementary Table SI is available upon request.

Supplementary Table SII. Replicate phosphopeptide quantification at t=1h, t=3h and t=5h.

SGN-ID[a]	Peptide sequence[b]	Cf-4/Avr4 compared to control seedlings[c] t=1h		
		Ratio 1	Ratio 2	Ratio 3
SGN-U312354 SGN-U312357 SGN-U313363	EDQLEYLEER	1.11 ± 0.16	2.09 ± 0.28	1.22 ± 0.17
SGN-U313365	ELISNSSDALDK	1.21 ± 0.19	1.95 ± 0.26	1.06 ± 0.14
SGN-U312354	EISDDEDEEEK	0.77 ± 0.34	0.73 ± 0.10	0.31 ± 0.04
SGN-U312357	EISDDEEEEEK	0.68 ± 0.23	0.51 ± 0.07	1.59 ± 0.22
SGN-U313363 SGN-U313365	EISDDEDDEPK	1.51 ± 0.58	0.66 ± 0.09	1.49 ± 0.20
SGN-U313363	EISDDEDDEPKKDEEGAVEEVDEDK			
SGN-U313365	EISDDEDDEPKKEQEGDIEEVDEDK			
SGN-U312661	NLAGDIIGtRtEVADVK			
SGN-U312844	SISTPFmNTASK	1.33 ± 0.22		0.83 ± 0.11
SGN-U312863	AALAAGADKDEEDSEGR KSPESSTVEAPSGEGR	1.06 ± 0.18 1.23 ± 0.29		1.37 ± 0.19 0.76 ± 0.10
SGN-U313210 SGN-U313218	FGEAVWFK			
SGN-U313210	SAPSSSPWYGPDR SAPSSSPWYGPDR			
SGN-U313218	PASSGSPWYGPDR TAAKPKPASSGSPWYGPDR	1.44 ± 0.09 0.96 ± 0.10	29.95 ± 4.07	1.40 ± 0.19 0.51 ± 0.[redacted]
SGN-U313242	GGmtsHAAVVAR			
SGN-U313311	VETPIDANEIR VSTDFDYDGEG SPSGGR	0.53 ± 0.02 0.99 ± 0.51	0.38 ± 0.05	0.84 ± 0.[redacted] 0.03 ± 0.00
SGN-U313649 SGN-U313650	GLDIETIQQSY TV			
SGN-U313547 SGN-U315949	GLDIETIQQHY TV			
SGN-U313599	RFGTTGTVK			
SGN-U313650	TLHGLQVPDTK	1.05 ± 0.31		0.91 ± 0.12
SGN-U313858	KEEPKEESDDDmGFSLFD	0.96 ± 0.49		0.37 ± 0.05
SGN-U314961	IASESDVSVHSTFASR			
SGN-U315162	VADSGASPPASSANPQHPASR			
SGN-U315274	TPVTEsAsFK	[redacted]		[redacted]
SGN-U315305	YHGHsmsDPGSTYR	0.50 ± 0.07	5.56 ± 0.76	3.66 ± 0.50
SGN-U315592	VSSFEALQPVNR	1.24 ± 0.31		0.72 ± 0.10
SGN-U315632	LRDGEASDEEEEYEAK			
SGN-U315720	SHAVDA SDDEmDDDENDANIK			
SGN-U315821	ALGSFRSNATN			
SGN-U315990	AAATIAKEPEEK ANEESDAQVA TVR	1.10 ± 0.18 1.03 ± 0.47	0.70 ± 0.10 0.36 ± 0.05	2.26 ± 0.31 1.27 ± 0.17
SGN-U316572	ALGsFRsNQTN ALGSFRSNQTN			
SGN-U317145	QLmLEYAGSER			
SGN-U317356	NSAEGYVPIHAL sEsPK			
SGN-U317388	VSTLPSENPQ SPSDQPK			
SGN-U317660	EAVAD mSEDLSEGEK			
SGN-U317742 SGN-U317743	SVVELTSGT SDDGHDK			
SGN-U317758	KVSPIPESR	0.72 ± 0.09	1.05 ± 0.14	0.50 ± 0.07
SGN-U317838	QLSIDQFENEGR			
SGN-U318020	VDGLLtssssPR			
SGN-U318050	GLEHSFSTGFR			

Supplementary Table SII. Continued from left page.

SGN-ID[a]	Cf-4/Avr4 compared to control seedlings [c]					
	t=3h			t=5h		
	Ratio 1	Ratio 2	Ratio 3	Ratio 1	Ratio 2	Ratio 3
SGN-U312354						
SGN-U312357	0.97 ± 0.19	0.28 ± 0.03	1.93 ± 0.20	1.09 ± 0.10		
SGN-U313363						
SGN-U313365				1.14 ± 0.24	0.63 ± 0.07	1.77 ± 0.20
SGN-U312354	0.62 ± 0.14	1.56 ± 0.16	0.28 ± 0.03	**1.49 ± 0.37**	**2.17 ± 0.17**	
SGN-U312357	1.73 ± 1.46	0.98 ± 0.10	0.75 ± 0.08	**12.41 ± 2.22**	**5.27 ± 0.60**	**1.22 ± 0.14**
SGN-U313363	0.71 ± 0.74	0.21 ± 0.02		1.47 ± 0.34	0.14 ± 0.02	1.12 ± 0.09
SGN-U313365						
SGN-U313363	0.71 ± 0.04	5.10 ± 0.52	0.62 ± 0.06			
SGN-U313365	1.06 ± 0.08	1.27 ± 0.13	1.10 ± 0.11			
SGN-U312661	2.80 ± 0.50	0.46 ± 0.05	2.78 ± 0.28	1.49 ± 0.23	0.84 ± 0.10	0.57 ± 0.06
SGN-U312844				2.56 ± 0.26	0.35 ± 0.04	1.09 ± 0.09
SGN-U312863						
SGN-U313210				1.36 ± 0.20	0.05 ± 0.01	
SGN-U313218						
SGN-U313210				1.77 ± 0.29	0.12 ± 0.01	3.49 ± 0.28
SGN-U313218				1.44 ± 0.11	1.36 ± 0.15	0.31 ± 0.03
					1.50 ± 0.17	
SGN-U313242				0.91 ± 0.25	0.36 ± 0.04	1.09 ± 0.12
SGN-U313311				1.98 ± 0.17		
	0.46 ± 0.04	2.07 ± 0.21	1.24 ± 0.13	0.95 ± 0.08	0.91 ± 0.10	0.57 ± 0.06
SGN-U313649	1.24 ± 0.38	0.23 ± 0.02	2.23 ± 0.23	0.86 ± 0.09		
SGN-U313650						
SGN-U313547	1.23 ± 0.28	0.67 ± 0.07	2.65 ± 0.27	0.98 ± 0.15	0.84 ± 0.10	2.66 ± 0.30
SGN-U315949						
SGN-U313599						
SGN-U313650				0.71 ± 0.12	1.43 ± 0.16	1.71 ± 0.19
SGN-U313858	2.13 ± 0.26	0.70 ± 0.07	3.74 ± 0.38	1.29 ± 0.48	0.94 ± 0.11	1.01 ± 0.11
SGN-U314961	0.73 ± 0.04		3.56 ± 0.36	1.71 ± 0.40	0.79 ± 0.09	
SGN-U315162				1.72 ± 0.36	0.33 ± 0.04	
SGN-U315274				0.30 ± 0.03	0.66 ± 0.07	3.06 ± 0.35
SGN-U315305				1.31 ± 0.33	0.33 ± 0.04	0.96 ± 0.11
SGN-U315592	1.32 ± 0.07	0.14 ± 0.01	1.76 ± 0.18	1.37 ± 0.14	2.08 ± 0.24	0.89 ± 0.10
SGN-U315632	1.51 ± 0.21	0.35 ± 0.04	0.85 ± 0.09	0.85 ± 0.09		
SGN-U315720	1.04 ± 0.28	0.60 ± 0.06				
SGN-U315821	0.90 ± 0.09		0.73 ± 0.07			
SGN-U315990	2.66 ± 1.94	3.45 ± 0.35		1.32 ± 0.40		
	0.97 ± 0.08	2.45 ± 0.25	0.33 ± 0.03	0.46 ± 0.06		
SGN-U316572	1.05 ± 0.11	0.23 ± 0.02	0.47 ± 0.05	1.34 ± 0.21	0.33 ± 0.04	0.48 ± 0.05
	1.28 ± 0.23		1.43 ± 0.15	1.22 ± 0.15	1.82 ± 0.21	0.85 ± 0.10
SGN-U317145	0.36 ± 0.02	0.37 ± 0.04	3.78 ± 0.38			
SGN-U317356	1.02 ± 0.30	1.09 ± 0.11	4.95 ± 0.50			
SGN-U317388	0.52 ± 0.05	1.77 ± 0.18	0.11 ± 0.01	0.84 ± 0.15		0.81 ± 0.09
SGN-U317660	0.63 ± 0.13	1.20 ± 0.12				
SGN-U317742	1.01 ± 0.30	9.29 ± 0.94				
SGN-U317743						
SGN-U317758						
SGN-U317838	0.77 ± 0.20	0.15 ± 0.01	6.47 ± 0.66			
SGN-U318020	0.87 ± 0.08		0.79 ± 0.08			
SGN-U318050	0.80 ± 0.11	0.40 ± 0.04	1.53 ± 0.15	1.66 ± 0.16	0.25 ± 0.03	0.61 ± 0.07

Supplementary Table SII. Continued.

SGN-ID [a]	Peptide sequence [b]	Cf-4/Avr4 compared to control seedlings [c] t=1h		
		Ratio 1	Ratio 2	Ratio 3
SGN-U318935	LHFSNHSSSPAPASSSSD **S**DDEK			
SGN-U319866	ISSEDE**m**AG**m**DLTR	3.17 ± 1.49	0.29 ± 0.04	0.60 ± 0.08
SGN-U319978	**m**A**S**IDAQLR			
SGN-U320093	VEEPHNVAEQPI **S**PKDER			
SGN-U320785	TDVGEG **S**FHAISR **S**IDVFDPASTHDGANLASSSR TSEESNLGAEEPRV **S**QDLK	1.19 ± 0.48	0.45 ± 0.06	1.21 ± 0.16
SGN-U322822	GR**S**FDDSPVSITDR			
SGN-U323143	EIEAG**S**DLEVK			
SGN-U323433	DDHWDEE **S**LQR IYLHQEAGP **ss**R			
SGN-U325962	AT**S**PQTGSQQVGGNLK			
SGN-U327750	EANGGFI**ms**A**s**HNPGGPEYDWGIK			
SGN-U328413	LPEMP**S**SKGLKR			
SGN-U333128	GEN**S**SSEINIVR**S**			
SGN-U337595	QEEP**T**KGKLEK	1.04 ± 0.10		0.48 ± 0.06

[a] Gene identifier from the *Solanaceae* Genomics Network (SGN).

[b] The phosphorylated residue in the peptide sequence is indicated in bold, or in lower case bold when it is unclear from the spectrum which residue is phosphorylated. Methionine (M) oxidation is indicated in lower case bold.

[c] The ratio represents the ion intensities of a peptide in the Cf-4/Avr4 seedlings versus the control seedlings. Average ratios per experiment are presented in Table III. Ratios of which the average ratios is significantly different from 1.00 with 95% and 99% confidence, are indicated in light and dark grey, respectively.

Supplementary Table SII. Continued from left page.

SGN-ID[a]	Cf-4/Avr4 compared to control seedlings [c]					
	t=3h			t=5h		
	Ratio 1	Ratio 2	Ratio 3	Ratio 1	Ratio 2	Ratio 3
SGN-U318935	0.98 ± 0.23		1.15 ± 0.12			
SGN-U319866	0.99 ± 0.19		1.19 ± 0.12			
SGN-U319978	0.50 ± 0.07			1.77 ± 0.24	1.46 ± 0.17	0.93 ± 0.11
SGN-U320093				2.15 ± 0.13	0.88 ± 0.10	0.72 ± 0.08
				1.15 ± 0.27	0.69 ± 0.08	
SGN-U320785				0.88 ± 0.12		
				0.81 ± 0.09	0.46 ± 0.05	1.71 ± 0.19
SGN-U322822	1.03 ± 0.13		2.57 ± 0.26			
SGN-U323143				1.26 ± 0.19	0.65 ± 0.07	
SGN-U323433	0.96 ± 0.30	0.46 ± 0.05	0.78 ± 0.08			
SGN-U325962	0.92 ± 0.16	0.27 ± 0.03	0.60 ± 0.06	1.78 ± 0.26	0.99 ± 0.11	
SGN-U327750				0.73 ± 0.13	1.11 ± 0.13	0.91 ± 0.10
SGN-U328413				1.15 ± 0.14	0.79 ± 0.06	0.50 ± 0.04
SGN-U333128						
SGN-U337595						

Supplementary Table SIII.
Transcriptional regulation of genes encoding pathogenesis-related proteins, proteins involved in photosynthesis and involved in glycolysis

Code[a]	Microarray ID	SGN-ID[b]	Annotation	Ratio[c] t=1h	Ratio[c] t=3h	Ratio[c] t=5h
PR	Les.4693.1.S1_at	SGN-U314796	Pathogenesis-related protein PR1a (P4) precursor	5.06	5.31	**36.04**
PR	LesAffx.10495.1.S1_at	SGN-U313773	P69C protein	-1.17	1.04	1.36
PR	Les.5611.1.S1_at	SGN-U330434	P69D protein	1.12	1.17	-1.11
PR	LesAffx.5691.1.S1_at	SGN-U314863	Pathogenesis related protein isoform b1 precursor (Solanum phureja)	1.46	1.07	1.34
PR	Les.3408.1.S1_at	SGN-U314797	Pathogenesis-related leaf protein 6 precursor (P6)	1.95	**2.24**	**3.83**
PR	Les.3408.1.S2_at	SGN-U314797	Pathogenesis-related leaf protein 6 precursor (P6)	1.17	1.58	3.31
PR	Les.4496.1.S1_at	SGN-U312368	Pathogenesis-related protein 10 (Solanum virginianum)	**1.94**	1.94	**2.85**
PR	Les.54.1.S1_at	SGN-U315428	Pathogenesis-related protein 1A1 precursor (PR-1A1)	-1.05	**1.81**	2.80
PR	Les.4460.1.S1_at	SGN-U316008	Pathogenesis-related protein P2 precursor	1.92	3.09	**4.74**
PR	LesAffx.55504.1.S1_at	SGN-U327156	Pathogenesis-related protein-like protein (Medicago truncatula)	1.24	-1.20	-3.09
PR	Les.3648.1.S1_at	SGN-U313772	Subtilisin-like endoprotease (P69A protein)	-1.02	-1.12	-1.25
PR	Les.3635.1.S1_at	SGN-U313775	Subtilisin-like protease (P69B protein)	1.38	1.60	**1.80**
PR	Les.1609.1.S1_at	SGN-U315668	Beta-1,3-endoglucanase 14 (Arabidopsis thaliana)	**-1.87**	1.29	2.33
PR	Les.1609.2.A1_at	SGN-U315668	Beta-1,3-endoglucanase 14 (Arabidopsis thaliana)	-1.01	1.21	**3.12**
PH	Les.147.1.S1_at	SGN-U312438	Chlorophyll a,b binding protein type I (Solanum tuberosum)	-1.15	-1.10	-1.35
PH	Les.1603.1.A1_at	SGN-U315963	Chlorophyll a-b binding protein 8	-1.07	-1.21	-1.58
PH	Les.1736.1.A1_at	SGN-U319612	Putative chlorophyll A-B binding protein (Arabidopsis thaliana)	-1.07	-1.04	-1.25
PH	Les.2092.1.S1_at	SGN-U312336	Secretory peroxidase (Nicotiana tabacum)	-1.10	-1.74	**-2.22**
PH	Les.2092.2.S1_at	SGN-U312336	Secretory peroxidase (Nicotiana tabacum)	**-1.68**	-3.69	-1.50
PH	Les.2286.1.S1_at	SGN-U312827	Light-harvesting complex protein (Arabidopsis thaliana)	1.03	-1.09	-1.44
PH	Les.233.1.S1_at	SGN-U312436	Chlorophyll a-b binding protein 4	-1.02	-1.04	-1.10
PH	Les.2478.1.S1_a_at	SGN-U313214	Chlorophyll a-b binding protein 3C-like (Solanum tuberosum)	-1.02	-1.03	-1.13
PH	Les.2478.1.S1_at	SGN-U313214	Chlorophyll a-b binding protein 3C-like (Solanum tuberosum)	1.00	-1.07	-1.09
PH	Les.2924.1.S1_at	SGN-U313159	Sulfur (Nicotiana tabacum)	-1.07	-1.06	-1.34
PH	Les.3016.1.S1_at	SGN-U314750	Chlorophyll a-b binding protein 12	-1.09	1.05	-1.44
PH	Les.3054.1.S1_at	SGN-U314748	Chlorophyll a-b binding protein 13	-1.00	-1.06	-1.16
PH	Les.3062.1.S1_at	SGN-U312661	Chloroplast pigment-binding protein CP29 (Nicotiana tabacum)	-1.12	-1.04	-1.29
PH	Les.3062.2.S1_at	SGN-U312661	Chloroplast pigment-binding protein CP29 (Nicotiana tabacum)	1.13	-3.83	1.38
PH	Les.3073.1.S1_at	SGN-U312967	Photosystem II 22 kDa protein	-1.03	-1.09	-1.21
PH	Les.3123.1.S1_at	SGN-U334377	Geranylgeranyl reductase (Nicotiana tabacum)	-1.20	-1.03	-1.62
PH	Les.3297.1.S1_at	SGN-U312593	Chlorophyll a/b-binding protein (cab-11)	-1.08	-1.06	-1.38
PH	Les.3297.2.S1_at	SGN-U312593	Chlorophyll a/b-binding protein (cab-11)	1.42	-4.81	1.52
PH	Les.3775.1.S1_at	SGN-U312713	Chlorophyll a-b binding protein 6A	-1.05	-1.11	-1.24
PH	Les.4083.1.S1_at	SGN-U312663	Chlorophyll a-b binding protein 7	-1.02	-1.15	-1.22
PH	Les.4259.1.S1_at	SGN-U312843	Chlorophyll a-b binding protein 8	**-1.11**	**-1.17**	**-1.54**

Supplementary Table SIII. Continued.

Code[a]	Microarray ID	SGN-ID[b]	Annotation	Ratio[c] t=1h	Ratio[c] t=3h	Ratio[c] t=5h
PH	Les.4345.1.S1_at	SGN-U313210	Chlorophyll a-b binding protein 1B	1.01	-1.03	-1.03
PH	Les.4345.2.A1_a_at	SGN-U313217	Chlorophyll a-b binding protein 1B	-1.10	-1.10	-1.18
PH	Les.4345.2.A1_x_at	SGN-U313217	Chlorophyll a-b binding protein 1B	-1.12	-1.10	-1.25
PH	Les.4345.3.S1_x_at	SGN-U313211	Chlorophyll a-b binding protein 1B	-1.06	-1.09	-1.13
PH	Les.4345.4.A1_at	SGN-U313211	Chlorophyll a-b binding protein 1B	1.03	-1.18	-1.18
PH	Les.4345.4.A1_x_at	SGN-U313211	Chlorophyll a-b binding protein 1B	1.03	-1.11	-1.17
PH	Les.4359.1.S1_at	SGN-U313221	Chlorophyll a-b binding protein 3C	-1.11	1.22	1.49
PH	Les.4359.2.A1_at	SGN-U313221	Chlorophyll a-b binding protein 3C	1.03	1.33	2.15
PH	Les.4492.1.S1_at	SGN-U312334	Chlorophyll a-b binding protein CP24 10A	-1.34	-5.81	1.17
PH	Les.4492.2.S1_at	SGN-U312334	Chlorophyll a-b binding protein CP24 10A	-1.08	-1.07	-1.43
PH	Les.4492.3.S1_at	SGN-U312336	Secretory peroxidase (Nicotiana tabacum)	-1.10	-1.04	-1.53
PH	Les.608.1.S1_at	SGN-U312449	Type I (26 kD) CP29 polypeptide	-1.08	-1.11	-1.35
PH	LesAffx.41489.1.S1_at	SGN-U321924	Hypothetical protein	-1.26	-1.09	-1.02
PH	LesAffx.57669.1.S1_at	SGN-U319612	Putative chlorophyll A-B binding protein (Arabidopsis thaliana)	-1.33	1.10	-1.52
PH	Les.4228.1.A1_at	SGN-U314594	Chloroplast photosystem I reaction center V	1.06	-1.10	-1.05
PH	Les.4228.3.S1_at	SGN-U314594	Chloroplast photosystem I reaction center V	1.01	-1.09	-1.10
PH	Les.1305.1.A1_at	SGN-U315765	Ultraviolet-B-repressible protein (Gossypium hirsutum)	1.10	1.15	-1.04
PH	Les.2377.1.S1_at	SGN-U314018	Ultraviolet-B-repressible protein (Gossypium hirsutum)	-1.02	-1.03	-1.39
PH	Les.2377.2.A1_at	SGN-U314018	Ultraviolet-B-repressible protein (Gossypium hirsutum)	1.05	-1.06	-1.22
PH	Les.5812.1.S1_at	SGN-U315764	Ultraviolet-B-repressible protein (Gossypium hirsutum)	1.04	1.08	-1.13
PH	Les.1290.1.A1_at	SGN-U314676	Photosystem II 10 kDa polypeptide (Solanum tuberosum)	1.41	-1.00	1.00
PH	Les.3099.1.S1_at	SGN-U312648	Photosystem I subunit XI (Nicotiana attenuata)	-1.06	-1.05	-1.11
PH	Les.324.1.S1_at	SGN-U314260	Putative photosystem I subunit III (Nicotiana tabacum)	-1.11	-1.08	-1.22
PH	Les.867.1.S1_at	SGN-U312640	Photosystem I reaction center subunit II (Solanum lycopersicum)	-1.03	1.01	-1.19
PH	LesAffx.482.1.S1_at	SGN-U345822	Photosystem I assembly protein ycf4 (Solanum tuberosum)	**1.46**	-1.10	-1.38
PH	Les.2168.1.S1_at	SGN-U313179	Photosystem I reaction centre subunit N (Medicago truncatula)	1.01	1.06	-1.25
PH	Les.3175.1.S1_at	SGN-U313090	Putative desaturase-like protein (Trifolium repens)	-1.06	-1.13	-1.25
PH	Les.1472.1.S1_at	SGN-U312871	Photosystem II oxygen-evolving complex protein 3 precursor	-1.03	-1.04	-1.15
PH	Les.3029.1.S1_at	SGN-U312532	Oxygen-evolving enhancer protein 1	-1.06	-1.14	-1.22
PH	Les.4007.1.S1_at	SGN-U312531	Oxygen-evolving enhancer protein 1	-1.02	-1.04	-1.36
PH	Les.482.1.S1_at	SGN-U312572	Oxygen-evolving enhancer protein 2	-1.01	-1.04	-1.13
PH	Les.5738.1.S1_at	SGN-U317040	Oxygen evolving complex protein-like (Oryza sativa)	-1.10	-1.08	-1.35
PH	Les.626.1.S1_at	SGN-U318866	putative PsbP domain protein (Arabidopsis thaliana)	1.15	1.19	-1.11
PH	Les.626.2.S1_at	SGN-U318866	putative PsbP domain protein (Arabidopsis thaliana)	1.09	1.17	-1.38
PH	Les.626.3.S1_at	SGN-U318866	putative PsbP domain protein (Arabidopsis thaliana)	1.05	1.20	-1.15

Supplementary Table SIII. Continued.

Code[a]	Microarray ID	SGN-ID[b]	Annotation	Ratio[c] t=1h	Ratio[c] t=3h	Ratio[c] t=5h
PH	LesAffx.48402.1.A1_at	SGN-U323580	Thylakoid lumenal 21.5 kDa protein (Arabidopsis thaliana)	-1.15	-1.23	-1.08
PH	LesAffx.48402.1.S1_at	SGN-U323580	Thylakoid lumenal 21.5 kDa protein (Arabidopsis thaliana)	-1.05	1.04	-1.45
PH	LesAffx.67937.1.S1_at	SGN-U326478	Hypothetical protein (Arabidopsis thaliana)	-1.20	-1.24	-1.52
PH	LesAffx.51226.1.A1_at	SGN-U342407	Apocytochrome f precursor (Solanum tuberosum)	**2.32**	1.11	1.06
PH	LesAffx.51226.1.S1_at	SGN-U342407	Apocytochrome f precursor (Solanum tuberosum)	2.12	-1.13	1.08
PH	LesAffx.66410.1.S1_at	SGN-U343039	Photosystem II CP43-chlorophyll (Populus trichocarpa)	-1.34	-1.02	-1.72
PH	Les.3011.1.S1_at	SGN-U314192	NADPH:protochlorophyllide oxidoreductase (Nicotiana tabacum)	-1.29	-1.43	-2.05
PH	Les.5120.1.S1_at	SGN-U313279	NADPH:protochlorophyllide oxidoreductase (Nicotiana tabacum)	-1.21	-1.20	-1.89
PH	Les.5850.1.S1_at	SGN-U313280	NADPH:protochlorophyllide oxidoreductase (Nicotiana tabacum)	-1.37	-1.24	-1.89
G	LesAffx.71366.1.S1_at	SGN-U322121	Hypothetical protein (Arabidopsis thaliana)	-1.20	-1.07	1.13
G	Les.3182.1.S1_at	SGN-U312518	Hypothetical protein (Solanum tuberosum)	-1.08	-1.05	-1.27
G	Les.4336.1.S1_at	SGN-U313176	Phosphoglycerate kinase (Solanum tuberosum)	-1.36	-1.10	-1.44
G	Les.4336.2.A1_at	SGN-U313176	Phosphoglycerate kinase (Solanum tuberosum)	-1.02	-1.11	-1.23
G	Les.4336.3.S1_at	SGN-U313176	Phosphoglycerate kinase (Solanum tuberosum)	-1.16	-1.05	-1.30
G	Les.1829.1.S1_at	SGN-U314788	Putative plastidic aldolase (Oryza sativa subsp. japonica)	-1.03	-1.09	1.27
G	Les.246.1.S1_at	SGN-U314331	Fructose-bisphosphate aldolase-like protein (Solanum tuberosum)	1.17	1.04	1.09
G	Les.3060.1.S1_at	SGN-U312609	Plastidic aldolase NPALDP1 (Nicotiana paniculata)	-1.04	-1.11	-1.14
G	Les.3174.1.S1_at	SGN-U312608	Plastidic aldolase NPALDP1 (Nicotiana paniculata)	-1.16	-1.18	-1.26
G	Les.4275.1.S1_at	SGN-U312344	Plastidic aldolase (Nicotiana paniculata)	-1.05	-1.14	-1.13
G	Les.5598.1.S1_at	SGN-U314332	Fructose-bisphosphate aldolase-like (Solanum tuberosum)	-1.04	-1.03	1.13
G	Les.3516.1.S1_at	SGN-U316705	Hexokinase	1.08	1.10	1.13
G	Les.3815.1.S1_at	SGN-U335794	Hexokinase	-1.25	-1.05	1.00
G	Les.1509.1.S1_at	SGN-U313534	Pyruvate kinase isozyme A (Nicotiana tabacum)	-1.08	-1.23	-1.23
G	Les.2323.1.S1_at	SGN-U313639	Putative pyruvate kinase (Arabidopsis thaliana)	1.00	-1.05	1.08
G	Les.3129.1.S1_at	SGN-U314040	Pyruvate kinase, cytosolic isozyme (Solanum tuberosum)	-1.14	-1.16	-1.32
G	Les.3129.2.S1_at	SGN-U314040	Pyruvate kinase, cytosolic isozyme (Solanum tuberosum)	-1.34	-1.18	**-1.71**
G	Les.4288.1.S1_at	SGN-U334503	Pyruvate kinase family protein (Oryza sativa subsp. japonica)	-1.27	-2.78	-1.82
G	Les.4562.1.S1_at	SGN-U312582	Pyruvate kinase (Arabidopsis thaliana)	-1.03	-1.27	-1.09
G	Les.5326.1.S1_at	SGN-U313540	Putative pyruvate kinase (Oryza sativa subsp. japonica)	1.09	-1.36	1.06
G	Les.5649.1.A1_at	SGN-U320512	Pyruvate kinase (Nicotiana tabacum)	-1.04	-1.46	-1.12
G	Les.5649.1.S1_at	SGN-U320512	Pyruvate kinase (Nicotiana tabacum)	-1.41	-1.34	-1.31
G	LesAffx.61184.1.S1_at	SGN-U313534	Pyruvate kinase isozyme A (Nicotiana tabacum)	-1.29	-1.14	-1.51
G	LesAffx.66367.1.S1_at	SGN-U320005	Pyruvate kinase, cytosolic isozyme (Nicotiana tabacum)	-1.16	-1.15	-1.41
G	Les.186.1.S1_at	SGN-U315933	Glyceraldehyde-3-phosphate dehydrogenase (Nicotiana tabacum)	-1.30	-1.21	-1.26
G	Les.262.1.S1_at	SGN-U314312	Glyceraldehyde 3-phosphate dehydrogenase (Solanum tuberosum)	-1.11	1.01	1.13

Supplementary Table SIII. Continued.

Code[a]	Microarray ID	SGN-ID[b]	Annotation	Ratio[c] t=1h	Ratio[c] t=3h	Ratio[c] t=5h
G	Les.2888.1.S1_at	SGN-U312461	Glyceraldehyde-3-phosphate dehydrogenase A (Nicotiana tabacum)	-1.10	-1.00	-1.32
G	Les.2933.1.S1_at	SGN-U312804	Glyceraldehyde-3-phosphate dehydrogenase B subunit (Glycine max)	-1.11	-1.15	-1.34
G	Les.3072.1.S1_at	SGN-U312459	Glyceraldehyde-3-phosphate dehydrogenase A (Nicotiana tabacum)	-1.15	-1.15	-1.50
G	Les.3072.2.S1_at	SGN-U312459	Glyceraldehyde-3-phosphate dehydrogenase A (Nicotiana tabacum)	-1.43	-1.14	-2.08
G	Les.3072.3.S1_at	SGN-U312459	Glyceraldehyde-3-phosphate dehydrogenase A (Nicotiana tabacum)	-1.28	-1.19	-1.94
G	Les.3242.1.A1_at	SGN-U312802	Glyceraldehyde-3-phosphate dehydrogenase B subunit (Glycine max)	-1.07	-1.19	-1.40
G	Les.3242.2.S1_at	SGN-U312802	Glyceraldehyde-3-phosphate dehydrogenase B subunit (Glycine max)	-1.34	-1.14	-1.89
G	Les.3242.3.S1_at	SGN-U312802	Glyceraldehyde-3-phosphate dehydrogenase B subunit (Glycine max)	-1.23	-1.13	-1.85
G	Les.4797.1.S1_at	SGN-U317897	Glucose-6-phosphate isomerase	-1.17	-1.23	-1.53
G	LesAffx.2135.1.S1_at	SGN-U315951	Glucose-6-phosphate isomerase	-1.33	1.05	-1.81
G	LesAffx.2135.3.S1_at	SGN-U315951	Glucose-6-phosphate isomerase	-1.07	-1.08	-1.26
G	LesAffx.2135.4.S1_at	SGN-U315951	Glucose-6-phosphate isomerase	-1.43	-1.01	-1.67
G	Les.2900.1.S1_at	SGN-U315352	Pyrophosphate--fructose 6-phosphate 1-phosphotransferase subunit beta (Solanum tuberosum)	-1.06	-1.37	-1.25
G	LesAffx.51723.1.S1_at	SGN-U320209	Phosphofructokinase, putative (Phosphofructokinase) (Medicago truncatula)	-1.65	-1.53	-1.10
G	LesAffx.62009.1.S1_at	SGN-U318557	Putative pyrophosphate-fructose-6-phosphate 1-phosphotransferase (Arabidopsis thaliana)	-1.72	-1.01	-1.15
G	LesAffx.68197.1.S1_at	SGN-U314840	Pyrophosphate--fructose 6-phosphate 1-phosphotransferase alpha subunit (Solanum tuberosum)	-1.15	-1.11	-1.46
G	Les.303.1.S1_at	SGN-U312379	Enolase	-1.07	-1.08	-1.03
G	Les.3932.1.S1_at	SGN-U312378	Enolase	-1.64	1.05	-1.31
G	Les.3932.2.S1_at	SGN-U312378	Enolase	**-1.66**	1.04	-1.48
G	Les.3932.3.S1_at	SGN-U312378	Enolase	-1.13	1.08	-1.07
G	Les.5741.1.S1_at	SGN-U318766	Putative enolase (Arabidopsis thaliana)	-1.16	-1.12	1.25
G	Les.96.1.A1_at	SGN-U327280	L-lactate dehydrogenase	-1.01	1.41	**4.55**
G	Les.97.1.S1_at	SGN-U326680	L-lactate dehydrogenase	1.04	**1.96**	**3.58**
G	Les.4801.1.S1_at	SGN-U316396	Pyruvate dehydrogenase complex E2 subunit 1 (Arabidopsis thaliana)	-1.19	1.01	1.05
G	LesAffx.3802.1.S1_at	SGN-U316577	Dihydrolipoamide succinyltransferase (Medicago truncatula)	**-1.66**	-1.23	-1.47
G	LesAffx.3802.2.S1_at	SGN-U316577	Dihydrolipoamide succinyltransferase (Medicago truncatula)	-1.51	1.02	-1.28

[a] PR refers genes that encode pathogenesis-related proteins. Proteins encoded by genes indicated with PH or G are functionally related to these processes according to the Biological Process GO annotation.
[b] Gene identifier from the *Solanaceae* Genomics Network.
[c] The values shown in bold indicate significantly different gene expression between the Cf-4/Avr4 and control seedlings $P \leq 0.01$). Ratios were used for the expression profiles presented in Figure 5.

Chapter 5

Resistance of tomato to *Cladosporium fulvum* requires the hypersensitive response and host cell wall-related defence responses that are specifically suppressed by the fungus in susceptible plants

Iris J.E. Stulemeijer, Antoine H. America, Johannes P.C. Visser, Henk L. Dekker, Chris G. de Koster, Jan H. Cordewener and Matthieu H.A.J. Joosten

SUMMARY

To study the apoplastic defence response of tomato, MM-Cf-4 (resistant) and MM-Cf0 (susceptible) tomato plants were inoculated with an Avr4-producing strain of the extracellularly colonizing fungal pathogen *Cladosporium fulvum*. Apoplastic protein patterns from resistant and susceptible plants were first analyzed at four stages after *C. fulvum* inoculation by 2-dimensional fluorescence difference gel electrophoresis. This revealed a similar protein pattern in resistant and susceptible plants, although proteins accumulated faster and stronger in resistant plants as compared to susceptible plants. In addition, *C. fulvum*-specific proteins accumulated at later stages of the colonization process in susceptible plants. Next, the apoplastic proteome of these plants was analyzed by a robust comparative LC-MS/MS^E analysis, leading to the identification of 66 proteins that were confirmed or predicted to be apoplastic. These included pathogenesis-related proteins, cell wall-related proteins and, in susceptible plants, effectors from *C. fulvum*. Quantification of the apoplastic tomato proteome revealed a fast and strong, but transient protein accumulation over time in resistant plants upon inoculation with *C. fulvum*. In the susceptible plants, a subset of these proteins accumulates slowly upon *C. fulvum* inoculation, while the remainder does not accumulate. The observed protein abundances correlate to a large extent with the levels of transcription of their encoding genes. Since transcription of these genes also appeared to be stimulated by the Cf-4/Avr4-triggered HR initiation, the difference in gene expression and subsequent protein accumulation between resistant and susceptible plants is likely caused by the Cf-4-mediated Avr4 recognition. Furthermore, our data indicate that *C. fulvum* is able to specifically suppress a subset of genes encoding cell wall proteins, of which the accumulation hampers the proliferation of *C. fulvum* in resistant plants. Possibly, effectors of *C. fulvum* successfully target a microbe-associated molecular pattern-receptor in susceptible plants, eventually leading to suppression of transcription of these genes.

INTRODUCTION

Plants, world's suppliers of food and oxygen, are mercilessly exposed to the world's abiotic and biotic threats. However, plants have developed two layers of defence to protect

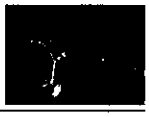

themselves against invading pathogens (Jones and Dangl, 2006; De Wit, 2007). First, microbe-associated molecular patterns (MAMPs), molecules essential for microbial life, are recognized by pattern recognition receptors (PRRs), which induce MAMP-triggered immunity (MTI) (Jones and Dangl, 2006). For example, the highly conserved flagellin protein from the bacterial flagellum required for bacterial motility, is recognized by the PRR FLS2 (Gómez-Gómez and Boller, 2000). In addition to this first line of defence, specific effectors produced by the pathogen, which aim at suppression or avoidance of MTI, are recognized by the cognate resistance (R) proteins present in resistant plants, thereby inducing effector-triggered immunity (ETI) (Jones and Dangl, 2006). ETI is generally associated with a hypersensitive response (HR), consisting of a type of programmed cell death at the site of pathogen penetration, and a vast set of additional defence responses (Joosten and De Wit, 1989; Lamb and Dixon, 1997; Gabriëls *et al.*, 2006; Chapter 3). This generally local and lethal process for the plant prevents invading pathogens such as viruses, bacteria, fungi, oomycetes and nematodes with a biotrophic lifestyle, from further proliferation. Effectors that are recognized by the plant can therefore also be regarded as avirulence factors (Avrs) and are also referred to as race-specific elicitors, as they are strain-specific in most cases. In susceptible plants, none of the effectors that are produced by the pathogen are recognized, allowing the pathogen to successfully counteract MTI with its effectors, thereby provoking effector-triggered susceptibility (ETS).

The interaction between tomato (*Solanum lycopersicum*) and the biotrophic fungal pathogen *Cladosporium fulvum* is a typical model system to study ETI and ETS, as this interaction fully complies with the gene-for-gene hypothesis and both partners in the interaction are genetically well-defined (Flor, 1942; De Wit, 1992; Joosten and De Wit, 1999). Tomato plants that express a *Cf* resistance gene are resistant to strains of *C. fulvum* that secrete the cognate elicitor encoded by the avirulence (*Avr*) gene. Upon recognition of an Avr, Cf-proteins trigger a HR (Rivas and Thomas, 2005). One of the main advantages of the *C. fulvum* – tomato interaction concerning studies on ETI and ETS is that the fungus remains strictly apoplastic in the leaves of both resistant and susceptible plants without the formation of specific feeding structures (De Wit, 1992). In fully colonized leaflets of susceptible plants, the pathogen grows in close association with the cell walls of its host, with the highest hyphal density in the vicinity of the vascular tissue from which the fungus probably obtains most of its nutrients (De Wit, 1977; Joosten *et al.*, 1990b; Van den Ackerveken *et al.*, 1994).

Therefore, the extracellular communication between fungus and plant can be studied by identification of the (proteinaceous) compounds present in apoplastic washing fluids, which provides insight into the extracellular response of tomato to invasion by *C. fulvum* and manipulation of this response by *C. fulvum* (Joosten and De Wit, 1999).

Several defence-related responses are initiated during the induction of MTI and ETI (Jones and Dangl, 2006; Bittel and Robatzek, 2007; De Wit, 2007; Ferreira *et al.*, 2007; He *et al.*, 2007). These responses include cell wall modifications (Asselbergh *et al.*, 2007; Van Baarlen *et al.*, 2007), synthesis of secondary metabolites with antimicrobial activities (Dixon, 2001), an oxidative burst and pathogenesis-related (PR) protein accumulation (Van Loon *et al.*, 2006). PR proteins are mainly secreted into the apoplast of the plant, were they are anticipated to act against invading pathogens such as viruses, bacteria, fungi or oomycetes. Different types of PR proteins are induced in several plant species and these proteins have been classified into 17 families, of which subsets are induced either through salicylic acid (SA), jasmonic acid (JA) and/or ethylene (Van Loon *et al.*, 2006). Since some PR proteins have direct antifungal activity, such as 1,3- ß-glucanases (PR-2) and several types of chitinases (PR-3, -4, -8, and -11) that target 1,3- ß-glucan and chitin in the fungal hyphae, respectively, PR proteins have been suggested to inhibit pathogen proliferation within the plant (Van Loon and Van Strien, 1999). However, PR proteins were shown not to provide the first line of defence against invading pathogens. Since PR protein expression is a hallmark for pathogen-induced systemic acquired resistance (SAR), PR proteins are thought to enhance defence against a second invasion (Van Loon *et al.*, 2006).

PR protein accumulation has been extensively studied in the interaction between tomato and *C. fulvum*. Many years ago, it has already been found that swift accumulation of the apoplastic protein "P14" (a 14 kDa protein) is a typical marker for incompatibility (De Wit and Van der Meer, 1986). Later, it was found that in fact three 14 kDa proteins strongly accumulate, of which one (P2) is related to PR-4, while the other two proteins are both serologically related to the tobacco PR-1 protein (P4 and P6) (Joosten *et al.*, 1990a). However, a clear biological role for these proteins was never found (Van Loon and Van Strien, 1999; Van Loon *et al.*, 2006). The function of some other PR proteins appears to be more clear. As mentioned above 1,3-ß-glucanases and chitinases, which are strongly expressed in resistant plants upon *C. fulvum* inoculation, directly target the fungal hyphae (Joosten and De Wit, 1989; Wubben *et al.*, 1992). Although *C. fulvum* itself appears to be

insensitive to these hydrolytic enzymes (Joosten *et al.*, 1995), they have deleterious effects on other fungi (Van den Burg *et al.*, 2006; Van Esse *et al.*, 2007). The Avr4 effector enhances virulence of the pathogen by binding and subsequently protecting the chitin of the penetrating hyphae against plant chitinases (Van den Burg *et al.*, 2006; Van Esse *et al.*, 2007). In addition, the Avr2 effector, which matches the Cf-2 resistance protein, allows *C. fulvum* to resist a particular aspect of the host defence response since this effector specifically inhibits the activity of the Rcr3 protease that is secreted by tomato (Rooney *et al.*, 2005). Non-race specific effectors produced by all strains of *C. fulvum* are the extracellular proteins (Ecps), which also contribute to virulence. Ecp1 and Ecp2 are both required for full virulence (Laugé *et al.*, 1997) and the recently identified Ecp6 protein has also been shown to significantly contribute to *C. fulvum* virulence on tomato (Bolton *et al.*, 2008). Ecp6 contains lysine motifs (LysM domains) that are carbohydrate-binding modules, and homology-based modelling suggests that this effector binds to chitin. Possibly Ecp6 also shields and protects chitin as was suggested for Avr4. Alternatively, it could act as a 'stealth' factor implying that Ecp6 captures chitin oligomers that are released from the hyphae during colonization of the apoplast and which might function as MAMPs (Whiteford and Spanu, 2002).

Since *C. fulvum* induces a differential apoplastic response in resistant plants compared to susceptible plants (Joosten and De Wit, 1989), an extensive study of the apoplastic proteome of tomato leaves was performed to study the apoplastic defence response in tomato. Furthermore, we anticipated to obtain additional information on the manipulation of this response by *C. fulvum*. Therefore, *Cf-4*-containing (resistant) and *Cf-4*-lacking (susceptible) tomato plants were inoculated with an Avr4-producing strain of *C. fulvum* and apoplastic fluid (AF) was isolated from the leaflets at several stages after inoculation. We subsequently analyzed the apoplastic proteins present in the AF by quantitative 2-dimensional fluorescence difference gel electrophoresis (DIGE-2DE) and by comparative LC-MS/MS^E analysis. Eventually, we identified 66 apoplastic proteins and results from both studies revealed that protein accumulation occurred much faster in the resistant plants than in the susceptible ones. In addition, various effectors secreted by *C. fulvum* were found to accumulate in susceptible plants. Our comparative LC-MS/MS^E analysis provides a highly detailed overview of the apoplastic proteome and its changes upon *C. fulvum* inoculation. Furthermore, quantification of a subset of the apoplastic proteins from tomato and comparison to gene expression data of the *C. fulvum*-inoculated plants and Cf-4/Avr4 seedlings, which specifically mount a HR,

reveals new insights into the dynamics of the apoplastic leaf proteome during the interaction between tomato and *C. fulvum*. Furthermore, these combined data provide indications that, to exert ETS, *C. fulvum* specifically triggers the downregulation of host genes encoding cell wall proteins of tomato. Since *C. fulvum* grows in close association with the cell wall, this would lead to an increase in nutrient and water supply.

RESULTS

Analysis of the tomato apoplastic proteome by quantitative DIGE-2DE gels

Earlier analysis revealed that the apoplastic proteome of tomato plants inoculated with *C. fulvum* changes rapidly (De Wit and Van der Meer, 1986; Joosten and De Wit, 1989). Here, we describe an extensive analysis of the changes in the apoplastic proteome of resistant (R; MM-Cf-4) and susceptible (S; MM-Cf0) tomato plants inoculated with a strain of *C. fulvum* expressing Avr4. We analyzed four stages of symptom development (A-D), in which stage A represents the day of inoculation, stage B approximately 6 days after inoculation, stage C approximately 10 days after inoculation and stage D approximately two weeks after inoculation (Table I) (Bolton *et al.*, 2008). At each of these four stages, apoplastic fluid (AF) was isolated from leaflets collected from multiple inoculated plants. Approximately 0.5 ml of AF was obtained per gram of fresh leaf weight from MM-Cf-4 as well as MM-Cf0 plants (Figure 1). The Coomassie-stained protein profile of equal volumes of AF was determined by one dimensional SDS-PAGE and the

Table I. Symptoms of resistant and susceptible tomato plants at four stages after inoculation with *C. fulvum* expressing Avr4.

Stage	Resistant plants	Code	Susceptible plants	Code
A	No symptoms (day of inoculation)	R_A	No symptoms (day of Inoculation)	S_A
B	Bending of leaves (epinasty)	R_B	Just before manifestation of the first visual symptoms	S_B
C	Bending of leaves (epinasty)	R_C	Mycelium is visible	S_C
D	Bending of leaves (epinasty) and chlorosis	R_D	Extensive mycelium growth and sporulation on lower side of the leaves	S_D

Table II. Average protein concentrations of apoplastic fluid (AF) and the corresponding amount of protein loaded on the DIGE-2DE gels.

Code	ug/ul in AF [a]	ug/2DE [b]
R_A	7.7 ± 2.3	30.5
R_B	5.6 ± 2.1	22.0
R_C	9.2 ± 3.6	36.4
R_D	7.6 ± 2.6	29.9
S_A	5.5 ± 2.3	21.7
S_B	4.7 ± 2.1	18.2
S_C	7.3 ± 1.2	29.2
S_D	12.0 ± 3.3	47.5

[a] Average protein concentration of 10 times concentrated apoplastic fluid.
[b] Average protein amounts present in 40 µl of apoplastic fluid that was loaded on a DIGE-2DE gel.

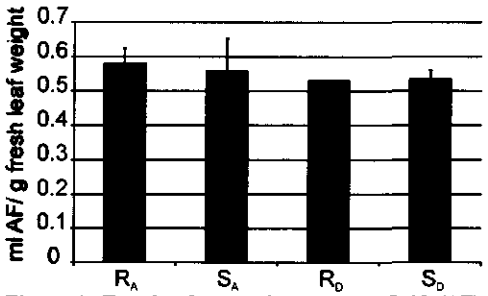

Figure 1. Equal volumes of apoplastic fluid (AF) are obtained from leaflets of resistant (R) and susceptible (S) tomato plants.
Apoplastic fluid was isolated at the day of inoculation (R_A and S_A) and at stage D (R_D and S_D), when *C. fulvum* has completed its life cycle on the susceptible plants. At the latter stage, the susceptible leaflets are fully colonized by the fungus.

results proved to be similar to earlier observations (Figure 2A) (De Wit and Van der Meer, 1986; Joosten and De Wit, 1989). The amount of 35 kDa 1,3-ß-glucanase, 26 kDa chitinase and 14 kDa PR protein increases fast in the resistant compared to susceptible plants. However, the increase of these proteins in resistant plants is transient, and at later stages these proteins accumulate to higher amounts in the susceptible plants than in the resistant plants (compare lanes R_D and S_D).

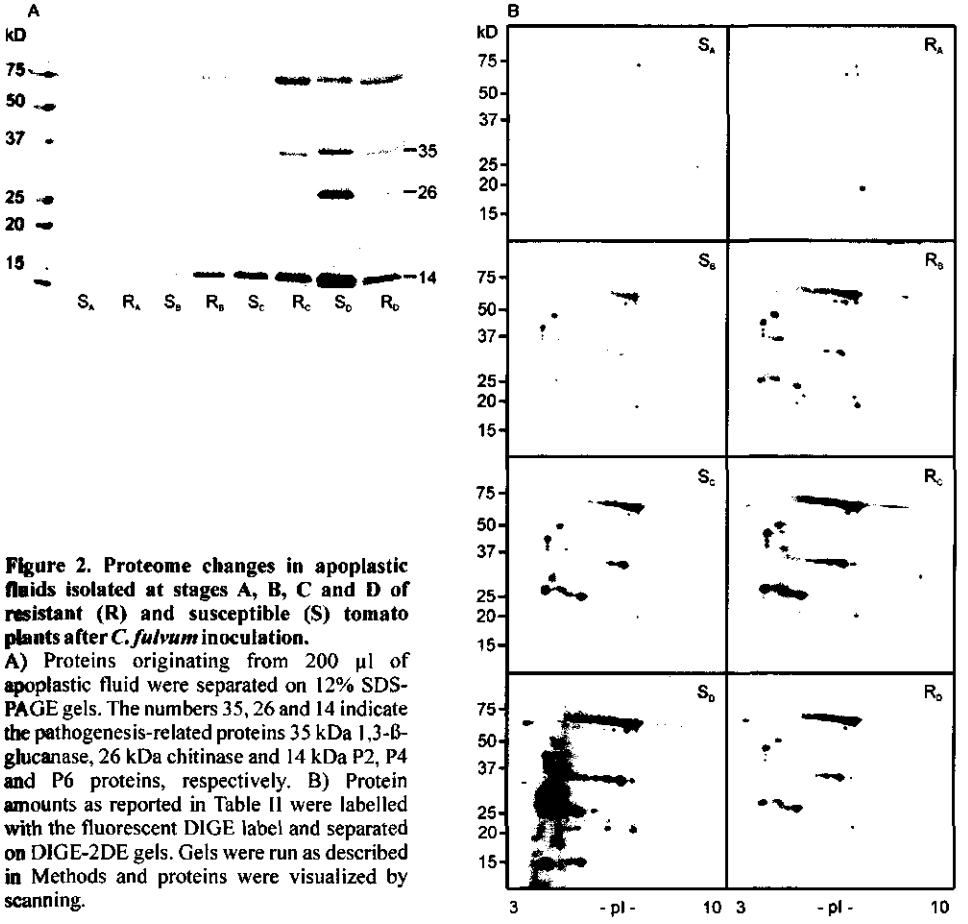

Figure 2. Proteome changes in apoplastic fluids isolated at stages A, B, C and D of resistant (R) and susceptible (S) tomato plants after *C. fulvum* inoculation.
A) Proteins originating from 200 µl of apoplastic fluid were separated on 12% SDS-PAGE gels. The numbers 35, 26 and 14 indicate the pathogenesis-related proteins 35 kDa 1,3-ß-glucanase, 26 kDa chitinase and 14 kDa P2, P4 and P6 proteins, respectively. B) Protein amounts as reported in Table II were labelled with the fluorescent DIGE label and separated on DIGE-2DE gels. Gels were run as described in Methods and proteins were visualized by scanning.

To study the apoplastic proteome changes in more detail, proteins present in 40 µl of AF obtained at the four different stages, in three replicate inoculation experiments of resistant and susceptible plants, were separated on quantitative DIGE-2DE gels (Figure 2B, Table II). In both resistant and susceptible tomato plants, the abundance of many proteins increased significantly in time over the various stages after inoculation. However, the pattern of the proteins changes the most between stages A and B in both resistant and susceptible plants, and from stage C to D in susceptible plants. Principle component analysis (PCA) of the DIGE-2DE images also reveals a change in proteome between stages A and B in both resistant and susceptible plants, and a clear deviation of stage S_D from the other stages (Figure 3A). In addition, this analysis revealed that the apoplastic response in the three replicate inoculations of resistant and susceptible plants is similar, since the biological replicates of each sample cluster in the same quadrant of the plot (Figure 3A). Although the stages R_B, R_C, R_D, S_B and S_C are hard to separate in this plot, some deviation between these stages seems to exist.

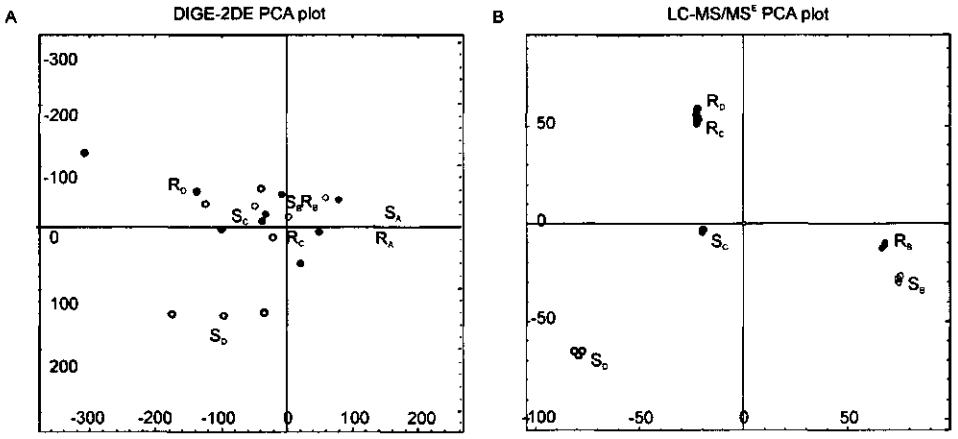

Figure 3. Principle component analysis (PCA) of DIGE-2DE images and LC-MS/MS^E data. A and B) Closed circles represent samples from resistant plants while open circles represent samples from susceptible plants. The lightest grey represents stage A (only in panel A), while ●○ , ●● and ●● represent stages B, C and D, respectively.

For the identification of proteins present in AF obtained at several stages, samples were separated on preparative 2D gels. Proteins were excised from the gels, trypsin-digested, and peptides were analyzed by mass spectrometry. In Figure 4, 18 spots are indicated on a 2D SDS-PAGE gel representing proteins in AF isolated from stage S_D. The identity of most of them is given in Table III. Many previously described pathogenesis-related (PR) proteins,

Table III. Protein identification from preparative 2DE gels.

Spot number	Protein name	Protein ID	Exp. pI	Theor. pI	Exp. mass (kDa)	Theor. mass (kDa)	# peptides identified in 2DE spot	VEMS score	E-value	Sequence coverage (%)
1	P69B	SGN-U313775	6.2	6.3	76	79	15	2397	0.0E+00	23
2			4.9		48					
3	1,3-beta-glucanase[a]	sp|Q01412.1	6.0	6.6	35	38	13	187	0.0E+00	51
4			6.5		33					
5	Basic 30 kDa endochitinase	SGN-U312562	6.5	6.2	31	34	7	766	0.0E+00	25
6	Ecp6[b]	-	5.0	4.6	32	21	8	977	0.0E+00	38
7	PIP1	gb|ABG23376.1	4.9	4.9	30	38	2	153	5.2E-50	7
8	Acidic 26 kDa endochitinase[a]	dbj|BAC76900.1	5.7	5.9	27	28	12	179	0.0E+00	57
9			5.7		23					
10			6.2		22					
11	PR P23	emb|CAA50059.1	8.2	6.1	21	24	8	1117	0.0E+00	22
	PR-5x	emb|AAM23272.1	8.2	6.6	21	25	8	1009	0.0E+00	18
12	CfPhiA[b]	-	5.0	5.0	19	19	6	78	0.0E+00	39
13	Ecp2	emb|CAA78401.1	5.1	4.7	17	18	11	1114	0.0E+00	70
14			5.7		17					
15			4.7		15					
16	PR P2	SGN-U316008	8.2	8.5	14	16	20	2039	0.0E+00	64
	PR P4	emb|CAA09671.1	8.2	7.6	14	17	5	566	0.0E+00	32
17	Plastocyanin	SGN-U312690	4.8	5.1	13	17	2	219	6.0E-62	11
18	Ecp1	emb|CAA78400.1	5.8	5.6	12	10	2	472	0.0E+00	31

[a] These proteins were identified with peptide mass fingerprinting instead of LC-MS/MS analysis.
[b] The sequence of this protein has not yet been submitted to publicly available databases.

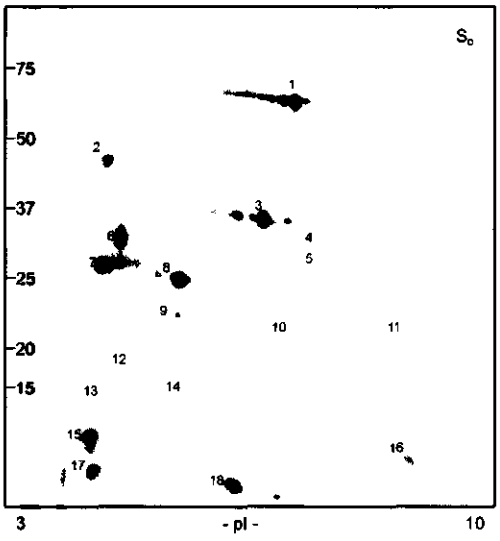

Figure 4. Preparative 2DE gel for identification of protein spots.
One milligram of total apoplastic protein obtained at stage D from susceptible plants inoculated with *C. fulvum* was separated by 2D-SDS-PAGE. The spots indicated with 1-18 were excised from the gel, proteins were trypsin-digested and the peptides were characterized by mass spectrometry. Protein identifications are reported in Table III.

including subtilisin-like protease P69B, 1,3-ß-glucanase, and chitinase were identified (Joosten and De Wit, 1989; Van Kan *et al.*, 1992; Jorda and Vera, 2000). Furthermore, the extracellular proteins Ecp1, -2 and -6, which are secreted by *C. fulvum* and accumulate in the apoplast of susceptible plants, and a phialide-related protein from *C. fulvum*, CfPhiA, were identified (Table III and Figure 4) (Van den Ackerveken *et al.*, 1993; Bolton *et al.*, 2008).

Labelling with the fluorescent DIGE labels allowed relative protein quantification from the gel images. The changes in protein abundance are presented relative to R_A, in which the abundance of each protein was set to 1 (Figure 5). As expected, the *C. fulvum* effectors and CfPhiA accumulate in the apoplast at late stages of colonization of the susceptible plants (S_C and S_D; spots 6, 12 and 13; Figure 5). The Ecp1 protein (spot 18; Figure 4) could not be quantified since this protein was not present on all

gels. Furthermore, the typical PR proteins (spots 1, 3, 5, 7, 8, 11 and 16) increase in abundance in both the resistant and the susceptible plants, and decrease after stage C in the resistant plants compared to the susceptible plants, as was described previously for some of these proteins (Figure 5) (De Wit and Van der Meer, 1986; Joosten and De Wit, 1989). Finally, spot 17 was identified as a plastocyanin protein. This is an abundant small thylakoid lumen protein that functions as an electron transfer agent between photosystem (PS) II and PS I. It is most likely that this abundant protein is a contaminant in the AF, which is present as a result of damage to the cells during AF isolation.

LC-MS/MS^E analysis of the tomato apoplastic proteome and comparison to the results obtained by DIGE-2DE analysis

The analysis by DIGE-2DE gels clearly visualized the general proteome dynamics in the apoplast of resistant and susceptible tomato plants after *C. fulvum* inoculation and confirmed earlier findings. However, it was difficult to identify and quantify low abundant proteins from the gels and in addition the dynamic range of this system appeared to be limited (see below). This implies that by using this approach, only abundant proteins that have already been described extensively in the past could be identified. To obtain a more detailed and possibly exhaustive overview of the changes in the apoplastic proteome, proteins in AFs from leaflets at stages B to D of resistant and susceptible plants from one of the three inoculation series used for DIGE-2DE were digested with trypsin and analyzed in triplicate by a Q-TOF Premier mass spectrometer. This type of mass spectrometers allows collection of very accurate masses and retention times of peptides in combination with precise quantification. To reveal overall differences between the samples, a PCA plot was made of the quantified data. This plot revealed a very low technical variation since the triplicate LC-MS/MS^E runs of each sample cluster very close together (Figure 3B). In addition, this large dataset allowed distinction between the different stages (B-D) and between stage B and even more between stage C and D of resistant and susceptible plants. The proteome does not seem to change from R_C to R_D, while a major change in the proteome occurs between S_C and S_D, probably because of the accumulation of *C. fulvum*-secreted proteins at S_D (Figure 3B).

Figure 5. Average abundance of the proteins indicated in Figure 4 and Table III, as determined by 2DE DIGE and LC-MS/MS^E (left and right panels, respectively, for each spot). The changes in protein abundance are presented relative to R_A (DIGE-2DE) or R_B (LC-MS/MS^E), in which the abundance of each protein was set to 1. From spots indicated with an asterisk, either no or more than one protein was identified.

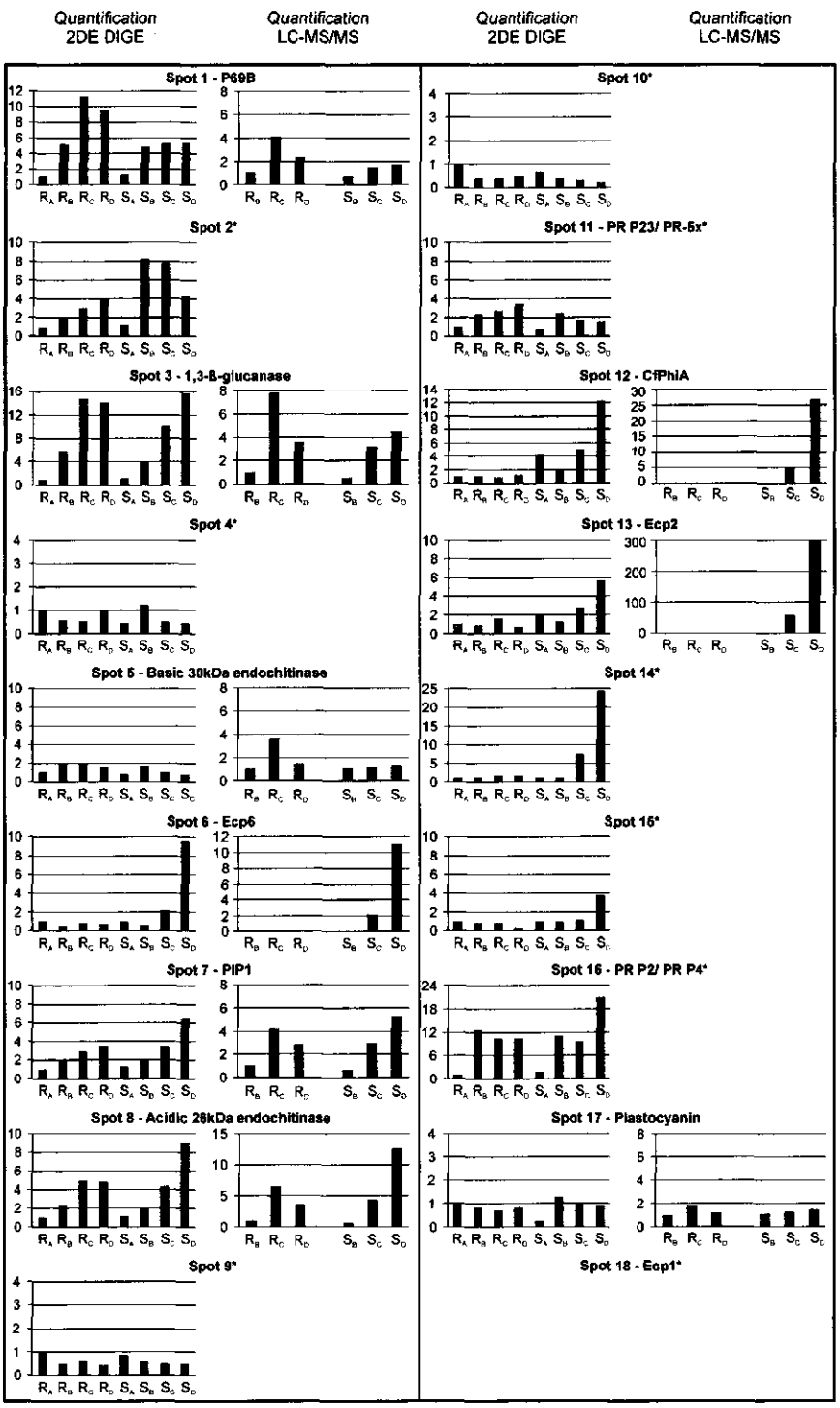
Quantification 2DE DIGE
Quantification LC-MS/MS
Quantification 2DE DIGE
Quantification LC-MS/MS
Spot 1 - P69B
Spot 2*
Spot 3 - 1,3-ß-glucanase
Spot 4*
Spot 5 - Basic 30kDa endochitinase
Spot 6 - Ecp6
Spot 7 - PIP1
Spot 8 - Acidic 26kDa endochitinase
Spot 9*
Spot 10*
Spot 11 - PR P23/ PR-5x*
Spot 12 - CfPhiA
Spot 13 - Ecp2
Spot 14*
Spot 15*
Spot 16 - PR P2/ PR P4*
Spot 17 - Plastocyanin
Spot 18 - Ecp1*

Quantitative LC-MS/MS^E and DIGE-2DE analysis of the same samples should lead to similar results concerning protein quantification. MS analysis of tryptic peptides obtained from 9 of the 17 quantified spots shown in Figure 4 led to an unambiguous identification (Table III) and this set of proteins was used to compare DIGE-2DE and LC-MS/MS^E quantification (Figure 5; right panels). LC-MS/MS^E protein quantifications are based on non-redundant peptides that were quantified in at least 17 of the 18 LC-MS/MS^E runs. The changes in protein abundance are presented relative to R_B, in which the abundance of each protein was set to 1 (Figure 5). Proteins secreted by *C. fulvum* (spots 6, 12 and 13; Figure 5) are quantified based on non-redundant peptides identified in at least the triplicate runs of S_C and S_D. Since the peptides were not identified in R_B, the abundance of these proteins at S_C was set to the abundance of S_C in the DIGE-2DE gels. The relative changes in apoplastic protein abundance at the different stages after inoculation revealed by both methods revealed similar protein patterns although the *C. fulvum*-secreted effectors and CfPhiA (spots 6, 12 and 13) seem to be present in substantial amounts in AFs of resistant plants and early stages of susceptible plants when analyzed on DIGE-2DE gels. However, this is caused by some minor background detection in the gel in combination with the way the data are presented (for DIGE-2DE the protein abundance at $R_A = 1$). Furthermore, it is clear that the dynamic range (the ratio between proteins with the lowest and the highest abundance) of the LC-MS/MS^E analysis is much larger and therefore, the actual changes in protein abundance are often much more pronounced than determined by DIGE-2DE analysis. This is also clear from the more discriminating PCA plot of the LC-MS/MS^E analysis compared to the PCA plot of the DIGE-2DE analysis (Figure 3). In addition, the DIGE-2DE quantification is based on three biological replicates while the LC-MS/MS^E quantification is based on triplicate analysis of one of these replicates. This is also reflected by the PCA plots since the technical replicates cluster much better than the biological replicates (Figure 3). Since quantification profiles as determined by LC-MS/MS^E prove to be comparable to the results obtained with DIGE-2DE gels, we concluded that the samples used for LC-MS/MS^E analysis are representative for the apoplastic proteome of resistant and susceptible plants at the various stages after *C. fulvum* inoculation. Therefore, the LC-MS/MS^E data were used for further analysis and subsequent biological interpretation of the events that take place in the apoplast of leaflets of resistant and susceptible tomato plants upon inoculation with *C. fulvum*.

LC-MS/MS^E analysis reveals massive changes in the apoplastic proteome after inoculation of resistant and susceptible tomato plants with *C. fulvum*

LC-MS/MS^E analysis in triplicate of AFs obtained from stages B, C and D of resistant and susceptible plants from one inoculation series led to the identification of 66 proteins, based on two or more peptides, which are predicted by MultiLoc (Höglund *et al.*, 2006) to localize to the apoplast or to the plasma membrane (PM). This set of proteins includes members of almost all PR protein families that were described by Van Loon *et al* (2006) (Table IV). It also contains the low abundant papain-like cysteine protease Rcr3 (Table IV, #31), which is guarded by Cf-2 and is targeted by Avr2 (Rooney *et al.*, 2005). Also the Rcr3-related proteases, referred to as *Phytophthora*-inhibited protease 1 (PIP1) (Table IV, #15) (Tian *et al.*, 2007) and cysteine protease TDI-65 (CYP1) (Table IV, #33) (Hao *et al.*, 2006) were identified. Furthermore, the CfPhiA protein (Table IV, #66) (Bolton *et al.*, 2008) and several effectors of *C. fulvum* were identified in S_C and S_D, of which some were to a (very) low extent also present in S_B and R_B, R_C and/or R_D. The effectors include the highly abundant extracellular protein Ecp6 from *C. fulvum* (Table IV, #64), but also the less abundant extracellular proteins Ecp2, -4, -5 and -7 (Table IV, #61, #62, #63 and #65, respectively) (Van den Ackerveken *et al.*, 1993; Laugé *et al.*, 2000; Bolton *et al.*, 2008). Ecp1 and the race-specific elicitor Avr9 were identified based on only one peptide (results not shown) and therefore not included in Table IV. In addition, several PM-localized proteins were identified including two Cf-like LRR proteins (Table IV, #17 and #26), the tomato brassinosteroid LRR receptor kinase (BRI1) (Table IV, #25) and three fasciclin-like arabinogalactan proteins (Table IV, #21, #22 and #24). The latter proteins can be (transiently) anchored into the PM and are probably involved in cell adhesion (Johnson *et al.*, 2003).

A subset of 47 of the identified apoplastic proteins was quantified based on the constraints described in the Methods. This analysis provided a detailed overview of protein accumulation in the apoplast through the various stages after inoculation with *C. fulvum* of resistant MM-Cf-4 and susceptible MM-Cf0 tomato plants. The changes in protein abundance are relative to R_B, in which protein abundance was set to 1 or -1. Based on the accumulation patterns, the quantified proteins were divided over three types of accumulation profiles (Table IV; Figure 6, left graphs). Profile 1 matches proteins of which the abundance increases rapidly between R_B and R_C, after which there is a rapid decline between R_C and R_D. At the same time,

Table IV. LC-MS/MS^E-based apoplastic protein identification and quantification in resistant and susceptible tomato plants inoculated with *C. fulvum*, and transcriptional regulation of the encoding genes upon *C. fulvum* inoculation and in Cf-4/Avr4 seedlings mounting the HR.

		Protein identification				Protein quantification		
#	Annotation	# peptides for ID	Highest peptide score	Protein score	Sequence coverage %	Acc. Profile	# peptides for quantification	Highest peptide score
1	PR-1; Pathogenesis-related protein P4	4	343	781	43	1	1	104
2	PR-1; Pathogenesis-related protein P6	5	352	1125	57			
3	PR-1-like	4	155	244	37			
4	PR-2; Acidic beta-1,3-glucanase	42	440	3086	76	1	9	117
5	Beta-1,3-glucanase-like protein	4	117	283	44	1	1	55
6	PR-3; Acidic 26 kDa endochitinase	18	465	1563	67	1	4	465
7	PR-3; Acidic 27 kDa endochitinase	4	184	295	33	1	1	52
8	PR-3; Class IV chitinase-like	2	126	185	31	1	1	126
9	PR-4; Pathogenesis-related protein P2	14	325	1139	65	1	2	325
10	PR-7; Subtilisin-like protease (P69B protein)	67	492	5985	69	1	20	438
11	PR-7; Subtilisin-like protease (P69C protein)	27	382	3559	58	1	4	275
12	PR-8; Acidic endochitinase III (CHIB1)	9	385	1084	49	1	2	385
13	PR-11; Chitinase, class V	8	242	634	52	1	1	212
14	Cysteine proteinase 3	7	161	325	19	1	4	132
15	Phytophthora-inhibited protease 1 (PIP1)	12	388	1242	46	1	6	367
16	Plastocyanin-like (CT099)	6	188	512	37	1	3	188
17	Putative disease resistance protein	6	86	294	27	1	2	74
18	Subtilisin-like protease precursor (ARA12-like)	19	177	955	46	1	5	177
19	Proline-rich protein	4	186	188	11	1	2	186
20	Hypothetical protein	5	165	434	42	1	1	165
21	Fasciclin-like arabinogalactan protein	3	149	231	22	1	1	149
22	Fasciclin-like arabinogalactan protein	4	79	233	24	1	1	79
23	Putative beta-galactosidase	10	236	681	36	1	1	61
24	Fasciclin-like arabinogalactan protein	7	216	471	30			
25	Brassinosterold LRR receptor kinase (BRI1)	2	55	319	4			
26	Leucine-rich repeat protein	5	147	483	39	1	3	145
27	Serine carboxypeptidase	5	161	276	28	1	3	161
28	Alpha-L-arabinofuranosidase	11	142	434	30	2	1	60
29	Alpha-mannosidase	10	123	369	44	2	2	89
30	Putative beta-galactosidase	14	236	1133	33	2	3	191
31	Cysteine protease 1 (Rcr3)	7	135	201	24	2	1	92
32	Basic PR-1-like	6	155	441	51	2	1	150
33	Cysteine protease TDI-65 (CYP1)	4	119	272	24	2	1	77
34	ß-D-xylosidase (LEXYL1)	4	111	360	13	2	1	111
35	PR-3; Basic 30 kDa endochitinase	8	450	874	49	2	1	450
36	PR-9; Peroxidase	15	430	1809	56	2	3	119
37	Low-temperature-induced cysteine proteinase	5	119	258	32			
38	Hypothetical protein	2	146	182	46	2	1	146
39	PR-15; 24K germin like protein	2	380	386	26	2	1	87
40	Germin-like protein	6	175	214	46	2	3	175
41	PR-15; 24K germin like protein	10	380	1401	56	2	2	89
42	Pectinesterase	3	55	247	28	2	1	52
43	Alpha-galactosidase	5	165	463	43	2	1	50
44	Xyloglucan endotransglycosylase LeXET2	5	120	339	47	2	2	111
45	Pectinacetylesterase-like	2	83	251	22			
46	PR-6; Ethylene-responsive proteinase inhibitor 1	3	267	447	41	2	1	267
47	PR-7; Subtilisin-like protease (P69F protein)	7	127	505	23	2	1	52
48	PR-7; Subtilisin-like protease (P69A protein)	14	492	2177	32			
49	PR-7; Subtilisin-like protease (P69D protein)	11	127	476	24			
50	Arabinosidase ARA-1	8	172	482	30			
51	PR-9; Peroxidase	4	143	216	26	2	1	64
52	Cationic peroxidase	5	100	288	28			
53	PR-14; Lipid transfer protein LTP1-like	2	90	124	24	2	1	90
54	Non-specific lipid transfer protein	4	163	296	46	3	1	147
55	PR b1-like precursor	3	197	407	63	3	1	197
56	Haem peroxidase	2	106	214	33	3	1	106
57	PR-5; Thaumatin-like protein	2	65	164	22	3	1	65
58	Glucan endo-1,3-beta-D-glucosidase	12	340	1678	65			
59	Hypothetical protein	2	102	126	11			
60	Pathogenesis-related protein PR P23	3	148	349	27			
61	Ecp2 (*Cladosporium fulvum*)	7	309	719	65			
62	Ecp4 (*Cladosporium fulvum*)	4	297	430	75			
63	Ecp5 (*Cladosporium fulvum*)	4	326	377	34			
64	Ecp6 (*Cladosporium fulvum*)	8						
65	Ecp7 (*Cladosporium fulvum*)	3						
66	PhiC (*Cladosporium fulvum*)	9						

[a] Ratios refer to gene expression in Cf-4/Avr4 seedlings compared to the control seedlings.
[b] Values indicated in bold are significantly different from the values shown for the previous stage.
[c] Ratios indicated in bold represent significantly different transcription in Cf-4/Avr4 seedlings as compared to the controls.

Table IV. Continued.

	Relative protein abundance							Relative gene expression						HR-induced transcription[a]		
#	R_A	R_B	R_C	S_A	S_B	S_C	Exp. Profile	R_A	R_B[b]	R_C	S_A	S_B	S_C	*HR 1h*[c]	*HR 3h*	*HR 5h*
1	1.0	5.6	1.9	0.1	4.4	10.1	1A	1.0	**4.9**	4.0	2.8	2.5	6.0	**5.1**	**5.3**	**36.0**
2																
3																
4	1.0	7.8	3.6	0.5	3.2	4.5										
5	1.0	7.1	2.0	0.8	1.5	3.7	1A	1.0	2.4	1.7	1.1	1.8	2.2	**0.5**	**1.6**	**1.9**
6	1.0	6.5	3.5	0.6	4.3	12.6	1A	1.0	**9.6**	9.2	6.4	6.6	13.0	**1.8**	**1.9**	2.2
7	1.0	1.1	1.0	0.5	1.7	5.8	1A	1.0	1.1	2.6	2.6	1.0	**5.3**	1.1	1.1	1.7
8	1.0	3.9	1.5	1.0	1.5	2.6	1A	1.0	**13.1**	20.5	17.2	6.8	**37.3**	**2.8**	**3.5**	**4.0**
9	1.0	14.1	8.9	0.9	8.1	13.2	1A	1.0	**16.8**	14.9	7.3	8.2	22.1	**1.9**	**3.1**	**4.7**
10	1.0	4.1	2.4	0.7	1.6	1.7	1A	1.0	**4.0**	3.1	2.7	2.5	4.0	1.4	**1.6**	**1.8**
11	1.0	4.6	2.4	0.5	0.9	1.6	1A	1.0	**8.7**	2.2	2.3	4.4	2.6	0.9	1.0	1.4
12	1.0	4.5	2.0	0.6	1.6	2.2	1A	1.0	**5.1**	3.5	2.5	4.1	5.5	1.4	1.3	1.3
13	1.0	6.2	3.5	0.6	1.5	3.0										
14	1.0	2.4	1.6	0.7	1.4	2.3	1A	1.0	1.3	2.3	1.6	1.2	2.3	**1.1**	0.8	0.8
15	1.0	4.2	2.9	0.7	2.9	5.3	1A	1.0	**12.1**	14.4	8.9	7.5	17.7	1.2	1.3	**1.9**
16	1.0	2.7	1.6	0.7	1.5	2.0	1A	1.0	1.0	1.3	1.0	0.8	**1.6**	1.0	0.9	1.0
17	1.0	5.5	1.2	0.7	1.0	2.6	1A	1.0	**2.2**	1.3	0.9	1.2	1.2	1.0	**2.9**	**3.2**
18	1.0	2.5	1.4	0.8	1.3	1.4	1B	-1.0	-1.5	-1.5	-1.2	-1.3	-1.7	**-1.3**	-1.5	-2.1
19	1.0	3.0	1.5	0.8	1.0	1.6	1B	-1.0	-7.3	-3.0	0.6	-2.4	**-101.7**	-1.2	-1.7	-1.5
20	1.0	2.5	1.4	0.7	1.9	4.1	1B	-1.0	-3.0	-2.6	0.8	-1.5	**-5.7**	-1.3	-1.1	-1.2
21	1.0	1.8	0.9	0.7	1.2	1.6	1B	-1.0	**-10.3**	-3.8	0.6	-2.6	**-80.9**	-1.0	-1.0	-2.4
22	1.0	2.3	1.0	0.8	1.2	2.2	1B	-1.0	**-4.2**	-3.2	0.7	-2.0	**-62.5**	-1.2	-1.3	-1.9
23	1.0	7.7	2.3	0.5	4.6	10.5	1B	-1.0	-1.2	-1.6	1.1	**-1.1**	-2.4	**-1.2**	-1.6	**-2.2**
24																
25																
26	1.0	4.3	3.2	0.6	2.1	3.8										
27	1.0	2.9	1.5	1.2	1.7	1.7										
28	1.0	2.1	1.5	0.8	1.1	1.3										
29	1.0	2.5	1.5	1.0	1.4	1.5										
30	1.0	2.5	1.5	1.1	1.3	1.2										
31	1.0	4.3	3.1	0.7	2.0	1.8										
32	1.0	5.9	3.6	1.0	0.0	0.4	2A	1.0	**23.3**	1.0	9.6	9.0	5.6	0.9	**1.8**	**2.8**
33	1.0	2.7	1.5	0.7	0.9	1.2	2A	1.0	**1.4**	2.3	1.4	1.0	**2.5**	0.7	0.6	**0.5**
34	1.0	1.5	1.3	0.8	0.9	0.8	2A	1.0	1.0	0.9	1.2	1.1	1.1	1.1	0.9	1.1
35	1.0	3.6	1.5	1.1	1.2	1.4	2A	1.0	**2.7**	1.2	1.4	1.7	1.8	1.3	**4.1**	**2.8**
36	1.0	3.8	2.2	0.9	1.5	1.8	2A	1.0	**4.5**	2.1	2.3	3.1	3.5	**1.7**	**2.0**	**2.1**
37																
38	1.0	2.6	1.2	0.6	0.8	1.2										
39	1.0	1.7	1.2	0.7	0.7	1.1										
40	1.0	1.6	1.3	0.7	0.9	0.9	2B	-1.0	-2.2	-2.4	-1.4	-1.5	**-5.3**	-1.2	-1.0	-1.1
41	1.0	1.8	1.2	0.8	0.7	1.1	2B	-1.0	**-2.9**	-2.4	-1.1	-1.4	**-15.4**	-1.1	-1.2	-1.1
42	1.0	3.5	1.9	0.6	1.1	1.4	2B	-1.0	-2.1	-2.8	-1.4	-1.2	**-4.0**	-1.1	-1.2	**-1.3**
43	1.0	4.1	1.8	0.7	0.8	0.8	2B	-1.0	-2.6	-3.1	-1.6	-1.4	**-27.7**	**-1.5**	-1.5	**-2.0**
44	1.0	2.2	0.8	0.7	0.8	0.7	2B	-1.0	-1.5	-1.3	-1.3	-1.1	**-1.5**	-1.4	**-2.0**	-2.8
45																
46	1.0	2.2	1.0	0.8	1.1	0.9										
47	1.0	2.0	0.8	0.9	0.9	1.1										
48																
49																
50																
51	1.0	4.4	1.4	0.3	0.6	0.7										
52																
53	1.0	7.1	2.5	1.3	1.2	1.9										
54	-1.0	-0.5	-0.9	-1.2	-1.7	-2.1	3	-1.0	-1.2	**-1.9**	-1.2	-1.2	-1.6	1.0	1.0	1.0
55	-1.0	-0.4	-0.7	-1.2	-2.4	-2.5	3	-1.0	-1.9	-2.1	-1.3	-1.2	**-3.5**	1.5	1.1	1.3
56	-1.0	-0.9	-1.9	-1.2	-1.7	-5.7	3	-1.0	-0.9	-1.0	-0.9	-0.7	-1.0	2.1	1.4	1.4
57	-1.0	-0.3	-0.5	-0.9	-1.0	-2.4										
58																
59																
60																
61																
62																
63																
64																
65																
66																

the abundance of these proteins continuously increases in the susceptible plants. Profile 2 is similar to Profile 1 in the resistant plants, whereas the abundance of the same proteins in the apoplast of the susceptible plants remains more or less unaltered. The accumulation of proteins of the resistant plants matching Profile 3 is similar to Profiles 1 and 2, albeit less pronounced, whereas their abundance decreases in the susceptible plants.

Most PR proteins that were quantified match Profile 1, which is a behaviour that is typical for PR proteins. Proteins that match this profile include members of the PR-1, -2, -3, -4, -7, -8 and -11 families, and several plasma membrane-localized proteins (Table IV). The PR-7 subtilisin-like protease P69 family consists of 7 members, of which five (P69A to -D and P69F; Table IV, #10, #11, #47, #48 and #49) were identified in the LC-MS/MS^E analysis. P69B and P69C have been described to be transcriptionally upregulated upon inoculation with an avirulent or virulent pathogen (Jorda and Vera, 2000), thereby matching our data and protein abundance Profile 1. The P69 family members A, D and F are not transcriptionally upregulated in a compatible interaction, while upregulation in an incompatible interaction was not studied (Jorda *et al.*, 1999; Jorda and Vera, 2000). Here, P69F was found not to accumulate in susceptible plants and to accumulate in resistant plants (Profile 2), thereby suggesting that the encoding gene is transcriptionally upregulated in incompatible interactions. Furthermore, the P69 family members E and G were not identified in this analysis, which confirms the observation that these family members are only expressed in roots (Jorda and Vera, 2000; Kavroulakis *et al.*, 2006). Since our results, and results presented by other groups, show that individual members of the P69 family have increased gene expression and increasing protein accumulation (Jorda *et al.*, 1999), and one of them (P69B) is targeted by two independent protease inhibitors secreted by *Phytophthora infestans* (Tian *et al.*, 2004; Tian *et al.*, 2005), these apoplastic subtilisin-like proteases seem to play an important role in plant defence.

In addition to apoplastic proteins, contaminating proteins not predicted to localize to the apoplast were identified in all AF samples. In other studies on the leaf apoplastic proteome, the activity of cellular malate dehydrogenase (MDH) has been used as a marker for intracellular protein contamination of AFs (Boudart *et al.*, 2005; Dani *et al.*, 2005). Two different MDHs were identified in the tomato apoplast (Supplementary Table S1) and quantification of these MDHs revealed that they match Profile 2. Also most additional contaminating non-apoplastic proteins match Profile 2 (Supplementary Table S1 and Figure

S1). This expression pattern might be explained by the HR-associated cell death that takes place at R_B and R_C due to Cf-4-mediated recognition of Avr4, which locally causes release of the cellular content into the apoplast. Since the abundance of most of these contaminating proteins does not change during *C. fulvum* proliferation in the leaves of susceptible plants, these data also show that *C. fulvum* remains restricted to the apoplast without damaging the tomato cells.

Changes in the apoplastic proteome related to transcriptional regulation due to a challenge with *C. fulvum*, and comparison to HR-associated transcriptional regulation

To study transcriptional regulation of genes encoding apoplastic proteins in response to *C. fulvum* inoculation, Affymetrix tomato microarrays were hybridized with RNA isolated at stages A, B and C of new inoculation series of resistant and susceptible plants. To be able to compare expression patterns, the expression level of the various genes at R_A was set to 1 or -1 (Table IV; Figure 6, middle graphs). In addition to studying gene expression upon *C. fulvum* inoculation, HR-associated expression of the same subset of genes was studied using transgenic tomato seedlings expressing both the *Cf-4* and *Avr4* gene (see Methods for details; Table IV; Figure 6, right graphs). For this, the Affymetrix arrays were hybridized with RNA isolated from Cf-4/Avr4 and control seedlings at 1, 3 and 5 hours after the temperature shift that initiates a synchronized HR. Genes present on the microarray that encode the proteins listed in Table IV were selected for further analysis.

Microarrays that were hybridized with RNA isolated from the *C. fulvum*-inoculated plants revealed that the increased apoplastic abundance of most of the proteins that match Profile 1 is the result of an increased transcription of the encoding gene in both resistant and susceptible plants, although some genes were not transcriptionally regulated (Profile 1A, Figure 6; middle graphs). Analysis of the expression of the same subset of genes present on the microarrays hybridized with RNA from Cf-4/Avr4 seedlings mounting a HR revealed that for most of the genes that match Profile 1A, transcription also increases during the HR (Table IV; Figure 6, right graphs). The proteins matching Profile 1A are mainly PR proteins that accumulate as a result of increased gene expression (Table IV), such as 1,3-ß-glucanases, chitinases and the PR-1-related proteins P4 and P6 (De Wit and Van der Meer, 1986; Joosten and De Wit, 1989; Joosten *et al.*, 1990a; Wubben *et al.*, 1992).

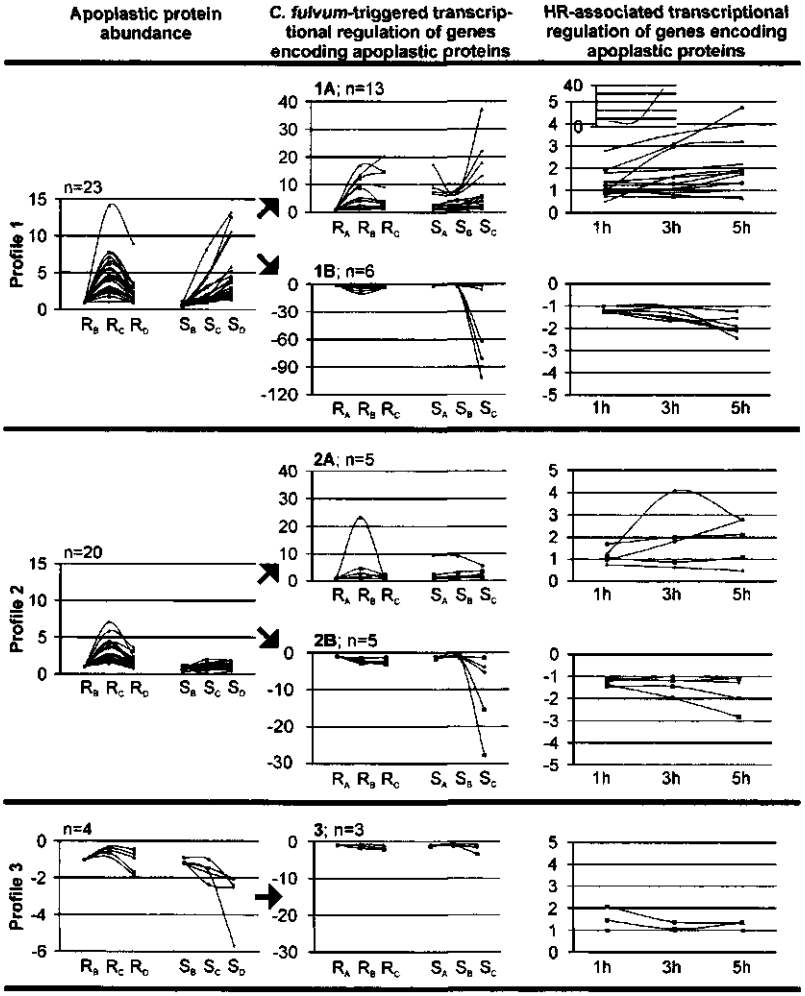

Figure 6. The relation between protein accumulation in the apoplast and transcriptional regulation of the encoding genes in *C. fulvum*-inoculated resistant and susceptible tomato plants and Cf-4/Avr4 seedlings. Abundance profiles of apoplastic proteins identified and quantified by LC-MS/MS^E at stages B, C and D in resistant and susceptible plants are classified into Profiles 1, 2 and 3 (see text for details). Protein abundances are shown relative to R_B, of which protein abundance was set to 1 or -1 (left graphs). The encoding genes of approximately 70% of the identified proteins are present on the Affymetrix tomato microarray. Transcriptional regulation of these genes was determined for stages A, B and C of resistant and susceptible plants inoculated with *C. fulvum*. Gene expression is shown relative to R_A, of which gene expression was set to 1 or -1 (middle graphs). In addition, microarrays were hybridized with RNA isolated from Cf-4/Avr4 tomato seedlings that execute a synchronized hypersensitive response (HR). In this case, transcriptional regulation of the genes encoding the quantified apoplastic proteins was determined at 1, 3 and 5 hours after HR initiation and presented as the expression in Cf-4/Avr4 versus control seedlings (right graphs; see Table IV for details).

Surprisingly, genes encoding a subset of proteins matching Profile 1 are transiently downregulated in the resistant plants and strongly downregulated in the susceptible ones upon challenge with *C. fulvum*. In the resistant plants there was a slight and transient increase in the abundance of the encoded proteins, whereas in the susceptible plants there was some increase at later stages of colonization of the leaflets (Profile 1B; Table IV; Figure 6, left and middle graphs). These genes also appear slightly downregulated in the Cf-4/Avr4 seedlings mounting the HR (Table IV; Figure 6, right graphs). However, the strong downregulation, particularly in the heavily colonized leaflets of susceptible plants of stage S_C, suggests that this is the result of *C. fulvum*-mediated suppression of host gene expression. Interestingly, four out of the six proteins of which the expression of the encoding gene is downregulated are localized at the plasma membrane and/or cell wall. These proteins include two fasciclin-like arabinogalactan proteins (Table IV, #21 and #22), that might be involved in cell adhesion (Seifert and Roberts, 2007), a proline-rich protein (Table IV, #19), and a beta-galactosidase (Table IV, #23).

About 50% of the genes encoding proteins matching Profile 2 are transcriptionally upregulated in the resistant plants, which causes accumulation of the encoding proteins in the apoplast (Profile 2A; Table IV; Figure 6, left and middle graphs). In addition, transcription of some of these genes is also stimulated in susceptible plants and by the HR (Table IV; Figure 6, middle and right graphs). These genes encode proteins such as a basic PR-1-like protein (Table IV, #32) and the PR-9 peroxidase (Table IV, #36), which have both been described to be transcriptionally upregulated upon inoculation with various pathogens (Vera *et al.*, 1993; Tornero *et al.*, 1994; Tornero *et al.*, 1997). We find that the increase in mRNA in susceptible plants does not lead to an increase in protein in the apoplast. Possibly, the sustained presence of *C. fulvum* in the apoplast results in a high turn-over of these enzymes, while in the resistant plants *C. fulvum* has been defeated, leading to transient protein accumulation. Similar to Profile 1, approximately half of the genes encoding proteins matching Profile 2 appear to be downregulated by *C. fulvum* (Profile 2B; Table IV; Figure 6), mainly in the susceptible plants but also more or less transiently in the resistant plants. This profile again mostly accounts for cell wall-localized proteins, such as two germin-like proteins (Table IV, #40 and #41), a pectinesterase (Table IV, #42), an alpha-galactosidase (Table IV, #43) and a xyloglucan endotransglycosylase (Table IV, #44). Finally, the genes encoding apoplastic proteins that match Profile 3 are neither transcriptionally regulated in *C. fulvum*-inoculated plants, nor in

plants mounting the Cf-4/Avr4-initiated HR (Table IV; Figure 6). Most likely, these proteins gradually decrease in abundance because of protein turn-over and a lack of transcriptional regulation.

DISCUSSION

Apoplastic fluid isolation as a tool to study the apoplastic proteome

The volumes of apoplastic fluid isolated per gram of fresh weight of healthy and diseased leaves are very similar (Figure 1), illustrating that the volume of the mycelium that grows in the apoplast of susceptible leaves is negligible compared to the volume of the intercellular spaces of the leaf mesophyll. In addition, HR-related cell collapse that leads to the release of the cellular content into the apoplast also does not seem to add much to the volume of apoplastic fluid obtained. Since a similar volume of AF was obtained from leaflets of resistant and susceptible plants before and after inoculation with *C. fulvum* (Figure 1), the dynamics of the apoplastic proteome could be studied by comparing the protein contents of identical volumes of AF. The observation that similar volumes of AF are isolated from leaflets at different stages suggests that the apoplastic volume is very large. Indeed, the volume of the apoplastic space represents about 30% of the total leaf volume since we isolated about 5 ml of apoplastic fluid from 10 grams (fresh weight) of leaves, which have a volume of about 16 ml themselves. The apoplast consists of intercellular spaces filled with air and a water layer in and on the cell walls surrounding the cells (the apoplastic water volume), in which the apoplastic proteins are localized. During AF isolation, the intercellular spaces, which are in particular large in the spongy parenchyma, are filled with water that is subsequently removed by centrifugation, thereby washing out and diluting the apoplastic proteins. This implies that the actual local protein concentrations in the apoplast are higher than in the AF. Indeed, Rico and Preston (2008) calculated that the apoplastic water volume from tomato is about 2-3 fold diluted upon AF isolation. Since the apoplastic response in resistant plants is accelerated by the HR that is mounted at the various, strictly localized sites of *C. fulvum* penetration into the leaf, the local concentration of apoplastic proteins at these sites in the resistant plants mounting HR (stages R_B and R_C) is anticipated to be very high.

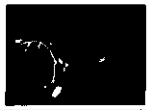

Apoplastic proteome analysis by DIGE-2DE gels

AFs originating from three independent biological replicates of *C. fulvum*-inoculated resistant and susceptible plants, isolated at stages A, B, C and D were analyzed by DIGE-2DE gels. To avoid incorrect protein quantification caused by more intense fluorescence or more efficient labelling of a particular sample with the Cy3 or Cy5 label, labelling of the replicates with either Cy3 or Cy5 was alternated. In addition, one biological replicate was analyzed twice, in which the samples were alternately labelled with Cy3 and Cy5. No significant differences in protein abundance were found between these two experiments and therefore, it was assumed that protein quantification was not influenced by DIGE labelling.

The number of the various (abundant) proteins making up the apoplastic proteome appears to be relatively low, which makes 2DE analysis a useful method for proteome analysis. However, the dynamic range of the apoplastic proteome proved to be extremely large since proteins such as the subtilisin-like protease P69B show a huge increase in abundance, which made identification of low abundant proteins from preparative 2D gels difficult. Although the DIGE-2DE gels were suitable to identify the previously described apoplastic proteins, DIGE-2DE gels were not suitable to identify new proteins involved in apoplastic defence responses of *C. fulvum*-inoculated tomato plants.

In one of the inoculation experiments, non-inoculated MM-Cf-4 and MM-Cf0 plants were included. These plants were incubated in the same compartment as the inoculated ones and AF was isolated at stage C. Based on DIGE-2DE gels, the apoplastic proteome of these plants was similar to the proteome pattern of R_B and S_B (results not shown), suggesting that the induced responses in the inoculated plants also lead to signalling from plant to plant, resulting in an elevated state of defence also in untreated plants. Genes encoding PR proteins have been reported to be induced by plant hormones such as salicylic acid and ethylene (Van Loon *et al.*, 2006). Indeed, inoculated leaflets of resistant plants show severe epinasty at stages B to D (Table I), which is a hallmark for ethylene production (Ursin and Bradford, 1989). The released ethylene possibly triggers defence in the neighbouring non-inoculated plants.

Apoplastic proteome analysis by LC-MS/MS^E

LC-MS/MS^E analysis of the apoplastic proteome at stages B-D of one representative biological replicate of both resistant and susceptible plants inoculated with *C. fulvum*, was

performed in triplicate to eliminate technical variation. To obtain a robust dataset of peptides for apoplastic protein quantification, only peptides quantified in 18 LC-MS/MS^E runs (6 samples, each with 3 replicates), or a minimum of 17 runs, were used for further analysis (Table IV). Protein quantification is based on the total intensity of the quantified non-redundant peptide(s).

As mentioned above, AF was isolated at the various stages and SDS-PAGE gels revealed protein patterns conform to earlier observations (Figure 2A) (De Wit and Van der Meer, 1986; Joosten and De Wit, 1989; Joosten *et al.*, 1990a). However, in addition to a large set of apoplastic proteins, LC-MS/MS^E analysis of these AFs revealed a substantial number of non-apoplastic proteins (Supplementary Table S1), which is caused by the sensitivity and robustness of the method of analysis, in combination with the relatively small apoplastic proteome. Since also the relatively insensitive approach of spot identification from the 2DE gels revealed a non-apoplastic protein (spot 17, Figures 4 and 5), indeed a large number of contaminating non-apoplastic proteins identified through LC-MS/MS^E analysis was expected.

Most non-apoplastic proteins do not increase in abundance at any of the stages, except for stage R_C. At this stage the HR has occurred in the resistant plants, which probably leads to leakage of cellular proteins into the apoplast (Profiles 1 and 2; Supplementary Figure S1). Non-apoplastic proteins matching Profile 1 have been described to increase in abundance in the cells of leaflets of susceptible plants. This set of proteins includes the basic 1,3-ß-glucanase (PR-2) and PR-10 protein that accumulate in the vacuole and the cytoplasm, respectively (Van Kan *et al.*, 1992; Liu and Ekramoddoullah, 2006), and the expression of the encoding genes increases in susceptible plants upon inoculation with various pathogens (Van Kan *et al.*, 1992; McGee *et al.*, 2001; Liu and Ekramoddoullah, 2006). Indeed, several of the genes encoding proteins in Profile 1 are transcriptionally upregulated in susceptible plants (Supplementary Figure S1). Therefore, we assume that the increased amounts of these contaminating proteins in the AFs of susceptible plants, is caused by their increased abundance inside the cells. Finally, a set of non-apoplastic proteins decreases in abundance in the AFs from susceptible and also resistant plants (Profile 4; Supplementary Figure S1). Many proteins in this subset are involved in photosynthesis and glycolysis and the decrease in protein abundance suggests that these pathways are inactivated. Indeed, initiation of the HR was shown to specifically inactivate the photosynthesis pathway in a phosphorylation-dependent manner (Chapter 4) which might lead to a decrease in protein abundance at a later

stage. Susceptible plants do not execute a HR but the metabolism and gas exchange of such plants are disturbed since the stomata are clogged with mycelium at the later stages of infection (Thomma *et al.*, 2005). Microarray analysis revealed that the genes encoding non-apoplastic proteins matching Profiles 2 or 4 are either transcriptionally unaltered or downregulated. Since protein accumulation differs between Profile 2 and 4, the observed protein patterns seem to depend on the stability of the protein (Supplementary Figure S1).

The LC-MS/MS^E analysis provides a robust overview of the apoplastic tomato proteome. However, the low abundant effectors Avr2, Avr4 and Avr4E were not identified in this analysis, which indicates that also this technique has its limitations. In addition, this analysis did not reveal any new effectors secreted by *C. fulvum*, since the full genomic sequence of *C. fulvum* is not available. When available, a database search of the LC-MS/MS^E data is anticipated to reveal novel effectors of the pathogen that are secreted into the apoplast. This is the first time that a subset of *C. fulvum*-secreted effector proteins has been identified in AFs originating from resistant plants (results not shown). Particularly Ecp2 has been identified in some of the replicates of R_A, R_B and R_C. Previously, Avr4-promoter-GUS fusions revealed that the Avr4 gene is highly expressed by *C. fulvum* upon inoculation of resistant plants. However, the Avr4 protein was never detected in AF isolated from an incompatible interaction (Joosten *et al.*, 1997). This suggests that also in resistant plants, effectors of *C. fulvum* are initially able to manipulate plant defence responses (see below) before Avr perception and subsequent HR initiation stops proliferation of the pathogen.

The differences between the dynamics of the apoplastic proteome of resistant and susceptible plants

Almost all apoplastic proteins match Profiles 1 and 2 (Table IV; Figure 6). The clear transient protein accumulation in resistant plants, in contrast to a sustained increase or unaltered protein abundance in the susceptible plants, illustrates that tomato has defeated *C. fulvum* around stage R_C, as after this stage protein abundances decrease again. From these expression patterns, it is clear that the resistant MM-Cf-4 plants, which mount a fast HR upon Avr4 recognition, are substantially faster with their response to *C. fulvum* than the susceptible plants.

The observation that the susceptible plants also differentially accumulate substantial amounts of apoplastic proteins upon inoculation, despite the lack of HR-associated resistance

to *C. fulvum*, is probably the result of massive colonization of the leaflets by *C. fulvum*. The increase in fungal biomass at the later stages of colonization probably leads to the release of large amounts of MAMPs, leading to MAMP-triggered immunity (MTI) in a relatively large area of the leaf (Jones and Dangl, 2006). However, *C. fulvum* is able to colonize the leaflets of these plants and must therefore, at least at the earlier stages of infection, be able to avoid and/or suppress MTI, most likely through its secreted effectors that might interfere in the activation and/or effectiveness of the various components of the host defence response (effector-triggered susceptibility, ETS) (Jones and Dangl, 2006) (see below). Since a slow apoplastic defence response of susceptible tomato plants is observed, the effectors probably do not induce complete ETS during colonization. However, MTI appears to be repressed sufficiently or is successfully circumvented by *C. fulvum*, and therefore the fungus is able to colonize the tomato leaves. Upon recognition of Avr4 by *Cf-4*-expressing tomato plants, HR-associated effector-triggered immunity (ETI) occurs (Jones and Dangl, 2006), which renders the plant fully resistant to *C. fulvum*. These data typically show that the resistance of Cf-4 plants is an accumulation of basal (MTI) and specific resistance (ETI), as was proposed by Jones and Dangl (2006). Furthermore, these data show that proteins matching Profile 1 are induced as a result of MTI and ETI, while proteins matching Profile 2 are mainly ETI-induced as the latter do not increase in abundance in the susceptible plants.

For a subset of proteins, transcriptional regulation of the encoding genes does not correlate with their abundance profile in the AF (Profiles 1B and 2B; Table IV; Figure 6). It has been reported previously that mRNA expression levels do not always correlate with the actual protein abundance (Greenbaum *et al.*, 2003). In eukaryotic cells, proteins destined to the extracellular space are synthesized on the endoplasmic reticulum (ER) and subsequently translocated to the ER lumen where they obtain their native conformation. After these processing steps they are transported to the Golgi and secreted. However, proteins can also be stored in protein storage vacuoles that are destined for regulated secretion, a sorting process which is mediated by quality control in the early secretory pathway (Neuhaus and Rogers, 1998). Furthermore, a decrease in protein abundance caused by transcriptional down regulation of the encoding gene strongly depends on the stability of the encoded protein.

Interestingly, the genes encoding the proteins that match profiles 1B and 2B are slightly, and more or less transiently, transcriptionally downregulated in resistant plants and very strongly in susceptible plants, after inoculation with *C. fulvum* (Profiles 1B and 2B;

Table IV; Figure 6). These proteins significantly accumulate in resistant plants at stage C, which implies that these proteins are required for defence against *C. fulvum* (Table IV; Figure 6). Since this subset mainly consists of proteins involved in cell wall modifications, and a clear difference between protein abundance and gene expression is observed, these proteins are likely to be stable. For instance, two germin-like proteins (Table IV, #40 and #41) belong to this subset, and these proteins are involved in cell wall stiffening and cross-linking, possibly via their oxalate-oxidase or superoxide dismutase activity, which leads to hydrogen peroxide production (Lamb and Dixon, 1997). In addition, pectinesterase (Table IV, #42), a protein that also accumulates at stage R_C, catalyses de-esterification of pectin, a process which precedes cell wall stiffening to mount resistance (Ficke *et al.*, 2004; Pelloux *et al.*, 2007). Another protein in this subset, alpha-galactosidase (Table IV, #43), hydrolyses α-D-galactose from cell wall polymers (Chrost *et al.*, 2007) to modify the cell wall. Possibly, this enzyme releases oligogalacturonide fragments from the cell wall that stimulate plant defence or accelerates senescence, since a gene encoding a barley alpha-galactosidase is upregulated during senescence. Finally, two fasciclin-like arabinogalactans (FLAs; Table IV, #21 and #22), which are proteins that function as cell adhesion molecules, reside in this subset. FLAs belong to the family of arabinogalactan proteins (AGPs) that form a subgroup within the hydroxyproline-rich glycoproteins (HRGPs) (Seifert and Roberts, 2007). Most FLAs are anchored in the plasma membrane with a GPI-anchor (Johnson *et al.*, 2003) that can be cleaved to release the protein from the membrane into the cell wall (Schultz *et al.*, 1998; Sun *et al.*, 2004). Induced GPI-anchor cleavage would allow identification of these FLAs in the AFs, and might also explain why for these proteins the abundance does not correlate with gene transcription. In addition, this subset contains a proline-rich protein with clear homology to extensin-like HRGPs based on conserved domains (Table IV, #19).

We find that all of the genes encoding the proteins in Profile 1B and 2B described above, and which appear to be important for resistance to *C. fulvum*, are strongly downregulated in heavily colonized leaflets of susceptible plants. Genes encoding FLAs have been reported to be downregulated as a result of the accumulation of abscisic acid (Johnson *et al.*, 2003), suggesting a stress-induced transcriptional downregulation in the host. However, transcription of these genes hardly changes in the Cf-4/Avr4 seedlings (Table IV; #21 and #22), which renders aspecific stress-induced down regulation of these genes highly unlikely. Furthermore, there is an example of downregulation of an extensin-like protein by several

isolates of endophytic *Trichoderma* (Bailey *et al.*, 2006). On the contrary, HRGPs are important for defence responses to pathogen attack and an increase in HRGP transcripts was observed in an incompatible interaction between pearl millet and the oomycete *Sclerospora graminicola* (Deepak *et al.*, 2007). Furthermore, overexpression of an extensin in Arabidopsis causes these plants to be resistant to *Pseudomonas syringae* (Wei and Shirsat, 2006). Conformably, genes encoding germin-like proteins were shown to be transcriptionally upregulated upon pathogen attack suggesting a role for these proteins in basal defence (Park *et al.*, 2004; Zimmermann *et al.*, 2006). Since *C. fulvum* colonizes the apoplast in close association with the cell walls of its host from where it obtains water and nutrients (De Wit, 1977; Joosten *et al.*, 1990b), accumulation of host cell wall proteins that stiffen the cell wall and cause impermeability, thereby blocking water and nutrient uptake, is a potential threat for the fungus. Furthermore, cell wall proteins such as FLAs might stimulate a tight adhesion between the individual host cells, thereby preventing growth of *C. fulvum* in between these cells. Since most of the genes encoding these proteins are (strongly) transcriptionally downregulated in susceptible plants, we propose that *C. fulvum* is able to mediate active suppression of these genes, as also proposed for *Pseudomonas syringae* inoculated on *Arabidopsis thaliana* (Truman *et al.*, 2006). This allows the fungus to loosen the host cell-to-cell contacts in order to grow in between the cells and to prevent an increase of the stiffness and impermeability of the host cell walls. In this way, the outer surface of the fungal hyphae can remain in close contact with the plant cells, allowing uptake of water and nutrients. Therefore, we suggest that an effector of *C. fulvum* targets an extracellular MAMP-receptor in susceptible plants, thereby suppressing MAMP-induced transcription of the genes encoding the above-mentioned cell wall proteins. In this way, an essential part of the plant defence response aimed at restricting proliferation of the fungus is counteracted.

Accumulation of proteins matching the Profiles 1A and 2A is stimulated by increased gene expression of their encoding genes (Table IV, #Figure 6). Furthermore, their accelerated accumulation in resistant plants originates from enhanced gene expression, stimulated by the Cf-4/Avr4-triggered HR. Therefore, we conclude that Cf-4-mediated resistance to *C. fulvum* is the outcome of a combination of the HR and enhanced apoplastic defence responses. The observation that Cf-4-mediated resistance does not rely on the HR only, was also reported in Chapter 3.

METHODS

Inoculation of tomato plants with *Cladosporium fulvum* and isolation of apoplastic fluid

Tomato plants were grown under standard greenhouse conditions: 21°C during the 16 hour day period, 19°C at night, 70% relative humidity (RH) and 100 Watt/m^2 Supplementary light when the sunlight influx was below 150 Watt/m^2. Tomato cultivar MoneyMaker that does not contain resistance genes against *C. fulvum* (MM-Cf0), and a near isogenic line containing the *Cf-4* locus (MM-Cf-4) were used for all inoculations. A race 5 strain of *C. fulvum*, avirulent on MM-Cf-4 plants due to secretion of Avr4, was grown on PDA plates containing additional agar (30g/l in total) and after 8-10 days conidia were harvested by covering the plate with distilled water and rubbing the surface to release the conidia. Conidial suspensions were washed with water twice by centrifugation (4,000g) and the supernatant was discarded. Five-week-old plants were spray-inoculated with approximately 1 x 10^6 spores per ml on the lower side of the leaves and plants were kept at 100% relative humidity under a plastic transparent cover for 48 hours. Leaflets were subsequently collected from multiple resistant and susceptible plants at several stages after *C. fulvum* inoculation (see also Table I) and apoplastic fluids were obtained via vacuum infiltration as described by De Wit and Spikman (1982). Briefly, entire leaflets were infiltrated with distilled water *in vacuo* and carefully dried at the outside, after which the apoplastic fluid was isolated via centrifugation (10 minutes at 3,000g). Aliquots of 10 ml of apoplastic fluid were freeze-dried and the residue was dissolved in 1 ml of MilliQ water and centrifuged at 16,000g for 10 minutes. The supernatant was applied to a PD-10 desalting column (GE Healthcare) and proteins were eluted with 3.5 ml of MilliQ water, freeze-dried and again dissolved in 1 ml of MilliQ water. Protein concentrations were determined by a Bradford protein assay (Bio-Rad) with BSA as a standard. This procedure was followed for the apoplastic fluids of three replicate inoculations, obtained at stages A, B, C and D after inoculation of resistant (R) and susceptible (S) plants, resulting in samples R_A to R_D and S_A to S_D (Table I).

Protein DIGE-labelling

An aliquot of the desalted apoplastic protein preparations was freeze-dried and dissolved in TUC (7M Urea, 2M Thiourea, 4% (w/v) CHAPS, 50 mM Tris (pH 8.5)) to a final protein concentration of 5 µg/µl. The samples were labelled with 0.4 nmol Cy3 or Cy5 DIGE

label per 50µg of protein in a volume of 10 µl according to the instructions of the manufacturer (GE Healthcare). In addition, a reference sample consisting of an aliquot of each sample was labelled with 0.4 nmol Cy2 DIGE label. The labelling reaction was stopped by adding 10 mM lysine and TUCCDT (5M Urea, 2M Thiourea, 2% (w/v) CHAPS, 2% (w/v) 3-(4-Heptyl)phenyl-3-hydroxypropyl)dimethylammoniopropanesulfonate (C7BzO), 20 mM DTT and 5 mM (2-Carboxyethyl) phosphine (TCEP)). The amount of protein that was loaded onto the gels originated from equal volumes of apoplastic fluid (Table II).

Two-dimensional polyacrylamide gel electrophoresis (2DE-PAGE)

Apoplastic protein samples obtained from the same stage of resistant and susceptible plants that were differentially labelled with Cy3 or Cy5 were mixed with the Cy2-labelled reference. The volume was adjusted to 450 µl and IPG buffer (pH 3-10) was added to a final concentration of 0.5% (v/v). A 7 cm IPG strip (pI 3-10, non-linear; GE Healthcare) covered with mineral oil was rehydrated with the protein mixture in a ceramic strip holder. Subsequently, proteins loaded in the strips were focussed on an Ettan IPGphor II IEF System using the Manifold tray (GE Healthcare) at 20°C to a maximum of 9,000 Volt hours, according to the instructions of the manufacturer. Subsequently, the strips were incubated in equilibration buffer (50 mM Tris (pH 8.8), 6 M Urea, 30% (v/v) glycerol and 2% (w/v) SDS) enriched with 1% (w/v) dithiothreitol (DTT) and subsequently in equilibration buffer enriched with 2,5% (w/v) iodoacetamide (IAA), both for 15 minutes. The strips were laid onto 12.5% SDS-PAGE gels, covered with 0.5% agarose including bromophenol blue and run for 30 minutes at 5 mA per gel followed by 15 mA per gel, until the bromophenol blue front had reached the end of the gel. Gels were immediately scanned on a FX scanner (Bio-Rad) or an Ettan DIGE Imager (GE Healthcare). Images were exported as tiff files with Quantity One software (Bio-Rad). For protein identifications, preparative 2D gels were run from strips loaded with approximately 1 mg of total protein. For this, 18 cm IPG strips with varying pI ranges (GE Healthcare) were rehydrated with a protein sample, focused with a Multiphor II (GE Healthcare), further separated on SDS-PAGE gels (Protean, Bio-Rad) and subsequently stained with Coomassie Brilliant Blue.

Protein identification from 2DE gels

Protein spots that were clearly visible after Coomassie staining were excised from the gel and digested with trypsin (Promega), following the in-gel method according to (Shevchenko *et al.*, 1996). The collected extracts of the resulting tryptic peptides were dried overnight in a vacuum centrifuge (v/v), and stored at -20°C. The peptides were re-dissolved in 8 µl of 50% acetonitrile (ACN) and 5% formic acid (FA) in H_2O (v/v/v). MS and MS/MS information was acquired with a Q-TOF I (Waters, Manchester, UK) coupled to a nano-LC Ultimate system (LC Packings Dionex, Sunnyvale, CA). One or two µl of sample was 12 times diluted with H_2O and peptides were separated on a nano-analytical column (75 µm internal diameter x 15 cm, C18 PepMap, LC Packings, Dionex) using a gradient of 2-50% ACN and 0.1% FA in H_2O (v/v/v) in 20 minutes. The flow of 300 nl/min was directly infused into the Q-TOF I, operating in data-dependent MS and MS/MS modes. The resulting MS/MS spectra were processed with Masslynx software (Waters, Manchester, UK). For MALDI-TOF analysis, a 1 µl volume of the dissolved peptide sample was spotted onto a target plate after mixing the sample 1:1 (v/v) with a solution of 10 mg/ml α-cyano-4-hydroxycinnamic acid in 50% ethanol/50% ACN/0.1% TFA (v/v/v). Reflectron MALDI-TOF spectra were acquired on a TofSpec 2E (Waters, Manchester, UK). Both the MS/MS spectra from the Q-TOF I as well as the peptide mass lists from the MALDI-TOF were used to search in the Virtual Expert Mass Spectrometrist (VEMS) software using the non-redundant database LycoperClado3 (see below for details). The following constraints were used for LC-MS/MS spectra: tryptic peptides only, up to 2 missed cleavages sites allowed, initial tolerance of 0.3 Da for MS ions and 0.6 Da for MS/MS fragment ions, carbamidomethyl cysteine as fixed modification and methionine oxidation and asparagines and glutamine deamidation as variable modification. For MALDI peptide lists, similar constraints were used with a tolerance of 0.3 Da and a charge state of 1+. Proteins reported in Table III are identified by at least two peptides and have a protein score higher than 100.

Quantification of 2DE protein spots

Apoplastic protein samples originated from three independent biological replicates. The samples from the first biological replicate were analyzed in duplo, whereas the samples from the 2nd and 3rd biological replicates were analyzed once by DIGE-2DE analysis. The gel images were loaded into Decyder software (version v6.0) and the reference samples were

matched between all gels. Samples were compared with t-statistics in the Biological Variation Analysis (BVA) package (Decyder, GE Healthcare). No significant differences were observed between the proteins quantified in the two technical replicates of biological replicate 1 ($P \leq 0.05$; results not shown). Protein quantifications as presented in Figure 5 originate from quantification of one of the two technical replicates of biological replicate 1, and biological replicates 2 and 3. XML data from all detected spots were exported from Decyder and Principle Component Analysis plot of all data was made in GeneMaths (Applied Maths).

Database compilation

To compile the LycoperClado3 database, several databases with tomato or *C. fulvum* sequences were combined, since each database contains information that is lacking from another database. The tomato sequences came from NCBI (ftp://ftp.ncbi.nih.gov/repository/UniGene/, 17012007) and SGN (Tomato_200607_build_1; http://www.sgn.cornell.edu/) databases. The *C. fulvum* sequences came from COGEM (http://cogeme.ex.ac.uk/sequence.html; 17012007) and NCBI (http://www.ncbi.nlm.nih.gov/Taxonomy/Browser/wwwtax.cgi?id=5499) databases, which were enriched with in-house sequenced proteins. To these sequences were added the *Mycosphaerella graminicola* sequences from NCBI (http://www.ncbi.nlm.nih.gov/Taxonomy/Browser/wwwtax.cgi?id=54734) and the sequences from trypsin, keratin and the yeast enolase that was spiked into the samples. This resulted in a highly redundant database for tomato and *C. fulvum* and therefore, the total database was analyzed with BLAST (Altschul *et al.*, 1990) to align similar sequences. From sequences with 100% homology, only the longest sequence was retained in the database. Eventually, the LycoperCladoV3 database consisted of 40,183 sequences.

LC-MS/MS^E analysis and protein identification

An aliquot of 100 µg of the apoplastic protein samples from stages R_B, R_C, R_D, S_B, S_C and S_D (Table I) from one of the inoculation series was digested with trypsin (Promega), desalted, freeze-dried and dissolved in 100 µl of 0.1% TFA, 5% ACN in H_2O (v/v/v). The samples were analyzed in triplicate, resulting in 6 x 3 LC-MS/MS^E runs, according to the following protocol. An aliquot of 0.5 µg of trypsin-digested apoplastic protein, spiked with 100 fmol of digested yeast enolase as internal quantification standard, was used for LC-

MS/MS analysis. Tryptic peptides were separated on a NanoAcquity LC system (Waters Corporation, Milford USA) with a Symmetry C18 precolumn (5 µm particle size, 5 mm x 300 µm internal diameter) and an Atlantis C18 analytical reversed phase column (3 µm particle size, 15 cm x 75 µm internal diameter (Waters Corporation)). Peptides were transferred to the precolumn in solution A (0.1% FA (v/v) in H_2O) with a flow rate of 4 µl/min. Sequential elution of peptides was accomplished in 90 minutes using a linear gradient of 3% (v/v) of solution B (0.1% FA (v/v) in ACN) to 40% (v/v) of solution B in solution A, with a flow rate of 300 nl/minute. Subsequently, the columns were rinsed for ten minutes with 90% (v/v) of solution B in solution A and equilibrated with solution A for 20 minutes, after which the next sample was loaded. During analysis, the column temperature was maintained at 35°C. Upon elution, peptides were injected into a Q-TOF Premier mass spectrometer (Waters, Manchester, UK) that operated in the V-mode with a resolving power of at least 10,000 full-width half maximum (FWHM) and in the positive electronspray ionisation (ESI) mode. The TOF analyzer was externally calibrated with a NaI mixture from m/z 50 to 1990. The data were post-acquisition lock mass corrected using the monoisotopic mass of the doubly charged precursor of [Glu^1]-Fibrinopeptide B, which was delivered with a constant flow rate of 200 nL/min through the reference sprayer of the NanoLockSpray source of the mass spectrometer and sampled with 30 sec intervals. LC-MS/MS data were collected during alternating low energy modes with a constant collision energy of 4 eV and high collision energy modes with a ramping collision energy from 15 eV to 40 eV. The spectral acquisition time was 1.5 seconds with an interscan delay of 0.1 seconds which resulted in a data collection cycle of 3.2 seconds (Bateman *et al.*, 2002). The radio frequency (RF) allowed only ions with m/z 300 to 2,000 to enter the quadrupole mass analyzer, which ensured that ions with m/z smaller than 300 originated from dissociations in the source of the collision cell.

Accurate masses and retention times (RT) were obtained in the low energy mode, whereas sequence information from the eluting peptides was obtained in the high energy mode. To increase the number of sequenced peptides, additional data-dependent acquisition (DDA) experiments were performed with include lists of peptides that had an altered abundance between the samples in the above described analysis. A maximum of 5 parent ions was selected per MS scan with a dynamic exclusion of 120 sec. Eventually, all datasets were processed against the LycoperCladoV3 database using the ion accounting algorithm (IAA) in ProteinLynx Global Server (V2.3, Waters, Millford USA). The following constraints were

used: low energy threshold 250 counts, elevated energy threshold 100 counts, lock mass window of 0.5 Da, intensity threshold of 1,000 and an automatic TOF resolution. Peptides that were quantified in all 18 runs and have a peptide score > 50 were taken along for further analysis. Apoplastic proteins identified based on at least two peptides with a score > 50, of which at least one is non-redundant, are reported (Table IV). The number of peptides that identified the protein, the highest peptide score, the protein score and the sequence coverage (%) are reported in Table IV. Subcellular protein localization was predicted by MultiLoc (Höglund *et al.*, 2006) and manually validated.

Protein quantification and data analysis

For quantitative analysis, the data were processed in ProteinLynx Global Server (V2.3, Waters, Millford USA) using the peak clustering algorithm that results in an experimental mass retention time (RT) pair (EMRT) table in which all quantitative data are collected. EMRT data were processed with the post alignment clustering procedure (PACP) to correct peak repeats within 10 mDa in multiple alignments (De Groot *et al.*, 2008). Quantitative data from the EMRT table were matched to peptide identifications from the IAA based on peptide mass (Δmass < 0.01) and RT (ΔRT < 2 min). Peptides with a RT of more than 57 min were not used for quantification since a high intensity peak caused by the detergent CHAPS eluting from the column after this RT. Peptide identifications from the DDA experiments were not matched to the EMRT data since these experiments were not performed in series and therefore, the RT deviated too much. Data were normalized based on the intensities of the yeast enolase internal standard peptides that were quantified in all 18 LC-MS/MS runs. Non-redundant peptides quantified in 17 or 18 of the LC-MS/MS runs were used for protein quantification. Peptides that match a protein from *C. fulvum* had to be quantified in at least the triplicate runs of S_C and S_D. The number of peptides used for quantification, including the highest peptide score, is reported in Table IV. The average peptide intensity was obtained from the triplicate runs and the total intensity of one or more non-redundant peptides per protein was used for quantification. Total intensities of the technical replicates were very similar, indicating that the replicates were very reproducible (America *et al*, data not shown). The PCA plot was made in GeneMaths (Applied Maths).

Microarray experiments and further analysis

Total RNA was extracted and purified (NucleoSpin RNA/Protein kit, Machery-Nagel, GmbH & Co., Dueren, Germany) from leaflets of transgenic MM-Cf0:*Hcr9-4D* (Cf-4; resistant) and MM-Cf0:*Avr4* (susceptible) tomato plants, inoculated with a race 5 strain of *C. fulvum* producing Avr4, which were harvested at stages R_A, R_B, R_C, S_A, S_B and S_C (Table I). Three biological replicates were performed. Hybridization of the microarrays (Affymetrix GeneChip® Tomato Gene Array) and subsequent data analysis was similar to the procedure described for the microarray analysis of the Cf-4/Avr4 seedlings (Chapter 4). For the latter, RNA was obtained from Cf-4/Avr4 and control (a mixture of the parental lines) seedlings. These Cf-4/Avr4 seedlings result from a cross between the above mentioned MM-Cf0:*Hcr9-4D* and MM-Cf0:*Avr4* tomato plants. At 20°C, they develop a constitutive HR soon after germination, which can be suppressed at 33°C and 100% relative humidity. After a subsequent shift from 33°C to 20°C, a synchronized HR is induced which allows the collection of leaf material at several stages after HR initiation (De Jong *et al.*, 2002; Gabriëls *et al.*, 2006; Chapter 3).

ACKNOWLEDGEMENTS

The authors would like to thank Froukje van der Wal for assistance with DIGE-2DE analysis and Joost de Groot for providing the non-redundant LycoperCladoV3 database.

REFERENCES

Altschul SF, Gish W, Miller W, Myers EW, Lipman DJ (1990) Basic local alignment search tool. J Mol Biol 215: 403-410.

Asselbergh B, Curvers K, Franca SC, Audenaert K, Vuylsteke M, Van Breusegem F, Höfte M (2007) Resistance to *Botrytis cinerea* in *sitiens*, an abscisic acid-deficient tomato mutant, involves timely production of hydrogen peroxide and cell wall modifications in the epidermis. Plant Physiol 144: 1863-1877.

Bailey B, Bae H, Strem M, Roberts D, Thomas S, Crozier J, Samuels G, Choi I-Y, Holmes K (2006) Fungal and plant gene expression during the colonization of cacao seedlings by endophytic isolates of four *Trichoderma* species. Planta 224: 1449-1464.

Bateman RH, Carruthers R, Hoyes JB, Jones C, Langridge JI, Millar A, Vissers JPC (2002) A novel precursor ion discovery method on a hybrid quadrupole orthogonal acceleration time-of-flight (Q-TOF) mass spectrometer for studying protein phosphorylation. J Am Soc Mass Spectrom 13: 792-803.

Bittel P, Robatzek S (2007) Microbe-associated molecular patterns (MAMPs) probe plant immunity. Curr Opin Plant Biol 10: 335-341.

Bolton MD, Van Esse HP, Vossen JH, De Jonge R, Stulemeijer IJE, Stergiopoulos I, Van den Berg GCM, Borras-Hidalgo O, Dekker HL, De Koster CG, De Wit PJGM, Joosten MHAJ, Thomma BPHJ (2008) The novel *Cladosporium fulvum* lysine motif effector Ecp6 is a virulence factor with orthologs in other fungal species. Mol Microbiol: accepted for publication.

Boudart G, Jamet E, Rossignol M, Lafitte C, Borderies G, Jauneau A, Esquerré-Tugayé M-T, Pont-Lezica R (2005) Cell wall proteins in apoplastic fluids of *Arabidopsis thaliana* rosettes: Identification by mass spectrometry and bioinformatics. Proteomics 5: 212-221.

Chrost B, Kolukisaoglu U, Schulz B, Krupinska K (2007) An α-galactosidase with an essential function during leaf development. Planta 225: 311-320.

Dani V, Simon WJ, Duranti M, Croy RRD (2005) Changes in the tobacco leaf apoplast proteome in response to salt stress. Proteomics 5: 737-745.

De Groot JCW, Fiers MWEJ, Van Ham RCHJ, America AHP (2008) Post alignment clustering procedure for comparative quantitative proteomics LC-MS data. Proteomics 8: 32-36.

De Jong CF, Takken FLW, Cai X, De Wit PJGM, Joosten MHAJ (2002) Attenuation of Cf-mediated defense responses at elevated temperatures correlates with a decrease in elicitor-binding sites. Mol Plant-Microbe Interact 15: 1040-1049.

De Wit PJGM (1977) A light and scanning-electron microscopic study of infection of tomato plants by virulent and avirulent races of *Cladosporium fulvum*. Neth J Plant Pathol 83: 109-122.

De Wit PJGM (1992) Molecular characterization of gene-for-gene systems in plant-fungus interactions and the application of avirulence genes in control of plant pathogens. Annu Rev Phytopathol 30: 391-418.

De Wit PJGM (2007) How plants recognize pathogens and defend themselves. Cell Mol Life Sci 64: 2726-2732.

De Wit PJGM, Van der Meer FE (1986) Accumulation of the pathogenesis-related tomato leaf protein P14 as an early indicator of incompatibility in the interaction between *Cladosporium fulvum* (syn. *Fulvia fulva*) and tomato. Physiol Mol Plant Pathol 29: 159-172.

Deepak S, Shailasree S, Kini R, Hause B, Shetty S, Mithöfer A (2007) Role of hydroxyproline-rich glycoproteins in resistance of pearl millet against downy mildew pathogen *Sclerospora graminicola*. Planta 226: 323-333.

Dixon RA (2001) Natural products and plant disease resistance. Nature 411: 843-847.

Ferreira RB, Monteiro S, Freitas R, Santos CN, Chen Z, Batista LM, Duarte J, Borges A, Teixeira AR (2007) The role of plant defence proteins in fungal pathogenesis. Mol Plant Pathol 8: 677-700.

Ficke A, Gadoury DM, Seem RC, Godfrey D, Dry IB (2004) Host barriers and responses to *Uncinula necator* in developing grape berries. Phytopathology 94: 438-445.

Flor HH (1942) Inheritance of pathogenicity in *Melampsora lini*. Phytopathology 32: 653-669.

Gabriëls SHEJ, Takken FLW, Vossen JH, De Jong CF, Liu Q, Turk SCHJ, Wachowski LK, Peters J, Witsenboer HMA, De Wit PJGM, Joosten MHAJ (2006) cDNA-AFLP combined with functional analysis reveals novel genes involved in the hypersensitive response. Mol Plant-Microbe Interact 19: 567-576.

Gómez-Gómez L, Boller T (2000) FLS2: an LRR receptor-like kinase involved in the perception of the bacterial elicitor flagellin in Arabidopsis. Mol Cell 5: 1003-1011.

Greenbaum D, Colangelo C, Williams K, Gerstein M (2003) Comparing protein abundance and mRNA expression levels on a genomic scale. Genome Biol 4: 117.111-117.118.

Hao L, Hsiang T, Goodwin PH (2006) Role of two cysteine proteinases in the susceptible response of *Nicotiana benthamiana* to *Colletotrichum destructivum* and the hypersensitive response to *Pseudomonas syringae* pv. *tomato*. Plant Science 170: 1001-1009.

He P, Shan L, Sheen J (2007) Elicitation and suppression of microbe-associated molecular pattern-triggered immunity in plant-microbe interactions. Cell Microbiol 9: 1385-1396.

Höglund A, Dönnes P, Blum T, Adolph H-W, Kohlbacher O (2006) MultiLoc: prediction of protein subcellular localization using N-terminal targeting sequences, sequence motifs and amino acid composition. Bioinformatics 22: 1158-1165.

Johnson KL, Jones BJ, Bacic A, Schultz CJ (2003) The fasciclin-like arabinogalactan proteins of Arabidopsis. A multigene family of putative cell adhesion molecules. Plant Physiol 133: 1911-1925.

Jones JDG, Dangl JL (2006) The plant immune system. Nature 444: 323-329.

Joosten MHAJ, Bergmans CJB, Meulenhoff EJS, Cornelissen BJC, De Wit PJGM (1990a) Purification and serological characterization of three basic 15-kilodalton pathogenesis-related proteins from tomato. Plant Physiol 94: 585-591.

Joosten MHAJ, De Wit PJGM (1989) Identification of several pathogenesis-related proteins in tomato leaves inoculated with *Cladosporium fulvum* (syn. *Fulvia fulva*) as 1,3-ß-glucanases and chitinases. Plant Physiol 89: 945-951.

Joosten MHAJ, De Wit PJGM (1999) The tomato-*Cladosporium fulvum* interaction: A versatile experimental system to study plant-pathogen interactions. Annu Rev Phytopathol 37: 335-367.

Joosten MHAJ, Hendrickx LJM, De Wit PJGM (1990b) Carbohydrate composition of apoplastic fluids isolated from tomato leaves inoculated with virulent or avirulent races of *Cladosporium fulvum* (syn. *Fulvia fulva*). Neth J Plant Pathol 96: 103-112.

Joosten MHAJ, Verbakel HM, Nettekoven ME, Van Leeuwen J, Van der Vossen RT, De Wit PJGM (1995) The phytopathogenic fungus *Cladosporium fulvum* is not sensitive to the chitinase and ß-1,3-glucanase defence proteins of its host, tomato. Physiol Mol Plant Pathol 46: 45-59.

Joosten MHAJ, Vogelsang R, Cozijnsen TJ, Verberne MC, De Wit PJGM (1997) The biotrophic fungus *Cladosporium fulvum* circumvents Cf-4-mediated resistance by producing unstable AVR4 elicitors. Plant Cell 9: 367-379.

Jorda L, Coego A, Conejero V, Vera P (1999) A genomic cluster containing four differentially regulated subtilisin-like processing protease genes is in tomato plants. J Biol Chem 274: 2360-2365.

Jorda L, Vera P (2000) Local and systemic induction of two defense-related subtilisin-like protease promoters in transgenic Arabidopsis plants. Luciferin induction of PR gene expression. Plant Physiol. 124: 1049-1058.

Kavroulakis N, Papadopoulou KK, Ntougias S, Zervakis GI, Ehaliotis C (2006) Cytological and other aspects of pathogenesis-related gene expression in tomato plants grown on a suppressive compost. Ann Bot 98: 555-564.

Lamb C, Dixon RA (1997) The oxidative burst in plant disease resistance. Annu Rev Plant Biol 48: 251-275.

Laugé R, Goodwin PH, De Wit PJGM, Joosten MHAJ (2000) Specific HR-associated recognition of secreted proteins from *Cladosporium fulvum* occurs in both host and non-host plants. Plant J 23: 735-745.

Laugé R, Joosten MHAJ, Van den Ackerveken GFJM, Van den Broek HWJ, De Wit PJGM (1997) The *in planta*-produced extracellular proteins ECP1 and ECP2 of *Cladosporium fulvum* are virulence factors. Mol Plant-Microbe Interact 10: 725-734.

Liu J-J, Ekramoddoullah AKM (2006) The family 10 of plant pathogenesis-related proteins: their structure, regulation, and function in response to biotic and abiotic stresses. Physiol Mol Plant Pathol 68: 3-13.

McGee JD, Hamer JE, Hodges TK (2001) Characterization of a PR-10 pathogenesis-related gene family induced in rice during infection with *Magnaporthe grisea*. Mol Plant-Microbe Interact 14: 877-886.

Neuhaus J-M, Rogers JC (1998) Sorting of proteins to vacuoles in plant cells. Plant Mol Biol 38: 127-144.

Park CJ, An JM, Shin YC, Kim KJ, Lee BJ, Paek KH (2004) Molecular characterization of pepper germin-like protein as the novel PR-16 family of pathogenesis-related proteins isolated during the resistance response to viral and bacterial infection. Planta 219: 797-806.

Pelloux J, Rusterucci C, Mellerowicz EJ (2007) New insights into pectin methylesterase structure and function. Trends Plant Sci 12: 267-277.

Rico A, Preston GM (2008) *Pseudomonas syringae* pv. *tomato* DC3000 uses constitutive and apoplast-induced nutrient assimilation pathways to catabolize nutrients that are abundant in the tomato apoplast. Mol Plant-Microbe Interact 21: 269-282.

Rivas S, Thomas CM (2005) Molecular interactions between tomato and the leaf mold pathogen *Cladosporium fulvum*. Annu Rev Phytopathol 43: 395-436.

Rooney HCE, Van 't Klooster JW, Van der Hoorn RAL, Joosten MHAJ, Jones JDG, De Wit PJGM (2005) Cladosporium Avr2 inhibits tomato Rcr3 protease required for *Cf-2*-dependent disease resistance. Science 308: 1783-1786.

Schultz C, Gilson P, Oxley D, Youl J, Bacic A (1998) GPI-anchors on arabinogalactan-proteins: implications for signalling in plants. Trends Plant Sci 3: 426-431.

Seifert GJ, Roberts K (2007) The biology of arabinogalactan proteins. Annu Rev Plant Biol 58: 137-161.

Shevchenko A, Wilm M, Vorm O, Mann M (1996) Mass spectrometric sequencing of proteins silver-stained polyacrylamide gels. Anal Chem 68: 850-858.

Sun W, Zhao ZD, Hare MC, Kieliszewski MJ, Showalter AM (2004) Tomato LeAGP-1 is a plasma membrane-bound, glycosylphosphatidylinositol-anchored arabinogalactan-protein. Physiol Plant 120: 319-327.

Thomma BPHJ, Van Esse HP, Crous PW, De Wit PJGM (2005) *Cladosporium fulvum* (syn. *Passalora fulva*), a highly specialized plant pathogen as a model for functional studies on plant pathogenic Mycosphaerellaceae. Mol Plant Pathol 6: 379-393.

Tian M, Benedetti B, Kamoun S (2005) A second kazal-like protease inhibitor from *Phytophthora infestans* inhibits and interacts with the apoplastic pathogenesis-related protease P69B of tomato. Plant Physiol 138: 1785-1793.

Tian M, Huitema E, Da Cunha L, Torto-Alalibo T, Kamoun S (2004) A kazal-like extracellular serine protease inhibitor from *Phytophthora infestans* targets the tomato pathogenesis-related protease P69B. J Biol Chem 279: 26370-26377.

Tian M, Win J, Song J, Van der Hoorn RAL, Van der Knaap E, Kamoun S (2007) A *Phytophthora infestans* cystatin-like protein targets a novel tomato papain-like apoplastic protease. Plant Physiol 143: 364-377.

Tornero P, Conejero V, Vera P (1994) A gene encoding a novel isoform of the PR-1 protein family from tomato is induced upon viroid infection. Mol Gen Genet 243: 47-53.

Tornero P, Gadea J, Conejero V, Vera P (1997) Two *PR-1* genes from tomato are differentially regulated and reveal a novel mode of expression for a pathogenesis-related gene during the hypersensitive response and development. Mol Plant-Microbe Interact 10: 624-634.

Truman W, Zabala MT, Grant M (2006) Type III effectors orchestrate a complex interplay between transcriptional networks to modify basal defence responses during pathogenesis and resistance. Plant J 46: 14-33.

Ursin VM, Bradford KJ (1989) Auxin and ethylene regulation of petiole epinasty in two developmental mutants of tomato, *diageotropica* and *epinastic*. Plant Physiol 90: 1341-1346.

Van Baarlen P, Woltering EJ, Staats M, Van Kan JAL (2007) Histochemical and genetic analysis of host and non-host interactions of Arabidopsis with three *Botrytis* species: an important role for cell death control. Mol Plant Pathol 8: 41-54.

Van den Ackerveken G, Dunn RM, Cozijnsen AJ, Vossen JP, Van den Broek HW, De Wit PJGM (1994) Nitrogen limitation induces expression of the avirulence gene *Avr9* in the tomato pathogen *Cladosporium fulvum*. Mol Gen Genet 243: 277-285.

Van den Ackerveken G, Van Kan JAL, Joosten MHAJ, Muisers JM, Verbakel HM, De Wit PJGM (1993) Characterization of two putative pathogenicity genes of the fungal tomato pathogen *Cladosporium fulvum*. Mol Plant-Microbe Interact 6: 210-215.

Van den Burg HA, Harrison SJ, Joosten MHAJ, Vervoort J, De Wit PJGM (2006) *Cladosporium fulvum* Avr4 protects fungal cell walls against hydrolysis by plant chitinases accumulating during infection. Mol Plant-Microbe Interact 19: 1420-1430.

Van Esse HP, Bolton MD, Stergiopoulos I, De Wit PJGM, Thomma BPHJ (2007) The chitin-binding *Cladosporium fulvum* effector protein Avr4 is a virulence factor. Mol Plant-Microbe Interact 20: 1092-1101.

Van Kan JAL, Joosten MHAJ, Wagemakers CAM, Van den Berg-Velthuis GCM, De Wit PJGM (1992) Differential accumulation of mRNAs encoding extracellular and intracellular PR proteins in tomato induced by virulent and avirulent races of *Cladosporium fulvum*. Plant Mol Biol 20: 513-527.

Van Loon LC, Rep M, Pieterse CMJ (2006) Significance of inducible defense-related proteins in infected plants. Ann Rev Phytopathol 44: 135-162.

Van Loon LC, Van Strien EA (1999) The families of pathogenesis-related proteins, their activities, and comparative analysis of PR-1 type proteins. Physiol Mol Plant Pathol 55: 85-97.

Vera P, Tornero P, Conejero V (1993) Cloning and expression analysis of a viroid-induced peroxidase from tomato plants. Mol Plant-Microbe Interact 6: 490-794.

Wei GUO, Shirsat AH (2006) Extensin over-expression in Arabidopsis limits pathogen invasiveness. Mol Plant Pathol 7: 579-592.

Whiteford JR, Spanu PD (2002) Hydrophobins and the interactions between fungi and plants. Mol Plant Pathol 3: 391-400.

Wubben JP, Joosten MHAJ, Van Kan JAL, De Wit PJGM (1992) Subcellular localization of plant chitinases and 1,3-ß-glucanases in *Cladosporium fulvum* (syn. *Fulvia fulva*)-infected tomato leaves. Physiol Mol Plant Pathol 41: 23-32.

Zimmermann G, Baumlein H, Mock H-P, Himmelbach A, Schweizer P (2006) The multigene family encoding germin-like proteins of barley. Regulation and function in basal host resistance. Plant Physiol 142: 181-192.

SUPPLEMENTARY DATA

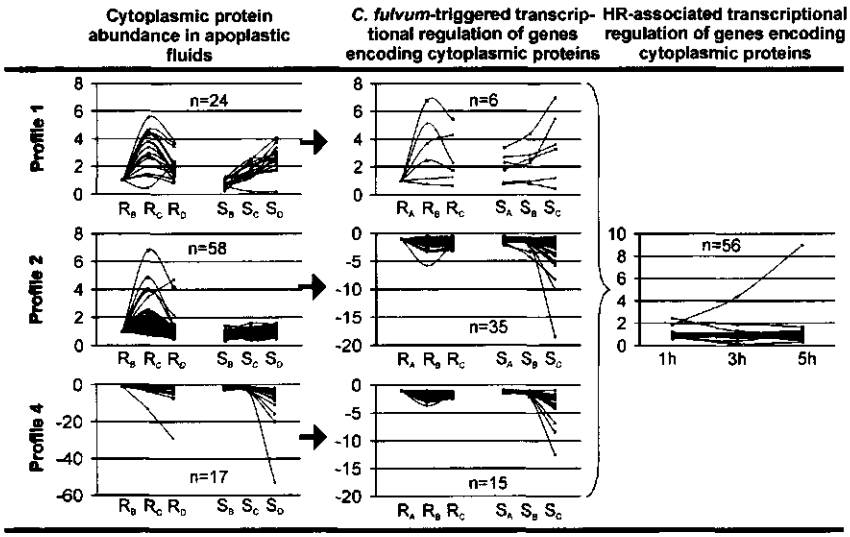

Supplementary Figure S1. The relation between apoplastic contamination by cellular proteins and transcriptional regulation of the encoding genes.

Abundance patterns of cytoplasmic proteins identified and quantified by LC-MS/MS^E in AF obtained at stages B to D from resistant and susceptible plants inoculated with *C. fulvum*, are classified into Profiles 1, 2 and 4 (left graphs). Patterns of Profiles 1 and 2 are similar to the patterns of Profiles 1 and 2 of the genuine apoplastic proteins while Profile 4 was not found for apoplastic proteins (Figure 6). Approximately 60% of the encoding genes are present on the Affymetrix tomato microarray and transcriptional regulation of these genes was studied at stages A, B and C in resistant and susceptible plants inoculated with *C. fulvum* (middle graphs). In addition, microarrays were hybridized with RNA isolated from Cf-4/Avr4 tomato seedlings that execute a synchronized hypersensitive response (HR). In this case, transcriptional regulation of the genes encoding the quantified cellular proteins was determined at 1, 3 and 5 hours after the HR initiation (right graphs; see Supplementary Table I for protein identifications).

Supplementary Table S1. Cellular proteins identified as contaminants in the apoplastic proteins samples.

#	Annotation	# peptides for ID	Highest peptides score	Protein score	Sequence coverage %	# peptides for quantification	Highest peptide score[a]	Acc. Profile
1	Pathogenesis-related protein 10 - Solanum virginianum	8	126	374	70	5		1
2	Putative aminotransferase - Oryza sativa subsp. Japonica	5	82	495	46	1		1
3	NADH-ubiquinone oxidoreductase 17.8 kD subunit	3	58	143	32	1		1
4	Peptidyl-prolyl cis-trans isomerase, chloroplast precursor - Spinacia oleracea	3	56	168	38	3		1
5	F11F12.2 protein - Arabidopsis thaliana	5	56	197	11	1		1
6	Enolase	16	291	1246	61	14		1
7	Ubiquitin	7	59	316	76	1		1
8	Plastidic aldolase - Nicotiana paniculata	2	52	199	39	2		1
9	Glutamine synthetase - Nicotiana plumbaginifolia	4	140	340	32	3		1
10	Presequence protease 1, chloroplast/mitochondrial precursor - Arabidopsis thaliana	3	53	554	19	7		1
11	Chromosome 05 contig 1, DNA sequence - Ostreococcus tauri	4	51	213	67	1		1
12	Glutathione S-transferase, class-phi [Solanum commersonii]	6	97	249	54	2		1
13	PR-2; Basic beta-1,3-glucanase	13	295	1261	53	5		1
14	Photosystem II oxygen-evolving complex protein 3 precursor	8	70	438	36	2		1
15	Mitochondrial malate dehydrogenase	9	119	618	43	1	49	2
16	Malate dehydrogenase	7	290	421	28	2		2
17	LEXYL2	19	290	1776	47	2		2
18	Pathogenesis-related protein	8	60	1132	78	1		2
19	polyphenoloxidase; P2	10	70	664	32	1		2
20	ADP-glucose pyrophosphorylase large subunit	2	75	414	32	1		2
21	Alpha-mannosidase - Arabidopsis thaliana	7	119	307	40	5	119	2
22	Aminotransferase 2 - Cucumis melo	13	103	1156	64	2		2
23	Aminotransferases class-I pyridoxal-phosphate-binding site - Medicago truncatula	7	67	393	20	2		2
24	Carbonic anhydrase	9	124	653	43	1		2
25	Carboxypeptidase type III	3	55	320	20	1		2
26	Chaperonin 21 precursor	3	67	232	33	1	65	2
27	Chaperonin-60 beta subunit precursor - Solanum tuberosum	8	61	433	43	5		2
28	Chloroplast HSP70 - Cucumis sativus	24	110	944	38	7		2
29	Cucumisin-like serine protease - Arabidopsis thaliana	4	56	469	28	2		2
30	Cytosolic cysteine synthase - Solanum tuberosum	9	61	379	48	2		2
31	FER1	6	277	437	33	2		2
32	Ferredoxin--NADP reductase - Nicotiana tabacum	11	63	1148	50	1		2
33	Glycine dehydrogenase - Solanum tuberosum	4	134	282	40	4		2
34	Glycine dehydrogenase - Solanum tuberosum	20	234	1325	37	9		2
35	Glycolate oxidase - Brassica napus	19	174	1966	62	3		2
36	H-Protein - Flaveria pringlei	4	114	268	40	2		2
37	Hypothetical protein - Solanum tuberosum	8	65	518	46	3		2
38	Hypothetical protein - Streptococcus agalactiae	9	101	639	61	1		2
39	Hypothetical protein - Trifolium pratense	7	81	543	35	5		2
40	Hypothetical sodium:dicarboxylate symporter - Photobacterium profundum	3	56	219	54	1		2
41	Inorganic pyrophosphatase - Medicago truncatula	6	66	293	32	2		2
42	Inorganic pyrophosphatase - Medicago truncatula	5	54	302	36	1		2
43	LEXYL1 protein	4	250	680	62	1		2
44	NADP-dependent glyceraldehyde-3-phosphate dehydrogenase - Nicotiana plumbaginifolia	2	74	333	16	2		2
45	Os06g0650100 protein - Oryza sativa subsp. Japonica	6	81	326	36	1		2
46	Phosphoenolpyruvate carboxylase 1 - Gossypium hirsutum	8	87	478	23	3		2

#	Annotation	# peptides for ID	Highest peptides core	Protein score	Sequence coverage %	# peptides for quantification	Highest peptide score[a]	Profile
47	Phosphoglycerate kinase - Solanum tuberosum	13	67	1441	43	3		2
48	Phosphoglycerate kinase - Solanum tuberosum	10	128	819	67	2		2
49	Phosphoglycerate mutase - Solanum tuberosum	5	98	280	36	1		2
50	Plastocyanin, chloroplast precursor	3	214	723	77	1		2
51	Protease-associated PA - Medicago truncatula	3	80	311	27	1		2
52	Protein At1g09340, chloroplast precursor - Arabidopsis thaliana	22	214	1267	55	15		2
53	PSBP	9	117	604	45	3		2
54	Putative peptidylprolyl isomerase - Oryza sativa subsp. Japonica	11	268	738	50	3		2
55	Putative rubisco subunit binding-protein alpha subunit - Trifolium pratense	6	64	571	34	2		2
56	Putative thioredoxin m2 - Pisum sativum	5	128	328	66	8		2
57	Ribosome recycling factor - Spinacia oleracea	3	150	272	35	3		2
58	Serine carboxipeptidase - Cicer arietinum	6	197	512	92	6		2
59	Serine hydroxymethyltransferase - Solanum tuberosum	13	183	752	51	3		2
60	Thioredoxin M-type - Brassica napus	5	81	257	44	3		2
61	Thioredoxin peroxidase - Nicotiana tabacum	4	343	887	43	4		2
62	Transketolase, chloroplast precursor - Solanum tuberosum	25	199	2003	52	4		2
63	Transketolase, chloroplast precursor - Solanum tuberosum	7	117	590	59	1		2
64	Triose phosphate isomerase cytosolic isoform-like - Solanum tuberosum	9	119	698	46	4		2
65	Triosephosphate isomerase - Spinacia oleracea	9	170	622	44	6		2
66	UTP:alpha-D-glucose-1-phosphate uridylyltransferase - Solanum tuberosum	9	60	379	32	2		2
67	Ribulose bisphosphate carboxylase large chain	24	226	4303	63	3		4
68	Plastidic aldolase NPALDP1 - *Nicotiana paniculata*	10	167	866	46	2		4
69	Ribulose bisphosphate carboxylase small chain 3B	5	83	926	71	2		4
70	Ribulose bisphosphate carboxylase large chain precursor	24	83	1382	32	1		4
71	Ribulose bisphosphate carboxylase/oxygenase activase - Solanum pennellii	4	56	553	15	1		4
72	Phosphoribulokinase (Hypothetical protein) - Oryza sativa subsp. Indica	13	165	1180	58	3	136	4
73	Ribulose bisphosphate carboxylase small chain 3B	4	52	966	50	1		4
74	LEXYL2 protein (Fragment) - Solanum lycopersicum	22	132	1789	46	5		4
75	Fructose-1,6-bisphosphatase (EC 3.1.3.11) - Solanum tuberosum	10	157	595	36	1	102	4
76	Ferredoxin–NADP reductase, leaf-type isozyme - Nicotiana tabacum	5	61	397	34	3		4
77	Sedoheptulose-1,7-bisphosphatase - Spinacia oleracea	17	198	794	37	6		4
78	Glutamate synthase (Ferredoxin) - Nicotiana tabacum	21	79	996	50	2		4
79	HAD-superfamily hydrolase, subfamily IIA - Medicago truncatula	9	76	597	54	4		4
80	mRNA binding protein precursor	10	61	603	60	2		4
81	Ribulose-phosphate 3-epimerase - Solanum tuberosum	5	250	775	38	3		4
82	Fructose-bisphosphate aldolase - Glycine max	9	146	500	53	2		4
83	Glyceraldehyde-3-phosphate dehydrogenase B subunit - Glycine max	4	66	199	16	1		4
84	Glyceraldehyde-3-phosphate dehydrogenase A - Nicotiana tabacum	4	52	232	29	1		4
85	Hypothetical protein - Medicago truncatula	5	103	254	22	4		4
86	Phosphoglycerate kinase-like - Solanum tuberosum	12	133	923	49	5		4
87	Methionine synthase - Solanum tuberosum	12	396	872	31	1		4
88	Glycolate oxidase	14	57	1455	74	2		4

a The highest peptide score is only reported when different from the highest peptide score for protein identification.

Chapter 6

Summarizing discussion

SUMMARIZING DISCUSSION

Temperature-sensitivity of the HR in Cf-4/Avr4 seedlings

Most work described in this thesis has been performed employing Cf-4/Avr4 seedlings. These seedlings originating from seeds obtained from a cross between transgenic tomato line expressing the *Cf-4* resistance gene and a transgenic tomato line expressing *Avr4*, a gene which originates from *Cladosporium fulvum*. Upon incubation of the seedlings at 33°C and 100% relative humidity, the hypersensitive response (HR) is suppressed and a synchronized HR can be induced by a temperature shift of the plants from 33°C to 20°C (De Jong *et al.*, 2002). Temperature sensitivity is not unique for the Cf-4 response, since also Cf-9 (De Jong *et al.*, 2002) and Cf-2 (unpublished data) mediated defence responses are suppressed at elevated temperatures. Furthermore, the NB-LRR resistance protein N of tobacco providing resistance to Tobacco Mosaic Virus (TMV), is also temperature-sensitive (Whitham *et al.*, 1994). However, the molecular basis of this temperature sensitivity remains unclear.

Heat-shock proteins are temperature-sensitive molecular chaperones that, amongst others, assist in protein folding to prevent the accumulation of miss-folded proteins in the cell (Sangster and Queitsch, 2005). An intriguing genetic study in *Drosophila* showed that Hsp90 buffers the genetic variation of proteins and that this buffering capacity was released by elevated temperatures. In addition, heat stress enhances the phenotypes of heterozygous *Hsp90* mutants that display multiple phenotypes caused by the expression of genetically altered proteins, which are normally covered by the buffering capacity of Hsp90 (Rutherford and Lindquist, 1998). A similar observation has been done in Arabidopsis, in which reduced Hsp90 levels and elevated growth temperatures synergistically affect several phenotypes (Sangster *et al.*, 2007). In plants, it has become apparent that Hsp90 plays a crucial role in R protein-mediated defence signalling and Hsp90 has been related to N, RPM1, Rx, I-2 and Cf-4 function, which are resistance proteins that confer resistance to TMV, *Pseudomonas syringae*, potato virus X, *Fusarium oxysporum* and *C. fulvum*, respectively (Sangster and Queitsch, 2005; Gabriëls *et al.*, 2006). Also R proteins harbour a high degree of sequence polymorphism, probably as a result of selection pressure imposed by new variants of a pathogen, and these polymorphisms may lead to unstable proteins under normal conditions (Rose *et al.*, 2004; Kruijt *et al.*, 2005b). Therefore, Hsp90 is hypothesized to stabilize polymorphic R proteins to retain these altered proteins and allow positive selection during

evolutionary adaptation in the battle between plants and their pathogens (Sangster and Queitsch, 2005). Indeed, Hsp90 interacts with the LRR domain of both the N and I-2 protein (Liu *et al.*, 2004; De la Fuente van Bentem *et al.*, 2005). Furthermore it was found that loss of Hsp90 from the R protein complex leads to instability and subsequent degradation of Rx and RPM1 (Sangster and Queitsch, 2005; Botër *et al.*, 2007). Upon heat stress, Hsp90 binds to many cellular proteins to prevent their unfolding and to maintain cellular functioning, which causes a massive demand on Hsp90. This probably induces diversion of Hsp90 from the R proteins, resulting in R protein degradation and inhibition of R protein-mediated signalling (Rutherford and Lindquist, 1998). This hypothesis is confirmed by studies with the Hsp90-binding inhibitors geldanamycin and radicicol that both induce similar phenotypes as observed when exposed to heat stress (Rutherford and Lindquist, 1998; Yamada *et al.*, 2007). The increased requirement for Hsp90 proteins to maintain cellular functions would also explain heat-shock-related transcriptional activation of *Hsp90-1* (Krishna and Gloor, 2001).

The above described hypothesis for malfunctioning of R proteins at elevated temperatures is valid for intracellularly localized R proteins. However, Cfs are plasma membrane proteins that for the greater part are located extracellularly and lack a clear cytoplasmic signalling domain (Kruijt *et al.*, 2005a). Still, Hsp90 is required for the Cf-4/Avr4-mediated HR (Gabriëls *et al.*, 2006), and different isoforms of phosphorylated Hsp90 specifically change in abundance upon initiation of the Cf-4/Avr4-triggered HR (Chapter 4). The Cf-like receptor CLAVATA2 (CLV2) from Arabidopsis, which mediates cell proliferation and cell differentiation in the apical shoot meristem (Clark, 2001), forms a complex with the receptor-like kinase (RLK) CLV1 that harbours a cytoplasmic kinase domain and mediates downstream signalling upon direct binding of the CLV3 ligand (Ogawa *et al.*, 2008). Similarly, Cf proteins might form a complex with another plasma membrane-localized protein which is possibly an RLK that might also directly bind the Avr, since the Cf proteins do not seem to interact directly with their cognate avirulence factors (Avrs) (Joosten and De Wit, 1999). This putative Avr binding subsequently trigger downstream signalling into the cytoplasm. The Cf complex might be stabilized by Hsp90 through interaction with the cytoplasmic kinase domain of the RLK, thereby rendering it temperature-sensitive. The observation that Cf-4 tobacco cells need about 20 hours to completely loose their responsiveness to Avr4 after incubation at 33°C (De Jong *et al.*, 2002), suggests that a gradual release of Hsp90 from the R protein complex upon elevated temperatures is possible. Upon

relief of the heat stress, protein synthesis is required to restore defence. This is supported by the observation that the lost response to Avr4 is recovered in Cf-4 tobacco cells within 45 minutes, which is sufficient time for *de novo* protein synthesis of Cf-4 (De Jong *et al.*, 2002). Furthermore, this could imply that at elevated temperature Cf-mediated signalling is inhibited upstream, at the level of Avr perception. This is supported by the inhibition of Cf-4-mediated medium alkalization, which is one of the first responses of transgenic Cf-4 tobacco cell suspensions treated with Avr4, at elevated temperatures (De Jong *et al.*, 2002). In addition, the amount of the Avr9 high-affinity binding site (HABS) at the plasma membrane, which is hypothesized to be the (co-)receptor for Avr9, is reduced by 80% at elevated temperatures (De Jong *et al.*, 2002), which also confirms the temperature-sensitivity at the level of Avr perception. On the other hand, the hypothesis is contradicted by the already significantly different gene expression between the Cf-4/Avr4 and control seedlings at t=0h (33°C) (Gabriëls *et al.*, 2006; unpublished results). However, this might suggest that residual Hsp90 activity leads to a low level of signalling that does not reach the threshold to develop a HR. Another reason why Hsp90 is thought to stabilize the receptor complex is based on the observation that the short cytoplasmic tail of Cf-9 binds to vesicle-associated protein (VAP) 27, which is a VAP33-like protein (Laurent *et al.*, 2000). VAP33 is required for transport of proteins through the Golgi and has been shown to interact with Hsp90, which also plays an essential role in the secretory pathway (McClellan *et al.*, 2007; Richter *et al.*, 2007). In addition, it was shown that Cf-9 is functional in the plasma membrane, probably in association with one or more proteins that mask its ER retention signal (Van der Hoorn *et al.*, 2001). Therefore, the Cf-9 complex is delivered at the plasma membrane through the Golgi and possibly this complex consists of the Cf protein, an RLK, Hsp90 and VAP27.

Another possibility is that Hsp90 does not stabilize the receptor complex itself but a complex required for defence signalling further downstream in the pathway. Previously, a NB-LRR protein required for resistance to *C. fulvum* (NRC1) was found to be required for Cf-mediated signalling (Gabriëls *et al.*, 2006). NRC1 might, for example, interact with Hsp90 as described for I-2 and N, thereby rendering this complex temperature-sensitive, resulting in hampered Cf-mediated signalling when exposed to elevated temperatures. This hypothesis is supported by the observation that the Hsp90-interacting co-chaperones RAR1 and SGT1 (Takahashi *et al.*, 2003; Liu *et al.*, 2004) are required for the NRC1-induced HR, which places these proteins at the same level as NRC1 in a defence signalling cascade (Gabriëls *et al.*,

2007). Finally, it might also be possible that NRC1 is, together with Hsp90, part of a Cf/RLK-complex that stabilizes Cf-4, or that different isoforms of Hsp90 bind different complexes.

Cf-4/Avr4 seedlings as a model system for Cf-4-mediated HR and resistance

The Cf-4/Avr4 seedlings provide a very clean synchronized model system in which the HR can be induced without the interference of wound responses or artificial microbes such as *Agrobacterium tumefaciens*. Still, heat-shock-related stress signals might interfere with HR signalling in the Cf-4/Avr4 seedlings. However, the results of several experiments make this hypothesis unlikely. The mitogen-activated protein kinase (MAPK) activity assays described in Chapter 3 show that activation of LeMPK1, -2 and -3 at two hours after the temperature shift only occurs in the Cf-4/Avr4 seedlings and not in the control seedlings. In addition, elevated MAPK activity at t=0h in the Cf-4/Avr4 seedlings disappeared within 30 minutes after the temperature shift, indicating that the heat stress-related signals disappear during recovery at 20°C (Chapter 3). Furthermore, microarray analysis to study gene expression in the Cf-4/Avr4 and control seedlings revealed a slight decrease in the number of differentially expressed genes at t=1h (n=72) compared to t=0h (n=95), suggesting there is a recovery of the plants from possible heat stress within one hour. After this recovery, a massive transcriptional reprogramming occurrs upon HR-induction, since 408 differentially regulated genes were found at t=3h and 1616 at t=5h ($P \leq 0.01$; unpublished results). These results suggest that the Cf-4/Avr4 seedlings recover from the heat stress before the HR is initiated.

Protein phosphorylation is a very rapid and transient post-translational modification (PTM). Therefore, a very reproducible and synchronized biological system is required to study changes in the phosphoproteome. In Chapter 3, LeMPKs were described to be reproducibly activated after the temperature shift of the Cf-4/Avr4 seedlings and the activated kinases were subsequently shown to play a role in HR-development and resistance to *C. fulvum* in Cf-4 plants. In addition, several phosphopeptides were reproducibly identified with altered abundance in the Cf-4/Avr4 seedlings, which implies differential phosphorylation and subsequently altered activity of these proteins. These results pointed for example to a swift decrease in photosynthetic activity upon HR-initiation, an observation that was confirmed by chlorophyll fluorescence measurement in the Cf-4/Avr4 seedlings (Chapter 4). In addition, photosynthetic activity seemed to be decreased in resistant tomato plants inoculated with *C.*

fulvum, as was shown by the decreased abundance of cellular proteins involved in photosynthesis that contaminated the apoplastic protein samples. (Supplemental data Chapter 5). These data show that the temperature-sensitive Cf-4/Avr4 seedlings are a very clean and reproducible tool to study the Cf-4/Avr4-initiated HR, without the presence of the fungus to produce the Avr. In addition, the Cf-4/Avr4 seedlings disclose processes that occur in Cf-4 tomato plants inoculated with an Avr4 producing strain of *C. fulvum*.

Finally, comparison of the responses occurring in Cf-4/Avr4 seedlings to the response of tomato plants either lacking or expressing the *Cf-4* resistance gene, upon inoculation with an Avr4-producing strain of *C. fulvum*, allows to separately study the Cf-4/Avr4-triggered plant responses and additional responses of the host occurring during challenge by *C. fulvum*. The data in Chapter 5 revealed that MAMP-triggered immunity (MTI) in susceptible tomato plants is probably actively suppressed by effectors secreted by *C. fulvum*, leading to effector-triggered susceptibility (ETS) of tomato. In resistant plants, in addition to the induction of cell death, the Cf-4/Avr4-induced HR accelerates the already apparent MTI response in the apoplast, which renders this response much faster and stronger, thereby resulting in resistance.

The role of post-translational modifications in Cf-4-mediated defence signalling

In Chapter 3, the MAP kinases LeMPK1, -2 and -3 are shown to be rapidly activated in Cf-4/Avr4 seedlings that mount a HR. MAP kinases are activated by upstream MAPK kinases that phosphorylate a conserved motif of the MAP kinase, containing a threonine and tyrosine phosphorylation site (Pedley and Martin, 2005). In addition to LeMPK activation, 50 phosphoproteins were identified of which 13 showed an altered abundance upon initiation of the HR (Chapter 4). These data illustrate that protein phosphorylation plays a major role in the Cf-4/Avr4-mediated HR and subsequent resistance.

The phosphoproteins identified in Chapter 4 do not include the activated LeMPKs themselves, most likely because these proteins are very low abundant and therefore they are rarely detected in large phosphoproteome analyses. However, based on the substrate phosphorylation motifs that were determined for LeMPK1, -2 and -3 (Chapter 3), a few potential substrates of these LeMPKs might have been identified. For example, UDP-glucose glycosyltransferase and the YT521-ß-like protein contain the well-known MAPK phosphorylation motif PxSP. However, both proteins were not differentially phosphorylated

during the HR. In addition, the hexose transporter that was identified as a target for LeMPK3 contains the Sxx[KR] motif. However, the phosphopeptide matching this protein has a significantly decreased abundance in the Cf-4/Avr4 seedlings as compared to the controls. Therefore, it is unlikely that any of these three proteins are substrates of LeMPK1, -2 or -3 under the described conditions.

In addition to phosphorylation, preliminary data suggest that sumoylation plays a role in Cf-4/Avr4-mediated defence signalling. We found that virus-induced gene silencing (VIGS) of the gene encoding tomato SUMO(s) significantly decreased the Cf-4/Avr4-triggered HR (unpublished results). In addition, western blot analysis of total soluble protein extracts of Cf-4/Avr4 and control seedlings at 0, 6, 8 and 24 hours after the temperature shift appeared to show an increase in the abundance of sumoylated proteins. However, these results were difficult to reproduce, which might be a consequence of the relatively insensitive antibody-based approach in combination with SDS-PAGE gels and/or the instability of the SUMO modification. Similarly, a phospho-specific antibody-based approach was not successful to identify changes in the phosphoproteome of Cf-4/Avr4 seedlings, although we have been able to show that significant changes are present in the Cf-4/Avr4 seedlings (Chapters 3 and 4), which indicates that this antibody approach is not suitable for high-throughput screening for post-translational modifications. Further analysis should reveal the importance of protein sumoylation in the Cf-4/Avr4-induced HR.

An indirect indication that PTMs play a role in the early stages after HR-initiation was obtained from microarray expression profiling and quantitative DIGE-2DE analysis of Cf-4/Avr4 and control seedlings. Major transcriptional changes were only found at t=3h after the temperature shift, when MAPK activity is already apparent, whereas 2DE analysis of the total proteome of these seedlings hardly revealed any differences in the first hours after HR-initiation and only a few after 24 hours (results not shown). Although changes in the amount of less abundant proteins might be overshadowed by more abundant ones, major proteome changes did not seem to occur within 24 hours. Therefore, transcriptional profiling as well as proteome analysis suggests that the initial HR-induced responses, such as an oxidative burst and ion channel activation, eventually leading to cell death and protein accumulation in the apoplast, occur through PTMs.

The relation between HR and other processes occurring in plants

The HR is a form of programmed cell death (PCD) that typically occurs in plants as the result of effector-triggered immunity (ETI). Senescence, which is the aging-related yellowing and subsequent dying of the leaves of plants, is also a form of PCD (Quirino *et al.*, 2000). Although opinions differ on whether senescence, HR and PCD refer to the same process (Heath, 2000; Thomas *et al.*, 2003; Van Doorn and Woltering, 2004; Della Mea *et al.*, 2007), striking similarities between the three processes have been observed. Upon initiation of senescence, but also of the HR, a decrease in photosynthetic activity is observed that subsequently leads to chloroplast degradation, visible as yellowing of the leaves (Quirino *et al.*, 2000; Yoshida, 2003; Chapters 3 and 4). Furthermore, a process referred to as autophagy seems to play an important role in both leaf senescence and HR. Autophagy is required for the recovery of nutrients during leaf senescence but recently it has also been shown to be involved in degradation of oxidized proteins that accumulate as a result of oxidative stress. Furthermore, it is involved in the removal of protein aggregates and possibly damaged cellular components, to maintain normal cell function. Interestingly, senescence accelerates in the absence of autophagy. This shows that autophagy promotes cell survival under abiotic stress conditions (Bassham, 2007). In agreement with this observation, autophagy has recently been reported to restrict HR-induced cell death and thus to play a pro-survival role in the cells that surround HR lesions (Patel *et al.*, 2006). As mentioned above, autophagy can be responsible for the removal of oxidized proteins under oxidative stress conditions (Hanaoka *et al.*, 2002; Xiong *et al.*, 2007) and it is intriguing that the production of reactive oxygen species (ROS), which is one of the first responses upon pathogen recognition, stimulates autophagy (Xiong *et al.*, 2007) and inhibits the spread of cell death (Torres *et al.*, 2005). These data suggest that the production and subsequent spread of ROS stimulate autophagy in the surrounding tissue, in which superfluous cell death is subsequently inhibited. Indeed, plants that are unable to perform autophagy display an uncontrolled HR (Patel *et al.*, 2006). The HR initiated in the Cf-4/Avr4 seedlings was also found to be under strict control (Chapter 3). The spread of necrotic lesions that have started to develop and eventually will result in complete leaf necrosis upon a shift from 33°C to 20°C, can be stopped by incubating the Cf-4/Avr4 seedlings again at 33°C. This suggests that the HR is initiated in a limited amount of cells and that the surrounding tissue survives, possibly in an autophagy-dependent way. The mechanism that limits superfluous spread of the HR might also cause the formation of

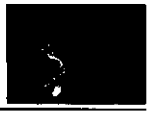

localized necrotic lesions at 20°C, instead of systemic necrosis throughout the cotyledons. Finally, both the HR and senescence induce the expression of pathogenesis-related (PR) proteins, salicylic acid and ROS, thereby showing the overlap between these two forms of PCD (Yoshida, 2003).

Recently, a link between brassinosteriod-induced developmental growth signalling and defence signalling has been revealed. The BRASSINOSTEROID-INSENSITIVE 1 (BRI1) receptor kinase forms a heterodimer with the BRI1-associated receptor-like kinase 1 (BAK1) upon perception of brassinosteroids, to mediate endocytosis (Karlova and De Vries, 2006). Just recently, the FLS2 receptor, mediating recognition of bacterial flagellin, has also been found to interact with BAK1 (Chinchilla *et al.*, 2007; Heese *et al.*, 2007). This implies that plasma membrane receptor proteins are involved in several processes and these data suggest a link between plant growth and development pathways on the one hand and defence signalling on the other.

The specific recognition of a pathogen by a plant leads to the rapid activation of several defence processes. ROS are produced, phosphorylation-dependent pathways are activated, cells are transcriptionally reprogrammed and PR proteins are synthesized and secreted (Joosten and De Wit, 1989; Lamb and Dixon, 1997; Gabriëls *et al.*, 2006; Benschop *et al.*, 2007; Chapters 2-5). As mentioned above, these processes are not only required for defence signalling, but also for many additional processes in the plant such as development, senescence and abiotic stress responses (Quirino *et al.*, 2000; Dani *et al.*, 2005; Niittylä *et al.*, 2007). It would be energetically and evolutionary highly unfavourable to have these tools only available for defence against invading pathogens. This conclusion, and the above described connections of defence with photosynthesis, autophagy, senescence and brassinosteroid signalling, indicates that resistance and HR cannot be seen as an independent process executed in plants that have recognized a pathogen. On the contrary, signalling cascades seem to depend on similar components and on cascades that possibly converge, eventually leading to a similar response. For example, the MAPK cascade is activated by a very large range of biotic and abiotic stress stimuli but also by plant hormones and during cell division (Zhang *et al.*, 2006). Furthermore, in Chapter 3 the LeMPKs were shown to have a different role in defence signalling, which shows that these kinases are involved in different processes. Upon perception of an external stimulus, which in this case is the Avr4 elicitor of

C. fulvum, many processes will be affected and possibly inhibited or stimulated, to eventually trigger HR development in the cell.

The Cf-4/Avr4-mediated hypersensitive response that leads to resistance of tomato plants to *C. fulvum*

Based on the results described in this thesis, in combination with previously described results, the following hypothesis for Cf-4/Avr4-mediated signalling is proposed and summarized in Figure 1.

Conidia from *C. fulvum* reaching the abaxial side of a tomato leaflet germinate, after which the emerging runner hyphae enter the leaf mesophyll through open stomata. In susceptible plants, *C. fulvum* is able to actively suppress and/or circumvent MTI, which is triggered via the recognition of MAMPs such as chitin and 1,3-ß-glucan fragments. Eventually, in densely colonized leaflets the MAMP concentrations have become so high that the effectors of *C. fulvum* are not capable anymore to fully suppress MTI, leading to the transcriptional upregulation of a subset of genes encoding PR proteins and other (apoplastic) proteins. However, this response is too late to resist full invasion of the apoplast by *C. fulvum* (Chapter 5). In resistant tomato plants harbouring the Cf-4 resistance protein, *C. fulvum* also secretes its effectors. However, in addition to the MAMP-triggered response, a specific and fast defence response is triggered upon perception of Avr4 (Chapter 5). As one of the first responses, Cf-4 triggers the production of phosphatidic acid (PA) in a PLC-dependent manner. PA subsequently stimulates the production of ROS, which plays a role in direct pathogen inhibition, signalling and cell wall reinforcement through cross-linking of cell wall components, such as arabinogalactans (Lamb and Dixon, 1997; De Jong *et al.*, 2004). Subsequently, LeMPK1, -2 and -3 are activated (Chapter 3), possibly via PA as was described for a MAP kinase in soybean (Lee *et al.*, 2001). This activation leads to phosphorylation of downstream targets, most likely related to the MAPK targets described in Arabidopsis and tobacco. LeMPK1 is involved in resistance to *C. fulvum* (Chapter 3) and its closest orthologue in Arabidopsis, AtMPK6, phosphorylates the rate-limiting enzyme 1-aminocyclopropane-1-carboxylate synthase (ACS) in the ethylene biosynthesis pathway, thereby elevating ethylene production (Liu and Zhang, 2004). Indeed, Cf-4 plants inoculated with an Avr4-producing strain of *C. fulvum*, display clear epinasty, appearing approximately 6 days after inoculation and which is a phenotype correlated with ethylene production (Chapter 5). In addition,

LeMPK1 might phosphorylate WRKY-transcription factors that subsequently induce transcription of defence genes such as PR proteins and proteins involved in cell wall modifications (Kim *et al.*, 2003; Kim and Zhang, 2004; Menke *et al.*, 2005). Since VIGS of LeMPK1 leads to a decreased resistance to *C. fulvum* but not to a decreased HR upon Avr4 elicitation, LeMPK1 might have a role in MTI since the Cf-4-mediated resistance is proposed to be the sum of MTI and ETI-related Cf-4-triggered HR. LeMPK2 plays a role in HR development but not in resistance to *C. fulvum*, which might imply that LeMPK2 functions in a pathway parallel to LeMPK1 and/or MTI. Possibly, LeMPK3 stimulates other pathways since the phosphorylation motifs of its substrate proteins appear to differ from the motifs described for LeMPK1 and -2 (Chapter 3). Similarly to the tobacco orthologue WIPK, LeMPK3 might induce an increase in SA levels in Cf-4/Avr4 seedlings (Waller *et al.*, 2006).

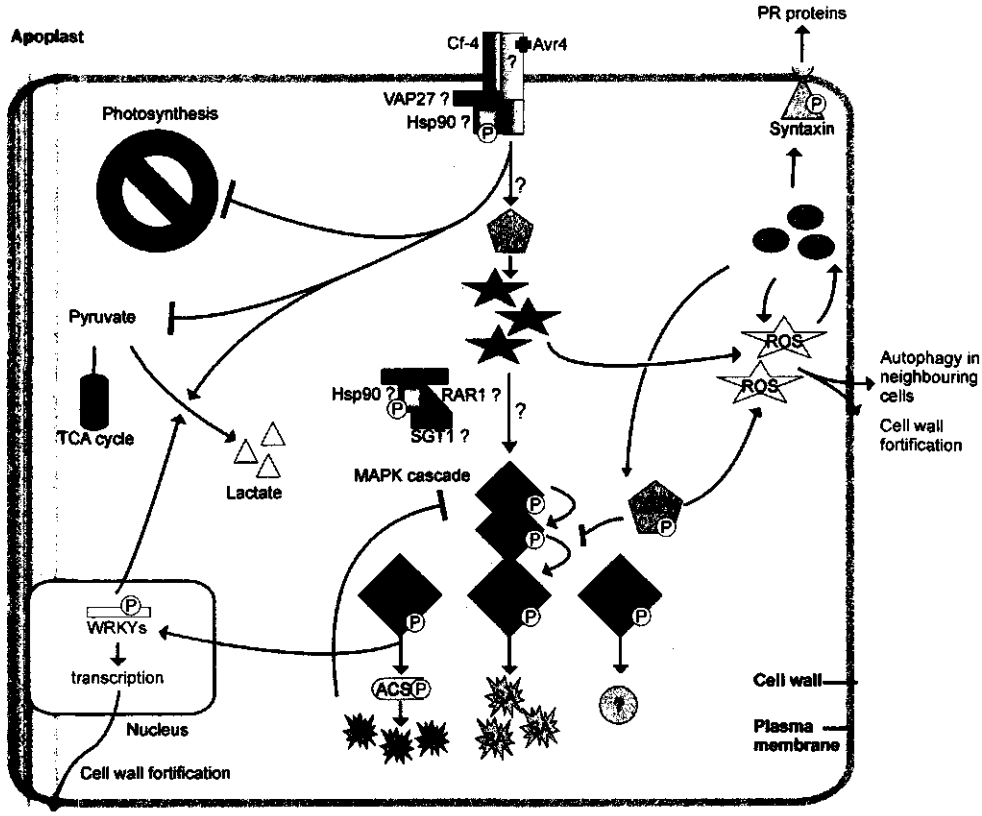

Figure 1. Tomato Cf-4-induced signal transduction cascades triggered after perception of Avr4 of the extracellular fungal pathogen *Cladosporium fulvum*.
Activation of the signalling cascades leads to the initiation of host defence responses, eventually resulting in host resistance. See text for details.

Concomitantly, phosphorylation-dependent signalling cascades decrease photosynthetic activity in the cell through the de-activation of essential components of this process (Chapter 4). Since the abundance of some phosphoproteins was already significantly altered before LeMPK activation was apparent, and no clear indications were found that the identified phosphoproteins involved in photosynthesis are targets of the LeMPKs, the pathway resulting in (de)phosphorylation of these proteins might be induced parallel to the MAPK cascade.

Massive ROS production, probably leads to oxygen depletion. Therefore, the pyruvate decarboxylase-dependent aerobic respiration switches to anaerobic respiration in which pyruvate is converted to lactate instead of entering the citric acid cycle, to facilitate energy production for the Cf-4/Avr4-induced response at low oxygen levels. Furthermore, ROS might signal to other cells where it induces autophagy that restricts the HR to the site of fungal penetration, leaving no visible trace of the HR on the Cf-4 tomato plants challenged with *C. fulvum* expressing Avr4. In addition, ROS production possibly stimulates a calcium burst in the cell that is required for the activation of other signalling components. For example, a calcium-dependent protein kinase (CDPK) is activated in a phosphorylation- and calcium-dependent manner upon Avr4-perception (Romeis *et al.*, 2001). However, no significantly altered abundance of a phosphorylated CDPK was observed during the development of the HR in the Cf-4/Avr4 seedlings (Chapter 5). Either another CDPK is differentially activated or this kinase is activated at a later stage of HR development since it compromises MAP kinase signalling in an ethylene-dependent way, thereby providing a feedback loop (Ludwig *et al.*, 2004). The calcium burst might also be required for the phosphorylation of a syntaxin, leading to the subsequent release of, for example, PR proteins into the apoplast (Heese *et al.*, 2005; Kalde *et al.*, 2007). Possibly, LeMPK1 plays a role in this process since this kinase has been shown to play a role in resistance to *C. fulvum* but not in the HR.

Finally, cytoplasmic Hsp90 plays a role in the Cf-4/Avr4-triggered defence response (Gabriëls *et al.*, 2006). Possibly, the individual isoforms of Hsp90 that were found to be differentially phosphorylated stabilize a Cf-4 receptor complex, a NRC1 complex, or both, and allow downstream signalling upon their (de)phosphorylation. However with the present data, it is not possible to conclude at which position(s) the different Hsp90s localize in the defence signalling cascade.

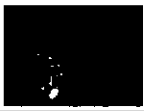

REFERENCES

Bassham DC (2007) Plant autophagy - more than a starvation response. Curr Opin Plant Biol 10: 587-593.

Benschop JJ, Mohammed S, O'Flaherty M, Heck AJR, Slijper M, Menke FLH (2007) Quantitative phosphoproteomics of early elicitor signalling in Arabidopsis. Mol Cell Proteomics 6: 1198-1214.

Botër M, Amigues B, Peart J, Breuer C, Kadota Y, Casais C, Moore G, Kleanthous C, Ochsenbein F, Shirasu K, Guerois R (2007) Structural and functional analysis of SGT1 reveals that its interaction with HSP90 is required for the accumulation of Rx, an R protein involved in plant immunity. Plant Cell 19: 3791-3804.

Chinchilla D, Zipfel C, Robatzek S, Kemmerling B, Nürnberger T, Jones JDG, Felix G, Boller T (2007) A flagellin-induced complex of the receptor FLS2 and BAK1 initiates plant defence. Nature 448: 497-500.

Clark SE (2001) Cell signalling at the shoot meristem. Nat Rev Mol Cell Biol 2: 276-284.

Dani V, Simon WJ, Duranti M, Croy RRD (2005) Changes in the tobacco leaf apoplast proteome in response to salt stress. Proteomics 5: 737-745.

De Jong CF, Laxalt AM, Bargmann BOR, De Wit PJGM, Joosten MHAJ, Munnik T (2004) Phosphatidic acid accumulation is an early response in the Cf-4/Avr4 interaction. Plant J 39: 1-12.

De Jong CF, Takken FLW, Cai X, De Wit PJGM, Joosten MHAJ (2002) Attenuation of Cf-mediated defense responses at elevated temperatures correlates with a decrease in elicitor-binding sites. Mol Plant-Microbe Interact 15: 1040-1049.

De la Fuente van Bentem S, Vossen JH, De Vries KJ, Van Wees S, Tameling WIL, Dekker HL, Koster CG, Haring MA, Takken FLW, Cornelissen BJC (2005) Heat shock protein 90 and its co-chaperone protein phosphatase 5 interact with distinct regions of the tomato I-2 disease resistance protein. Plant J 43: 284-298.

Della Mea M, Serafini-Fracassini D, Del Duca S (2007) Programmed cell death: similarities and differences in animals and plants. A flower paradigm. Amino Acids 33: 395-404.

Gabriëls SHEJ, Takken FLW, Vossen JH, De Jong CF, Liu Q, Turk SCHJ, Wachowski LK, Peters J, Witsenboer HMA, De Wit PJGM, Joosten MHAJ (2006) cDNA-AFLP combined with functional analysis reveals novel genes involved in the hypersensitive response. Mol Plant-Microbe Interact 19: 567-576.

Gabriëls SHEJ, Vossen JH, Ekengren SK, Ooijen GV, Abd-El-Haliem AM, Van den Berg GCM, Rainey DY, Martin GB, Takken FLW, De Wit PJGM, Joosten MHAJ (2007) An NB-LRR protein required for HR signalling mediated by both extra- and intracellular resistance proteins. Plant J 50: 14-28.

Hammond-Kosack KE, Silverman P, Raskin I, Jones JDG (1996) Race-specific elicitors of *Cladosporium fulvum* induce changes in cell morphology and the synthesis of ethylene and salicylic acid in tomato plants carrying the corresponding Cf disease resistance gene. Plant Physiol 110: 1381-1394.

Hanaoka H, Noda T, Shirano Y, Kato T, Hayashi H, Shibata D, Tabata S, Ohsumi Y (2002) Leaf senescence and starvation-induced chlorosis are accelerated by the disruption of an Arabidopsis autophagy gene. Plant Physiol 129: 1181-1193.

Heath MC (2000) Hypersensitive response-related death. Plant Mol Biol 44: 321-334.

Heese A, Hann DR, Gimenez-Ibanez S, Jones AME, He K, Li J, Schroeder JI, Peck SC, Rathjen JP (2007) The receptor-like kinase SERK3/BAK1 is a central regulator of innate immunity in plants. PNAS 104: 12217-12222.

Heese A, Ludwig AA, Jones JDG (2005) Rapid phosphorylation of a syntaxin during the Avr9/Cf-9-race-specific signaling pathway. Plant Physiol 138: 2406-2416.

Joosten MHAJ, De Wit PJGM (1989) Identification of several pathogenesis-related proteins in tomato leaves inoculated with *Cladosporium fulvum* (syn. *Fulvia fulva*) as 1,3-ß-glucanases and chitinases. Plant Physiol 89: 945-951.

Joosten MHAJ, De Wit PJGM (1999) The tomato-*Cladosporium fulvum* interaction: A versatile experimental system to study plant-pathogen interactions. Annu Rev Phytopathol 37: 335-367.

Kalde M, Nühse TS, Findlay K, Peck SC (2007) The syntaxin SYP132 contributes to plant resistance against bacteria and secretion of pathogenesis-related protein 1. Proc Natl Acad Sci USA 104: 11850-11855.

Karlova R, De Vries SC (2006) Advances in understanding brassinosteroid signaling. Sci. STKE 2006: pe36.

Kim CY, Liu Y, Thorne ET, Yang H, Fukushige H, Gassmann W, Hildebrand D, Sharp RE, Zhang S (2003) Activation of a stress-responsive mitogen-activated protein kinase cascade induces the biosynthesis of ethylene in plants. Plant Cell 15: 2707-2718.

Kim CY, Zhang S (2004) Activation of a mitogen-activated protein kinase cascade induces WRKY family of transcription factors and defense genes in tobacco. Plant J 38: 142-151.

Krishna P, Gloor G (2001) The Hsp90 family of proteins in *Arabidopsis thaliana*. Cell Stress Chaperon 6: 238-246.

Kruijt M, De Kock MJD, De Wit PJGM (2005a) Receptor-like proteins involved in plant disease resistance. Mol Plant Pathol 6: 85-97.

Kruijt M, Kip DJ, Joosten MHAJ, Brandwagt BF, De Wit PJGM (2005b) The *Cf-4* and *Cf-9* resistance genes against *Cladosporium fulvum* are conserved in wild tomato species. Mol Plant-Microbe Interact 18: 1011-1021.

Lamb C, Dixon RA (1997) The oxidative burst in plant disease resistance. Annu Rev Plant Biol 48: 251-275.

Laurent F, Labesse G, De Wit PJGM (2000) Molecular cloning and partial characterization of a plant VAP33 homologue with a major sperm protein domain. Biochem Biophys Res Commun 270: 286-292.

Lee S, Hirt H, Lee Y (2001) Phosphatidic acid activates a wound-activated MAPK in *Glycine max*. Plant J 26: 479-486.

Liu Y, Burch-Smith T, Schiff M, Feng S, Dinesh-Kumar SP (2004) Molecular chaperone Hsp90 associates with resistance protein N and its signaling proteins SGT1 and RAR1 to modulate an innate immune response in plants. J Biol Chem 279: 2101-2108.

Liu Y, Zhang S (2004) Phosphorylation of 1-aminocyclopropane-1-carboxylic acid synthase by MPK6, a stress-responsive mitogen-activated protein kinase, induces ethylene biosynthesis in Arabidopsis. Plant Cell 16: 3386-3399.

Ludwig AA, Romeis T, Jones JDG (2004) CDPK-mediated signalling pathways: specificity and cross-talk. J Exp Bot 55: 181-188.

McClellan AJ, Xia Y, Deutschbauer AM, Davis RW, Gerstein M, Frydman J (2007) Diverse cellular functions of the Hsp90 molecular chaperone uncovered using systems approaches. Cell 131: 121-135.

Menke FLH, Kang HG, Chen Z, Jeong MP, Kumar D, Klessig DF (2005) Tobacco transcription factor WRKY1 is phosphorylated by the MAP kinase SIPK and mediates HR-like cell death in tobacco. Mol Plant-Microbe Interact 18: 1027-1034.

Niittylä T, Fuglsang AT, Palmgren MG, Frommer WB, Schulze WX (2007) Temporal analysis of sucrose-induced phosphorylation changes in plasma membrane proteins of arabidopsis. Mol Cell Proteomics 6: 1711-1726.

Ogawa M, Shinohara H, Sakagami Y, Matsubayashi Y (2008) Arabidopsis CLV3 peptide directly binds CLV1 ectodomain. Science 319: 294.

Patel S, Caplan J, Dinesh-Kumar S (2006) Autophagy in the control of programmed cell death. Curr Opin Plant Biol 9: 391-396.

Pedley KF, Martin GB (2005) Role of mitogen-activated protein kinases in plant immunity. Curr Opin Plant Biol 8: 541-547.

Quirino BF, Noh YS, Himelblau E, Amasino RM (2000) Molecular aspects of leaf senescence. Trends Plant Sci 5: 278-282.

Richter K, Hendershot LM, Freeman BC (2007) The cellular world according to Hsp90. Nat Struct Mol Biol 14: 90-94.

Romeis T, Ludwig AA, Martin R, Jones JDG (2001) Calcium-dependent protein kinases play an essential role in a plant defence response. EMBO J 20: 5556-5567.

Rose LE, Bittner-Eddy PD, Langley CH, Holub EB, Michelmore RW, Beynon JL (2004) The maintenance of extreme amino acid diversity at the disease resistance gene, *RPP13*, in *Arabidopsis thaliana*. Genetics 166: 1517-1527.

Rutherford SL, Lindquist S (1998) Hsp90 as a capacitor for morphological evolution. Nature 396: 336-342.

Sangster TA, Bahrami A, Wilczek A, Watanabe E, Schellenberg K, McLellan C, Kelley A, Kong SW, Queitsch C, Lindquist S (2007) Phenotypic diversity and altered environmental plasticity in *Arabidopsis thaliana* with reduced Hsp90 levels. PLoS One 2: e648.

Sangster TA, Queitsch C (2005) The HSP90 chaperone complex, an emerging force in plant development and phenotypic plasticity. Curr Opin Plant Biol 8: 86-92.

Takahashi A, Casais C, Ichimura K, Shirasu K (2003) HSP90 interacts with RAR1 and SGT1 and is essential for RPS2-mediated disease resistance in Arabidopsis. Proc Natl Acad Sci USA 100: 11777-11782.

Thomas H, Ougham HJ, Wagstaff C, Stead AD (2003) Defining senescence and death. J Exp Bot 54: 1127-1132.

Torres MA, Jones JDG, Dangl JL (2005) Pathogen-induced, NADPH oxidase-derived reactive oxygen intermediates suppress spread of cell death in *Arabidopsis thaliana*. Nat Genet 37: 1130-1134.

Van der Hoorn RA, Van der Ploeg A, De Wit PJGM, Joosten MHAJ (2001) The C-terminal dilysine motif for targeting to the endoplasmic reticulum is not required for Cf-9 function. Mol Plant-Microbe Interact 14: 412-415.

Van Doorn WG, Woltering EJ (2004) Senescence and programmed cell death: substance or semantics? J Exp Bot 55: 2147-2153.

Waller F, Muller A, Chung KM, Yap YK, Nakamura K, Weiler E, Sano H (2006) Expression of a WIPK-activated transcription factor results in increase of endogenous salicylic acid and pathogen resistance in tobacco plants. Plant Cell Physiol 47: 1169-1174.

Whitham S, Dinesh-Kumar SP, Choi D, Hehi R, Corr C, Baker B (1994) The product of the tobacco mosaic virus resistance gene *N*: similarity to Toll and the Interleukin-1 receptor. *Cell* 78: 1101-1115.

Xiong Y, Contento AL, Nguyen PQ, Bassham DC (2007) Degradation of oxidized proteins by autophagy during oxidative stress in Arabidopsis. Plant Physiol 143: 291-299.

Yamada K, Fukao Y, Hayashi M, Fukazawa M, Suzuki I, Nishimura M (2007) Cytosolic HSP90 regulates the heat shock response that is responsible for heat acclimation in *Arabidopsis thaliana*. J Biol Chem 282: 37794-37804.

Yoshida S (2003) Molecular regulation of leaf senescence. Curr Opin Plant Biol 6: 79-84.

Zhang T, Liu Y, Yang T, Zhang L, Xu S, Xue L, An L (2006) Diverse signals converge at MAPK cascades in plant. Plant Physiol Biochem 44: 274-283.

Microbial plant pathogens impose a continuous threat on global food production. Similar to disease resistance in mammals, an innate immune system allows plants to recognise pathogens and swiftly activate defence. For the work described in this thesis, the interaction between tomato and the extracellular fungal pathogen *Cladosporium fulvum* serves as a model system to study host resistance and susceptibility in plant-pathogen interactions. Resistance to *C. fulvum* in tomato plants follows the gene-for-gene hypothesis, which requires the presence of a *Cf* resistance gene in tomato and presence of the cognate avirulence gene (*Avr*) in *C. fulvum*. Upon perception of the Avr by a tomato plant, a typical hypersensitive response (HR) is induced that renders the plant resistant to *C. fulvum*. In the years preceding this thesis work, most research was focussed on understanding which Avrs are produced by *C. fulvum* and how these Avrs are actually perceived by resistant plants (**Chapter 1**). The goal of the work described in this thesis is to reveal downstream signalling cascades triggered upon Avr perception. Therefore, the HR was studied by using a model system in which the Cf-4 protein of tomato and the Avr4 protein from *C. fulvum* were simultaneously expressed in tomato seedlings. Since the Cf-4/Avr-induced responses are inhibited at 33°C and high humidity, these Cf-4/Avr4 seedlings initiate a synchronized and reproducible HR after incubation at 33°C and a subsequent shift to 20°C, which allows studying downstream responses.

To prevent pathogen proliferation in the resistant plant, defence signalling cascades need to be activated extremely fast upon pathogen recognition. Therefore, many downstream signalling cascades depend on post-translational modifications (PTMs) that allow a rapid, reversible, controlled and highly specific transduction of perceived signals. An overview of the various types of PTMs and their role in the resistance response of plants to pathogens is provided in **Chapter 2**. In addition, examples are provided of successful pathogens that manipulate PTMs.

Protein phosphorylation seems to play an important role in the Cf-4/Avr4-triggered HR, since Avr4 perception leads to the specific activation of at least three mitogen-activated protein kinases, LeMPK1, -2 and -3, which requires phosphorylation by an upstream kinase (**Chapter 3**). Each of these three kinases seems to have a different role in downstream defence signalling, since the kinases were shown to have different phosphorylation specificities and therefore most likely have different downstream target substrates. Furthermore, these kinases appear to play a different role with regard to HR and full resistance to *C. fulvum* in tomato (**Chapter 3**).

Since protein phosphorylation was shown to play an important role in Cf-4/Avr4-induced defence signalling, the phosphoproteome of Cf-4/Avr4 and control seedlings after HR initiation was studied using a new approach (**Chapter 4**). This approach led to the identification of 50 phosphoproteins, most of which have not been described in tomato before. Quantification revealed 13 phosphoproteins with an altered abundance in the Cf-4/Avr4 seedlings as compared to the control, which implies HR-induced differential phosphorylation of these proteins. Phosphorylation-mediated regulation of the activity of these proteins pointed to a swift decrease in photosynthetic activity upon HR-initiation, which was confirmed by experiments in which the actual efficiency of the photosynthesis in the Cf-4/Avr4 seedlings was determined upon induction of the HR. Furthermore, a shift from aerobic to anaerobic respiration, which possibly results from oxygen depletion caused by a massive oxidative burst consuming large amounts of oxygen, seems to take place upon initiation of the HR. Finally, differential phosphorylation of the four cytoplasmic isoforms of the Hsp90 chaperone protein was observed, suggesting that they play distinct roles during defence signalling (**Chapter 4**).

In addition to the HR, other associated defence responses are initiated upon recognition of *C. fulvum*. One of these responses is the secretion of defence-related proteins into the apoplast, which is the environment where *C. fulvum* operates. Therefore, the dynamics of the apoplastic proteome of resistant, *Cf-4*-expressing plants and susceptible tomato plants lacking *Cf-4*, were studied after inoculation with a strain of *C. fulvum* that secretes Avr4 (**Chapter 5**). Analysis of the apoplastic proteome revealed a slow accumulation of defence proteins in the apoplast of susceptible plants, which is most likely the result of perception of general elicitors of *C. fulvum* by tomato. In resistant plants, the same set of proteins accumulates in the apoplast, but this occurs much faster and to higher levels. The accelerated response is caused by the Cf-4/Avr4-initiated HR that also leads to cell death. The HR, in combination with the accelerated protein secretion, renders the plants resistant to *C. fulvum*. In addition, in susceptible plants *C. fulvum* seems to specifically downregulate genes encoding cell wall proteins of which the accumulation possibly hampers nutrient and water uptake and thereby proliferation of the pathogen in the tomato apoplast. Possibly, an effector of *C. fulvum* targets a receptor for general elicitors, thereby suppressing transcription of these genes (**Chapter 5**).

Most data described in this thesis have been obtained from Cf-4/Avr4 seedlings in which the HR can be inhibited by incubating the plants at 33°C. The present data suggest that this temperature-sensitivity occurs at the site of signal perception. Possibly, cytoplasmic Hsp90 stabilizes R protein complexes localized at the plasma membrane. Upon high temperature stress, an increased demand for Hsp90 occurs in the cells to stabilize unfolding proteins that play a role in basal cellular processes, which could lead to the release and subsequent degradation of R protein complexes, rendering defence signalling temperature-sensitive (**Chapter 6**). The temperature-sensitivity of the Cf-4/Avr4-initiated HR provides a very clean and reproducible tool to study the HR, in the absence of the fungus that produces the Avr. Furthermore, the data described in this thesis provide evidence that the Cf-4/Avr4 seedlings recover from the temperature stress before the specific Cf-4/Avr4-triggered HR is initiated. The possibility to separate the events directly associated with the HR from the full resistance response of the plant to the invading fungus, provides new insight into the complexity of plant defence responses and their specific suppression upon successful colonization by *C. fulvum* (**Chapter 6**). Comparison of the defence response to other processes that occur in the cell underlines that resistance and HR execution cannot be seen as an independent and separate process in resistant plants that have recognized a pathogen. On the contrary, signalling cascades seem to depend on similar components and on cascades that possibly converge, eventually leading to a similar response (**Chapter 6**). Finally, an up to date model for the Cf-4/Avr4-triggered HR and resistance is proposed, based on data that have been published before and the results obtained with the research described in this thesis (**Chapter 6**).

Samenvatting

Pathogene micro-organismen kunnen plantenziekten veroorzaken en vormen een constante bedreiging voor de wereld voedselproductie. Net als bij zoogdieren en mensen hebben planten een afweersysteem dat micro-organismen als 'lichaamsvreemd' herkent waardoor een afweerreactie wordt geactiveerd. In dit proefschrift wordt de afweerreactie van tomaat tegen de pathogene schimmel *Cladosporium fulvum* bestudeerd. De interactie tussen deze extracellulaire ziekteverwekker en tomaat volgt de gen-om-gen hypothese en wordt gebruikt als een modelsysteem om resistentie en vatbaarheid van planten tegen pathogenen te bestuderen. Wanneer *C. fulvum* bladeren van de tomatenplant binnendringt door openstaande huidmondjes, worden diverse kleine eiwitten uitgescheiden door de schimmel die een rol spelen bij het infectieproces. Tussen deze eiwitten bevinden zich ook de zogenaamde avirulentie eiwitten (Avrs), welke gecodeerd worden door *Avr* genen. Een tomatenplant met een *Cf* resistentiegen kan een specifieke Avr herkennen, wat vervolgens leidt tot een overgevoeligheidsreactie. Deze reactie heeft lokale celdood tot gevolg wat de plant resistent maakt tegen *C. fulvum*. In de jaren voorafgaand aan het beschreven onderzoek is vooral bestudeerd welke Avrs *C. fulvum* maakt en hoe deze Avrs herkend worden door de plant (**Hoofdstuk 1**). Het doel van het hier beschreven onderzoek is het ontrafelen van de signalering die plaatsvindt in de tomatenplant na herkenning van een Avr, en hoe dit uiteindelijk leidt tot resistentie. Daarvoor is gebruik gemaakt van transgene tomatenzaailingen die zowel *Cf-4* van tomaat als *Avr4* van *C. fulvum* tot expressie brengen, wat leidt tot een overgevoeligheidsreactie in de plant. Deze reactie kan echter onderdrukt worden door de planten bij 33°C en hoge luchtvochtigheid te plaatsen, waarna een gesynchroniseerde en gecontroleerde overgevoeligheidsreactie kan worden geïnduceerd door de zaailingen naar 20°C terug te brengen. Deze Cf-4/Avr4 zaailingen vormen een zeer geschikt systeem om de signalering van planten in relatie tot ziekteresistentie te ontrafelen.

Signalering die leidt tot het activeren van een afweerreactie na herkenning van een pathogeen moet snel zijn om de ziekteverwekker geen kans te geven. De (de)activering van eiwitten betrokken bij signalering is vaak gebaseerd op post-translationele modificaties (PTMs) die zorgen voor een snelle, gecontroleerde, omkeerbare en zeer specifieke verandering van de activiteit van het eiwit. Daarom wordt in **Hoofdstuk 2** een literatuuroverzicht gegeven van allerlei typen PTMs en de rol die deze PTMs spelen in de resistentiereactie van planten. Bovendien worden voorbeelden gegeven van de manipulatie van deze PTMs door succesvolle ziekteverwekkers.

Eiwitfosforylatie lijkt een belangrijke rol te spelen bij de signalering geïnduceerd door Avr4 herkenning in resistente Cf-4 tomatenplanten, aangezien tijdens de afweerrespons in Cf-4/Avr4 zaailingen minstens drie mitogen-geactiveerde kinases, LeMPK1, -2 en -3, worden geactiveerd door fosforylatie (**Hoofdstuk 3**). Deze geactiveerde kinases fosforyleren vervolgens zelf ook eiwitten, waarmee de signalering wordt voorgezet. LeMPK1, -2 en -3 blijken een verschillende fosforylatiespecificiteit te hebben en spelen een verschillende rol in de overgevoeligheidsreactie en resistentie tegen *C. fulvum*. Daarom is het waarschijnlijk dat deze kinases elk een verschillende rol hebben in de afweersignalering (**Hoofdstuk 3**).

Aangezien fosforylatie een belangrijke rol speelt in de afweersignalering die geactiveerd wordt in de Cf-4/Avr4 zaailingen, wordt er in **Hoofdstuk 4** een nieuwe analyse beschreven waarin gefosforyleerde peptiden van Cf-4/Avr4 en controle zaailingen werden geïsoleerd. Deze analyse heeft geleid tot de identificatie van 50 gefosforyleerde eiwitten waarvan de meerderheid niet eerder werd beschreven voor tomatenplanten. Vergeleken met de controles waren 13 gefosforyleerde eiwitten in significant hogere of juist lagere hoeveelheden aanwezig in de Cf-4/Avr4 zaailingen, wat differentiële fosforylatie van deze eiwitten suggereert. Regulatie van de activiteit van deze eiwitten door fosforylatie suggereerde bijvoorbeeld dat er een snelle afname van de fotosyntheseactiviteit plaatsvindt als gevolg van het initiëren van de overgevoeligheidsreactie. Deze waarneming is bevestigd door metingen die laten zien dat de fotosyntheseactiviteit inderdaad zeer snel en specifiek afneemt in de Cf-4/Avr4 zaailingen. Daarnaast wijzen de data er ook op dat de plant overgaat van aerobe naar anaerobe respiratie wanneer de overgevoeligheidsreactie wordt geïnitieerd. Dit komt waarschijnlijk door de sterke oxidatieve reacties die tijdens deze respons plaatsvinden, welke leiden tot een gebrek aan zuurstof. Ten slotte wijzen de bevindingen ook op een differentiële rol voor de vier verschillende isovormen van cytoplasmatisch Hsp90 in de overgevoeligheidsreactie, aangezien de isovormen verschillend worden gefosforyleerd op hetzelfde geconserveerde fosforylatiemotief tijdens het activeren van de afweerrespons (**Hoofdstuk 4**).

Naast de overgevoeligheidsreactie worden er ook andere reacties geïnduceerd in tomatenplanten die *C. fulvum* herkennen, zoals het uitscheiden van afweergerelateerde eiwitten in de extracellulaire ruimtes van het tomatenblad; de omgeving waar *C. fulvum* zich ophoudt. Om de dynamiek van deze uitscheiding van extracellulaire eiwitten te bestuderen, zijn tomatenplanten met en zonder het *Cf-4* resistentiegen geïnoculeerd met een fysio van *C.*

fulvum dat Avr4 produceert (**Hoofdstuk 5**). In vatbare planten, die Avr4 niet herkennen, accumuleren diverse extracellulaire eiwitten langzaam als gevolg van herkenning van algemene 'lichaamsvreemde' componenten afkomstig van *C. fulvum*. In resistente planten accumuleert dezelfde set eiwitten veel sneller en in veel grotere hoeveelheden, wat veroorzaakt wordt door de Cf-4/Avr4-geïnduceerde overgevoeligheidsreactie. De combinatie van de overgevoeligheidsreactie en het snelle uitscheiden van deze extracellulaire eiwitten leidt tot resistentie tegen *C. fulvum*. Verder lijkt *C. fulvum* actief de expressie van een set van genen te onderdrukken die coderen voor eiwitten die ophopen in de celwand. Accumulatie van deze eiwitten bemoeilijkt mogelijk de opname van water en voedingsstoffen uit de cel en daarmee de kolonisatie en sporulatie van *C. fulvum* (**Hoofdstuk 5**).

De resultaten beschreven in dit proefschrift zijn verkregen door Cf-4/Avr4 zaailingen te gebruiken waarin de overgevoeligheidsreactie kan worden onderdrukt bij 33°C. Eerdere resultaten suggereren dat de Cf-4/Avr4-geactiveerde afweerrespons temperatuurgevoelig is doordat de herkenning van Avr4 wordt geblokkeerd. Hsp90 is een eiwit dat andere eiwitten stabiliseert en dat mogelijk ook Cf-4 stabiliseert. Bij hoge temperaturen stabiliseert Hsp90 eiwitten die door de hoge temperatuur dreigen te ontvouwen en die nodig zijn voor basale celfuncties, waardoor de vraag naar Hsp90 toeneemt. Dit zou kunnen leiden tot destabilisatie en afbraak van Cf-4, waardoor de Avr4 herkenning temperatuurgevoelig wordt (**Hoofdstuk 6**). Doordat de overgevoeligheidsreactie in de Cf-4/Avr4 zaailingen temperatuurgevoelig is, zijn deze planten geschikt om synchroon en reproduceerbaar de overgevoeligheidsreactie te induceren zonder dat de aanwezigheid van de schimmel nodig is. De mogelijkheid om de Cf-4/Avr4-geïnduceerde overgevoeligheidsreactie te bestuderen, onafhankelijk van de totale set aan afweerresponsen van Cf-4 tomaat geïnoculeerd met een Avr-producerend fysio van *C. fulvum*, geeft nieuwe inzichten in de complexiteit van de plant afweerreacties en de onderdrukking van deze response door de schimmel in vatbare planten (**Hoofdstuk 6**). Een vergelijking van afweerreacties en andere processen die plaatsvinden in plantencellen laat zien dat de aan resistentie gerelateerde responsen niet als onafhankelijke processen in de cel gezien kunnen worden. Veel eiwitten die een rol spelen in afweerreacties zijn namelijk ook betrokken bij processen als ontwikkeling, veroudering en onderhoud van de cel (**Hoofdstuk 6**). Ten slotte wordt er in dit hoofdstuk een geïntegreerd overzicht gegeven van de Cf-4/Avr4-geïnduceerde overgevoeligheidsreactie en resistentie, gebaseerd op eerder verkregen resultaten en de resultaten beschreven in dit proefschrift.

Met gemengde gevoelens heb ik mijn leesversie ingeleverd bij het secretariaat voor promoties. Het is een mijlpaal waar ik erg trots op ben, maar daarentegen is het ook het einde van een leuke en leerzame tijd. In dit nawoord wil ik graag de mensen bedanken die me jarenlang hebben gesteund en geholpen, en die de afgelopen jaren tot een onvergetelijke tijd hebben gemaakt.

Matthieu, jouw VIDI project maakte het in september 2002 mogelijk dat ik als promovenda kon beginnen aan een veelomvattend project. Je hebt me de vrijheid gegeven om mijn eigen richting binnen het project te bepalen, wat ik erg gewaardeerd heb. Ik heb veel geleerd de afgelopen jaren en dankzij de precieze correcties van mijn manuscripten zal ik nooit meer een manuscript schrijven waarbij ik niet aan die adviezen zal denken. Verder hoop ik dat de resultaten uit mijn proefschrift een bodem hebben gelegd voor het onderzoek van de komende jaren.

Zonder mijn collega's van het Laboratorium voor Fytopathologie hadden de afgelopen jaren er heel anders uitgezien. Pierre, als promotor en hoofd van het laboratorium geef je je promovendi de mogelijkheid om zich te ontwikkelen tot zelfstandige onderzoekers. Bedankt daarvoor. Susan, bedankt voor je steun en enthousiasme en voor alle jaren dat we samen een kamer deelden. Nana, I was very lucky to supervise a hard working student like you. You did a lot of nice but difficult work that, unfortunately, did not make it into this thesis. Never-the-less, thank you for your work and the nice collaboration. Jack, bedankt voor je samenwerking binnen het VIDI project. Grardy, bedankt voor je hulp aan hoofdstuk 3 en de gezelligheid op het lab. Ahmed, bedankt voor je gezelschap op onze kamer en succes met je promotie. Wladimir en Bart, bedankt voor alle ideeën en de manuscripten die jullie gelezen en van commentaar voorzien hebben. Renier, bedankt voor je begeleiding in mijn eerste jaar. Nienke, zonder jouw enthousiaste begeleiding tijdens mijn afstudeervak had ik niet eens overwogen om aan een promotie te beginnen. Ik heb er geen spijt van gekregen. John, Peter, Emilie en Ursula bedankt voor de samenwerking en succes met het afronden van jullie promoties. Irene, Judith, Marco en Jos, bedankt voor de steun en de vaste theepauzes. Verder wil ik iedereen van het Laboratorium voor Fytopathologie bedanken voor de fijne samenwerking en succes wensen in zijn/haar verdere toekomst.

De experimenten beschreven in Hoofdstuk 5 zijn uitgevoerd in samenwerking met Twan, Jan, Hetty en Froukje van Plant Research International. Het heeft lang geduurd voor de

resultaten zichtbaar werden maar uiteindelijk heeft deze samenwerking tot een mooi resultaat geleid.

The experiments described in Chapter 4 have been performed in Odense, in the Department of Biochemistry and Molecular Biology of the University of Southern Denmark. I would like to thank Ole Jensen for the opportunity to work in his lab. It has been an incredible docile period that led to a very nice chapter in this thesis. I would like to thank Nadia, Kate, Pia, David, Martin, Tine, Christian and Andreas for their assistance and support in this project. Furthermore, I would like to thank the complete PR group for their warm welcome. I experienced Denmark as a very friendly country.

Verder wil ik een aantal mensen bedanken die niet direct bij het werk van dit proefschrift betrokken waren maar die wel belangrijk voor mij zijn geweest. Ik betwijfel namelijk of ik door de afgelopen jaren heen was gekomen zonder mijn muzikale vrienden. Daarom wil ik allereerst Lex, Peter, Martin, Ester, Martijn en Rozemarijn van de Freaky Fish bedanken. De wekelijkse repetities zorgden voor ontspanning en een vrolijk stemming voor de rest van de week. Martin, ik ben blij dat je na bijna elf jaar samen toeteren tijdens mijn verdediging mijn paranimf wilt zijn. Ook heb ik met veel plezier bij studentenorkest "De Ontzetting" gespeeld waarmee we vele mooie concerten hebben gegeven, gezellige weekenden en concertreizen hebben gehad, en elke week weer een enerverende repetitie. Petra, Marjan, Marleen en Yvette, bedankt voor de gezellige middagen en weekenden die we samen hebben doorgebracht. Femke, bedankt voor je vriendschap en steun, en de gezellige carnavals die weer energie voor een jaar opleverden.

Pap en mam, bedankt voor de eindeloze steun die ik van jullie krijg. Zonder jullie stimulans was ik nooit zo ver gekomen. Casper, bedankt voor je hulp als ik erom vroeg en ik hoop dat je Franse dromen uit zullen komen. Lauret, bedankt voor je gezelligheid en ik ben heel blij dat je mijn andere paranimf wilt zijn. Theo en Margot, Raoul en Rigel, bedankt voor alle gezellige weekenden en de leuke vakanties in Venezuela. Ten slotte, Yves, jij bent voor mij in de afgelopen jaren heel belangrijk geweest. Ik wil je bedanken voor je steun, vertrouwen en alle jaren dat je heen en weer hebt gereisd tussen Wageningen en Amsterdam, zodat ik vlak naast mijn werk kon wonen. Zelfs toen ik voor 6 maanden naar Denemarken vertrok, heb je me gesteund. Ik ben ontzettend blij dat ik jou mijn partner mag noemen en ik zal er ook in de toekomst altijd voor je zijn.

Jeis

Curriculum vitae

List of publications

CURRICULUM VITAE

Iris Johanna Elisabeth Stulemeijer werd geboren op 25 januari 1979 in Eindhoven. In 1997 behaalde zij haar VWO diploma aan het Thomas College te Venlo. Daarna begon zij de opleiding "Plantenveredeling en gewasbescherming" aan de Wageningen Universiteit. Tijdens deze studie deed zij een afstudeeropdracht bij het Laboratorium voor Plantenveredeling, waar ze onderzoek verrichtte aan kwantitatieve resistentie van tomaat tegen de schimmel *Botrytis cinerea*. Vervolgens bestudeerde zij bij het Laboratorium voor Fytopathologie de relatie tussen de structuur en de functie van het Avr4 eiwit dat uitgescheiden wordt door de schimmel *Cladosporium fulvum*. Om de opleiding af te ronden heeft zij ten slotte stage gelopen op het "Plant Breeding Institute" te Narrabri in Australië, waar ze zich bezig hield met de veredeling van tarwe. In de zomer van 2002 sloot zij haar studie af met het verkrijgen van de doctoraalbul. In september 2002 startte zij haar promotieonderzoek bij het Laboratorium voor Fytopathologie waarvan de resultaten beschreven staan in dit proefschrift. In januari 2006 kreeg ze een persoonlijke beurs toegekend van het "Netherlands Genomics Initiative" die haar in staat stelde om het werk beschreven in Hoofdstuk 4 van dit proefschrift uit te voeren in het "Department of Biochemistry and Molecular Biology" van Prof. Dr. O.N. Jensen van de "University of Southern Denmark" in Odense. Vanaf april 2008 heeft ze een positie geaccepteerd bij het Nederlands Kanker Instituut in de groep van Fred van Leeuwen, waar zij de rol van Dot1, een eiwit dat een rol speelt bij histon methylatie in chromosoom organisatie en epigenetica, gaat bestuderen.

LIST OF PUBLICATIONS

Stulemeijer IJE, America AH, Visser JPC, Dekker HL, De Koster CG, Cordewener JH, Joosten MHAJ (2008) Resistance of tomato to *Cladosporium fulvum* requires the hypersensitive response and host cell wall-related defence responses that are specifically suppressed by the pathogen in susceptible plants. In preparation.

Stulemeijer IJE, Joosten MHAJ, Jensen ON (2008) Quantitative phosphoproteomics reveals a swift suppression of photosynthetic activity and a differential role for Hsp90 isoforms in tomato defence signalling. Submitted.

Bolton MD, Van Esse HP, Vossen JH, De Jonge R, Stergiopoulos I, Stulemeijer IJE, Van den Berg G, Borrás-Hidalgo O, Dekker HL, De Koster CG, De Wit PJGM, Joosten MHAJ, Thomma BPHJ (2008) The novel *Cladosporium fulvum* lysine motif effector Ecp6 is a virulence factor with orthologs in other fungal species. Mol Microbiol: accepted for publication.

Stulemeijer IJE, Joosten MHAJ (2008) Post-translational modification of host proteins in pathogen-triggered defence signalling in plants. Mol Plant Pathol 9: doi: 10.1111/j.1364-3703.2008.00468.x.

Stulemeijer IJE, Stratmann JW, Joosten MHAJ (2007) Tomato mitogen-activated protein kinases LeMPK1, LeMPK2, and LeMPK3 are activated during the Cf-4/Avr4-induced hypersensitive response and have distinct phosphorylation specificities. Plant Physiol 144: 1481-1494.

The work in this thesis was performed within the graduate school of Experimental Plant Sciences at the Laboratory of Phytopathology, Wageningen University, The Netherlands. The research was financially supported by the Dutch Organization for Scientific Research (VIDI grant 864.02.008 to Matthieu H.A.J. Joosten) and the Netherlands Genomics Initiative (Fellowship 050-72-416 to Iris J.E. Stulemeijer). Printing of this thesis was financially supported by the J.E. Jurriaanse Stichting.

On the cover:
A slightly modified painting from Iris J.E. Stulemeijer (1995)

Images above the odd numbered pages display a Cf-4/Avr4 (left) and control (right) seedling. An impression of how the hypersensitive response proceeds in the Cf-4/Avr4 seedling can be obtained by flapping this book from start to end. See page 78 for more details.

Printed by Ponsen & Looijen, Wageningen

Education Statement of the Graduate School
Experimental Plant Sciences

The Graduate School EXPERIMENTAL PLANT SCIENCES

Issued to: Iris Stulemeijer
Date: 2 June 2008
Group: Fytopathology, Wageningen University and Research Centre

1) Start-up phase	date
▶ **First presentation of your project**	
Changes in the phosphoproteome during the hypersensitive response of resistant plants	06 Jun 2003
▶ **Writing or rewriting a project proposal**	
▶ **Writing a review or book chapter**	
▶ **MSc courses**	
▶ **Laboratory use of isotopes**	
Course 'Safe handling with radioactive materials and sources'	Nov 2002
Subtotal Start-up Phase	*3.0 credits**

2) Scientific Exposure	date
▶ **EPS PhD student days**	
EPS PhD student day, Utrecht University	27 Mar 2003
EPS PhD student day, Vrije Universiteit Amsterdam	03 Jun 2004
EPS PhD student day, Raboud University Nijmegen	02 Jun 2005
EPS PhD student day, Wageningen University	13 Sep 2007
▶ **EPS theme symposia**	
Theme 2 symposium 'Interactions between Plant and Biotic Agents', Wageningen University	12 Dec 2003
Theme 2 symposium 'Interactions between Plant and Biotic Agents', Utrecht University	17 Sep 2004
Theme 2 symposium 'Interactions between Plant and Biotic Agents', Leiden University	23 Jun 2005
Theme 2 symposium 'Interactions between Plant and Biotic Agents', University of Amsterdam	02 Feb 2007
▶ **NWO Lunteren days and other National Platforms**	
NWO-ALW Lunteren 'Experimental Plant Sciences' (each year)	2003-2007
NWO-Chemical Sciences Lunteren 'Protein Sciences'	2004, 2006, 2007
Netherlands Proteomics Platform (NPP)	2003-2007
Willie Commeling Scholten days	2004, 2007
▶ **Seminars (series), workshops and symposia**	
Flying seminars (attendance 2x per year)	2003-2007
Symposium in honour of Pierre de Wit	04 Nov 2004
Symposium in collaboration with KNAW-CBS	27 Jun 2003
▶ **Seminar plus**	
Discussion with Jeff Dangl	*09 May 2003*
▶ **International symposia and congresses**	
Keystone meeting: Plant Biology: Functions and Control of Cell Death	10-15 Apr 2003
XII International Congress on Molecular Plant-Microbe Interactions	14-19 Dec 2003
Non-specific and specific innate and acquired plant resistance	31 Aug-03 Sep 2005
Plant protein phosphorylation and dephosphorylation	22-25 May 2007
XIII International Congress on Molecular Plant-Microbe Interactions	21-27 Jul 2007
▶ **Presentations**	
Oral presentation WCS day	22 Jan 2004
Oral presentation at the laboratory of Biochemistry and Molecular Biology, SDU	13 Oct 2005
Oral presentation at Lunteren EPS 2006	04 Apr 2006
Oral presentation at NPP symposium	12 Oct 2006
Oral presentation at EPS-WCS symposium	02 Feb 2007
Oral presentation at Plant Research International	07 Mar 2007
Oral presentation at Lunteren Protein Sciences 2007	10 Dec 2007
Poster for autumnschool: Disease Resistance in Plants	14-16 Oct 2002
Poster presentation at Lunteren EPS	07-08 Apr 2003
Poster for XII MPMI conference	14-19 Dec 2003
Poster for Proteomics Basics summerschool	13-19 Aug 2006
Poster for Plant phosphorylation/dephosphorylation meeting USA	22-25 May 2007
▶ **IAB interview**	03 Jun 2005
▶ **Excursions**	
Subtotal Scientific Exposure	*25.6 credits**

3) In-Depth Studies	date
▶ **EPS courses or other PhD courses**	
Autumnschool: Disease Resistance in Plants	14-16 Oct 2002
Bioinformation Technology – 1	12-21 May 2003
Summerschool: Basics in Proteomics	13-19 Aug 2006
▶ **Journal club**	
▶ **Individual research training**	
Training in Mass Spectrometry analysis of phosphopeptides	Apr-Oct 2006
Training in protein work in the laboratory of S. Peck. (Norwich)	Oct 2003
Training in DIGE-2DE technology and analysis	Dec-Feb 2006
Subtotal In-Depth Studies	*8.1 credits**

4) Personal development	date
▶ **Skill training courses**	
Scientific Writing	Apr-Jun 2004
Career perspectives	Sep-Oct 2005
▶ **Organisation of PhD students day, course or conference**	
▶ **Membership of Board, Committee or PhD council**	
Subtotal Personal Development	*3.3 credits**

TOTAL NUMBER OF CREDIT POINTS*	40.2

Herewith the Graduate School declares that the PhD candidate has complied with the educational requirements set by the Educational Committee of EPS which comprises of a minimum total of 30 credits

** A credit represents a normative study load of 28 hours of study*